THESE DE DOCTORAT DE L'UNIVERSITE PARIS 6

Spécialité
Géologie Structurale

Présentée pour obtenir le grade de
DOCTEUR de l'UNIVERSITE PARIS 6
Par

Faram AHMADHADI

La fracturation de la formation Asmari (sud-ouest Iran) : typologie, chronologie, et relation avec le plissement et la collision Arabie-Eurasie

Apports de données de terrain et de modèles mécaniques

Mém. Sc. Terre Univ. P. et M. Curie, n° 2006-03

soutenue le 27 mars 2006 devant le jury composé de:

M.	B. MEYER	Université Pierre et Marie Curie, Paris, France, Président
M.	O. LACOMBE	Université Pierre et Marie Curie, Paris, France, Directeur
M.	J.M. DANIEL	IFP, Rueil-Malmaison, France, Co-Directeur
M.	J. COSGROVE	Imperial College, London, UK, Rapporteur
M.	J.P. PETIT	Université de Montpellier II, Montpellier, France, Rapporteur
M.	T. ENGELDER	Pennsylvania State University, Pennsylvania, USA, Examinateur
M.	W. SASSI	IFP, Rueil-Malmaison, France, Examinateur

Thèse préparée conjointement au Laboratoire de Géologie structurale de l'Institut Français du Pétrole (IFP) et au Laboratoire de Tectonique de l'Université Pierre et Marie Curie (Paris 6)

Acknowledgments

This thesis would not be completed without encouragement and scientific support of a person to whom I am fully indebted, Professor O. Lacombe. I appreciate his patience in answering my numerous questions. His kindness, scientific and social personalities are admirable.

I am especially grateful to J.-M. Daniel, a conscientious man and hard worker who practically taught me how and what should be observed on the outcrops during several field seasons. I am quite indebted to J. Letouzey whose advices were constructive in my thesis. Without his support I would not be able to continue my work during the years of my Ph.D. program.

Many thanks to M. Guiton who supported the last part of this thesis and performed the mechanical simulation by his code.

My appreciation goes to J.L. Faure, J.M. Mengus, J.L Rudkiewicz, for sharing their experiences of brittle tectonics and field work. Many thanks to W. Sassi and F. Roure for their patience in answering my questions.

I acknowledge my colleagues of NIOC and all members of IOR Asmari Project Group who participated in regional studies and field campaigns.

I would like to thank F. Mouthereau and J. Tensi, for precious scientific discussions on geodynamics and constructive remarks on part of this manuscript and also their fully collaboration in the part of the modeling of the flexure in the Central Zagros. K. Amrouch kindly gave me some information about the practical manipulation and microscopic study of calcite twins. Also, I would like to thank N. Bellahsen for his constructive comments for a part of the manuscript.

I acknowledge the members of my thesis jury, J. Cosgrove, J.M. Daniel, T. Engelder, O. Lacombe, B. Meyer, J.P. Petit, and W. Sassi.

The scholarship for this Ph.D. thesis was granted by the University of Petroleum Technology of National Iranian Oil Company (NIOC) and a complementary grant by TOTAL Co. for which I am greatly indebted.

I have also been greatly helped by my family, my wife and my children, Farhad and Parisa, to whom I shared this success. Their tolerance over the years of my Ph.D. research is greatly admirable and I will be indebted to them whole my life.

Résumé

Les systèmes de fractures affectant la formation Asmari ont été étudiés dans plusieurs anticlinaux de la ceinture de plissement-chevauchement du Dezful, Zagros, Iran. En plus des orientations des familles de fractures et de leur chronologie, une attention particulière a été portée sur leur relation avec le plissement et avec les états de contraintes régionaux et/ou locaux, ainsi qu'au calendrier de la déformation régionale et à son contrôle par les failles de socle.

Un modèle tectonique régional de fracturation est proposé sur la base des observations de chronologie relative (phases de remplissage calcitique, relations géométriques de recoupement et d'intersection, modes d'activation, géométrie par rapport au plissement), de l'analyse des failles à stries et de l'interprétation d'images aériennes et satellitaires sur plusieurs anticlinaux de la région. Selon ce modèle, la plupart des fractures observées dans les carbonates de la formation Asmari sont précoces par rapport au plissement de la couverture qui s'est produit au Mio-Pliocène. Ces fractures précoces se seraient formées en relation avec des plis forcés au-dessus de failles de socle réactivées dès l'Oligocène – Miocène inférieur. La réactivation précoce de failles de socle N-S et N140° est corroborée par les données sédimentologiques qui montrent des variations régionales de facies pendant le dépôt de la formation Asmari et suggèrent le développement de sous-basins dans le bassin du Zagros central à cette époque. Une famille de joints précoces N40°-50°, très réguliers, marque probablement le début de la transmission lointaine des contraintes orogéniques dans la région. En réponse à la réactivation précoce des failles de socle, des fractures orientées N140° et N-S se développent ensuite. Au début et pendant la phase majeure de plissement de la couverture, au Mio-Pliocène, les factures précoce ont été réactivées (ré-ouvertes et/ou cisaillées) tandis que se néoformaient des fractures en cisaillement « classiques », comme des duplex, des failles inverse à faible pendage et des chevauchements. Cette étude souligne la nécessité de prendre en compte soigneusement le développement de fractures ante-plissement à l'échelle régionale et/ou locale dans les modèles des réservoirs fracturés, ainsi que l'influence des failles de socle majeures. En bref, pour le réservoir carbonaté d'Asmari dans le Zagros central, nous proposons un modèle complexe de fracturation incluant le développement de fractures classiques liées au plissement, ainsi que des fractures précoces anté-plissement, certaines d'entre elles étant liées à la réactivation précoce des faille de socle.

Un modèle mécanique 3D a été construit sur un pli typique restauré de la région d'étude (l'anticlinal Asmari) afin de prédire la réactivation des fractures dans des positions structurales différentes du pli. Cette modélisation fournit un test mécanique préliminaire de la séquence d'activation/réactivation de fractures au début et pendant le plissement déduite des observations et mesures de terrain. Les résultats indiquent que le modèle tectonique proposé est mécaniquement viable ; ils fournissent également des informations sur l'intensité de la fracturation et les modes de réactivation (ouverture, glissement) des fractures à l'échelle de la structure plicative dans son ensemble.

Abstract

Regional fracture patterns in the Asmari Formation, one of the most famous petroleum carbonate reservoir in Iran, have been investigated in several anticlines in the central part of the Zagros folded belt. In addition to fracture orientations and chronology, attention was paid to regional deformation scheme, folding style, regional/local stress state, and fold/fracture relationships. Combining fracture chronology observations based on calcite-filling phases and cross-cutting relationships, fault-slip data analysis and aerial/satellite image interpretation on several anticlines in the region allowed us to propose a tectonic model involving pre-folding fracture development in the Central Zagros folded belt.

Most fractures in the Asmari carbonates predated folding of the sedimentary cover which occurred in Mio-Pliocene times. Early fracture sets developed presumably in relation to forced-folding above reactivated, N-S and N140° trending basement faults during Oligocene to Lower Miocene times. Early basement fault reactivation is supported by facies changes during deposition of the Asmari Formation and occurrence of different sub-basins in the Central Zagros at that time. An early regional joint set striking ≈N40°-50° presumably marked the onset of the far-field transmission of orogenic stresses in the region. In response to the early reactivation of the main Zagros basement faults under a mean NE compressional stress trend , ≈N140° and N-S trending joint sets were initiated as second and third early fracture families. At the onset and during the main Mio-Pliocene folding phase in the sedimentary cover, early fractures were reactivated (reopened and/or sheared) while shear fractures including duplexes, low angle reverse faults and thrusts newly formed as more classical fold-related fracture sets.

This study puts emphasis on the need of carefully considering regional/local fracture development predating folding of the cover in models of the fractured reservoirs as well as influence of possible underlying basement faults. Indeed, in the Asmari carbonate reservoirs in the Central Zagros, the complex fracture pattern include both classical fold-related fractures as well as prefolding joint sets, some of them being related to early reactivation of underlying basement faults.

Finally, a 3D mechanical modelling code is used to predict fracture development and reactivation within different structural positions during folding. Applied to the well-known Asmari anticline, such a modelling provides a preliminary mechanical test of the sequence of fracture activation/reactivation at the onset of and during folding as derived from field observations and measurements. The results indicate that the tectonic scenario of fracture

development is mechanically valid; they further provide accurate information about fracture intensity and modes of fracture reactivation at the scale of the entire fold structure.

Foreword

The base of fracture study is one of the branches in the structural geology which has a long history of challenge. It covers a vast area of applications and it needs a multidisciplinary approach especially in petroleum exploration/production domain. Each step of this approach, from outcrop study and field work to numerical modeling, involves different theoretical and practical activities. Furthermore, each step should be carefully treated before using it as an input for the next step.

The Asmari Formation is one of the main reservoir rocks of SW Iran with several decades of production history from different oil fields in the region. Despite a generally poor porosity and matrix permeability in this reservoir, production rates are high because of the fractures. Most of these reservoirs are near the final stage of their natural depletion phase (most of them produced with their own natural reservoir energy). At the best case and with suitable reservoir rock and fluid properties and reservoir conditions (good aquifer and gas cap deriving forces) of the Zagros fields, something between 20 to 25% of initial oil in place of these reservoirs may be exploited. Nowadays, the need for performing secondary and tertiary phases of oil recovery is vital to maintain the optimum or economic production rate for each individual oil field. As the role of fractures in production within Iranian carbonate reservoirs appeared to be important, it can not be overwhelmed within enhanced oil recovery plans in these reservoirs.

On the other hand, almost all of these reservoirs are structural traps (or simply, folds), and oil has occupied entire or part of structural closure. While structural style and folding mechanisms studies on the outcrops of the Zagros folded belt is essential for geophysical interpretation of underground structures and finally petroleum exploration, they form the preliminary steps in each field-based fracture study. Furthermore, the proper understanding of fracturing and deformation through local and regional deformation context in the Zagros region not only provides a complementary tool in exploration aspects but also improve the success of production plans within each local, individual explored field. To this regard, field observations, as the most practical and fundamental step in fracture study is important. However, fracturing should be considered as part of a brittle deformation phase during the evolution history of a basin. Folds, faults, fractures, and stylolites are some examples in the manifestation of rock failure in response to, in most cases, an external agent, called stress field. Thus, it should be always taken into account that any fracture study should be

accompanied by stress field analysis otherwise making a link between deformation history and different fracturing episodes would be a difficult task.

The main objective of this thesis is to find answers to the following questions in the Central Zagros:

1. Is there any relation between folds and fractures in the Asmari Formation?
2. What is the hierarchical fracture genesis in the Asmari Formation?
3. What is the relation between fracturing and deformation from the Zagros geodynamic and basin evolution view points?
4. If there is/are preexisting fracture set(s) how are they reactivated during folding (mechanical modeling)?

The first phase of this work was carried out during several months of field trips. Analysis of outcrops data (fracture orientation, genesis, chronology, fault-slip data) was combine with aerial and satellite images interpretation, use of existing geological maps and paleologs kindly provided by National Iranian Oil Company (NIOC), and coupled with an intensive bibliography on all aspects covered in this work including the Zagros deformation and sedimentary evolution, folding types and mechanisms, basic fracturing concepts (joints, faults, paleostress field definition, fold/fracture relationship, …), as well as previous works carried out on fracturing aspects in the Zagros folded belt. Furthermore, a simplified 3D kinematic and direct (mechanical) modeling on a typical anticline in the studied area (Kuh-e Asmari) was performed at the end of this study in order to test and verify some hypotheses regarding fractures development episodes in the Asmari Formation taking into account field observations and chronologies.

This work was carried out in the Structural Geology Department of the Institut Français du Pétrole (IFP) and the Tectonic laboratory of the Pierre and Marie Curie University (Paris VI) under the supervision of Dr. Jean-Marc DANIEL (IFP, thesis promoter) and Pr. Olivier LACOMBE (Paris VI, thesis supervisor).

Plan of the thesis

This thesis comprises four main parts, each of them including different chapters. Part one has a review on folding and fracturing typology and mechanisms. Geological and tectonic framework of the Zagros is presented in the second part. In this part previous works in the

Zagros folded belt are emphasized to give a general picture of geological setting of the Zagros folded belt, deformation and sedimentary evolution, and to introduce the Asmari Formation in which the study of fracture patterns is one of the main objectives of this thesis. Part three begins with fracture development in the Arabian plate and the Zagros area and different ideas in this regards are presented and then is followed by the main results about fracture development and deformation timing in the Central Zagros which obtained in this thesis. In the last part, the reactivations of the fractures are discussed using a mechanical modeling approach. The contents of the chapters are summarized as follows;

- Part one

Chapter I presents folding typology and mechanism especially in the Zagros folded belt. The elementary aspects of fold evolution, especially fault-related folds are reviewed briefly.

Chapter II starts with the basic concepts of the stress then followed by elementary mechanical concepts of joint development. Faults as another group of fractures are discussed in this chapter. It covers the criteria used to detect the sense of fault movements. Paleostress definition using inversion method on fault-slip data, as well as stylolitic peaks, is another part of this chapter which ends with an integrated discussion of fold/fracture relationships.

- Part two

Chapter III introduces geological setting and geodynamic evolution of the Zagros with a focus on paleogeography of the Zagros basin since Upper Cretaceous. Then, morphotectonical divisions of the Zagros based on different authors are discussed.

Chapter IV focuses on the Asmari Formation and covers the main characteristics of this Formation. A detailed review on litho- and bio-stratigraphical divisions of the Asmari Formation is presented in this chapter.

- Part three

Chapter V critically discusses the previous studies about fracturing in the Asmari Formation following an introduction on fracture pattern within the sedimentary cover of the northeastern margin of the Arabian plate and beyond the Zagros orogenic belt.

Chapter VI provides the main results of a regional fracture study in the Asmari Formation in the Central Zagros based on the observations, fracture data and aerial/satellite images analysis, fracture chronology and fault-slip data interpretation in the studied area. A conceptual model for a hierarchical regional scale fracture initiation and development is introduced in this chapter and followed by some supplementary remarks on the field observations.

Chapter VII argues evidence of forced-folding and basement-fault-related deformation in the Central Zagros before the onset of Mio-Pliocene main orogenic phase in the Central Zagros based on constructed lithostratigraphical transects and paleogeographic maps in the region. The effect of basement faults reactivation in the Asmari basin during its sedimentation is discussed and occurrence offsets of fractures observed in the studied anticlines, inconsistent with classical fold-related fracture model is argued.

Chapter VIII discusses deformation timing and proposes a geodynamic model for the Central Zagros following the arguments of the previous chapter about basement faults reactivation and intra-basin development.

- Part four

This part presents a 3D kinematics and mechanical modeling of the Kuh-e Asmari anticline as a representative anticline in the studied area. A 3D surface on top of the Asmari anticline was constructed based on the most recent structural transect and subsurface geophysical data on this anticline. After restoration of the constructed surface, a direct mechanical modeling was performed using Guitton (2002) method to examine the reactivation of prefolding and newly-formed fractures during the evolution of fold.

Finally, this manuscript is finished by a general conclusion and prospective regarding fracture study in the Central Zagros. Possible topics which could be covered by future studies in this area are proposed to complete the present work.

Table of contents

ACKNOWLEDGMENTS III

RÉSUMÉ V

ABSTRACT VII

FOREWORD IX

PLAN OF THE THESIS X

PART 1: BASIC NOTIONS ON FOLDING AND FRACTURING 7

CHAPTER I: FOLDING TYPOLOGY AND MECHANISMS 9

INTRODUCTION 9
I.1. BUCKLE FOLDS 9
I.1.1. States of strain within the buckle layer and folding mechanisms 10
I.1.2. Evidence of flexural-slip and neutral surface Folding 13
I.1.3. Buckling associated with basement wrench faults 14
I.1.4. Geometrical differences between two kinds of buckle folds 15
I.2. FORCED FOLDS 16
I.2.1. Folds associated with thrust faulting 16
I.2.2. Forced folding above oblique-slip faults 19
I.3. FOLD EVOLUTION FROM A DETACHMENT TO A FAULT RELATED (FAULTED DETACHMENT) FOLD 19
CONCLUSION 21

CHAPTER II: BASIC GEOMETRICAL AND MECHANICAL ELEMENTS OF FRACTURES AND THEIR RELATIONS WITH FOLDS 23

INTRODUCTION 23
II.1. STRESS 23
II.2. FRACTURES 25
II.2.A: SOME TERMS AND DEFINITIONS 25
II.2.B : JOINTS (MODE I FRACTURES) 27
II.2.B.1. Some mechanical aspects of Joints 28
II.2.B.2. Joint surface morphology 31
II.2.B.3. Joint continuity and propagation 32
II.2.B.4. General condition for joint creation 33
II.2.B.5. Joint sequence and chronology 35
II.2.C. FAULTS (MODE II & III) 36
II.2.C.1. Mechanical aspects of faulting 37
II.2.C.2. Criteria for the sense of movement on fault surfaces 40
II.2.C.3. Fault-slip analysis and paleostress reconstruction 42
II.2.C.4. Faults growth, terminations and relays zones 46
II.2.C.5. Calcite twins and paleostress determination 48
II.2.C.6. Sylolites and paleostress determination 49
II.2.D. FRACTURE PATTERNS ASSOCIATED WITH FOLDING 52
II.2.D.1. The bases of classification 53
II.2.D.2. Axial fractures 54
II.2.D.3. Transversal fractures 58
II.2.D.4. Oblique fractures 59
II.2.D.5. Regional joints 60
CONCLUSION 61

PART 2: GEOLOGICAL AND TECTONIC FRAMEWORK OF THE ZAGROS 65

CHAPTER III: PALEOGEOGRAPHY AND GEOLOGICAL SETTING OF THE ZAGROS FOLDED BELT, SOUTHWEST OF IRAN 67

INTRODUCTION 67
III.1. ARABIAN PLATE TECTONICS 67
III.1.1. Geodynamic evolution 67
III.1.2. Basement tectonic and related features 68
III.2. THE ZAGROS BELT 78
III.2.1. The orogenic movements and paleogeography of Zagros 78
III.2.2. Stratigraphic and structural division of the Zagros folded belt 82
III.2.3. Deformation style and kinematic of different groups 86
III.2.4. General tectonic and morphotectonic features 86
III.2.5. Morphotectonic units of the Zagros 89
III.2.6. Other classification 96
III.2.7. Timing of deformation in the Zagros folded belt 98
CONCLUSION 98

CHAPTER IV: THE ASMARI FORMATION 101

INTRODUCTION 101
IV.1. LITHOLOGY AND DISTRIBUTION 101
IV.2. BIO-CHRONO FACIES DIVISION OF THE ASMARI FORMATION 103
IV.3. THE MEMBERS OF THE ASMARI FORMATION 108
CONCLUSION 114

PART 3: FRACTURE DEVELOPMENT AND ITS RELATION WITH LARGE SCALE DEFORMATION IN THE CENTRAL ZAGROS 115

CHAPTER V: PREVIOUS STUDIES OF FRACTURE DEVELOPMENT IN THE ARABIAN PLATE / ZAGROS 117

INTRODUCTION 117
V.1. REGIONAL FRACTURE SETS IN ARABIAN COVER ROCKS 117
V.1.1. Stress conditions 117
V.1.2. Lineament trends in the east Arabian platform 118
V.1.3. Macro-fractures (map scale fractures) and regional joint sets in Arabian basement-cover rocks 120
V.1.4. Age of the mesofractures 123
V.1.5. Integration and interpretation of megatectonic and microtectonic 123
V.2. FRACTURE PATTERNS IN THE ASMARI FORMATION IN THE ZAGROS; PREVIOUS STUDIES 124
V.2.1. Bedding-Plane Distribution 125
V.2.2. Origin of Fractures 125
V.2.3. Fracturing and Dynamic Data in Asmari Reservoirs 126
CONCLUSION 131

CHAPTER VI: A NEW STUDY OF REGIONAL FRACTURE PATTERN IN THE ASMARI FORMATION 133

VI.A. FRACTURE PATTERNS WITHIN OLIGO-MIOCENE ASMARI FORMATION IN THE CENTRAL ZAGROS FOLDED BELT, SW OF IRAN; EVIDENCE FOR PRE-FOLDING JOINT DEVELOPMENT (PRE-PUBLICATION) 133
ABSTRACT 133
INTRODUCTION 134
VI.A.1. GEOLOGICAL SETTING 136
VI.A.1.1. Tectonic setting 136
VI.A.1.2.Lithostratigraphy 138
VI.A.1.3. Structural style 138

VI.A.2. DATA COLLECTION AND ANALYSIS 142
VI.A.2.1. Sampling strategy and type of collected outcrop data 142
VI.A.3.2. Orientation measurements analysis 143
VI.A.3.3. Fault-slip data 144
VI.A.3. OBSERVATIONS 145
VI.A.3.1. Structural types 145
VI.A.3.2. Examples of simple fracture patterns: Safid and Razi anticlines 145
VI.A.3.3. Asmari anticline 147
VI.A.3.4. Khaviz anticline 151
VI.A.3.5. Supplementary fracture data 156
VI.A.3.6. Supplementary fault-slip data 158
VI.A.4. INTERPRETATION OF THE RESULTS AND DISCUSSION 159
VI.A.4.1. Pre-folding fracture patterns in the central Zagros 160
VI.A.4.2. Fold-related fractures in the Central Zagros 165
CONCLUSION 167
VI.B. SUPPLEMENTARY RESULTS ON FRACTURE STUDY 170
VI.B.1. Second-order early fracture patterns (N-S and E-W) in the anticlines of Izeh zone in the Asmari Fm 170
VI.B.2. Tectonic stylolites in the Central Zagros folds and their relations to extensional fractures 175
VI.B.3. Comparison of the results of paleostress analysis using fault-slip data and calcite twins in veins from Khaviz and Dil anticlines 177
VI.B.4. Diagenesis and fracturing 178
VI.B.5. Fractures in Upper Cretaceous carbonate of the Sarvak Formation, a preliminary observation 182

CHAPTER VII: EARLY FRACTURE DEVELOPMENT WITHIN ASMARI CARBONATES: ROLE OF BASEMENT FAULTS ON LOWER TERTIARY FACIES CHANGES AND POSSIBLE FORCED-FOLDING 187

INTRODUCTION 187
VII.1. POSSIBLE LINKS BETWEEN PREFOLDING FRACTURE DEVELOPMENT IN THE ASMARI FM. AND FORCED FOLDING/FLEXURE RELATED TO BASEMENT FAULT REACTIVATION 188
VII.1.1. Early fracture patterns in the Asmari Formation 188
VII.1.2. Fold-related fracture pattern; reminder 191
VII.1.3. Our knowledge about the Zagros basement faults 197
VII.2. PALEOGEOGRAPHIC EVIDENCE OF EARLY BASEMENT FAULT REACTIVATION 200
VII.2.1. Constraints from paleofacies evolution from Upper Cretaceous to Lower Tertiary 201
VII.2.2. Possible control of basement fault reactivation on Intra-basins geometries 213
VII.3. NATURE OF VERTICAL MOTION ALONG REACTIVATED BASEMENT FAULTS : COMPRESSIONAL OR EXTENSIONAL ? 215
VII.3.1 Early fracturing in the Asmari carbonates and extension due to lithospheric foreland flexure 216
- Airy-type (1D) backstripping 216
- Geometrical fitting of decompacted depths by a deflection profile 220
VII.3.2 Early fracturing in the Asmari carbonates and compressional reactivation of basement faults due to early orogenic stress build-up 224
CONCLUSION 226

CHAPTER VIII: IMPLICATIONS FOR THE GEODYNAMIC EVOLUTION OF THE CENTRAL ZAGROS 227

INTRODUCTION 227
VIII.1.PREVIOUS ESTIMATES OF DEFORMATION TIMING IN THE ZAGROS FOLDED-BELT 227
VIII.2. POSSIBLE TIMING OF EARLY FRACTURES AND ONSET OF OROGENIC DEFORMATION AND STRESS BUILD-UP IN THE CENTRAL ZAGROS 228
VIII.3 GEODYNAMIC IMPLICATIONS 229
VIII.4. PETROLEUM EXPLORATION IMPORTANCE 234
CONCLUSION 234

PART 4: INHERITED FRACTURE REACTIVATION AND NEO-FRACTURING DURING FOLDING OF SEDIMENTARY STRATA : A MECHANICAL MODELLING 237

INTRODUCTION 239
1. DEFORMATION AND 3D MODELLING IN STRUCTURAL GEOLOGY; METHODOLOGY 240
1.1. Restoration 241
1.2. Direct (mechanical) modeling 242
1.3. Description of the model and mechanical parameters 249
2. MODELLING OF THE ASMARI ANTICLINE 251
2.1. 3D geometrical model 251
2.2. 3D restoration 257
2.3. Mechanical modelling of different fracture families in the Asmari anticline 258
CONCLUSION 267

GENERAL CONCLUSION AND PROSPECTIVE 269

GENERAL CONCLUSION 271
PROSPECTIVE 272

REFERENCES 275

ANNEX 1: SOME REMARKS ON SPOT 5 IMAGERY 291

ANNEX 2: FIEL EXAMPLES OF FRACTURE PATTERNS IN SOME ANTICLINES 295

Part 1

Basic notions on folding and fracturing

CHAPTER I: Folding typology and mechanisms

Introduction

Each morphotectonic unit of the Zagros folded belt shows different fold pattern based on structural setting, detachment levels, development of thrust faults and reactivation of possible deep-seated basement faults. So, it is difficult to say which kind of fold is more dominant in this area. Colman-sadd (1978) interpreted the Zagros folds as buckle folds. However, the presence of a high competency contrast between the sedimentary units, involved in in the folding, is necessary. Furthermore, field observations and seismic interpretations in the central Zagros suggest that fault-propagated folds well developed in this part of the Zagros. On the other hand, frequently observed parallel-bedding slickensides within the folds prove that flexural slip mechanisim play an important role in internal deformation and bedding interaction in a fold in this area. Detachment or buckle folds was considred, at least, as an early stage of fold growth in the Zagros belt based on recent investigations (Sherkati et al, 2005; Molinaro et al., 2005). Therefore, the characteristics of this type of folds is discussed first, then flexural slip and flexural flow as two folding mechanisms is presented briefly. Forced folding as another type of folds in the Zagros was taken into account in this chapte and finally the evolution of a typical fold from detachment fold to a faulted detachment fold (Mitra, 2002) is discussed.

I.1. Buckle folds

Satellite images and aerial photographs show numerous examples of anticlines with aspect ratios (half wavelength to axial length ratio) of between 1:5 and 1:10, which are typical of buckle folds on all scales and which display the characteristic en echelon spatial organization in plan view, in which as one fold dies out it is replaced by another with parallel axes but offset from the first fold (Fig.I.1).

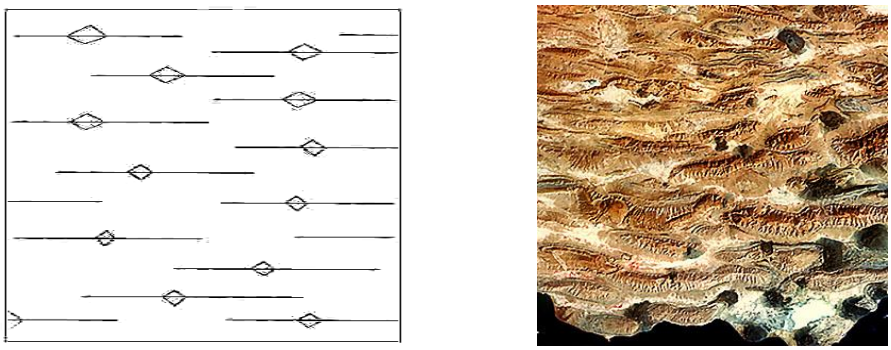

Fig.I.1a: Idealized spatial organization of buckle folds in plan view; After Price & Cosgrove (1990); b) (right). Satellite image (LANDSAT) of part of Zagros fold belt (Source: RST web-site).

Ideal parallel folds can be depicted as a series of approximately circular arcs, hence the synonym concentric folds. On any one fold the radius of curvature in the layers on the outer arc of the fold is much greater than in the layers near the core (Fig.I.2A&B). In anticlines there is a lower limit below which the folds no longer can follow the ideal parallel style; there is a corresponding upper limit in synclines.

Because parallel folds can not continue indefinitely either upward or downward, they must change in style to similar or chevron folds, or the folded layers must become detached from the rocks both above and below. The mechanical stratigraphy of the Zagros is particularly favorable for development of this kind of folds. In the case of the Competent group of the Zagros Mountains, there is a lower zone of detachment in the Lower Mobile group (Hormuz salt), and upper zone in the Upper Mobile group (Gachsaran formation) (Colman-Sadd, 1978).

A)

B)

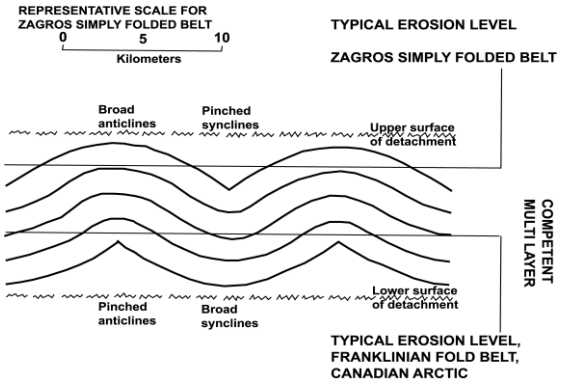

Fig.I.2: (A) Profile view of a parallel (buckle) fold with eroded crest (Source: RST web-site). (B): Concentricity of parallel folds. At higher erosion level anticlines are broad and synclines pitched ; at lower erosion level reverse is true. Potential faulting is omitted (Colman-Sadd, 1978).

Buckle folds in 3D space have a periclinal geometry; i.e. have the form of an elongated dome, basin or saddle. Buckle folds often die out rapidly in profile section (Cosgrove and Ameen., 2000) (Fig. I.3).

I.1.1. States of strain within the buckle layer and folding mechanisms

Folding by buckling maybe achieved by two mechanism, *flexural-slip and neutral-surface folding* (Hills, 1963; Ramsay, 1967). These mechanisms arise the problem of state of stress and related deformation and also second order structures due to shearing parallel to layer boundaries.

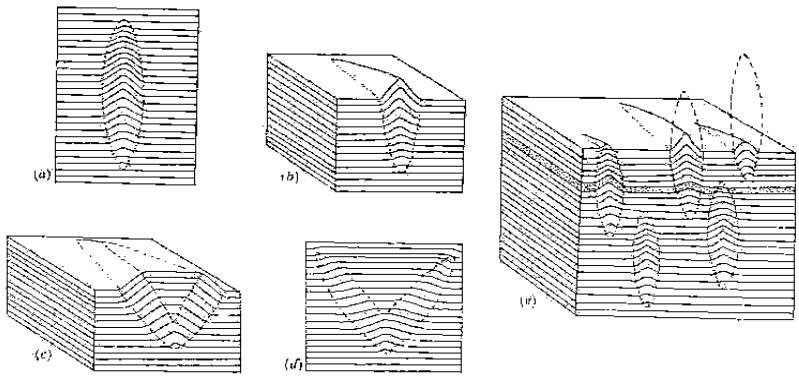

Fig.I.3 (a) Typical profile geometry of a fold in a multilayer. (b) Block diagram showing a fold dying out in both profile and plan view. (c) Block diagram and (d) profile geometry of a box fold. (e) The spatial organization of folds within a multilayer. Cosgrove & Ameen, 2000.

Shearing parallel to layer boundaries: Many sedimentary strata have a well-developed plane-parallel stratification, and this inherent weakness in the rocks frequently controls the type of internal deformation during buckling. The individual rock layers are flexed and the outermost layers slip over the inner layers toward the fold hinge zones. The folds developed in this way have a true parallel form (Class 1B) and are sometimes known as flexural folds. At any point in the fold this simple shear strain may be homogeneously distributed through the strata to produce *flexural-flow folds* (Fig.I.4A); or it may be inhomogeneously distributed with more movement on the layer boundaries then in the center of the layers (Fig.I.4B) and give rise to *flexural-slip folds* (Donath, 1962).

As a result of this flexural slip, various structures may develop in the rocks. Zones of en echelon quartz or calcite-filled extension fissures may begin to form on the flanks of structures where the dips attain the highest value in the fold (Fig.I.5). They always tend to dip at moderate to low angles toward the antiformal axial surface, and if the shearing is inhomogeneous they may be sigmoidally shaped. Slaty cleavage may develop on the fold limbs perpendicular to the maximum finite compressive strain (Ramsay, 1967) (Fig.I.5c). In this case internal deformation will be accommodated by development of these cleavages and/or sigmoid veins. Although flexural-slip folding develops in rocks, which have a well-marked stratification or layering, it may also be an important mechanism of internal deformation in rock sheets, which have no layered structure. So the slip will occur along the developed cleavages.

Longitudinal strains parallel to layer boundaries: The strains within buckled layers may be developed in ways other than those of flexural slip. *Tangential longitudinal strain* is a type of internal deformation commonly developed in buckled nonstratified sheets whereby the

principal axes of strain are arranged tangentially and perpendicularly to the folded layers. It is possible to accommodate the internal strains of the layers entirely by this type of deformation, although in nature both tangential longitudinal strain and flexural slip generally proceed together. Within the buckled layer there is a surface known as the *neutral surface* (*or finite neutral surface*) along which the principal finite longitudinal strains are zero. This neutral surface need not be positioned exactly midway between the layer boundaries and it may, in practice, crosscut the internal layering at a low angle (FigI.6b). On the outer arc of the neutral surface the layers have been subjected to an extensive strain, while on the inner arc they have been compressed (Ramsay, 1967) (Fig.I.6a).

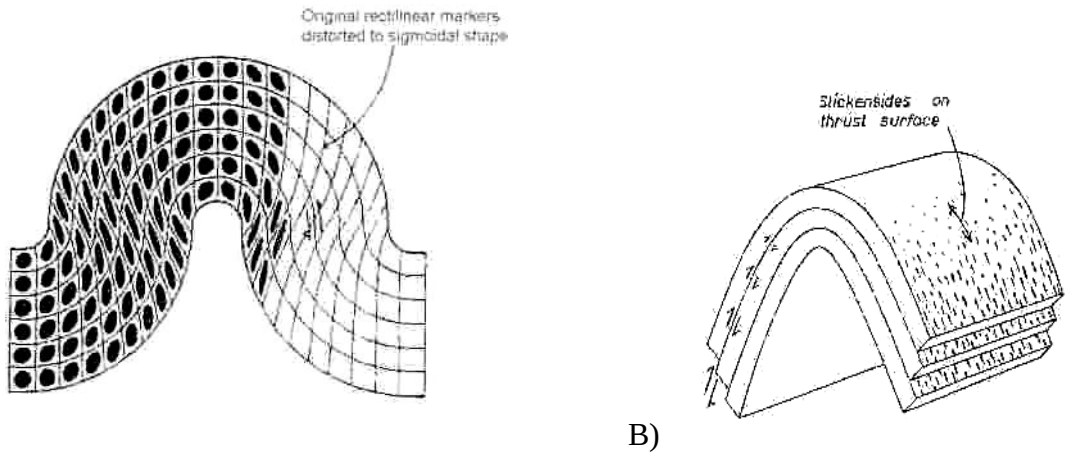

A) B)

Fig.I.4: (A) Internal strain in a layer deformed by flexural-flow (Ramsay, 1967) (B): Development of thrusts in a flexural-slip fold.

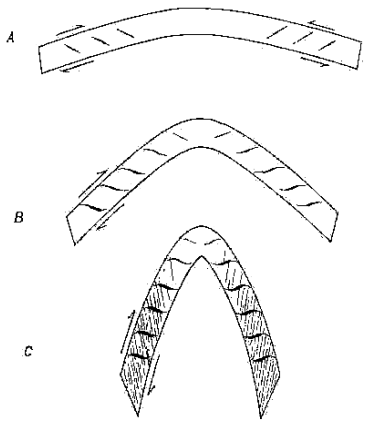

Fig.I.5. Progressive development of sigmoidal tension fissures and slaty cleavage as a result of progressive fold development with internal deformation by flexural flow (Ramsay, 1967).

The nature of the small-scale structures which are developed as a result of longitudinal strain in the buckled layer depends to a large extend on the properties of the layer under a given strain rate. In the inner arc of the fold the strong compressive strain perpendicular to the

layering may lead to the development of slaty cleavage around the fold hinge and sometimes to the formation of tension fissures subparallel to the layering. If the layer is not completely ductile (perhaps during the closing stages of the fold history), the last strain increments may lead to the development of sets of conjugate shears fractures (mode II & III) and to the formation of thrust faults which themselves may become involved in the folding (Fig.I.7). In the outer arc of the fold the principal strain along the layers is extensive and this may lead to the development of extension fractures cutting across the layering. Such fractures are often infilled with crystalline material that has migrated outward from the strongly compressed inner arc of the structure. Individual thin competent-layer components making up the buckled sheet may develop boudinage structures in the outer fold arc (Ramsay, 1967). Fracture mechanism and fold-fracture relationship will be discussed in more details in section II.

Parallel folding is generally achieved by a combination of the two mechanisms and this is the case in the folding of the Competent group of the Zagros folded belt (Colman-Sadd, 1978).

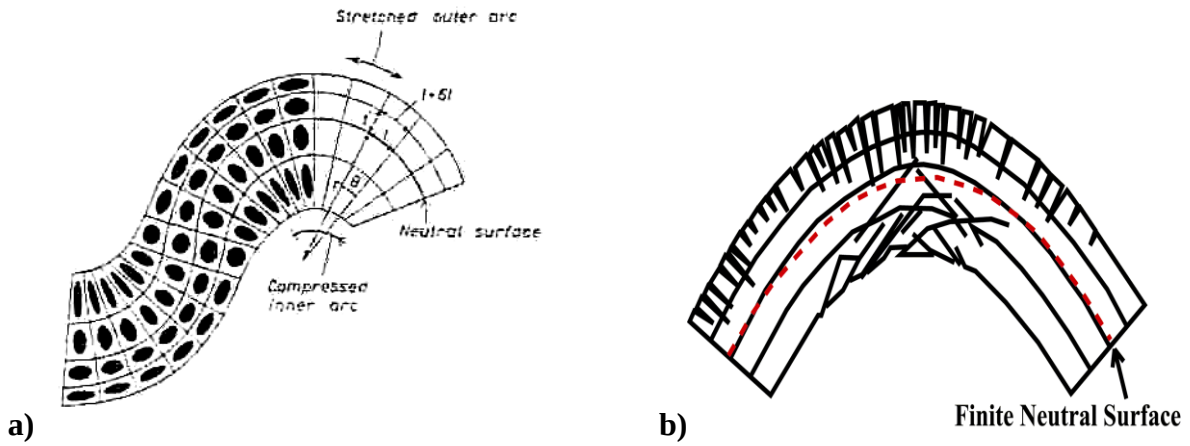

Fig.I.6. Buckled layer with internal deformation developed by tangential longitudinal strain (a), Buckled layers with neutral surface crosscut the internal layering at a low angle (b) (Ramsay, 1967).

I.1.2. Evidence of flexural-slip and neutral surface Folding

Indication of movement between the layers of the Competent group are provided by numerous bedding-plane slickensides on fold limbs which are normal to the fold axes (Colman-Sadd, 1978). Another evidence of flexural-slip is the variation in the thickness of individual, incompetent evaporite beds between massive carbonate members, especially in more deeply eroded anticlinal cores (e.g. Kuh-e Surmeh), where folding has tended toward the chevron style and the evaporites have been squeezed from the limbs to the hinges of the folds (Colman-Sadd, 1978).

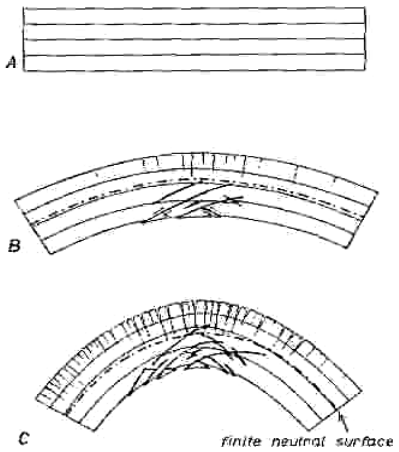

Fig.I.7: Structures developed in a layer progressively folded and deformed by tangential longitudinal strain (Ramsay, 1967).

Supposing Hormuz salt as the main and unique detachment level in the Zagros folds, neutral surface should be somewhere in lower part of Bangestan groupe (Kazhdumi formation) to upper part of Khami group (Fahlyan to Dariyan formations). However folding geometry and fracturing style indicating several complementary detachment surfaces (incompetent shaly intervals) and several neutral surfaces in competent group (Sherkati, 2004).

The outer arcs of anticlines in the Competent group are well exposed and provide numerous examples of extension structures. Widespread development of joints in almost all the Asmari anticlines has been given as a good evidence of extension structures above neutral surface by some authors (e.g., Colman-Sadd, 1978). Compressive structures in fold cores can be observed in the few anticlines that have been eroded or drilled below the neutral surface, and can be seen in some of the synclines where they have not been hidden by alluvium (Colman-Sadd, 1978).

I.1.3. Buckling associated with basement wrench faults

The recent seismicity of the Zagros belt (see e.g. Jackson & McKenzie 1984; Ni & Barazangi 1986; Berberian, 1995; Jackson et al, 1995; Talebian & Jackson, 2004)), and experimental work on analogue models (F. Odonne & P. Vialon, 1983) show that strike-slip faults exist in the basement underlying the Zagros fold belt and that movement on these faults has resulted in folding of the cover rock. This experimental work shows that, depending on the mechanical and rheological properties of the cover rock, they may deform in either a brittle or ductile manner and produce arrays of fractures and folds, or combination of the two.

The pattern and distributions of these structures can be used to determine both the existence of an underlying strike-slip fault and its sense of movement.

The folds produced when a cover sequence responds in a ductile manner to basement strike-slip faulting are buckle folds, and as such form with an aspect ratio of between 1:5 and 1:10. In plan view they are arranged so that they are consistently offset from each other, either to the right or to the left (Fig.I.8). One example in the Zagros fold belt is the E-W-trending en echelon array of anticlines above the Bala Rud line, with a sinistral motion, which marks the northern boundary of the Dezful Embayment (Sattarzadeh et al., 2000) (Fig.I.9).

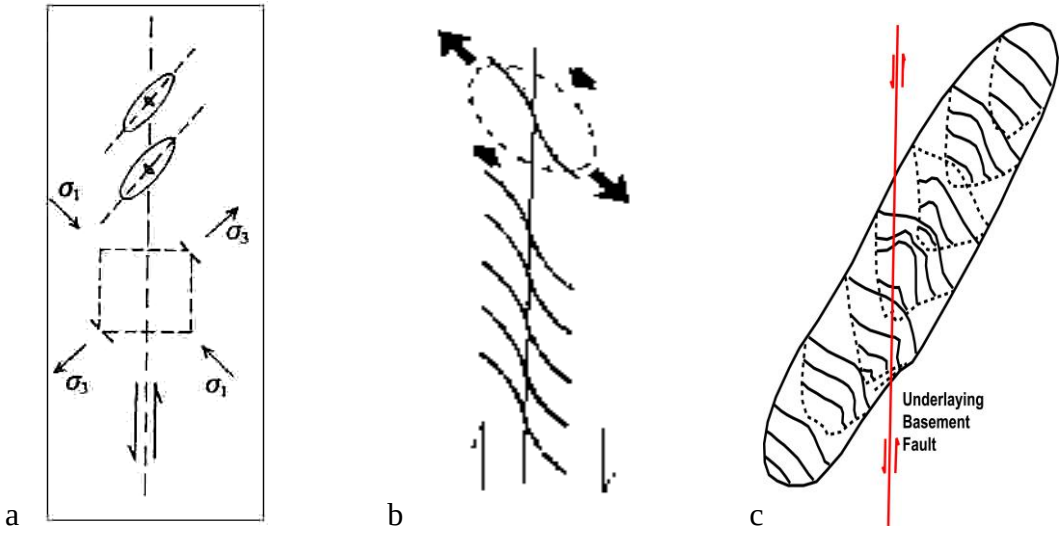

Fig.I.8(a): Shear along a basement wrench fault induces compression in the cover rocks which may produce en echelon folds along the sinistral strike-slip fault, (b) Schematic diagram showing the predicted orientation of folds axes (gently curved lines) in a cover sequence above a dextral strike-slip fault in the basement. (c) The form and structure are represented by a series of profiles. Note the reversal of symmetry of the fold on opposite sides of the basement fault (from Oliver 1987).

I.1.4. Geometrical differences between two kinds of buckle folds

In addition to their spatial organization, the buckle folds formed in association with basement strike-slip faulting may have second-order features that enable them to be distinguished from buckle folds formed as a result of a regional compression. For example they may become sigmoidal in plan view (Fig.I.8b) as a result of rotation of the earlier (central) part of the fold before the growth of the younger (peripheral) portions, in a manner similar to the formation of sigmoidal veins. In addition, they may develop a more complex profile geometry, which changes its symmetry when traced from one end of the fold to the other (Sattarzadeh et al., 2000) (Fig.I.8c).

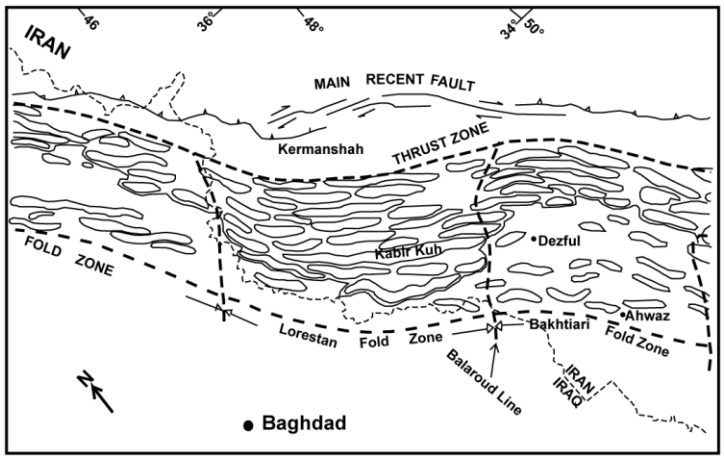

Fig.I.9: Distribution of folds in parts of the Zagros folded belt above the Bala Rud line (Sattarzade et al., 2000). See text for details.

I.2. Forced folds

According to Stearns 1978, Forced folds are "folds in which the final overall shape and trend are dominated by the shape of some forcing member below". Thus, in order for such folds to form when the forcing member is a fault block, it is necessary for them to be an element of dip-slip movement on the underlying fault. These kind of folds could be divided into two main groups: (1) those associated with thrust faulting in the cover rocks. Fault-bend folds and fauly propagation folds are two main examples in this group; (2) those associated with the movement of basement blocks; drape folds are placed in this group.

I.2.1. Folds associated with thrust faulting

I.2.1.1. Fault-bend folds

In this type of forced folding, the folding is not the result of the movement of rigid fault blocks in the basement but rather the result of fault movement within the cover rocks. They generally formed when layers move from flat to ramp or visa versa.(Fig.I.10). The two most widely recognized structural setting in which fault-bend folds form are: (1) in the hanging wall of a listric normal fault; and (2) in the hanging wall above a ramp in a thrust fault (Fig.I.10). This folding is not the result of frictional drag but is a result of bending (Cosgrove & Ameen, 2000).

As it was shown through different regional transect (e.g., McQuerrie, 2004, Molinaro et al., 2005; Sherkati et al., 2005) in chapter I, fault-bend fold above a ramp in a thrust fault seems to be common especially in the Dezful Embayment and Izeh zone (Fig.I.10, 12). Many of this folds are linked to underlying thrusts. This is often related, either directly or indirectly,

to the reactivation of basement normal faults during and subsequent to the major plate collision in the Miocene. As can be seen from Fig.I.11 , the forced folding in the Asmari limestone is often the result of fault-bend folding associated with the generation of new thrusts in the cover, whereas deeper in the succession, at the basement-cover contact, the forced folding of the Hormuz salt is the result of the reactivation of old basement normal faults (Sattarzadeh at al., 2000).

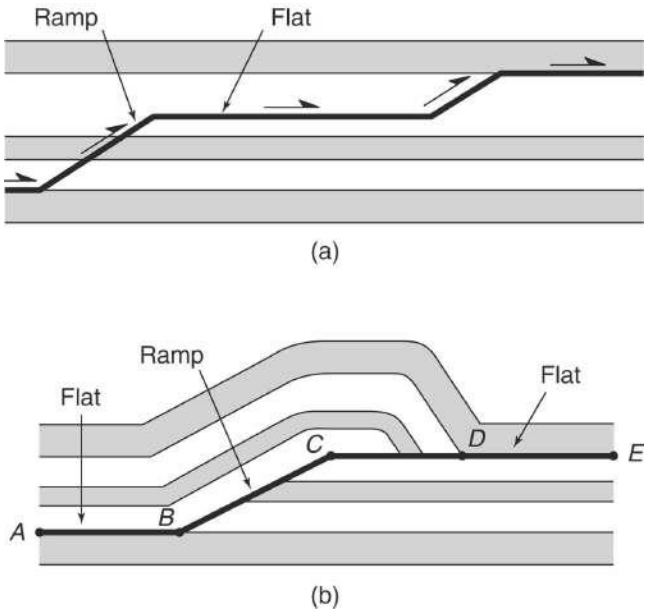

Fig.I.10: Schematic profile of a fault-bend fold formed in compression by two steps; (a) development of thrust in form of ramp and flat, (b) movement of layers from ramp to flat or visa versa (http://ic.ucsc.edu/~casey/eart150/Lectures/4ThrustFlts/4thrustfaults.htm).

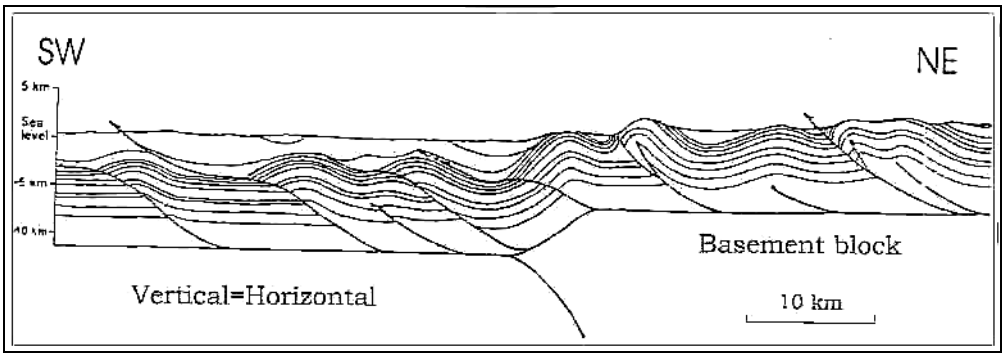

Fig.I.11. Part of a northeast-southeastern structural cross-section based on a seismic profile across 'Burujen' (51°12 =E -32°59 =N). After Payne (1990), Sattarzadeh et al. (2000).

Seismic sections have shown that many of the folds now visible at surface are linked to underlying blind thrusts (Fig.I.11). The growth of many of these fault-bend folds has been facilitated by the fact that they are near-surface structures with little or no overburden to inhibit their growth. Thus, many have the profile geometry of buckle folds formed near the

surface above a décollement horizon. However, these folds can often be easily distinguished from pure buckle folds by their aspect ratio. One of the most impressive is the Kabir Kuh anticline (Fig.I.12) which formed in the Lorestan folds zone and has a length of 200km (Sattarzadeh et al, 2000).

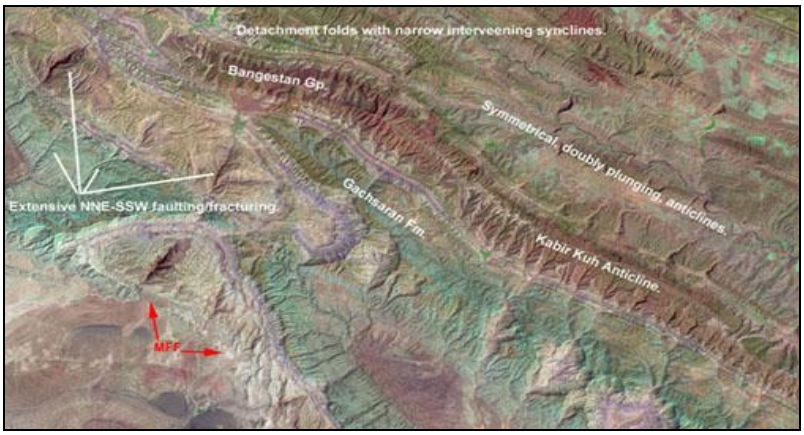

Fig.I.12: Satellite image of the Kabir-Kuh Anticline as an example of fault-bend fold regarding its aspect ratio. The axial length is about 200km (From NPA web-site).

I.2.1.1. Fault-propagation folds

Another group of folds associated with thrust faulting, are fault-propagation folds. In contrast with fold-bend folds in which thrust development predate folding, layers in advance of propagating fault tip are folded in a fault propagation fold (Fig.I.12). Through the constructed transects by the workers mentioned above, it is difficult to distinguish such a type of fold. Intermediate decollement levels with high competency contrasts with the surrounding series can influenced fold and fault geometry by favoring triangle shear zone and Fish tail structures (Harrison and Bally, 1988; Letouzey et al., 1995). These intermediate decollement series in the Central Zagros were discussed in detail by Sherkati et al. (2005). Furthermore, Sherkati and Letouzey (2004) stated that footwall synclines, high angle thrust faults, limb rotation and reduction in anticlinal wavelength during fold evolution are the specific characters of folds in the Central Zagros. Then they suggested that thses characteristics can be interpreted as a transition in deformation behavior from detachment folding to progressive fault propagation fold.

Fig.I.12: Fault-propagation fold ; layers in advance of propagating fault tip are folded.

I.2.2. Forced folding above oblique-slip faults

It is possible that the parent fault may be an oblique-slip fault, having components of both strike-slip and dip-slip motion. In such an example the resulting folds will possess two geometric characteristics which will declare their genetic link to the parent fault. These are the systematic offset of the adjacent folds and their high aspect ratio. An excellent example of such folding can be found in the southern part of the Zagros fold belt above the Minab basement fault (Sattarzadeh et al., 2000) (Fig.I.13). In addition to an important dextral component of movement, the fault also has a component of reverse dip slip motion, which has caused the eastern block to be thrust over the western block. The resulting fault scarp at the basement-cover contact has imposed a high aspect ratio on the resulting en echelon folds. In addition, continued movement along the fault has caused the folds to rotate clockwise and has produced a sigmoidal deflection of the fold axes.

One of the major differences in the geometry of forced folds and buckle folds is their aspect ratio; because the forcing members that generate the forced folds are generally from long linear steps (e.g. basement faults) in the basement. The resulting folds frequently have long aspect ratios and are frequently, although not always, asymmetric (Sattarzadeh et al., 2000).

I.3. Fold evolution from a detachment to a fault related (faulted detachment) fold

As it is shown in Fig.I.14, before propagation of a thrust within cover rocks we may have a decollement folding and then progressively the thrust propagate and finally a fold-thrust will shape. Passage from buckle fold to faulted detachment fold (Mitra, 2002) probably is a function of basal décollement thickness (Ramberg, 1970) ant its efficiency in addition to the anticlinal spacing. The path of fold development could be different in the case of involvement of intermediate décollement levels in folding and as a function of competency contrast between ductile units and competent rocks, at certain stage of fold growth, activation

of shearing in ductile units triggered new thrust faults in shallower décollement level (Sherkati et al., 2005).

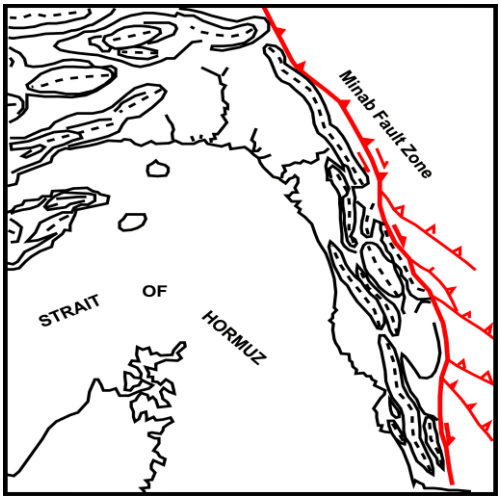

Fig.I.13. Folds and associated faults linked to the Minab fault zone adjacent to the Strait of Hormuz. The en echelon arrangement of the folds is the result of the component of strike-slip movement on the fault zone and their spatial organization indicates that the sense of movement is dextral. The long aspect ratio of the folds indicates that an important element of dip-slip movement occurred on the faults (after Y. Sattarzadeh et al.).

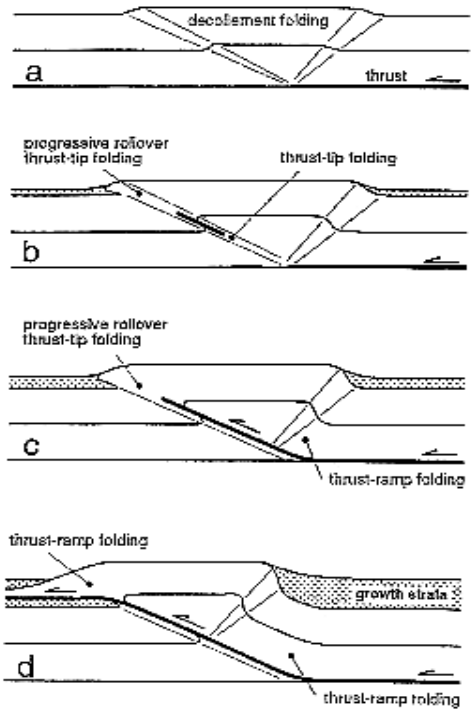

Fig.I.14. Conceptual model to show the evolutionary path observed during the growth of the experimental anticlines (Storti et al., 1997).

The fold maturity in he Fars area reaches by depletion of the ductile layers at the base of the synclines, causing local “touchdown” upon the basement which blocks the development

of the anticline and favors the progressive propagation of a fault through the forelimb (Molinaro et al., 2005).

Conclusion

Different mechanisms were engaged in folding and different fold type from detachment fold to forced fold could be distinguished in the Zagros folded belt although detachment folding seems to be in priority due to different mechanical behavior of basement, mobile, competent and incompetent groups in respond to folding of sediments. Especially where an underlain efficient decollement layer (e.g. Hormuz salt) is present. Fars and Lurestan areas in the Zagros are two regions in the Zagros where detachment folding style seems to be an outstanding fold geometry. In these regions, the mature stage in fold evolution achieve by lower decollement level depletion under the synclines and progressive propagation of a fault through the forelimb. In contrast, in the Izeh zone and the Dezful Embayment, forced folds appear to have a majority in the Central Zagros as the basal decollement level is presumably thin and weak. However, the first stage of folding in the Central Zagros may be started by detachment folding and then progressively evolve to a fault-propagation fold. Based on surface observations, folding intensity decreases from NE (high Zagros) with fault and ramp flat structures to SW (Zagros foredeep) with fault propagation and faulted detachment folds. The role of intermediate decollement levels is remarkable and affected the geometry and the wavelength of the folds in the Zagros area (Sherkati et al., 2004). However a detailed field survey is necessary to confirm it. Still more field studies and high quality seismic profiles need to determine the exact folding mechanism with emphasis on the kinematic evolution within different parts of the Zagros region.

CHAPTER II

Basic geometrical and mechanical elements of fractures and their relations with folds

Introduction

Before describing the characteristics of typical fractured structures in the Zagros area, it is worthy to have a review on basic geometrical and mechanical elements of the fractures (joints, faults,…) and define some terms in this domain. Both laboratory and nature occurrence of fractures were taken into account in this part. However, each one of these definitions may change according to their application in a specific case. First, the elementary mechanical aspects of the fractures are summarized, then some terms, which are generally used in fracture study, are defined and finally, the relation between fractures and folds will be discussed.

II.1. Stress

All of deformations are resulted from forces. In a homogenous media, a stress vector at a point on a surface element with normal n, is the limit of the ratio $\Delta F/\Delta A$ as ΔA, the surface element, tends to zero. ΔF is considered as a replaced single force acting at the center of ΔA (Fig.II.1a). In a body, the stress vector is generally oblique to ΔA; so the stress vector can be resolved into two components (Fig.II.1b): (1) σ_n, the normal stress directed along the normal to the surface, and (2) τ_n, the shearing stress directed along the line of intersection of the surface and the plane passing through $\mathbf{T}_n$ and **n**.

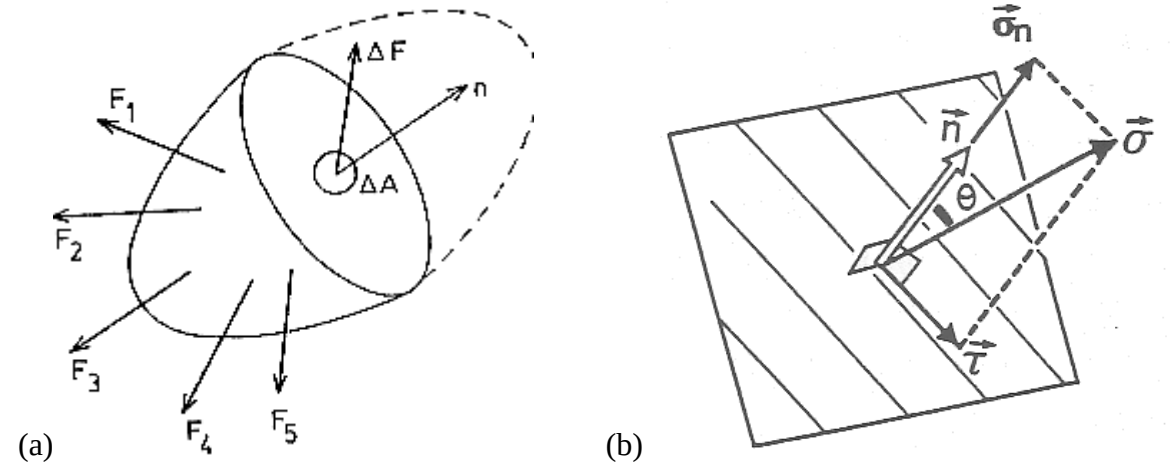

Fig.II.1: (a) Stress vector at a point on a surface element with normal **n**. The stress vector is the limit of the ration $\Delta F/\Delta A$ as ΔA, the surface element, tends to 0 (Ghosh, 1993). (b) Fault plane with its normal **n**. The stress, σ, combine from a normal, σn, and a shear stress, τ. θ is the angle between the vector σ and the normal to the fault plane.

To represent completely the state of stress at a given point, it is sufficient to give the stress vector on each of three mutually perpendicular planes. Consider a system of rectangular Cartesian axes, x, y and z with the origin at point O and with three surfaces perpendicular to the three axes. The stress vector on any one of these planes can be resolved into three components parallel to the coordinate axes, one normal and two shear ones. The state of stress at the point O can thus be completely represented by the elements of the following matrix:

$$\begin{bmatrix} \sigma_x & \tau_{xy} & \tau_{xz} \\ \tau_{yx} & \sigma_y & \tau_{yz} \\ \tau_{zx} & \tau_{zv} & \sigma_z \end{bmatrix} \qquad \text{(II.1)}$$

The matrix (II.1) may be called the stress matrix. The single subscript of the normal stress σ and the first subscript of the shear stress τ denote the direction of normal to the plane, while the second subscript of the shear stress denotes the direction of the stress component. The nine elements of the stress matrix are the components of a single entity, the stress at the point O. In fact, these nine elements are the components of a second order Cartesian tensor known as the stress tensor.

As the stress tensor, **T**, was defined it is easy to determine the applied stress vector σ applied on a plane in which the normal unity is the vector n:

$$\vec{\sigma} = \mathbf{T} \cdot \vec{n} \qquad \text{(II.2)}$$

The normal and shear stress vectors, σn and τ, are resulted as follow:

$$\vec{\sigma}_n = (\sigma \cdot \vec{n}) \qquad \text{(II.3)}$$

$$\vec{\tau} = \vec{\sigma} - \vec{\sigma}_n \qquad \text{(II.4)}$$

A normal stress is tensile if it tends to pull the material on one side of the plane from that on the other side. It is compressive if it tends to push the material from one side towards the other side.

There are three perpendicular planes, namely the principal planes of the stress, on which the shear component, τ, of the stress is null. On these 3 planes, the applied stress is equal to the normal stress σ_n. The intersections of these three planes define three perpendicular axes, namely principal stress axes. These three principal axes are the porters of the maximum intermediate, and minimum principal axes ($\sigma_1 \geq \sigma_2 \geq \sigma_3$). In the coordinate axes system of principal stress, the stress tensor is written as follow:

$$\begin{pmatrix} \sigma_1 & 0 & 0 \\ 0 & \sigma_2 & 0 \\ 0 & 0 & \sigma_3 \end{pmatrix}$$

The complete determination of the stress state in a point needs the knowledge of 6 parameters. Three parameters of these 6 parameters constitute the orientations of principal axes in the space and the 3 other parameters, define the magnitudes of the 3 principal stress.

- *Stress ellipsoid*

Stress ellipsoid in a point M is the geometrical place of the stress vector σ extremity applied in M. In other words, this ellipsoid correspond to the envelop of the stress vector extremities which applied on all the surfaces which pass from M. This ellipsoid comport, particularly, 3 orthogonal symmetrical axes which correspond o the three principal stress σ1, σ2 and σ3 (Fig.II.2). If the ellipsoid are identical in form and orientation in all the point of a considered volume, then the stress field in this volume is homogeneous or uniform. Otherwise, the stress field is heterogeneous.

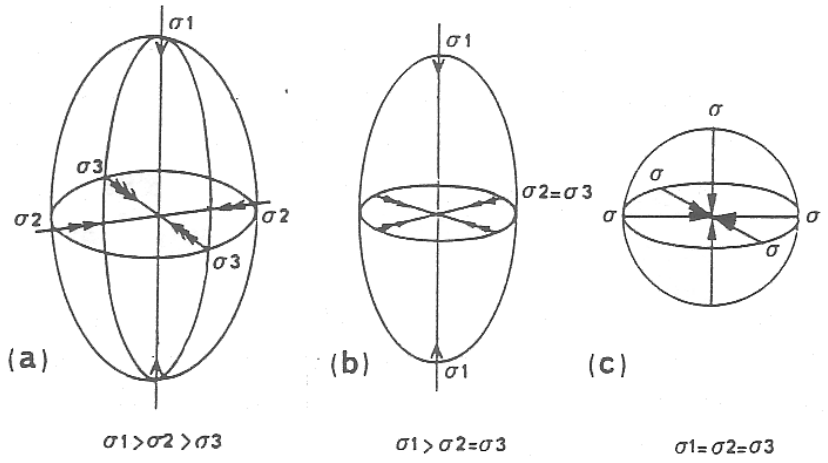

Fig.II.2: Representation of the stress state in term of stress ellipsoid. (a): triaxial; (b) monoaxial, here around σ1 axis (ϕ=0); (c): Hydrostatic (isotrop). After Mercier et Vergely (1992).

II.2. Fractures

II.2.A: Some terms and definitions

- *Fracture*: A fracture is a naturally occurring macroscopic surface discontinuity in rock due to deformation or physical diagenesis like dehydration (Nelson, 1985).

According to McQuillan (1973), fractures are considered to be the discontinuities which break rocks beds into blocks along cracks, fissures, joints or whatever they may called, and along which there is no displacement parallel with the planes of discontinuity. It is clear

that this definition could not be used for fault, which is another type of fracture in which, relative movement occurs either sides of fracture surface.

- *Shear Fractures:* Shear fractures have a sense of displacement parallel to the fracture plane. They form at some acute angle to the maximum compressive principal stress direction ($\sigma 1$) and at an obtuse angle to the minimum compressive stress direction ($\sigma 3$) within the rock sample (Fig.II.3A). Shear fractures form when all three principal stresses are compressive. The acute angle between shear fractures is called the conjugate angle and is dependent primarily on (Nelson, 1985):

- The mechanical properties of the material.
- The absolute magnitude of the minimum principal stress ($\sigma 3$)
- The magnitude of the intermediate principal stress ($\sigma 2$) relative to both the maximum ($\sigma 1$) and minimum ($\sigma 3$) principal stresses (as $\sigma 2$ approaches $\sigma 1$ the angle between $\sigma 1$ and the fracture plane decreases).

- ***Extension Fractures (Joints):*** Extension fractures have a sense of displacement perpendicular to and away from the fracture plane. They form parallel to $\sigma 1$ and $\sigma 2$ and perpendicular to $\sigma 3$ (Fig.II.3A). These fractures also form when all three principal stresses are compressive. The formation mechanisms of such a fracture still is not so clear.

- ***Fracture set and systems:*** A fracture set is a series of fractures characterized by a consistency of orientation of fracture plan attitudes over a given area. In most of the cases, two or more fracture sets make up the fracture system at a given outcrop (McQuillan, 1973).

There are other terminology based on fracture front propagation (lawn & Wilshaw, 1975), defined by three theoretical modes of fractures (Fig.II.3B):

Mode I (mode-one, opening mode): Stating that a fracture is a ***mode I*** fracture only implies that the walls moved perpendicularly away from the fracture plane when the fracture formed. So, we may suppose that stylolites be considered as anti-mode I as the walls of discontinuity moved perpendicularly towards each other.

Mode II (mode-two, sliding mode): It corresponds to a relative shearing on fracture surface in a direction perpendicular to fracture front.

Mode III (mode-three, tearing mode): It corresponds to a relative shearing parallel to fracture front.

All three modes can occur separately or in any combination. This nomenclature is purely descriptive, not genetic. For example, a mode I fracture can be formed by one or more mechanisms such as hydraulic fracturing, thermal contraction, and/or diagenetic shrinkage.
It was shown that in the brittle materials only mode (I) fracture could follows an unique plane with a directional stability (Lawn & Wilshaw, 1975). Also, from energetic point of view, it has been shown that the mode (I) fracture is created easier than the other modes (Evan, 1974).

II.2.B : Joints (Mode I fractures)

One of the most important groups of the fractures in petroleum industries, is joint. In a typical fractured reservoir, joints can severely affect the production scheme of the reservoir. Their effects could be both negative and positive. In both cases, finding their origin, spatial patterns, chronology, and other characteristics are important in economical point of view and sometimes are crucial in reservoir management. So, in this part, I tried to briefly review and discuss the mechanics and physical conditions of joint development in rocks.

A) 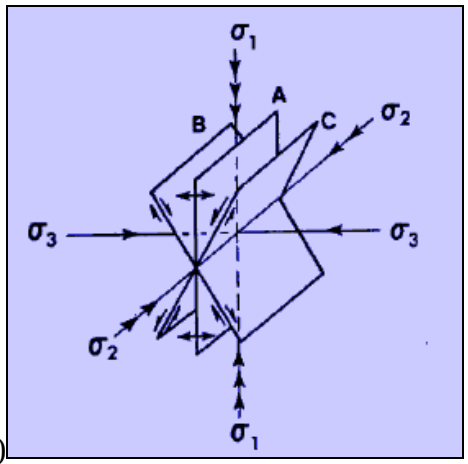

B) 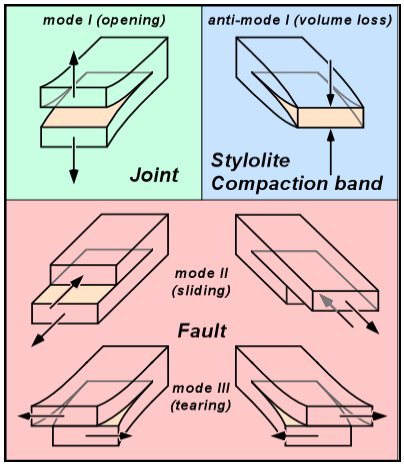

Fig.II.3: A) Potential fracture planes developed in laboratory compression tests. Extension fractures (a) and shear fractures (band c) are shown. B) Fracture mode terminology.

The mechanical origin of joints is still a controversial subject. However, most of the authors (Engelder, 1982, Bahat, 1991, Hancock et al., 1991…) believe that the joints are created in opening mode (Mode I). Joints are brittle fractures which may develop either by tensile failure or by shear failure (after Ghosh, 1993). Joints are defined as fracture surfaces along or across which the movement is negligibly small. This definition evidently depends on the scale of observation. A joint may not show a displacement in the mesoscopic scale, but may show evidence of displacement in the microscopic scale (Ghosh, 1993). A freshly exposed joint appears as a hairline crack. As weathering progresses, its opening may increase.

Some joints are filled with minerals. If the mineral fill is very thin (e.g. a few milimeters in thickness), it is still regarded as a joint when observed in the outcrop scale. However, when the same mineral fill is observed in a thin section, it is described as a vein. Joints form at different stages of the tectonic evolution of an area. They form in sediments which have not been lithified, they develop in buried rocks which are otherwise undeformed, they may form at different stages of formation of a system of folds, and a large number of joints form after the close of the tectonic cycle and during a slow uplift of the rocks. It is difficult, and often impossible, to distinguish among the different generations of joints when they occur together, and therefore it is often difficult to relate the joint pattern with the overall scheme of tectonic evolution of an area (Ghosh, 1993).

II.2.B.1. Some mechanical aspects of Joints

As it was mentioned, the joints are the fractures created in mode I, perpendicular to the minimum principal stress. Regarding the Mohr circle, this rupture could be formed in the point where Coulomb-Mohr curve intersects the abscissa axis when $\sigma 3eff = T0$. Based on the Griffith (1924) rupture criteria, only small circles can reach to this point of the curve. In other words, when $\sigma 1-\sigma 3 \leq 4To$ (Fig.II.4). For stronger differential stress, the fracture is shearing mode.

The Mohr-Coulomb curve of the rupture of a material is determined experimentally using uniaxial and triaxial tests. The value of $\sigma 3= To$ is defined using the direct extension tests or the Brazilian tests. The domain situated between T0 and the rupture threshold could not be determined experimentally (Fig.II.5). However, for some of the authors this part is the critical zone for joints and shear fractures development (Hancock, 1985; Bouroz, 1990).

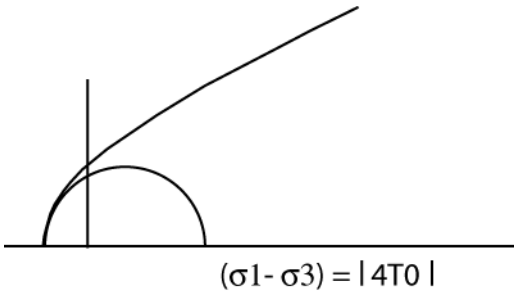

Fig.II.4: The biggest theoretical Mohr circle with $\sigma 3= To$ based on Griffith rupture criteria.

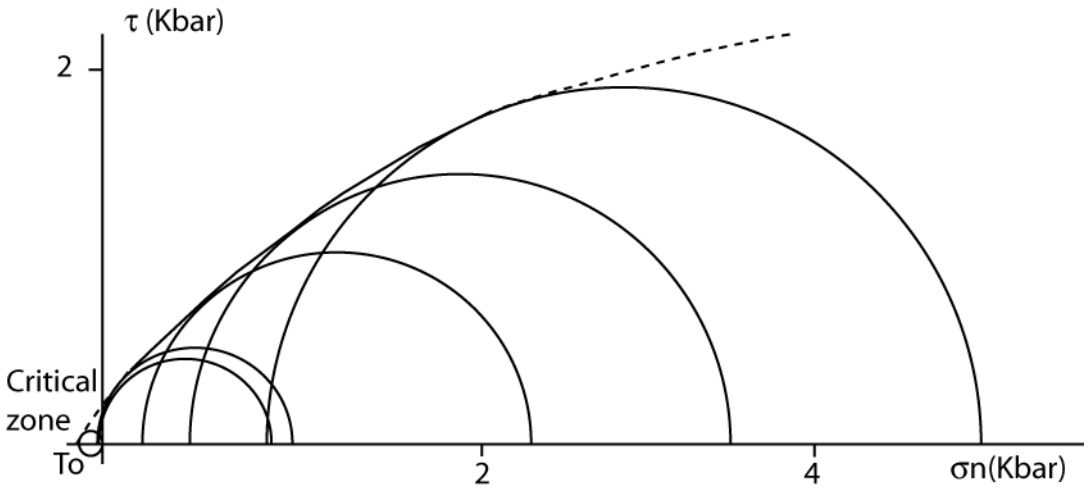

Fig.II.5: Experimental Mohr-Coulomb curve in the Villette limestone (Dogger, Briaçonnais). *To* has been determined in direct extension test. The rest of the curve is based on triaxial tests. The dashed parts of the curve have been extrapolated. Modified after Riffault (1969), Rives (1992).

In the experiences, which were done on rock plaques by Rives (1992), the fracture type depends on applied stress:

- If $\sigma 3eff = To$ (Fig.II.6A), then the rupture created in the form of one or more axial fractures parallel to the applied maximum principal stress.
- When the differential stress is large ($\sigma 1-\sigma 3 \geq 4\sqrt{2}To$, based on Griffith rupture criteria, Fig.II.6B), the rupture is done when Mohr circle tangent the Mohr-Coulomb curve and in the form of the conjugate fractures making an angle of 2θ between themselves. This shearing in early stage is done by en echelon cracks, making an angle of α with $\sigma 1$ then after the rupture of the bridges between the cracks in the materials, macroscopic fracture of the rock is formed.
- Within intermediate situation ($4To \leq \sigma 1-\sigma 3 \leq 4\sqrt{2}To$ based on Griffith rupture criteria, Fig.II.7C), the rupture should be done when Mohr circle tangent the Coulomb curve and in the form of the conjugate en echelon cracks, making a weak angle of 2θ between themselves (undetermined experimental domain). The created cracks should make a weak angle with $\sigma 1$ and they should be long and they lead to form a system of long conjugate fractures.

Some of the authors propose that the second group consist of shear joints (Hancock et al., 1987). However, this model could not be considered for all joints, as these conditions are quite restrictive to explain the joint ubiquity and lead us to consider the shear joints as a rare structure.

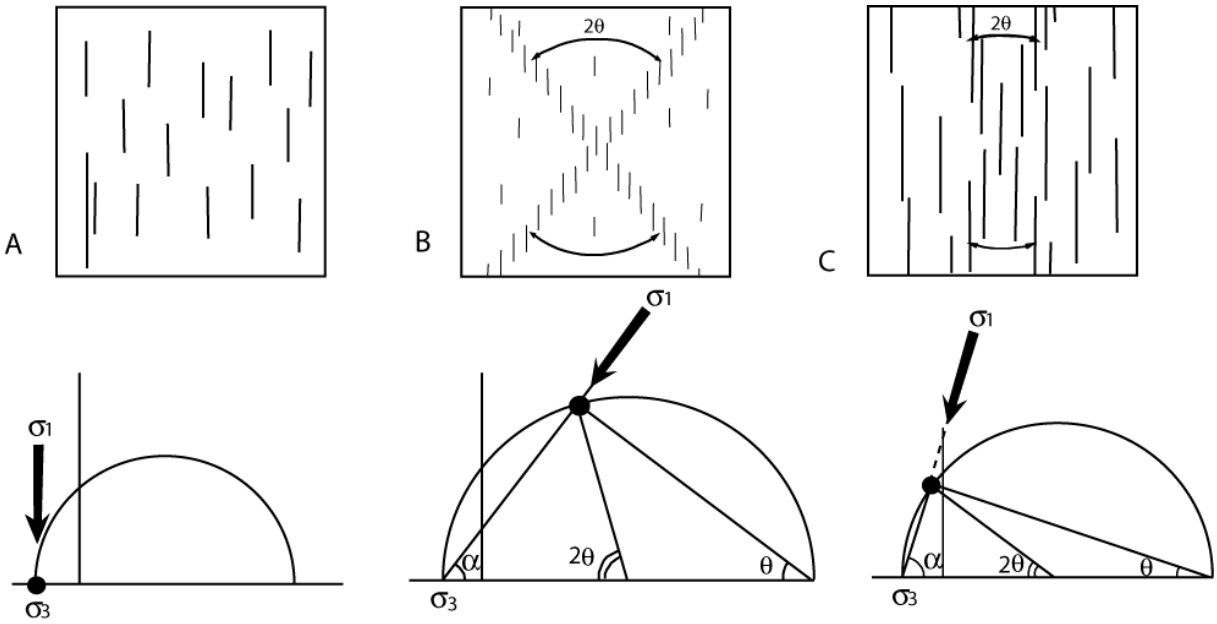

Fig.II.6: Different type of fractures in a rock plaque in the function of applied conditions. A) Axial fractures when σ3eff= T0. B) Conjugated shearing making a strong angle of 2θ with the applied maximum stress under the condition of σ1-σ3≥4√2To. C) Theoretical rupture under the condition of 4To≤σ1-σ3≤4√2To, conjugated shearing makes a weak angle of 2θ with the applied maximum stress and associated en echelon cracks (Rives, 1992).

Regardless of shear joint case in the classical analysis of rock mechanics, the rupture criterion for the joints is σ3eff= T0. To reach to this point on Mohr diagram, either the applied tectonic stress to boundaries should be a real extension, which does not seem to be realistic geologically or the other factors allow obtaining a negative minimum effective principal stress. On the other hand, differential stress (σ1-σ3) should be less than 4To. It means that the joints could be formed in a weak differential stress (at least in superficial part of earth crust) where the effective stress is not sufficient for brittle deformation or the folds (Rives, 1992).

Gramberg (1965) proposed ***dilatancy*** model, in which the joints form in a situation where the applied stress state is not sufficient to create macroscopic shear rupture. In this model, the micro-fissure or cracks form before macroscopic fractures. The domain of dilatancy has been shown in figure II.7 on τ /σ diagram. When a Mohr circle reach to this domain, the dilatancy starts and the rupture consists of micro-cracks in mode I, perpendicular to σ3 but the classical angular relation of Mohr theory could not be applied here. So, this domain should not be considered as Coulomb rupture curve. In the Gramberg (1965) hypothesis, the joints could formed in mode I without any necessary tangency between the Mohr circles and Coulomb curve in its intersection with abscissa axis. And also the minimum effective stress is not necessarily negative. However, because of the dilatancy fractures

morphologies in his experiences and discarding the effect of fluid in the fracturing, this theory was not quite accepted by geologists.

Using the Gramberg (1965) idea, Lorenz et al. (1991a) proposed that the dilatancy in a rock where the pore pressure is close to the minimum principal stress (but less than it) could lead to the formation of a joint family. The fracture propagation would be sub-critical (slow) and is controlled by tectonic stress increase. In this case the rupture criterion is not $\sigma 3eff = To$ any more, but corresponds to a differential stress, for which we can reach to the dilatancy domain.

So, using the model of dilatancy, it is easier to explain the joint ubiquity. In fact, the biaxial condition with a notable difference between the principal minimum and maximum stresses in the earth crust and is easier to realize than the condition, where $\sigma 1-\sigma 3 \leq 4To$ and $\sigma 3eff = To$.

In the nature there are two kinds of structures, which are created in Mode I: the *joints* and *tension cracks*. We can propose that the difference between these two structures is a criterion of different rupture. The joints correspond to a dilatancy phenomena in a big scale and tension cracks are formed when $\sigma 3eff = To$ (Rives, 1992).

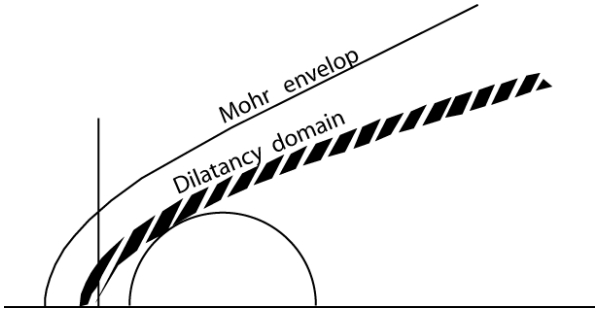

Fig.II.7: Mohr envelope and dilatancy rupture domain (supposed domain). Note that the rupture by dilatancy in Mode (I) happens in situations where the minimum principal stress is positive.

II.2.B.2. Joint surface morphology

The fractographical features (Plumoses structures) (Fig.II.8) on joint surfaces are generally observed in fine grain rocks. Experimentally, it was shown that these kinds of features are the characteristics of joint propagation in mode I. Furthermore, the preservation of such delicate structures indicates the absence of friction on fracture plane. Otherwise, it will be damaged or superimposed by sliding traces. However, the absence of such a fractographic feature on a joint does not mean necessarily that it has been created by other mechanisms. As noted by Pollard and Aydin (1988) and by Engelder et al. (1993), among others, the surface morphology of mode-I joints is unambiguously the result of separation of the joint walls perpendicular to the fracture. Previous notions that a high rate of joint

propagation (Roberts, 1961) or shearing of the fracture surface (e.g., Bucher, 1920, 1921; Parker, 1942; Hoppin, 1961) created plumose structure cannot be supported in the face of overwhelming observational and experimental evidence, as well as theoretical arguments, that convincingly demonstrate an opening-mode origin (e.g., Kulander and Dean, 1985).

Plumose structure refers to the chevronlike structure on some joint surfaces, with a collection of ***initiation point, axis and hackles.*** *Hackle Marks* are curvilinear boundaries with differential relief between adjacent surfaces. Hackles either radiate from the initiation point or fan away from a curvilinear axis.

Rib marks (or arrest lines) are also known as conchoidal structures. They are curvilinear ridges or furrows oriented at right angles to hackles and plume axes. In a profile that is parallel to hackle, rib marks express themselves as curves and kinks. They may be rounded or have sharp edge in profile.

A) 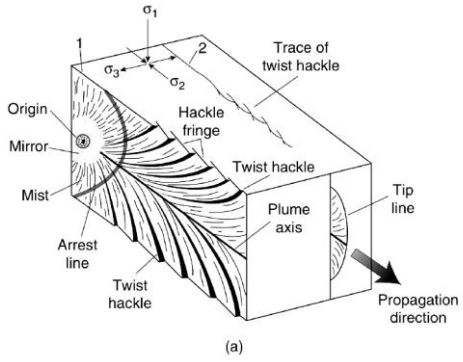

B) 

Fig.II.8: Plumose structure description on a joint surface. (B) : Joint surface in Asmari limestone with plumose structure.

II.2.B.3. Joint continuity and propagation

One of the other characteristics of joints is their continuity. In brittle materials, it was shown that only mode I fracture can follow a unique plane with directional stability (continuity) (Lawn & Wilshaw, 1975). Laboratory tests (Petit & Barquins, 1988) have shown that the joints propagate parallel to maximum principal stress σ_1 and perpendicular to minimum principal stress σ_3. Any obliquity in principal stress direction changes the fracture propagation scheme to shear mode (Fig.II.9). For a given stress state, there is only one plane perpendicular to σ_3 so two non-parallel joints could not be strictly contemporary.

In the rocks, the presence of friction trace (showing a quite weak displacement of fracture walls) on fracture surfaces does not mean necessarily a shear origin for them but mostly it means they are originally opening mode fractures which reactivated within a shearing stress.

However sometimes there are some fracture families and often conjugate which seem like joint families. Based on studies on these kinds of fractures (Petit & Barkins, 1988) and laboratory experiences (Rives, 1992), we can define conditions under which, an oblique fracture (relative to stress direction) can propagate along its direction. the conclusions are as follows (Rives, 1992):

- If lateral stress is strong, we will have a shear fracture (fault) with a considerable displacement.
- In most of the rocks, if lateral stress is weak or zero, the propagation of oblique fracture is done by branched fractures in the extremities of the fracture and by some en echelon fractures along its continuation (Fig.II.9).
- In a very porous rock, if lateral stress is weak or zero, an oblique fracture propagate along its surface by a quite fine shear band with a weak displacement. These particular types of fractures are quite frequent in almost all the quite porous rocks or little consolidated.

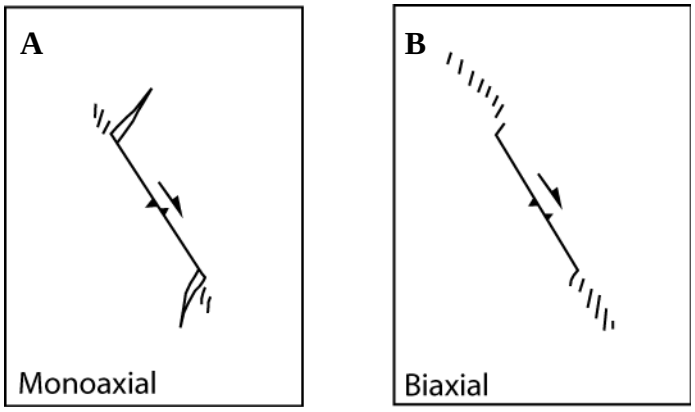

Fig.II.9: Experimental rupture pattern in plaques containing an oblique fracture in mode I. A: In monoaxial loading, the propagation of a branched fissure and a few en echelon cracks during the main fracture prolongation is seen. B: In biaxial loading, the development of en echelon open fractures during the prolongation of main fracture is seen. They normally form even before the shear propagation of the main fracture by rupture of the bridges between echelon cracks (after Petit & Barquins 1988).

II.2.B.4. General condition for joint creation

One of the well known model which was proposed by Price (1959) and then was completed by the others especially Voight & St. Pierre (1974) and Engelder (1985) is the traction development in a sedimentary basin during the uplift and after diagenesis process at subsurface (Loading, Diagenesis, Denudation = L.D.D. cycle). During diagenesis, the elastic properties of the materials change (Young Module, E, increased and Poisson coefficient, ν, decrease). So, the evolution of minimum horizontal stress (σh) curve has not the same path

during loading and uplift, relative to depth (Fig.II.10). In this model, tectonic stress is absent and ***unloading joints*** could be created in this way (Engelder, 1985).

The other type of joints, which was introduced by Engelder (1985), is called ***relaxation joints***. When the rocks are in depth they could be under compression. So, they can save part of this stress by their fabric, which is called residual tectonic stress. After uplift, when they are near the surface, the rock relaxation will lead to the creation of joint series perpendicular to the previous compression direction, afforded by rock. The joint direction in this case is controlled by rock fabric and not by the stress field at the time of relaxation.

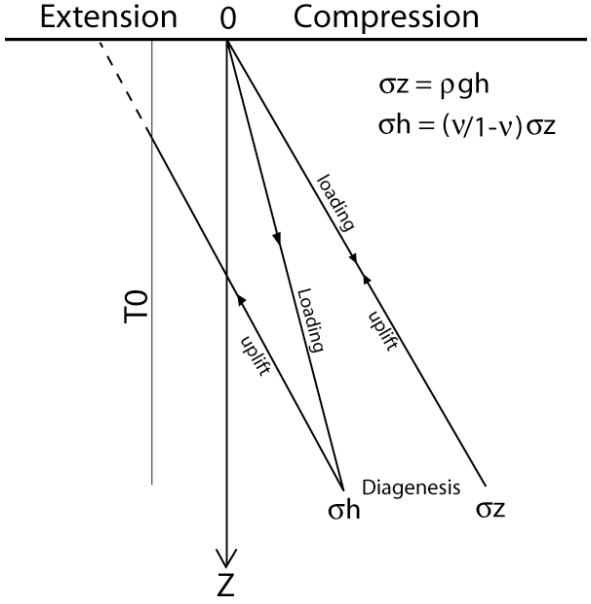

Fig.II.10: Stresses evolution in sediments as a function of depth during L.D.D. cycle in an elastic model without any tectonic stress. The rocks buried and then diagenesis process at depth change the elastic properties of the materials. Then they move towards surface during uplift. During uplift and erosion, the horizontal stresses cross extensional domain of stress and could pass beyond the rupture threshold of the rock (To). (Rives, 1992).

Regarding Mohr diagram and based on Griffith theory, opening mode fracture (mode I), is formed when differential stress is quite small ($\sigma1 - \sigma3 \leq 4To$), where To is rupture threshold of the rock in extension, where Mohr-coulomb curve cross the abscissa ($\sigma3 = To<0$). Engelder, (1985) proposed that the effective stresses during L.D.D. cycle could lead to the formation of joints when the minimum effective stress become equal to the rupture threshold of the rock. So, based on this model, the rocks should be either near the earth surface, in a real extension state or there is/are other factor(s) to establish these condition of effective stresses. One of the main agents helping to reach to this condition without any tectonic stress, is an abnormal fluid pressure, which is more than minimum principal stress. This pore pressure is more than hydrostatic pressure and could be developed when the porous media become impermeable. In this condition, the fluid trapped and its circulation reduced.

Regarding the Mohr criteria and regardless of lithostatic stress in depth, three kinds of stress evolutions lead to rupture, an increase in maximum principal stress (σ1), a reduction in the minimum principal stress (σ3) with Pf = constant or an increase in the pore pressure with the constant stress boundary limits. Based on Secor (1965), the ***hydraulic joints*** are developed within this later criterion (Fig.II.11).

Tectonic joints are another group which could be created during pore pressure increase resulted from tectonic stress (Engelder, 1985). So, these kinds of joints could be developed in shallower part of the earth crust compare to hydraulic joints.

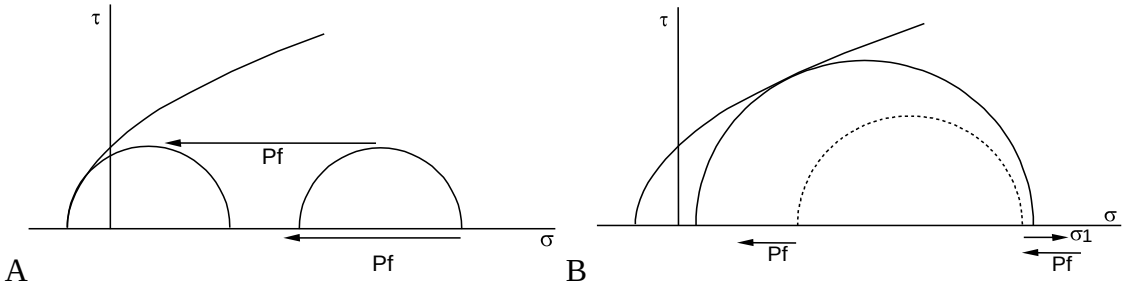

Fig.II.11: (A) The effect of fluid pressure in Mohr diagram. The deviatoric (differential) stress is not modified but the circle is shifted towards the Mohr-Coulomb curve (After Secor, 1965). (B) Mohr circle evolution towards the formation of tectonic joints by the increase of maximum principal stress and the fluid pressure Pf and enlarging the Mohr circle and its displacement towards Mohr-Coulomb curve (Engelder, 1985; Rives, 1992).

Some authors treat the joints like other structures in brittle tectonics using Mohr circle (Holst, 1982; Hancock, 1985; Suppe, 1985). These joints develop in opening mode, perpendicular to σ3 and when σ1-σ3 ≤ 4To and σ3eff = T0. In this case and in the presence of tectonic stress and/or abnormal pore pressure, the joints propagate independently of their evolution in L.D.D. cycle in the platforms or foothill regions (Rives, 1992). Hancock (1985) coated that shear joints develop making an angle of 30°(θ) with σ1 and when σ1-σ3 >8To and hybrid joints in an intermediate situation (Fig.II.12).

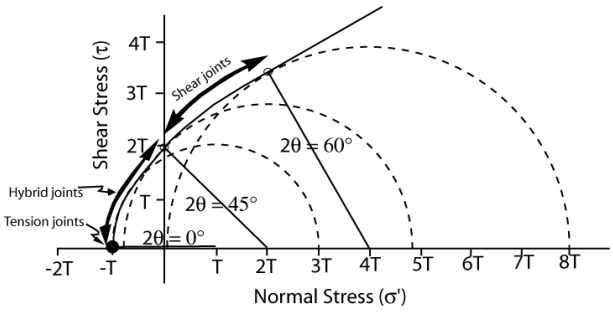

Fig.II.12: Different types of joints and Mohr circles based on Hancock (1985).

II.2.B.5. Joint sequence and chronology

Determining joint chronology and sequence is a task which should be done precisely in the field. However it is not always simple to find the sequential evidence of the fractures on the outcrops. This matter will be more important when specific joint(s) show no symmetrical relationship with the fold. he order of formation of neighbouring joints can be determined from three relationships. Based on Dunne and Hancock (1994), the order of formation of neighbouring joints can be determined from three relationships: (1) Where a joint is offset across a fault, vein or stylolites, the joint is the older structure (Fig.II.13a). (2) The trace of a younger joint segment abuts that of an older joint (Fig.II.13b). This relationship arises when a joint propagating through intact rock intersects an unsealed crack and is unable to jump the gap. (3) Where the short traces of small seal joints terminating in intact rock are cut by the long trace of a large joint, the shorter joints are the older joints (Fig.III13c). Where two joint traces cross each other, their relative ages cannot be determined because one of them must have been sealed when the other propagated across it (Fig.II.13d).

Although the relative ages of neighbouring joints can be determined easily, absolute ages are difficult to acquire. Letouzey and Trémolières' (1980) method of dating assemblages of small faults, veins and stylolites by relating directions of shortening inferred from them to a well-dated stratigraphic sequence can, in principal, also be applied to populations of joints. However, because younger joint sets are not everywhere superimposed on older sets (Hancock et al., 1991) the principal must be applied cautiously. Where a joint set is subject to later superimposed shear, faulted joints can result or distinctive patterns of en echelon cracks, horsetail fractures and kinked joint ends develop (Cruikshank et al., 1991).

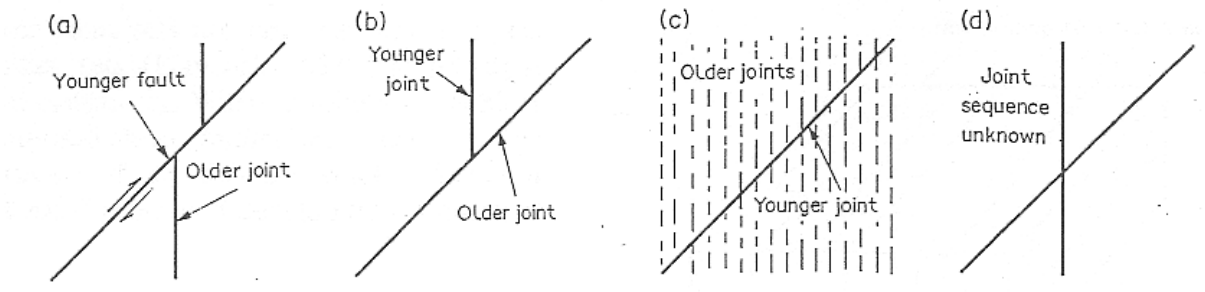

Fig.II.13: (a) an older joint trace offset by a younger fault. (b) A younger joint trace abutting an older joint trace. (c) Short traces of older sealed joints cut by the long trace of a younger joint. (d) Crossing traces of joints, the order of formation of which is not determinable.

II.2.C. Faults (Mode II & III)

Another group of the fractures which was taken into account limitedly in the fracture study of the Asmari Formation are faults. In this section we are not going to enter in detailed

into faulting in large scale and different crustal stress regime. The readers may refer to any text book in structural geology. As fault-slip data constitute part of our field data set, small-scale faults with small displacements and traces of movements (tectoglyphes) are the main part in the vast domain of fault study which is going to be considered. The main topics that we discuss briefly in this part are: the mechanical aspects of faulting, criteria for the sense of movement in fault analysis, and paleostress reconstruction based on fault-slip data analysis.

II.2.C.1. Mechanical aspects of faulting

- *Neo-formed and inherited faults*

In the case of natural deformations and faulting, we may encounter with two types of faulting: (1) neo-rupture in which we consider that the faults form under the applied stress to the rock (they are comparable to the experimental fracturing in rock mechanics). (2) the reactivation of pre-existing fracture planes; in this case the fault planes correspond to the pre-existing discontinuities on which slipping happen under applied stress field.

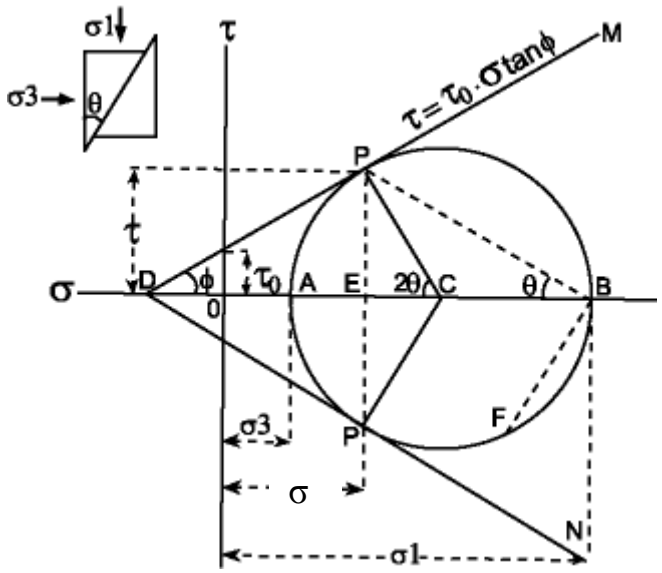

Fig.II.13: Mohr diagram of stress at shear failure (after Ghosh, 1993).

- *Criteria of brittle failure*

It is generally assumed that a fault develops when the shear stress acting along a plane is large enough to overcome the cohesive strength as well as the frictional resistance to movement along the fracture plane. A first approximation to the stress condition during the initiation of shear fracture was proposed by the French physicist Coulomb. He proposed the following criterion of shear failure:

$$|\tau| = \tau_0 + \sigma \tan\varphi \qquad \text{(II.5)}$$

where τ is the shear stress along the fracture plane, σ is the normal stress across the plane, $\tan\varphi$ ($= \mu_i$) is the coefficient of internal friction and τ_0 is the cohesive strength of the material. The significance of this equation can be understood from a Mohr diagram (Fig.II.13).

On a σ-τ diagram, DM and DN are the two straight lines represented by equation (II.5). The lines are at angles of $\pm\,\varphi$ with the σ-axis and intersect the τ-axis at $\pm\tau_0$. A point on either of these lines specifies the stress condition at which failure should occur. For example, P is one such point on DM in Fig.II.13. The Mohr circle for the condition of failure must have its centre C on the σ-axis and must touch the line DM at point P. If the normal to the fracture plane makes an angle θ with the σ_1-axis, then in the Mohr diagram the angle ACP = 2θ and the angle ABP = θ. BF, the perpendicular to BP, is parallel to the fracture plane. The normal and shear stresses, σ and τ, on the plane are given, respectively, by OE and PE, where PE is perpendicular to the σ-axis. From the triangle DCP, we find that

$$2\theta = 90° - \varphi,$$

or

$$\theta = 45° - \varphi/2 \qquad \text{(II.6)}$$

φ is known as the angle of internal friction. It should be noted that θ is the angle between the σ_1-axis and the normal to the shear fracture. Therefore the fracture surface itself makes an angle of θ with the σ_1-axis, the direction of maximum compressive stress. For non-zero φ, i.e. for cohesive materials, $\theta < 45°$. According to Coulomb criterion, two sets of shear fractures should form with an angle 2θ between them.; this angle is bisected by the direction of maximum compressive stress. Coulomb's criterion suggests that the initiation of shear fractures depends on two properties of the material, τ_0, the cohesive strength, and μ_i ($= \tan\varphi$), the coefficient of internal friction. For a particular combination of τ_0 and μ_I, we get according to the equation (II.5) two straight lines DM and DN on the σ-τ diagram. The angles between the two lines opens up towards the positive sides of the σ-axis, since according to our convention, compressive stress is taken as positive. Regarding the initiation of the fracture, the region between the two lines is stable and the region outside these lines is unstable and the shear fractures initiate when the Mohr circle touches these lines which form the border between the stable and unstable regions. Although the Coulomb criterion is not fully

satisfactory, it is in agreement with experimental data of brittle deformation of several rock types at moderate confining pressure (Handin & Kager, 1957, Handin, 1969).

The lines DM and DN from a Mohr envelope which separates fields of stable and unstable stresses. Mohr suggested that τ and σ may not have a linear relation. He suggested that the envelope represented by the general equation $\tau = f(\sigma)$ is curved and is different for different materials. This suggestion is in agreement with triaxial compression tests of brittle failure of rocks.

The strength of an ideal brittle solid is about one-tenth the Young's modulus (see Price, 1966, p.29). However the observed tensile strengths of materials are much less than this theoretical value. This led Griffith to suggest that most materials have fine flaws in the form of cracks; at a critical stress the cracks propagate and cause brittle failure. A confirmatory evidence of Griffith's theory is found from the fact that specially prepared flaw-free fibres have a tensile strength much closer to the theoretical strength. A simplified description of Griffith's theory (Griffith, 1920) is given by Odé (1960). From this analysis we find that, at the moment of rupture, the normal and shear stresses are related by the equation

$$\tau^2 = 4T_0^2 - 4T_0\sigma \qquad \text{(II.7)}$$

where T_0 is the uniaxial tensile strength. This is the equation of the Mohr envelop as predicted by Griffith's theory.

The equation (II.7) may written as

$$\tau^2 = 4T_0(\sigma - T_0), \text{ or}$$

$$Y^2 = -4\,T_0X, \qquad \text{where } Y = \tau,\ X = \sigma - T_0$$

This is the standard equation of a parabola in which the focus is to the right of the directrix (Fig.II.14). Although the parabolic form of the Mohr envelope agrees with some experimental data, there is often some discrepancy for fractures caused by compression. It has been argued that in the compressive stress field the Griffith cracks will tend to close. Using this concept, McClintock and Walsh (1962) have proposed a modified Griffith theory according to which τ and σ are linearly related:

$$|\tau| = 2T_0 + \mu_s\sigma, \qquad \text{(II.8)}$$

where μ_s is the coefficient of sliding friction. This eqution is similar to the Coulomb criterion if we replace $\tau 0$ by $2T_0$ and the coefficient of internal friction μ_i by the coefficient of sliding friction μ_s. This modified Griffith theory agrees fairly well with the experimental data for fractures in the compressive stress field.

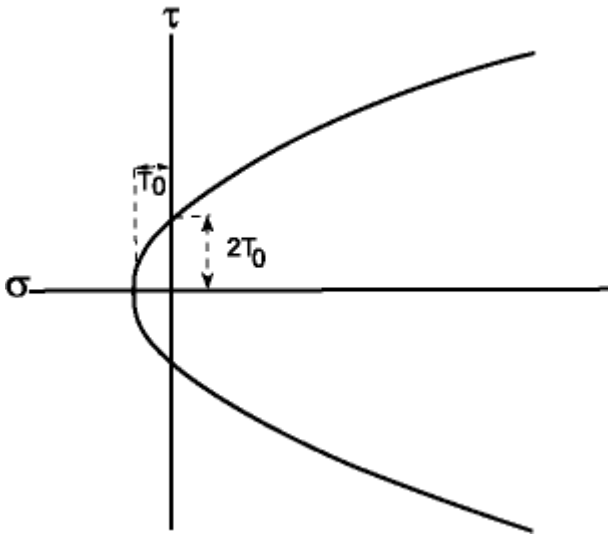

Fig.II.14: Parabolic form of Mohr envelope (after Ghosh, 1993).

II.2.C.2. Criteria for the sense of movement on fault surfaces

The determination of direction and sense of fault movement is a basic requirement in fault-slip data analysis. For detailed information in this regard, readers can refer to Petit (1987) and Mercier and Vergely (1992). Here, the cases which frequently observe in the Asmari Formation are discussed.

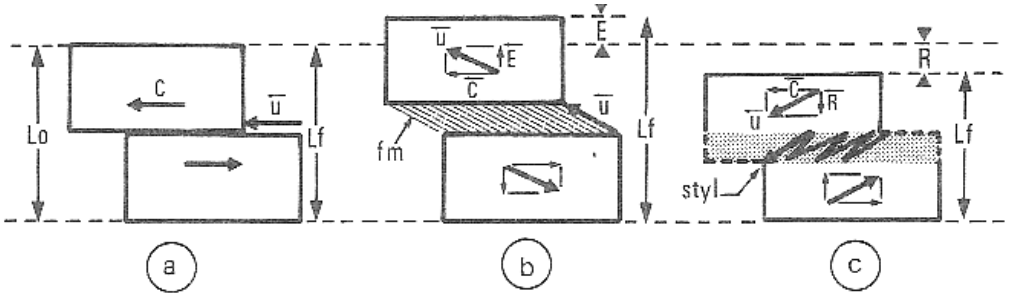

Fig.II.15: Displacement scheme of two separated blocs by a fault plane: (a) simple slide, (b) sliding with opening (E), (c) sliding with pressing (R). Lo: Initial thickness, Lf: final thickness. (after Mercier and Vergely, 1992).

In a fault, based on the movements of fault blocs, we may observe a simple sliding, sliding + opening, or sliding + pressing (Fig.II.15). The simple sliding (Fig.II.15a) is a displacement, **u**, parallel to the fault plane. It bears a friction of the blocs following by the abrasion of contact surfaces. Usually striations due to a ploughing element (Fig.II.16a) is generally seen in this case. This striation occurs from an element (a rock or gouge fragment or mineral grain) which is obviously harder than the wall it striates, although it may be of the same material. During friction it forms deep striae (grooves) terminated at the final ploughing element position. The end of the plough mark points towards the movement of the missing

wall (Dzulinski and Kotlarcyzk, 1965; Tjia, 1971; Hancock, 1985; Petit, 1987). This clear type of striation is mainly present in limestone (Petit, 1987).

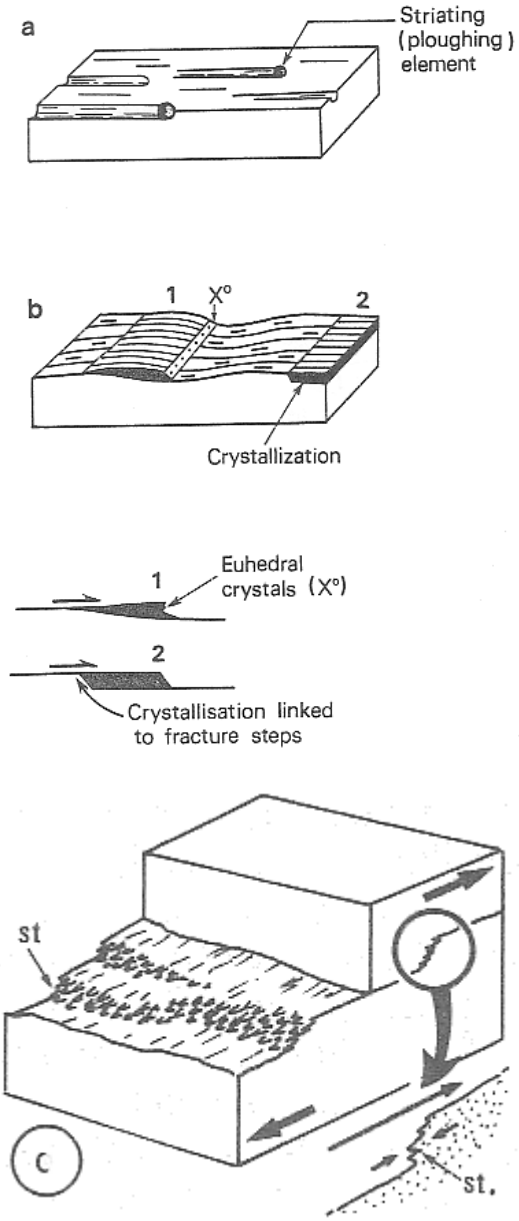

Fig.II.16: Principal marks of the movement (tectoglyphes) on the fault planes, (a) striation due to ploughing element; (b): crystallization on the lee side of asperities (see text for details) (Petit, 1987); (c) dissolution steps by compression (after Mercier and Vergely, 1992).

In sliding + opening (Fig.II.15.b), the crystallization of usually fibrous minerals may give directly the direction of displacement, **u**, which includes two movement components, parallel and perpendicular to the fault plane. Irregularities on the fault surface also exhibit lcal crystallization of fibrous minerals (e.g. calcite in limestone). They appear as a set of steps (accretion steps) whose risers are more or less perpendicular to the general striation and face in the same direction. These accretion steps are congruous (i.e. risers facing towards the

movement of the missing block) where euhedral crystal faces are observed on the risers (Petit, 1987) (Fig.II.16b2). This feature is also very common in limestone and sometimes associated with stylolites (Arthaud and Mattauer, 1969, Petit, 1987).

In the case of sliding + pressing (Fig.II.15c), like the previous case the direction of displacement, **u**, includes two movement components, parallel and perpendicular to the fault plane. The movement could be interpreted based on the localization of pressure-solution on contact surfaces. The indicator marks are in form of stylolitic striations (Fig.16.c). The obliquity of the stylolitic peaks indicates the direction of the displacement, **u**, of the blocs from which the shear and normal components of the movements on the fault plane could be deducted. The stylolitic striations and the crystallized fibrous minerals are resulted from slow displacements (0.1-10cm/yr), and probably aseismic, which are controlled by the dissolution-crystallization phenomena.

II.2.C.3. Fault-slip analysis and paleostress reconstruction

Fault-slip data including fault plane orientations and rake of slip trace on these planes (slickenside) are used to derive the local stress state. Following this hypothesis that the slickenside represents shear stress applied on the fault plane (Anderson, 1951; Walace, 1951); Bott (1959) showed that the orientation of this slickenside depends on 3 parameters of the orientations of stress trihedral which are shown by the function of Euler angles (Ψ, θ and φ) and the ratio of differential stress magnitude (R or ϕ). Wallace (1951) and Bott (1959) proposed that fault orientations may be arbitrary (as for inherited faults), but each slip (indicate by striae) has the direction and the sense of the shear stress that corresponds to a single common stress tensor.

There are different numerical methods using the stress tensor analysis and inversion proposed by different authors (e.g. Angelier et al, 1982; Angelier and Gaugle, 1979, Angelier,1984, 1990; Etchcopar, 1980; Armijo et al. 1982; Guiraud et al. 1989) to find the principal stress tensor directions. However, these methods are especially useful when we deal with many fault planes data. Also these methods work quite well when we have a simple mono-phase tectonic event. In the case of poly-phased tectonic evolution, the differentiation of several stress tensors engaged of deformation still is not so simple. Specially when we deal with a inhomogeneous medium displaying reactivated (inherited) discontinuities (Bedding planes, stylolites, fractures,..) and new formed faults.

- *Theory and principle of the fault-slip data inversion*

Stress conditions during brittle faulting can be approximated by inversion of fault-slip data (e.g. Angelier, 1984, 1990; Etchecopar et al., 1981; Reches, 1987). The geometry of potential faults during faulting is controlled by three factors: (1) the configuration of the stress tensor (orientation and relative magnitude of the principal stresses), (2) the yield characteristics of the rock mass, and (3) the orientations and properties of any discontinuities in the rock mass (Bott, 1959; Byerlee, 1968; Sibson, 1989).

The direction of slip along a discontinuity is a function of the tensor configuration (Bott, 1959). There are four key variables for slip on a frictionless surface: the orientation of principal stress axes, $\sigma1$, $\sigma2$, $\sigma3$, and the shape of stress ellipsoid, ϕ [where $\phi = (\sigma2 - \sigma3)/(\sigma1 - \sigma3)$]. Slickenlines measured on surfaces in the field are assumed to be parallel with the maximum resolved shear stress vector (τmax) on the surface. Analysis of critical stress state capable to overcome the shear strength on a pre-existing fault has been described by many authors (Bott, 1959; Jaeger and Cook, 1979; Sibson, 1974, 1985; Ranalli and Yin, 1990; Yin and Ranalli, 1992). These works suggest that the most important factors are the fault plane orientation relative to the orientation of the stress axes, and the type of the stress regime (extensional, strike-slip or compressional). It is generally admitted that before the creation of new faults, an ancient fault can be reactivated when its orientation with respect to tectonic stresses is favorable and when the total resistance on the fault is less than the resistance to failure of the intact material. However, the two mechanisms, new failure in the intact rock mass or reactivation of an ancient fault, may operate at the same time. This will essentially depend on the difference between the total resistance to failure of the intact rock mass and the resistance to failure along the pre-existing fault surface (Sassi et al., 1993).

Necessary conditions for obtaining quantitative information about the stress tensor using striation data have been given by many authors (e.g. Arthaud, 1969; Carey, 1976; Angelier, 1990, Lacobme et al., 2006). Fault slip inversion method assumes that (1) the analyzed body of rock is physically homogeneous and isotropic and if prefractured, is also mechanically isotropic, i.e., the orientation of fault planes is random, (2) the rock behaves as a rheologically linear material [Twiss and Unruh, 1998], and (3) displacements on the fault planes are small with respect to their lengths and there is no ductile deformation of the material and thus no rotation of fault planes. Moreover, the computation assumes that (4) a tectonic event is characterized by a single homogeneous stress tensor, (5) the slip responsible for the striation occurs on each fault plane in the direction and the sense of the maximum resolved shear stress on each fault plane (Wallace-Bott principle), the fault plane being the

preexisting fracture, and (6) the slip on each of the fault planes is independent of each other (Lacombe et al., 2006).

Using these assumptions, the stress state which is responsible for the observed displacement is characterized, in the referential frame of its principal directions, by a diagonal tensor:

$$\mathbf{T} = \begin{bmatrix} \sigma_1 & 0 & 0 \\ 0 & \sigma_2 & 0 \\ 0 & 0 & \sigma_3 \end{bmatrix}$$

When $\sigma_1 \geq \sigma_2 \geq \sigma_3$.

Two other variables must be considered because data are collected from natural surfaces: cohesion (C) and coefficient of friction (μ).These usually are related by the Mohr-Coloumb yield equation: $\tau \geq C + \mu\, \sigma_n$ (σ_n is the resolved component of stress normal to the fault plane). Coulomb behavior is exhibited at intermediate confining pressure by many rocks (Guiraud et al., 1989). In the situation of many minor slickensides, slip occurs along pre-existing discontinuities so that C and μ pertain to properties of the discontinuity, not the rock mass. The intensity and orientation of maximum shearing stress is governed by the relative values of σ_1, σ_2 and σ_3. Thus, even if σ_3 represents compression, if it is algebraically less than $\sigma_1$and σ_2, the effect on shearing stress would be the same as if it were an axis of tension (Wallace, 1951).

Based on Angelier (1990), the actual stress tensor has six degrees of freedom. The data are directions and senses of slip on fault plane whose orientation is known. Neither adding an isotropic stress or multiplying the tensor by a positive constant can modify the direction and the sense of slip on any fault. As a consequence, the actual tensor being $\mathbf{T}^*$, any tensor $\mathbf{T}$ equally solves the problem:

$$\mathbf{T} = t_1\mathbf{T}^* + t_2\mathbf{I} \qquad \text{(II.9)}$$

Where t_1 and t_2 designate any constants (t_1 positive) and $\mathbf{I}$ the unit matrix. The values of t_1 and t_2 can be determined provided that one adds rock mechanic parameters to data sets and adopts rupture-friction laws. The tensor $\mathbf{T}$ has four degrees of freedom so that one may adopt a particular form, which is called the 'reduced stress tensor' (Angelier et al., 1982). All tensor $\mathbf{T}$ obtained using equation (II.9) have the same directions of principal stress and the same 'shape ratio' Φ:

$$\Phi = (\sigma_2-\sigma_3) / (\sigma_1-\sigma_3) \qquad \text{(II.10)}$$

where σ_1, σ_2, σ_3 respectively designate the moduli of maximum compressional stress $\boldsymbol{\sigma_1}$, intermediate compressional stress $\boldsymbol{\sigma_2}$ and minimum stress $\boldsymbol{\sigma_3}$.

For a fault plate number k, called F_k in Fig.II.17, n_k and s_k are the unit normal to the fault and the unit stria on the fault, respectively (Fig.II.17a). **T** designs the unknown stress tensor, so that the stress vector $\boldsymbol{\sigma}_k$ for Fk (Fig.II.17.b) is given by

$$\boldsymbol{\sigma}_k = \mathbf{T}\mathbf{n}_k. \qquad \text{(II.11)}$$

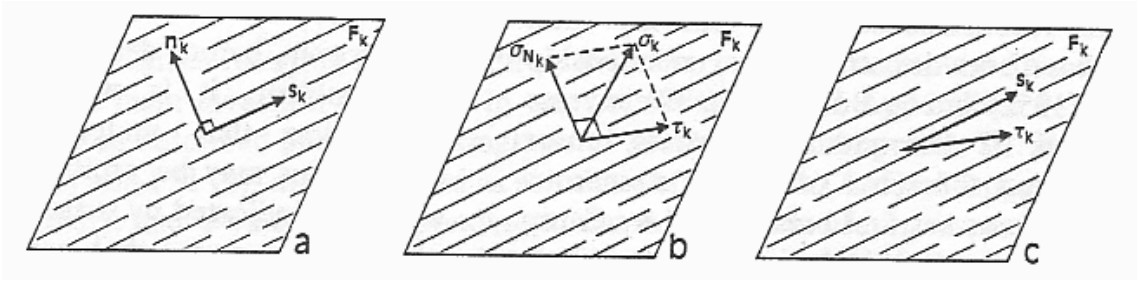

Fig.II.17: Fault-slip datum and computed stress. Index K designates datum number as in text. (a) Observed fault-slip: **F**, fault plane; **n**, normal fault (unit vector); **s**, unit slip vctor (parallel to striae). (b) Components of computed stress: σ_n, normal stress; τ, shear stress. (c) shear-stria angle: **s**, observed slip; τ, computed shear. (Angelier, 1990).

As Fig. II.17b shows, the normal stress σ_{Nk} in the component of $\boldsymbol{\sigma_k}$ on $\mathbf{n_k}$. The shear stress τ_k is consequently easily obtained:

$$\boldsymbol{\sigma}_{Nk} = (\boldsymbol{\sigma}_k \,.\, \mathbf{n}_k)\, \mathbf{n}_k\,, \qquad \text{(II.12)}$$

$$\boldsymbol{\sigma}_k = \boldsymbol{\sigma}_{Nk} + \boldsymbol{\tau}_k \qquad \text{(II.13)}$$

Finally, one may simply consider the angle $(\boldsymbol{\sigma_k}\,,\,\boldsymbol{\tau_k})$ between two vectors in the fault plane F_k (Fig.II.17c): the unit stria $\mathbf{s}_k$ indicating direction and sense of actual fault slip (observed), and the computed shear stress τ_k (related to unknown stress tensor **T**). Obviously this angle should be as small as possible for a tensor T consistent with fault slip datum number k; the ideal case being

$$(\mathbf{s}_k\,,\,\boldsymbol{\tau}_k) = 0 \qquad \text{(II.14)}$$

Using additional implicit assumptions of the least-squares method, one obtains the best fitting stress tensor for a given fault slip data set by minimizing function S_1, where N is the number of faults:

$$S_1 = \sum_{k=1}^{k=N} (\mathbf{s}_k\,,\,\boldsymbol{\tau}_k)^2 \qquad \text{(II.15)}$$

Because the sine of the half angle continuously increases from 0 to 1 as the angle increases from 0 to π, similar results are obtained by minimizing function S_2:

$$S_1 = \sum_{k=1}^{k=N} \sin^2(\mathbf{s}_k , \boldsymbol{\tau}_k)/2 \qquad \text{(II.16)}$$

Considering the field data, geologists measure a collection of slickensides within an area. They do not know if only a single stress state is responsible for all the slickensides. In general, there may be a sequence of different tectonic episodes in the local geologic history, and sometimes it is not clear from field observations how many of these events have occurred and to which of them an individual measurement can be attributed. In this case, measurements of faults with their planar orientations and senses of slip shown by linear slickensides on faults are dispersed in spherical space. Such dispersion may represent two cases. First, the set of fault-slip data may be composed of several dynamically homogeneous sub-sets which result from different single tectonic events. Secondly, the last tectonic event may have reactivated pre-existing fractures at the site of observation. In both cases, such data sets give rise to difficulties in computation of the principal stress axes, because these axes are calculated by assuming that the whole data set resulted from a single stress state. Thus the problem of the separating different tectonic phases arises.

II.2.C.4. Faults growth, terminations and relays zones

Two different situations could be found near fissures and faults terminations: (1) there is no fracture near the fracture termination, (2) the termination of two fractures are approached (with a distance less than half of the their lengths) and form a cover zone, namely, *relay* zone. These two situations are instable when a tectonic force applied to a fractured rocks because the fractures propagate (Mercier and Vergely, 1992).

- *Relay zones*

A relay is called ‘relay to right’ when an observer looks along the fault direction and see the next fault is situated to the right of the first fault and otherwise (to the left of the first fault) is called ‘relay to left’. Analogue modelling and numerical simulations (Segal and pollard, 1980) show the evolution of the bridges, formed between the two fracture planes, where are the privilege zone of the stress concentration (Fig.II.18a1 and a2). Based on the orientation of the regional stresses (σ1R and σ3R) and the relay’s orientation (to right or left),

local and perturbed stress field could be developed (Q1L and Q3L). From deformation point of view, two types of relays could be observed: compressive and extensive relays (Fig.II.18a1&2) with the new dominant compressive (or trans-compressive; CL, Fig.II.18b1) and extensive (or trans-extensive; TL, Fig.II.18b2) brittle structures, respectively. These new structures connect the initial major fractures by a system of the secondary fractures. These compressive and extensive relays could be co-existed in the same fracture zone. They are well known in the shear systems (Fig.II.19a), but we may find them in the compressive (inverse faults and thrusts, Fig.II.19b) and in extensional system (normal faults, Fig. II.19c).

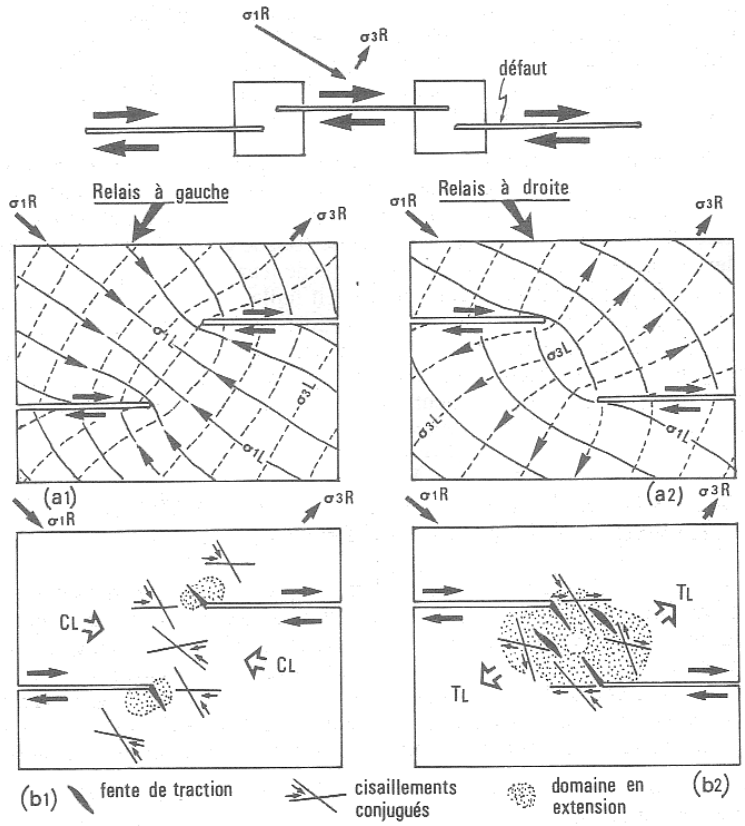

Fig.II.18: Stress state and deformation induced in the zones of compressive (a1, b1) and extensive (a2,b2) relays, (after Segall and Pollard, 1980, Mercier and Vergely, 1992).

- Fault terminations

During fracture formation, mechanical energy (elastic, cohesion, plastic) is released on the fracture surfaces. This released energy stops fracture propagation. Different tectonic processes are produced in the fault terminations, and consequently, lead to the stop of fault movement and creation of extensional and compressional structures at the fault terminations accompanying the accident branches (Fig.II.20).

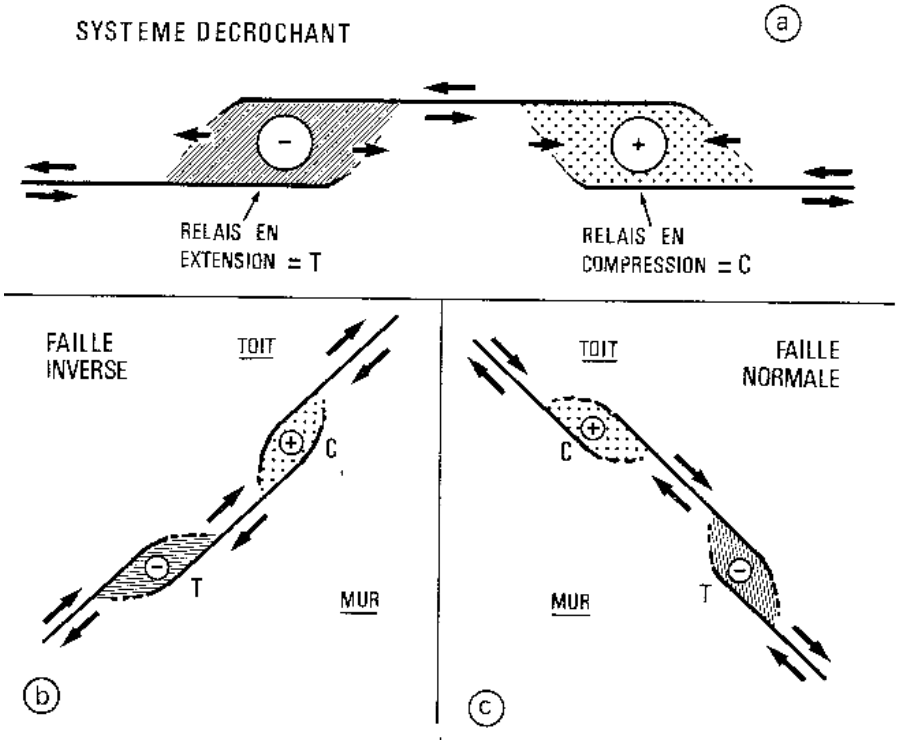

Fig.II.19: Compressive (+) and extensive (-) relays in a system of strike-slip (a), reverse (b) and normal (c) faults, (after Mercier and Vergely, 1992).

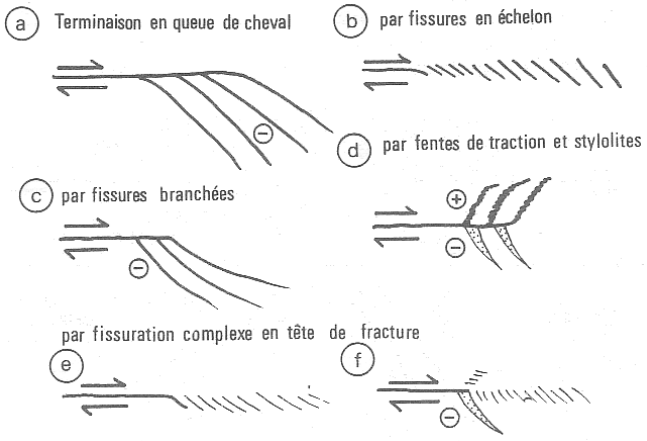

Fig.II.20: Fracture terminations, (a and b) after Granier (1986), (c) Segall and Pollard (1980), (d) Rispoli (1981), (e and f) Petit and Barquins (1987) and Petit (1987).

II.2.C.5. Calcite twins and paleostress determination

Calcite twins have been widely applied in tectonic studies. Turner (1962) developed a method to determine the stress axes from a population of e-lamellae in deformed calcite rocks. This method has been modified and refined in order to determine the principal directions and/or magnitude of paleo-stress (Groshong, 1972; Spang, 1972; Jamison and Spang, 1976; Tullis, 1980; Laurent et al. 1981, 1990; Pfiffner and Burkhard, 1987; Rowe and Rutter, 1990; Lacombe and Laurent, 1992). For more detailed explanation in this regards, readers could refer to Lacombe (1992, 2001).

From a geometrical point of view and for a given crystal, the e-lamellae {0112} are similar to micro-faults for which the five constitutive parameters (i.e. direction, plunge, pitch, sense of movement and value of real displacement), are all imposed by crystallography. Each calcite crystal has three symmetrically equivalent twins e_1, e_2 and e_3 (Fig.II.21a). The angle between optic axis (c axis) and the normal to a twin plane is about 26.5°. For a twin plane ei, the twin direction is along the edge $[e_i : r_j]$. The planes which contain both the optic axis and the normal to a twin plane $[e_i]$ also contain the direction of twining $[e_i : r_j]$ (Fig.II.21a). Fig. II.21b shows the geometry of a twin lamella when viewed in a section perpendicular to twin plane and parallel to twin direction. The width of twin lamellae associated with brittle deformation is about a fraction of a micron (Groshong, 1974; see also Barber & Wenk, 1976 and Goetze & Kohlsted, 1977). Therefore, when dynamic interpretation is carried out, there is no possibility of confusion between the host and the twinned part of the crystal (Friedman, 1964).

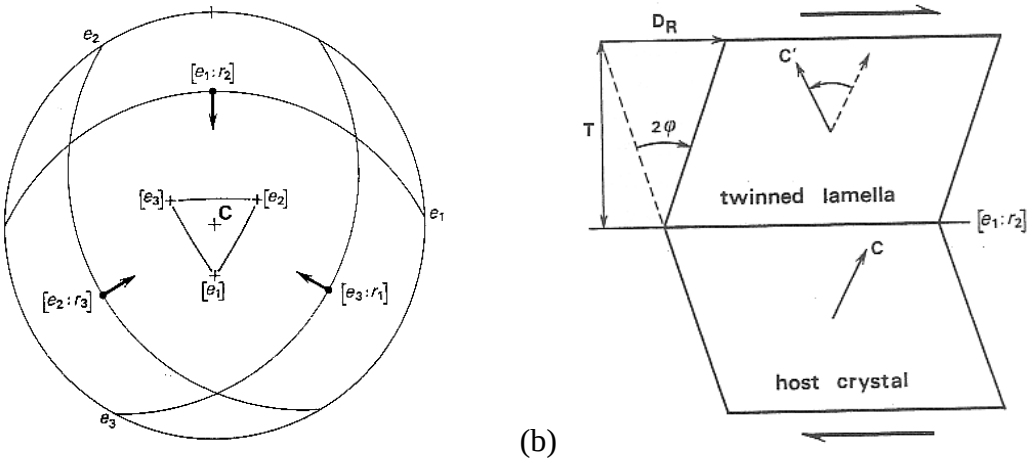

Fig.II.21: (a) Stereographic projection (lower hemisphere) of calcite twin planes {1012}. The optic axis c is vertical, at the center of the diagram. Poles to the three sets of twin planes are $[e_1]$, $[e_2]$ and $[e_3]$. Planes of twining are great circles e_1, e_2 and e3which contain directions of twining $[e_i : r_j]$. For each twin plane, the arrow is parallel to the twining direction; its head indicates that the upper part of the crystal moves upwards, towards the c axis like a reverse micro-fault, (b) The geometry of e-twining in calcite. The plane of the drawing is perpendicular to the twin plane e1 and contains both the direction of twining along the edge $[e_1 : r_2]$ and the optic axes (c for the host crystal and c' for the twined lamella). From the host crystal, the deformation is achieved by simple shear on the composition plane with a shear angle $2\phi = 38.3°$. Thickness of twin lamelle is T and total displacement is D_R. Notice that the rotation of the optic axis (c to c') is anticlockwise for a dextral sense of shear (Laurent, 1987).

II.2.C.6. Sylolites and paleostress determination

Stylolites are another group of discontinuities which generally observed besides the fractures within the rock mass. Their measurement and interpretation in addition to joints and fault-slip data measurement could be quite useful in determination of monophase or polyphase paleostress in a region. The measurement of stylolitic peaks should be a systematic

part of any fracture study. Here, stylolites and paleostress determination based on them are discussed based on Dunne and Hancock (1994).

Stylolites are solutions structures where shortening is mostly accommodated by volume loss (Park and Schot, 1968). Determination involves: (1) pressure-driven or free-face soltion (Engelder and Marshak, 1985); (2) chemical diffusional (Rutter, 1976) or physical advective transfer (Geiser and Sansone, 1981) of solute in a fluid phase; and (3) either local precipitation of solute in veins and fibrous overgrowths as a closed system, or solute export through an open system. Evidence for solution across stylolites includes: mutual penetration of fossil fragments, pit development in conglomerates, and elongation of clastic quartz grains by silica overgrowth (Groshong, 1975; Ramsy, 1977). However, stylolites do not pervade all shortened rocks because rock solution decreases with increasing temperature, increasing strain rate, increasing deviatoric stress, increasing grain size, decreasing clay content, and decreasing mineral solubility (Rutter, 1976; Kerrich et al., 1977; Engelder and Marshak, 1985; Houseknecht, 1987).

- *Stylolitic morphology and geometry*

Stylolite seams have a distinctive wave-form morphology and consist of two interpenetrating surfaces that are separated by an insoluble residue of clay minerals and oxides from rock dissolution. The wave forms are defined by first-order stylolites columns (Park and Scot, 1968) with teeth and sockets of hummocky, sutured, rectangular or peaked shape (Fig.II.22a) that contain smaller parasitic or second-order stylolite columns (Fig.II.22b). The parallel orientations of first-order columns define the stylolitic lineations, whereas the second-order columns only point towards the culminations of their host first-order (Fig.II.22b). The stylolitic lineation is parallel to the maximum shortening across stylolites. Commonly, stylolites accommodate less than 4% shortening and have greater than 5 cm spacing (Alvarez et al. 1978). For greater shortening, styloites are absent, and smooth or anastomosing solution structures develop. Stylolites do not have a unique geometry to bedding. They can be bedding-parallel structures that formed during burial in response to lithostatic load, or they can form obliquely or normal to bedding in reponse to tectonic compression (Fig.II.22c).

- *Related structures*

In clast-supported conglomerates where the clasts are in contact, transmit stress, and dissolve locally to yield interpenetrated pebbles, the following structures can form: (1) solution pits or sockets that develop in more soluble pebblesor those with broader radii of curvature; (2) slip-lineations from oblique solution or frictional wear between passing clasts;

and (3) fractured insoluble pebbles (McEwen, 1981; Schrader, 1988) (Fig.II.23a). Intraclast fracturing also occurs when the strain rate exeeds that of solution-related shortening.

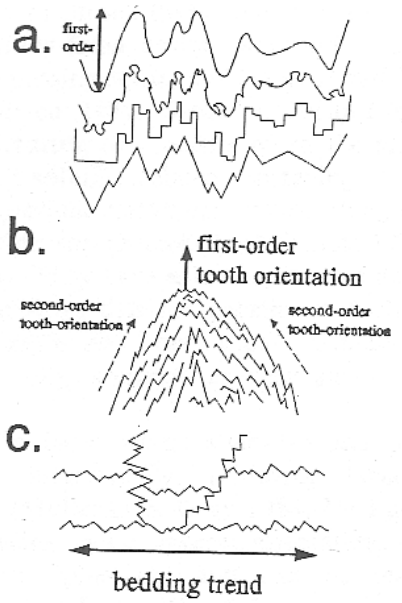

Fig.II.22: (a) Different stylolite morphologies: from top to bottom; hummocky, sutured, rectangular and peaked. (b) Sigle first order stylolite tooth or column with smaller second-order teeth. (c) Common geometries of stylolites with respect to bedding (Dunne and Hancock, 1998)

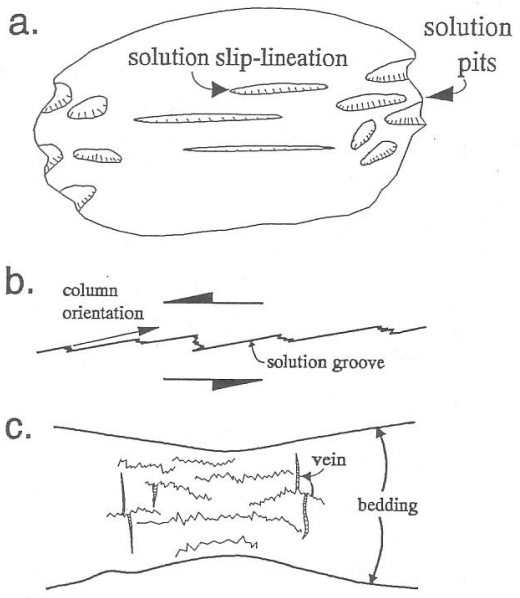

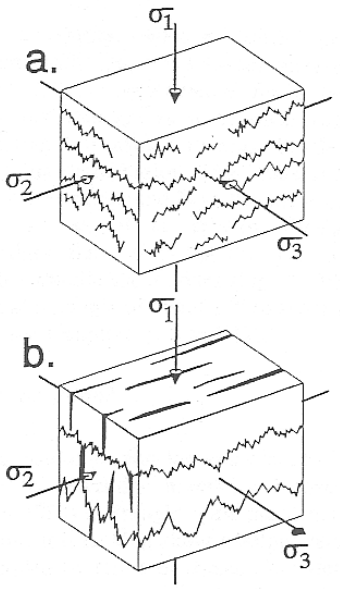

Fig.II.23 (left): (a) Pitted pebble. (b) Profile of slickolite with shear sense shown by coupled arrows. (c) Necking of a bed by styloboudinage (Dunne and Hancock, 1998).
Fig.II.24 (right): (a) Principal stress axes inferred from stylolite seams with surface-normal columns. (b) Principal stress axes inferred from coeval orthogonal stylolite seams and dilatation veins (Dunne and Hancock, 1998).

Slickolites (oblique stylolites) develop along faults by pressure-solution slip (Nitecki, 1962; Elliott, 1976). They have columns, but are dominated by solution grooves that are parallel to fault motion (Fig.II.23b). Slickolites are shear structures that accommodate displacements at very small, aseismic strain rates.

Styloboudins form where stylolites and dilational veins grown interactively, achieving layer parallel segmentation (Mullenax and Gray, 1984; De Paor et al., 1991). The veins cause layer segmentation, whereas stylolites cause 'pinching' and can be reactivated bedding-parallel stylolites (Fig.II.23c).

- *Paleostress determination*

Stylolites seams have been interpreted to have an anticrack origin (Fletcher and Pollard, 1981) and to have propagated normal to σ_1 (Tapp and Cook, 1988); that is, to be exactly the opposite of Mode (I) dilational cracks. Also, first-order stylolite columns are interpreted to form parallel to σ_1. Both geometries are well displayed where first-order stylolites columns are normal to their host surfaces (Fig.II.24a). However when columns are oblique to a solution surface, they are not parallel to σ_1. One cause for this oblique columnar geometry is solution along pre-existing fractures that act as conduits for the dissolving fluids but are oblique to the direction of σ_1 (Geiser and Sansone, 1981). Stylolitic columns on a slickolite seam are roughly parallel to σ_1, but can be refracted away from σ_1 towards the solution surface. Where coeval orthogonal stylolites and fibrous dilational veins form together (Fig.II.24b), paleostress geometry is completely defined (Nelson, 1981). The inferred direction of σ_1 is parallel to the stylolite columns, σ_2 is parallel to the intersects between stylolites and veins, and tensional σ_3 is parallel to vein fibres. The distribution of these paired dynamic indicators can be used to infer stress trajectories around faults (Rispoli, 1981) and stress conduction during burial and halokinesis (Watts, 1983) in limestoes.

II.2.D. Fracture patterns associated with folding

These kinds of fractures form during the initiation and growth of a fold. Because of complexity of the stress and strain history during fold evolution, the fracture patterns that develop within the fold are also complex. Each fold has uniqueness in its strain pattern during folding. The distribution of various elements of the fold related fracture geometry that is utilized on the structure during deformation would vary.

Based on Cosgrove and Ameen (2000), fractures formed in association with buckle folding may be the result of the regional stress field or the local stresses generated as a result of buckling (e.g. extension in the outer arc above the neutral surface and compression of the inner arc below). The principal stresses are constrained to being either sub-parallel or subnormal to bedding, and as a result of this stress deflection the fractures also form normal to bedding (Fig.II.25, left). Normal faults tend to be aligned parallel or perpendicular to the fold axis. Those forming parallel to the fold axis form in response to the local extension that occur in the hinge region of the fold above the neutral surface. Thrust fault form in the hinge regions below the neutral surface in the region of local compression. However, the most frequently developed shear fractures are strike- or oblique-slip faults, many of which exhibit very little movement and have often been termed joints.

In extensional forced folding (i.e. where the causative basement faults are normal dip-slip faults) the strain patterns generated in the folded layers are characterized by layer-perpendicular shortening and layer-parallel extension in the direction normal to strike of the fault, regardless of the amount of movement on the fault. The fracture density is predicted to increase with increased movement on the fault, but the fracture type will remain the same. This is in marked contrast to the fracture patterns generated during the forced folding of a cover sequence above a basement dip-slip fault reactivated by reverse movement which are found to vary both in time and space. The overlapping of different strain fields during fold amplification is a characteristic feature of forced folds formed over reverse dip-slip basement faults (Cosgrove & Ameen, 2000) (Fig.II.25, right).

The chronological evolution of the fracture is not always clear from filed data. This leads to propose mechanical modeling (e.g., Guiton, 2001) which take into account the contribution of perfrential orientations of fractures to the irreversible deformation in an opening or shearing mode. The accommodation of folding by an opening mode of axial joints and shearing activation of systematic joints with the creation of conjugate set are of the main results in these numerical models.

II.2.D.1. The bases of classification

The majority of the folds in the Zagros folded belt are buckle folds or more precisely, seems to be detachment folds or fault propagated fold in a more mature state (see section II). On the other hand, the classical fracture systems are frequently seen in the region (see field study section). So, it is worthy to describe different fractures and their spatial geometry in a classical buckle fold.

The principal groups of the observed fractures associated with the folds are called axial, transversal and oblique fractures (Fig.II.26). Furthermore a group of fractures whose direction are sub-parallel with fold axis also exist. They are a particular type of the compressive-shear fractures and developed in certain layers (Bazalgette, 2004). The height of the fractures could be limited between two specific bedding-contact or with high vertical persistence, they may cut several layers or whole the sedimentary series (fracture corridor or fracture swarm). It is important to mention that different types of fractures in folds may have two different origins: (1) new-formed, syn-folding fractures, and (2) pre-existing, reactivated fractures.

II.2.D.2. Axial fractures

Fracture strikes in this group are parallel with the fold axis regardless of their local responsible stress directions. But they could be classified as follows:

II.2.D.2.1. Simple joint network

One of the main characteristics of this group is their lateral persistent and weak aperture. They are parallel to sub parallel to the fold axis and orthogonal to sub-orthogonal to bedding. Their high density distribution is normally remarkable near crestal area particularly in the zones with high curvature. Generally, fracture spacing is almost uniform for this group but not in the case where fracture corridor is observed.

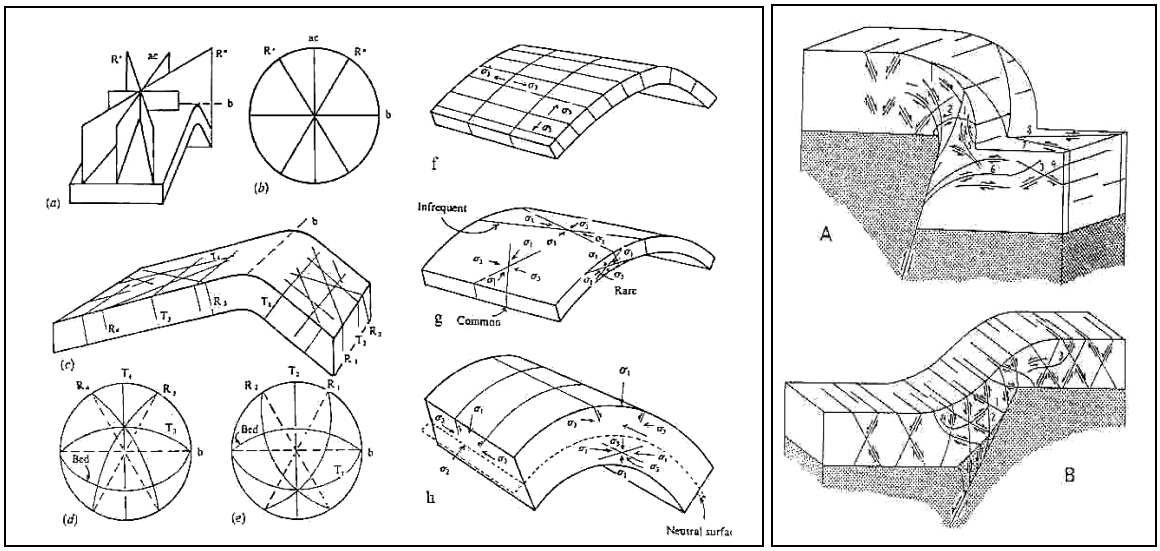

Fig.II.25: Left, (a)-(e) Typical fold-related fracture orientation diagrams depicting a portion of the total fracture geometry on folds. After Price (1966), (f) Typical relationship of dilational fractures to a fold, (g) Typical orientation of shear fractures in a thin bedded layer, (h) Typical orientation of normal faults and thrust which may develop in a thick, flexured unit (after Price & Cosgrove 1990). Right, Schematic block diagrams showing potential geometry and sense of movement of macrofaults in experimentally produced forced folds above (A), reverse and (B) normal basement faults (after Ameen 1990).

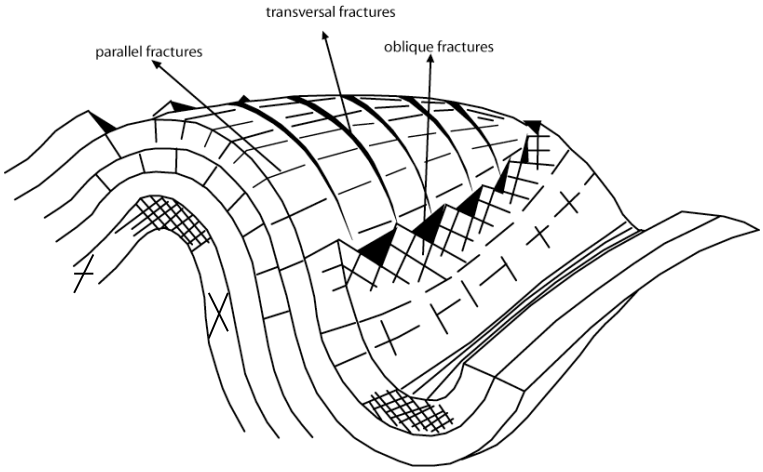

Fig.II.26: The principal groups of fold associated fractures, modified from Motiei (1995).

Axial fractures could have two different mechanical origins. First, syn-fold origin, which is due to the appearance of extension regime on the crest of the folds, after the initiation and amplification of elastic curvature in this area. The direction of this traction is parallel with the direction of regional shortening. The second mechanical origin is a pre-folding origin. In this case, the fracturing is inherited from other stress regimes than the one responsible of folding. Or they could have developed by relaxation effect after stress removal. The last hypothesis for the creation of these fractures could be explained by reopening of stylolite planes, which have been created within a regional compression. So, due to an inversion within a local traction during folding, the weak surfaces (stylolites) reopened as mode (I) fractures parallel to the fold axis (Fig.II.27).

The dynamic effect of axial fractures could be important in permeability anisotropy of reservoirs by creating a preferential axial direction for fluid flow. Especially when their density increase due to amplification of layer curvature.

II.2.D.2.2. Axial fracture corridors

Fracture corridors are remarkable structures in the folded formations (Fig.II.15). Sometimes under a favorable local stress regime, they may reactivate under shear stress. So, in this case, reactivated fracture corridor may be seen instead of non-reactivated, mode I fracture corridor (Bazalgette, 2004). Mechanical origin of this kind of fractures is not so clear but apparently they have a great role in curvature accommodation in a fold by articulation effect (Bazalgette, 2004). On the other hand, fracture corridors have important vertical and horizontal continuity. So, they could form the excellent drainage paths between apparently isolated reservoir units.

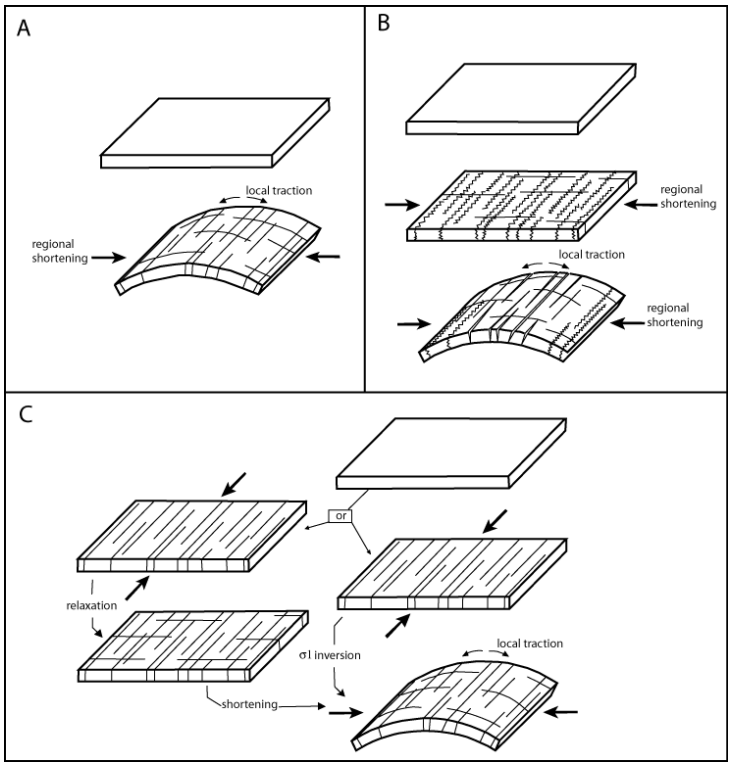

Fig.II.27: different mechanism for the creation of axial fractures in the folds. A) Syn-folding origin, where axial fractures form in an extensional regime due to elastic curvature of folding unit. B) Stylolitic origin in which, weak surfaces form before the curvature of folding due to compression. C) Pre-folding origin, where axial fractures are inherited and created within different tectonic stress regime. Bazalgette, 2004.

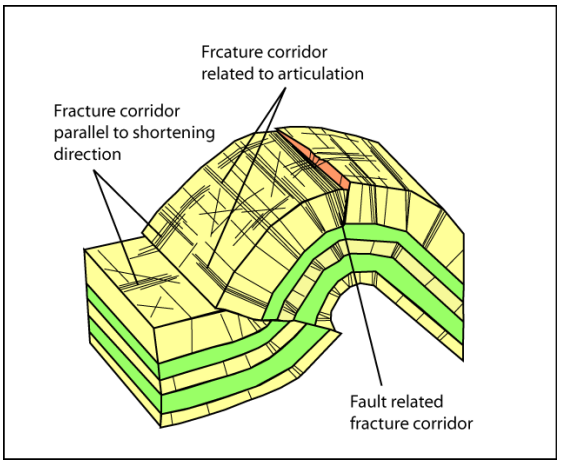

Fig.II.28: Fracture corridors in a fold, axial fracture corridor related to an axial fault or articulation effect. Modified from Bazalgette, 2004.

II.2.D.2.3. Axial faults

- *Axial normal faults*

There are many field examples of the presence of axial normal faults on the crestal area of the folds. Regarding the dip of the faults, two different kinds could be observed (Fig.II.29):

(1) Typically Andersonian normal faults. It means that fault plane makes a nearly 30° dip with the main principal stress (σ1).

(2) Non-Andersonian normal faults, which could be created by shear reactivation (syn-folding) of preexisting fractures (fracture corridors, inherited faults…). In this case, the fault geometry is severely controlled by the nature and the arrangement of inherited fractures.

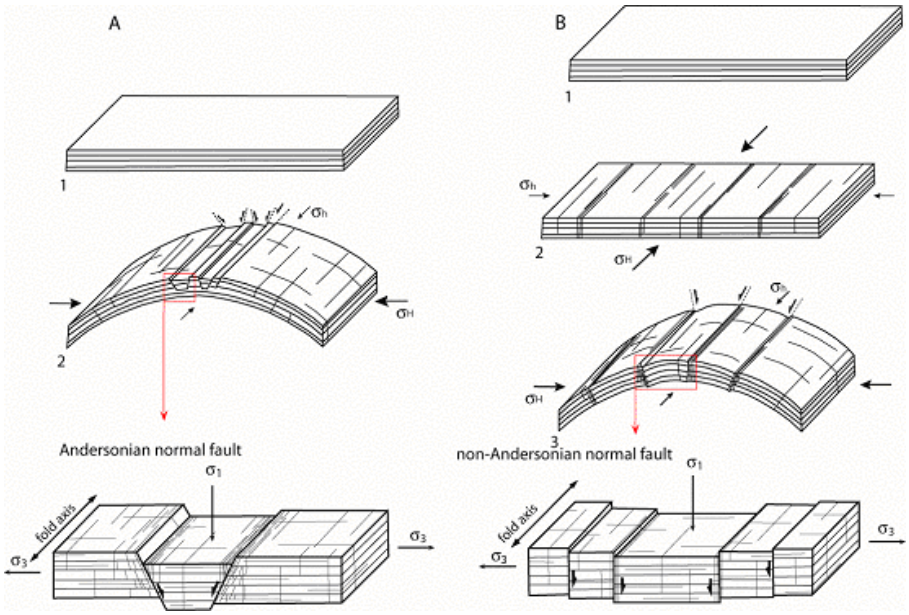

Fig.II.29: Different axial fault models and their mechanical origins. A) Syn-folding origin or Andersonain normal fault system in the zone of extrado as a new-formed fracture (fault) system. B) Pre-folding origins, where the faults are reactivated pre-existing fractures or fracture corridors (Bazalgette, 2004).

Andersonian normal faults have most probably a syn-folding origin. These kinds of faults could be created as newly-formed fractures under local traction regime in the zone of extrado (outer rim extension) (Fig.II.29A). In the case of non-Andersonian faults (shear reactivation of inherited faults, fracture corridors), the most probable scenario follows two stages: (1) a stage of initiation and propagation of fractures or fracture corridors parallel with the axis of the future fold; (2) an outer rim extension related to a syn-folding compression regime (Fig.II.29B).

In the function of the presence or lack of damaged materials in the fault zone and around it and the nature of the materials, axial faults could be excellent drains or barrier for the fluids of the reservoirs.

- *Axial reverse faults*

Axial reverse faults, in different scale and throw, could be seen frequently in buckle folds (Fig.II.30). One of the examples is bedding contact shearing due to the flexural-slip mechanism of the fold. Sometimes, when interfacial friction between the layers is strong then other type of fractures could develop within slipped layers. Other examples are the small conjugate or non-conjugate reverse faults with weak vertical continuity (limited by the thickness of the layer or mechanical unit). They are normally created just in the early stage of folding and before the onset of curvature of the sedimentary strata (II.30D). This case is mostly seen when internal decollement (like shale) with sufficient thickness exist. We can mention to the structures like ramp or duplex, which are developed in this manner (Fig.II.31).

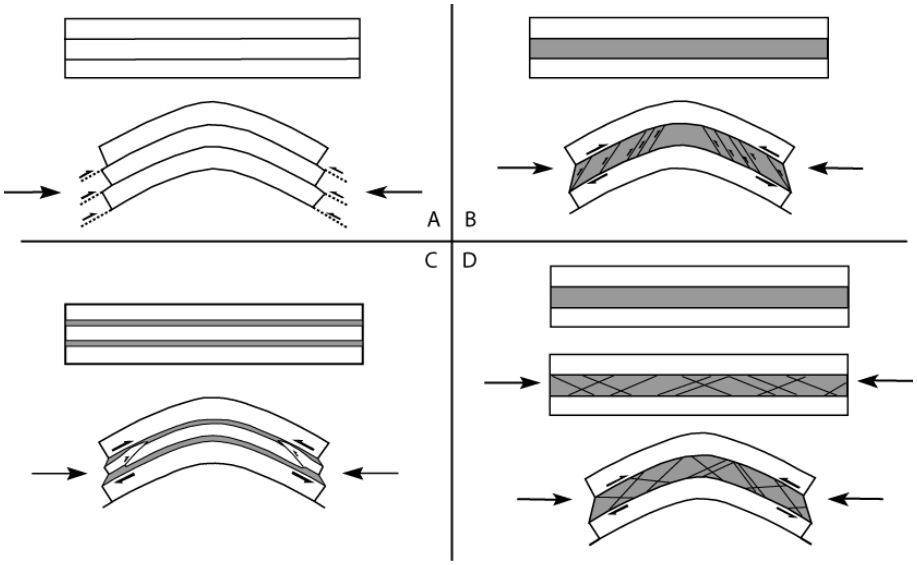

Fig.II.30: The formation of reverse faults associated with the folds. A) Bedding-parallel slip due to weak interfacial friction in flexural-slip mechanism. B) Small reverse faults network developed in a mechanical sub-unit with different and favorite mechanical properties (high porosity or high clay contents) compare to other layers. C) Flanking thrusts or duplex structures forming in competent beds inter-bedded with incompetent decollement layers. D) Pre-folding reverse fault network developed in the early stage of shortening (before appearance of layer curvature) in porous rocks or with high clay contents. Bazalgette, 2004.

II.2.D.3. Transversal fractures

Transversal fractures are often observed with axial fractures in a fold. Their directions are perpendicular to fold axis. In most cases transversal fracture network are of mode I type. Sometimes they could be accompanied by fracture corridors which are initiated and have propagated parallel to shortening direction (Fig.II.28). It is important to mention that these kinds of fractures could be found within foothill strata. It means that, in the contrary with axial fractures, they are not necessarily related to folding and they develop parallel with the maximum compression stress ($\sigma 1$). However after the initiation of the fold, some of transversal fractures could be reactivated in shear stress. If the throw of some of created faults

from reactivated transversal fractures be important, it leads to the creation of *segmented fold* (Bazalgette, 2004).

The presence of transversal fracture network superimposed by axial fractures normally tends to increase the permeability of reservoir in general but to decrease permeability anisotropy related to axial and bedding parallel fractures, supposing all of them are connected and conductive. Transversal fracture corridors could greatly affect the production, or if they are reactivated as normal faults with remarkable throw, they could compartmentalise the reservoir by *juxtaposition sealing*.

Fig.II.31: Axial reverse faults (flanking thrusts) in northern flank of Sefid anticline, southwest of Iran.

II.2.D.4. Oblique fractures

Oblique fractures are, classically, interpreted as shear fractures (Stearns and Friedman, 1972, Hancock, 1985). In fact, sometimes they appear in the form of two oblique sets with the appearance of conjugate strike-slip faults. However it is difficult to verify the shear origin of these fractures.

Oblique fractures often are joints (mode I) which are organised as sub-orthogonal network. They could be superimposed or not, with axial and transversal fracture families. In most cases, oblique fractures in "mode I", have an origin which has no relation with folding. They often form sub-orthogonal network, which could be the evidence of pre-folding stress. Normally, during the evolution of the fold, they could be reactivated by the shear component of the new stress field (Fig.II.31).

The hydraulic effect of oblique fractures as intersection paths between axial and transversal could be considerable. Generally, they could reduce permeability anisotropy.

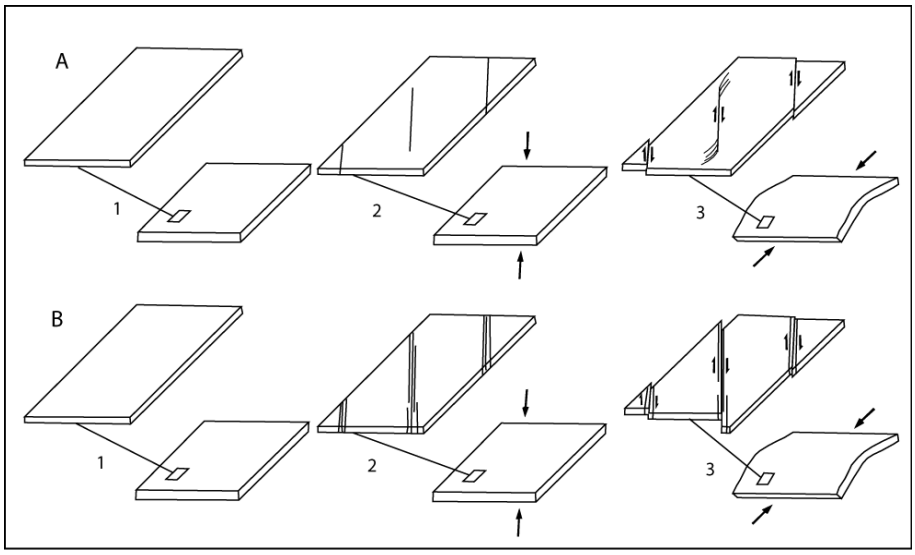

Fig.II.32: Formation of shear fractures during folding from A) oblique inherited joint set and B) inherited fracture corridor. Bazalgette, 2004.

II.2.D.5. Regional joints

Regional fractures are those that are developed over large areas of the earth crust with relatively little change in orientation. They show no evidence of offset across the fracture plane, and are always perpendicular to major bedding surfaces (Stearns, 1968a, 1968b, 1972; Nelson and Stearns, 1977). These fractures have also been called "systematic joints" by Price (1959, 1966, 1974), Hodgson (1961a) and Ziony (1966); "regional joints" by Babcock (1973, 1974a, 1974b); and simply "joints" by numerous authors, including Kelly and Clinton (1960). Regional fractures may form during the diagenesis of the sediments and affect fold formation resulting from exploitation of these kind of fractures (McQuillan, 1973). In other words, different sets of fractures could be developed under different regional stress regime and during folding they could be reactivated under another regional or local stress regime (Fig.II.33).

Regional joints are fracture families which appear on large surfaces and often in several geological stages. They show almost a constant direction over all outcrops like Appalachian plateau (Engelder & Geiser, 1980). It is thought that regional joints could be more sensible stress indicators than folds or faults especially in non-deformed regions. These fractures could develop in stress condition, which is not sufficient for faults or folds creation.
Rives (1992), classified regional joints as follows:

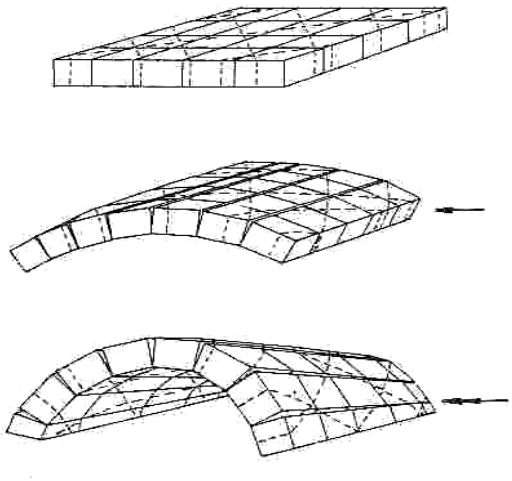

Fig.II.33: Fold formation from tectonic exploitation of preexisting fracture sets (McQuillan, 1973).

- Phase tectonic joints: The regional joints, which are related to a known tectonic event, like Appalachia joints or the North-Pyrenees foothill joints. The stress relaxation is the main agent for their creation (Fig.II.34a).
- Inter-phase tectonic joints: They develop under a stress field which is not sufficient to create associated faults and folds (Fig.II.34b) like the joints of Colorado plateau.
- Maturation joints: They are non-tectonics regional joints which are not related to a tectonic event, even weak, but are due to the evolution of petrophysical characteristics of materials during lithification or to an internal agent like fluid pressure (Fig.II.34c).

The direction of regional joints is not necessarily symmetric with the final deformation products (e.g. folds) in a region. They may be developed in a stress field which could be stongly oblique (e.g., Sheep mountain, Bellahsen et al., 2005, submitted) to the mean axial fold trends in a region, suggesting two different stress field directions. This indicate either a far-stress field rotation or block rotation (Lacombe et al., 2005) during the fa-field stress evolution in a region.

Conclusion

Brittle deformation is the main way that rocks and rock masses deform in both the shallow crust and at deeper levels when the conditions are right. Fractures are the main representatives of this deformation. One of the main fractures groups is joints or Mode I fractures. Joints really like to form in principal stress planes and will do everything they can to stay there, including rotate, twist, and break down into echelon arrays. They map out the trajectories (or flowlines) of stress during deformation so we can use them as paleostress indicators. One of the main factors in joint creation especially at deeper levels of earth crust,

is pore pressure. Based on this hypothesis, most of the joints create by dilatancy rather than a real extensional stress state (negative stress).

Different groups of fractures accompany the fold during its evolution. They are classical axial, transversal and oblique fractures. They consist of both joints and shear fractures (or faults). Between them, transversal and oblique fractures may have the origins, which are not directly related to fold formation but they could be reactivated during folding.

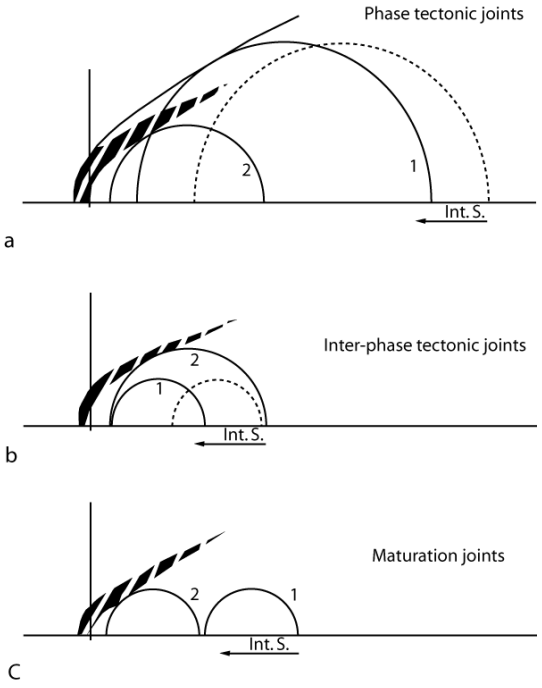

Fig.II.34: Mohr circles and their evolution (passing from stage 1 to stage 2) corresponding to three types of regional joints. (A): Phase tectonic joints, develop due to stress relaxation. (B): Inter-phase tectonic joints; a weak increase in maximum horizontal stress leads to regional joint development. (C) Maturation joints; internal stresses are sufficiently strong to create the rupture in an oriented stress field. Int. S. = Internal stress. (Rives, 1992).

Normally, the joints could be formed in a weak differential stress (at least in superficial part of earth crust) where the effective stress is not sufficient for other brittle deformation or fold creation. Regional joint set(s) is one of the main important groups, which can develop over a large area in this way. They could be classified to phase tectonic, inter-phase tectonic and maturation joints.

Another important group of fractures are faults. Their interpretation regarding paleostress state using fault-slip data is quite important to establish the chronological evolution of tectonic events in an area. Then, the interpretation of different joint families could be easier as chronological relationships among different joint sets are not always

possible. This may also achieve by mechanical modeling of different fracturing episodes during fold evolution (e.g., Guiton, 2001).

PART 2
Geological and tectonic framework of the Zagros

CHAPTER III
Paleogeography and Geological Setting of the Zagros Folded Belt, Southwest of Iran

Introduction

The importance of Zagros folded belt as a petroleum province is quite well known. Many efforts have been done towards better understanding of this prolific oil region. Maybe one of the main difficulties, through evolution of the Zagros belt, is the role of basement and its related structures beneath sedimentary cover. This role has been poorly understood.

Several authors have mentioned deep-seated basement faults and their influences on major structural features, folding style, diapirism and various lineaments in the Zagros area. However, the role of basement faults and their possible effect on paleogeography and the morphology of the Zagros basin and also the behavior of these faults during the sedimentation and folding of Phanerozoic strata are not so clear. Still many questions have remained without clear answers concerning the rifting phase between Arabian plate and Iranian block(s). The structures, which developed in this phase and also their rejuvenation during the collision of Arabian plate and central Iran, still have not been well understood. They not only have controlled different sedimentary environments, facies changes and structural framework along the general Zagros trend (NW-SE) and normal to it (NE-SW) but also have apparently had a noticeable effect on fracturing style and dynamic behavior of the oil reservoirs. So, at the beginning, attention will be given to basement tectonics mostly using what we know beyond Zagros folded belt in the Arabian plate. Then, the paleogeography of the Zagros basin from Upper Cretaceous to Neogene will be shown and finally different morphological classifications of the Zagros will be recalled and explained.

III.1. Arabian plate tectonics

III.1.1. Geodynamic evolution

The Arabian plate is one of over ten rigid lithospheric plates that make up the surface of the earth. The Arabian plate came into existence 25-30 million years ago (25-30 Ma), when the rocks that comprise what is now the Arabian Peninsula, Syria, Jordan, Iraq, and westernmost Iran began to separate from the African continent because of rifting along the margin of northeast Africa and the opening up of the Red Sea and Gulf of Aden. Although relatively young as a tectonic unit, the plate incorporates rocks that have evolved over a considerable span of geologic history. These rocks range in age from the Archean to the most

recent and make up a layer of continental crust as much as 45 km thick. The Precambrian rocks are extensively exposed in the southwest of the plate, and locally in the southeast, because of Mesozoic and Cenozoic uplift. Elsewhere the Precambrian rocks are concealed by a low-dipping sequence of Phanerozoic (Infracambrian-Tertiary) deposits that, in the Arabian Gulf, for example, reach a thickness of more than 10 km. The presence of Precambrian basement, where concealed, is attested by the extension of magnetic anomalies from areas of exposure into areas of concealment, by gravity data, by seismic surveys, and by widely scattered borehole intersections (Johnson, 1998).

The plate tectonics history of the Arabian Plate was influenced by events occurring around its margins, related to the rifting of Gondwana and later collision with Asia (Koop and Stoneley, 1982). Related rifting along the eastern and southeastern margin in Late Permian time resulted in separation of Central Iranian blocks and the Sanandaj-Sirjan zone of Iran from the Arabian plate (Fig. III.1a-g). These blocks moved north across Tethys. Arabia, as part of Gondwana, also moved north towards subtropical latitudes suitable for carbonate sedimentation. In Table 1, major tectonic events have been listed from Permian to Miocene time.

Series/Stage	Tectonic Event	Effect on Arabian Plate
Permian	Hercynian orogeny ends	Quiescent period, rifting of Central Iranian blocks from Arabian plate
L. Jurassic	Break-up of Atlantic begins	Unconformity with major erosion on margin of plate
Oxfordian	Rifting of India from Africa begins	Rifting in south, plate tilted down to north
Berriasian	Rifting of eastern Mediterranean begin	Uplift of western margin of plate, Hail-Jawf arch raised
Aptian	Opening of Mediterranean begins	Sub-basin form on Arabian Platform
Turonian	Ophiolite obduction in eastern Arabia	Fault reactivation, warping of plate with erosion and onlap
U. Eocene	Collision begins on northern margin	Mesopotamian foredeep of Zagros Fold belt formed
Miocene	Collision begins on eastern margin	Zagros-Oman Fold Belt formed, clastic pile formed

Table 1: List of the major tectonic events that affected the Arabian plate since the Late Paleozoic (Goff et al., 1994).

III.1.2. Basement tectonic and related features

As mentioned in section (III.1), basement tectonics might play an important role in the tectonic evolution of the Zagros folded belt and dependent features. However, its role has not been well understood yet. Specially, chronology of different striking basement faults and the movements of different blocks limited by these faults, which could be the main responsible for the formation of different sub-basins in these area, are not so clear.

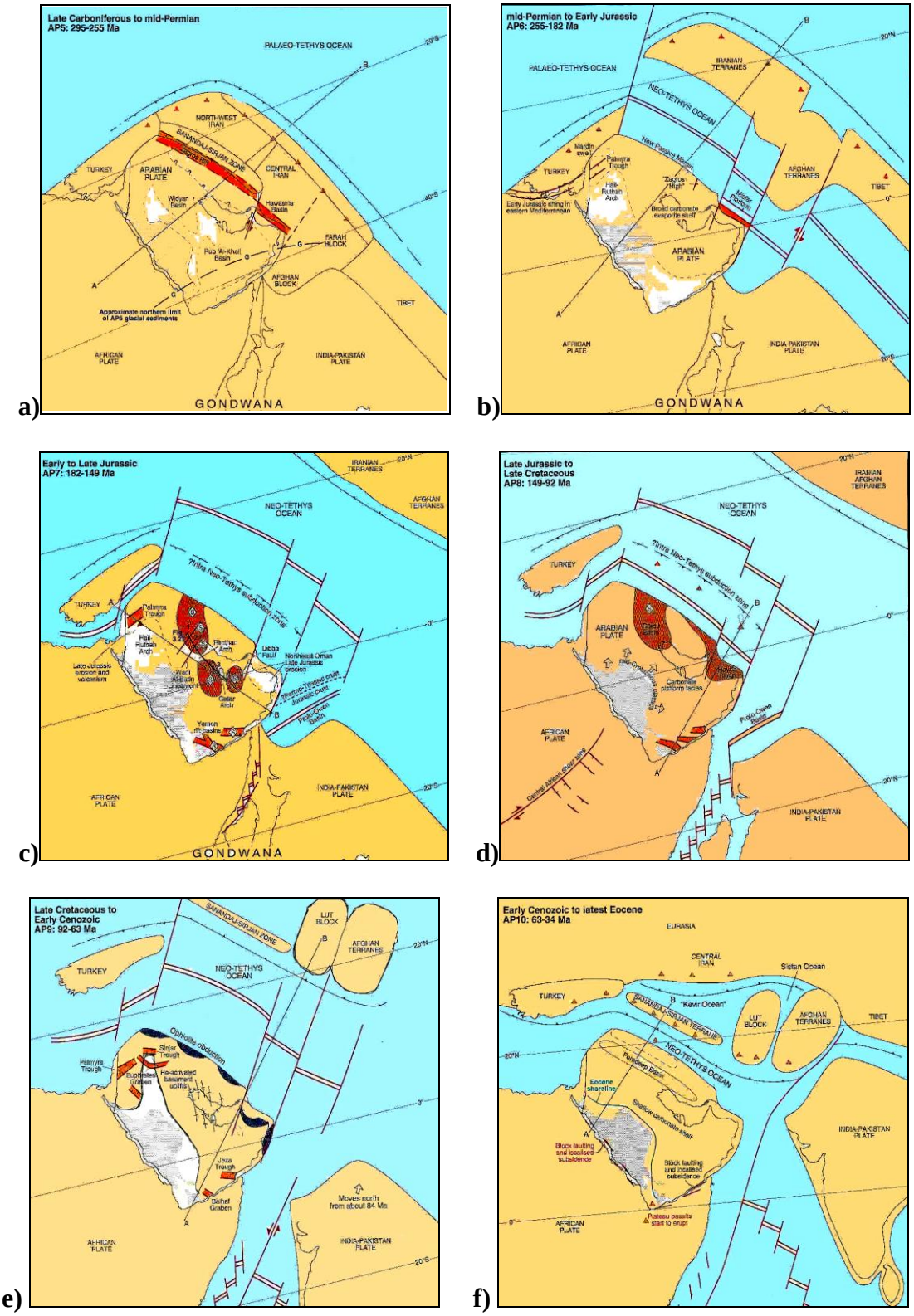

Fig. III.1: Schematic plate reconstruction; a) Late Carboniferous to mid-Permian; b) mid-Permian to Early Jurassic; c) early to Late Jurassic; d) Late Jurassic to Late Cretaceous; e) Late Cretaceous to Early Cenozoic; f) Early Cenozoic to latest Eocene (Sharland et al. 2001).

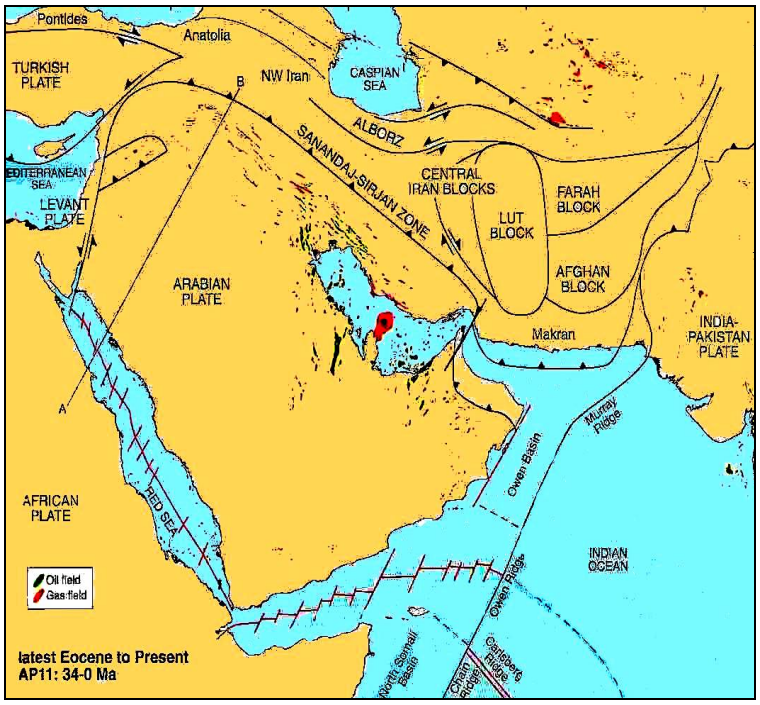

Fig.III.1g. (Cont.) Schematic plate reconstruction; latest Eocene to Present (Sharland et al. 2001).

Information on the Zagros basement are quite rare so I tried to find out some information relating to this topic beyond this area in Arabian plate where its Phanerozoic cover strata has not been affected by the Zagros orogeny, so overlain sediments can reflect basement features maybe better than in the Zagros area.

III.1.2.1. Late Precambrian-Cambrian tectonics of Arabian and adjoining plates

In the Stoesser and Camp (1985) model, the western part of the Arabian shield was initially formed by the fusion of three island-arc terranes: the Asir, Hijaj and Midyan (Fig.III.3). These three terranes were connected along the Bir Umq and Yanbu sutures at about 715 Ma. Between 680 and 640 Ma, the Afif terrane was added to the Arabian shield along the Nabitah suture. Finally, the Idsas collision sutured the Ar Rayn terrane to the Arabian shield around 640Ma. The schematic diagrams in Figure III.4 summarize these major tectonic events.

The Nabitah suture occurs within a 100 to 200-km wide zone of crustal deformation and Plutonism along the margins of the Asir, Hijaz and Afif terrane (Schmidt et al, 1979; Stoesser et al, 1984). This suture zone consists of broad, linear complexes of synorogenic plutonic and metamorphic rocks (Stosser et al 1984), as well as ophiolitic complexes (Frisch

and Shanti, 1977). Stoesser et al (1984) dated the synorogenic plutons within the southern part of the orogenic belt at 680 to 640 Ma.

Following the Nabitah orogeny, the Idsas orogeny completed the assembly of the Arabian plate along the Al Amar-Idsas suture (Fig.III.4). Between 670 and 630 Ma, the Al Amar area may have been an island arc (Nawab, 1979; Coulomb et al,1981; Shanti and Gass, 1983; Stacey et al, 1984; Le Bel and Laval, 1986), which coincides with a magnetic anomaly that extends in a north-south belt from Iraq to the Eastern edge of the Arabian shield (unpublished magnetic data from Director General of Mineral Resources of the Kingdom of Saudi Arabia and from Aramco).

Around 640Ma, the Al Amar arc appears to have collided with the Afif terrane (Shanti and Mitchel, 1976; Stoesser and Camp, 1985) as is evident from the widespread synorogenic plutonism in the vicinity of the Al Amar-Idsas suture (Calvez et al,1983; Stacey et al, 1984; Le Bel and Laval, 1986). East of the Al Amar arc, a large continental terrane, which is informally referred here to the Ar Rayn terrane, may also have participated in the collision; The Ar Rayn terrane probably included the eastern part of the Arabian plate, and central Iran's Lut block (Husseini, 1989).

The Idsas orogeny appears to have caused widespread deformation in the Ar Rayn terrane and may have initiated or reactivated the northwest-southeast, northeast-southwest, and north-south fracture grain of eastern Arabia (Husseini, 1989) (Fig.III.3). The rejuvenation of these fracture systems has controlled the accumulation of oil in the major fields in the Arabian plate, e.g., Ghawar in Saudi Arabia, Burgan in Kuwait and Bu Hasa in the United Arab Emirates (Salam et al., 2001).

In Iran, orogenic movements might also be equivalent to Iran's Assyntic orogeny (Stöcklin, 1968). In the Kerman area of central Iran, the Morad formation consists of metamorphic green slates and arkosic sandstones, containing Algonkian fauna. The Morad formation is intricately folded and overlain by the Rizu Formation, which has a radiometric age (from a synsedimentary ore deposit) of 760-595 Ma ± 120m.y.(Stöcklin, 1968).

The post-tectonic extensional stage evolved into the Arabian Infracambrian extensional system (Husseini, 1988) at about 600 to 580 Ma. This extensional regime (Fig.III.5) may have lasted up to 540 Ma. This system may have included a triple junction centered just east of the Sinai Peninsula, with one rift branch extending along the Jordan valley and Dead Sea; another rift branch extending across Sinai and northern Egypt; and a third rift wrench branch, the Najd fault system, extending southeast across the Arabian shield.

Aside from the paleomagnetic evidence for this Early Cambrian triple junction (Piper, 1983), the symmetry of the three arms (subtended by 120° angles) further support its development.
In the Zagros mountains and the Persian Gulf, the Hormuz Formation contains basalt and ryolite, suggesting tectonic extension in this area (Berberian and King, 1981). The Zagros fault and the Dibba fault (Fig.III.5) define the southeastern limit of the Hormuz Formation. As suggested by Fig.III.5, the Zagros fault may have moved dextrally and the Dibba fault may have moved normally resulting in the opening of several rift basins in the Persian Gulf and Zagros mountains (Husseini, 1989).

One of the prominent Late Precambrian to Early Cambrian tectonic signature, which is etched in the Arabian shield (Fig.III.6), is the extensive, NW-trending, Najd strike-slip fault system (Brown and Jackson, 1960). The Najd fault system accumulated 300 km of left-lateral dislocation (Moore and Al-Shanti, 1979) and provides quantitative evidence for the magnitude of Infracambrian tectonic movement within the Arabian shield. The regional extend of the Nabitah, Idsas and Najd systems, beyond the Arabian shield, is masked by thick Phanerozoic sediments, and in general, the relationship between these sutures and the Najd strike-slip fault system remains controversial (Stern, 1985).

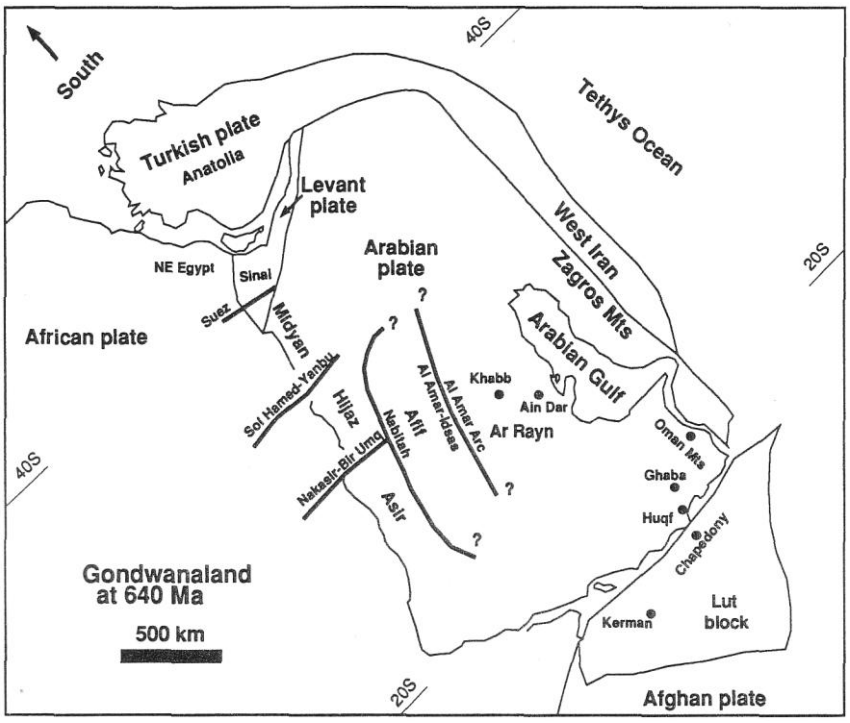

Fig. III.2: By about 640 Ma, present-day Arabian plate was formed by accretion and collision of terranes along northeastern flank of Arabian plate in the Gondwana. Eastern half of Arabian plate, western Iran and Lut block are informally grouped together as Ar Rayn terrane. Latitudes are appropriate for Early Cambrian (after Smith et al, 1981).

The eastern boundary of the Arabian plate, the Zagros fault (Fig.III.6), coincides with the eastern margin of the Infracambrian Hormuz evaporite. The Hormuz formation extends regionally beneath the Arabian Gulf and the Zagros Mountains (Stöcklin, 1968) and correlates with the Infracambrian Ara evaporite in the South Oman and Gaba basins (Fig.III.6). The Late Precambrian tectonic history of the Zagros fault and the depositional genesis of these evaporitic basins are poorly understood.

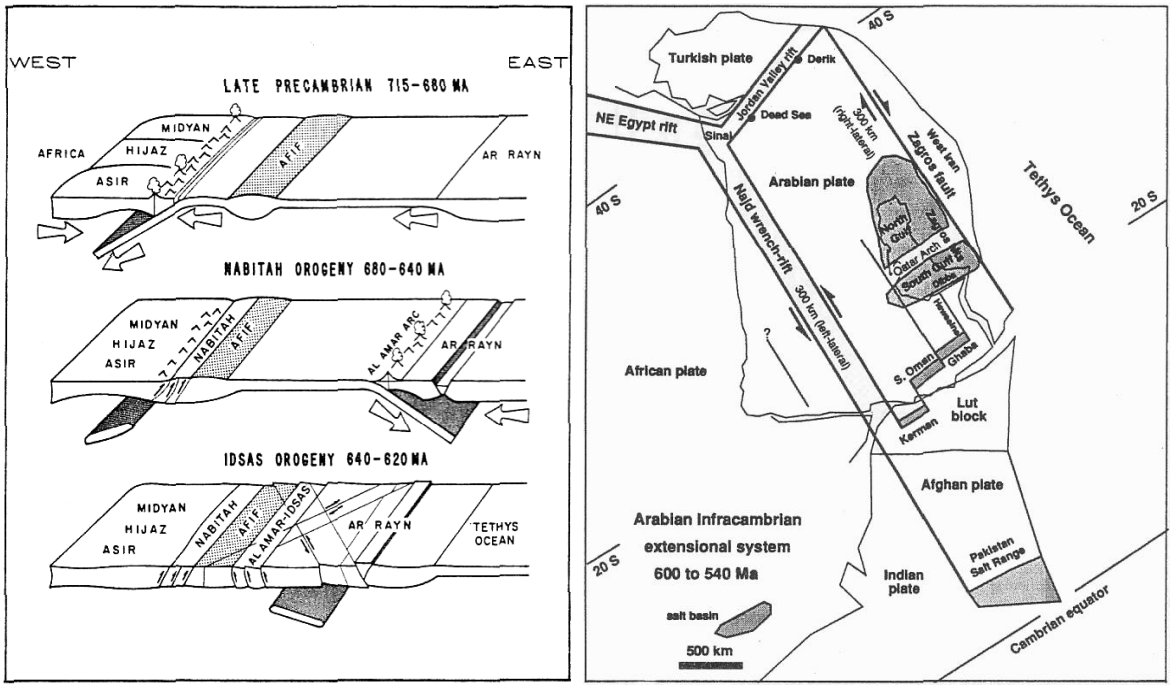

Fig.III.3:(left) Schematic reconstruction of accretionary evolution of Arabian shield. See text for more details. Idsas orogeny was probably responsible for initiation of major wrench and thrust faulting and folding. (Husseini, 1989).
Fig. III.4:(right) Arabian Infracambrian extensional system, which lasted from about 600 to 540 Ma. (Husseini, 1989).

III.1.2.2. Basement tectonics as related to oil field structures

In this part, we try to find a relation between oilfield trends in Saudi Arabia and some adjacent Arabian countries and basement structures based on H. S. Edgell (1992), as almost all oil and gas fields in these regions have generally been controlled by basement tectonics. Four trends of basement faulting which control the oil fields of Saudi Arabia (Henson 1951), are: The most prominently, N-S Arabian Trend, as well as the NE Aualitic Trend and the NW Erythraean Trend in offshore diapiric fields and finally, least conspicuous is the E-W Tethyan Trend.

All oil and gas fields of Saudi Arabia owe their origin to deep-seated tectonic movements in the Precambrian crystalline basement (Edgell, 1987). The thickness of the

sedimentary sequence varies from 4500m to 13700m by gradual thickening towards the northeast (Fig.III.10). Much of the evidence regarding depth to basement has been deduced from geophysical surveys, primarily gravity and magnetic investigations. In the case of the newly discovered oil fields at Al Hawtah, Dilam, Raghib and Nu'ayim (Fig.III.6), there is also direct seismic evidence of the depth to basement.

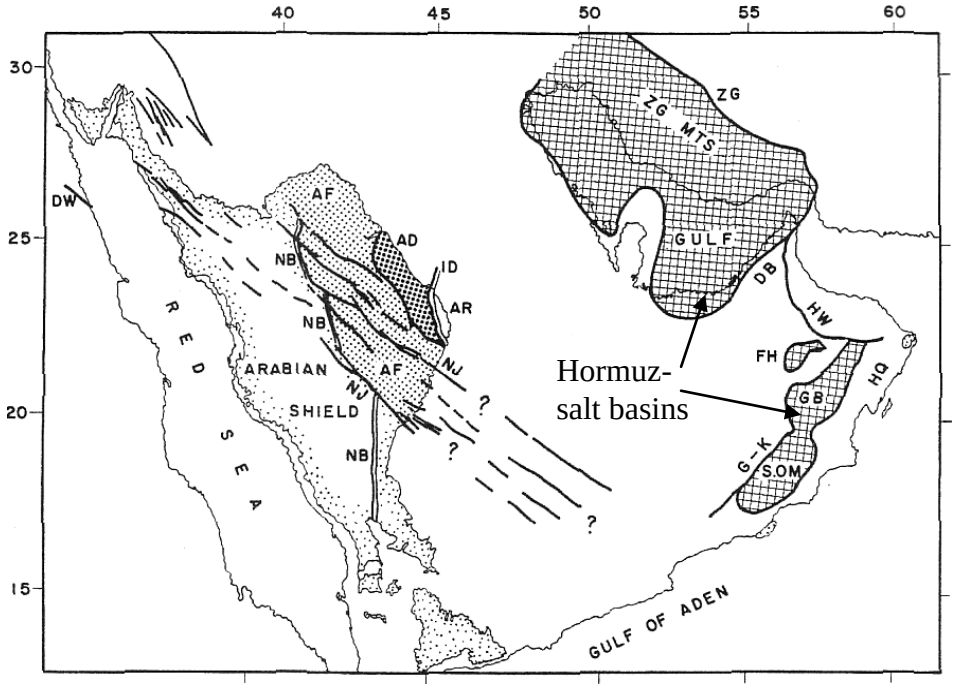

Fig.III.5: Arabian plate, showing Najd faults system, Infracambrian Hormuz salt basins with associated boundary faults (Husseini, 1988). AF, AD, AR; Afif, AD-Dawadimi and Ar-Rayn terranes; NB, ID; Nabitah and Idsas sutures; NJ, Najd fault system; DW: Duwai shear zone; ZB, DB: Zagros, Dibba faults; S.OM, GB: South Oman, Gaba Infracambrian evaporitic basins; G-K, HW: Ghudun-Khasfah, Hawasina faults; HQ, FH: Huqf anticline; FH: Fahud evaporitic basin.

Underlying the sediments in most of onshore northeastern Saudi Arabia, there is a faulted Precambrian basement, with alternating horsts and grabens directed along the N-S Arabian Trend. This is the 'old grain' of the Arabian Peninsula formed by repeated, E-W, extensional tectonism (Henson 1951). As a result, almost all the onshore oil fields of northeastern Saudi Arabia exhibit distinctive positive gravity anomalies due to the presence of denser uplifted basement beneath them (e.g. Ghawar field).

There is evidence to suggest that the basement was already faulted along the Arabian Trend in the Late Precambrian, so that the Proterozoic Hormuz Series sediments were deposited in a series of N-S troughs, between uplifts or headlands. Repeated rejuvenation of these uplifts, or basement horsts, particularly along the N-S Arabian Trend, is reflected in the pattern of deposition throughout the Phanerozoic (Fig.III.7). These horst and graben structures do not trend exactly N-S but mainly in a N l7° E direction, which Henson (1951) noted as the

main alignment of the Arabian Trend. The structural relief of basement horst blocks is interpreted as being up to 4.5 km with regard to adjacent basement troughs (Edgell, 1992). During the Mesozoic, and especially in the Triassic and Late Cretaceous, and even probably during the Permian, the N-S uplifts and basins of the Arabian Trend were intermittently reactivated, as seen in the Ghawar Anticline, Dibdibah Trough and Qatar Arch (Fig.III.7).

In offshore northeastern Saudi Arabia and adjacent coastal areas, more than 20 oil fields occur (Fig.III.6), all marked by distinctive negative gravity anomalies (Edgell, 1987). This is because basement faulting has also penetrated the Upper Precambrian halite beds of the Hormuz Series, thus triggering deep-seated salt diapirism and producing domal oil-field structures. Some of these oil fields, such as Karan, Abu Sa'afah, Abu Hadriyah and Dammam (Fig.III.6), have the typical circular shape of diapiric oil structures. Most offshore oil-field structures are elongated, doubly-plunging anticlines, such as Safaniyah, Khafji, Kurayn, Jana and Jurayd (Fig.III.6). They are elongated along a general NE to NNE direction (Aualitic Trend of Wissmann et al. 1942) and are due to left-lateral, strike-slip faulting in the basement, which has also penetrated the salt beds of the Hormuz Series causing diapiric salt-wall structures at depth (Player 1969), which have uplifted the overlying strata in elongated anticlines.

An E-W basement fault trend is less clearly seen in the oil fields of offshore Saudi Arabia and appears as alignments of gravity highs along this direction, both onshore and offshore. This E-W basement fault is clearly seen in the Central Arabian Graben System (Al-Kadhi and Hancock 1980; Hancock and Al-Kadhi 1985; Hancock and Bevan 1987), which continues eastward to truncate the southern end of the En Nala Anticlinal Axis (Fig.III.7). Only one, undeveloped, oil field at Hasbah/Farsi (Fig.III.7)(Mina et al. 1967), near the Saudi/Iranian offshore border, is clearly developed along an E-W structural alignment (III.e. the Tethyan Trend, Henson 1951).

A NE to NNE trend is clearly seen in major offshore oil field structures, such as Safaniya, Khafji, Marjan, Kurayn, Jana and Jurayd, as well as onshore in oil fields, such as Abqaiq and Khursaniyah. These fields are all related to faulting of the basement along a NE trend as seen in Kuh-e Namak in south part of Iran (Talbot and Jarvis 1984). The underlying basement faults are considered to be left-lateral strike-slip faults, which have also cut the thick saliferous Precambrian Hormuz Series providing release for the lighter halite.

In some cases, intersecting NE and NW basement faults have provided a focal point for salt diapirism and typical circular salt domes have been formed, as at Abu Hadriyah, Abu Sa'afah, Karan and Dammam. In the case of the Abu Sa'afah Oil Field, the second derivative

of the potential field of gravity indicates deep basement faults intersecting along NW-SE and N-S directions.

These diapiric structures are usually due to salt growth from Mid-Cretaceous to Recent and, in some cases, have started growth as far back as Late Jurassic. As stated by North (1985), some of the great productive oil regions of the world are characterized by traps due either to basement horst-block uplift, halokinesis (deep-seated salt movement) or a combination of both.

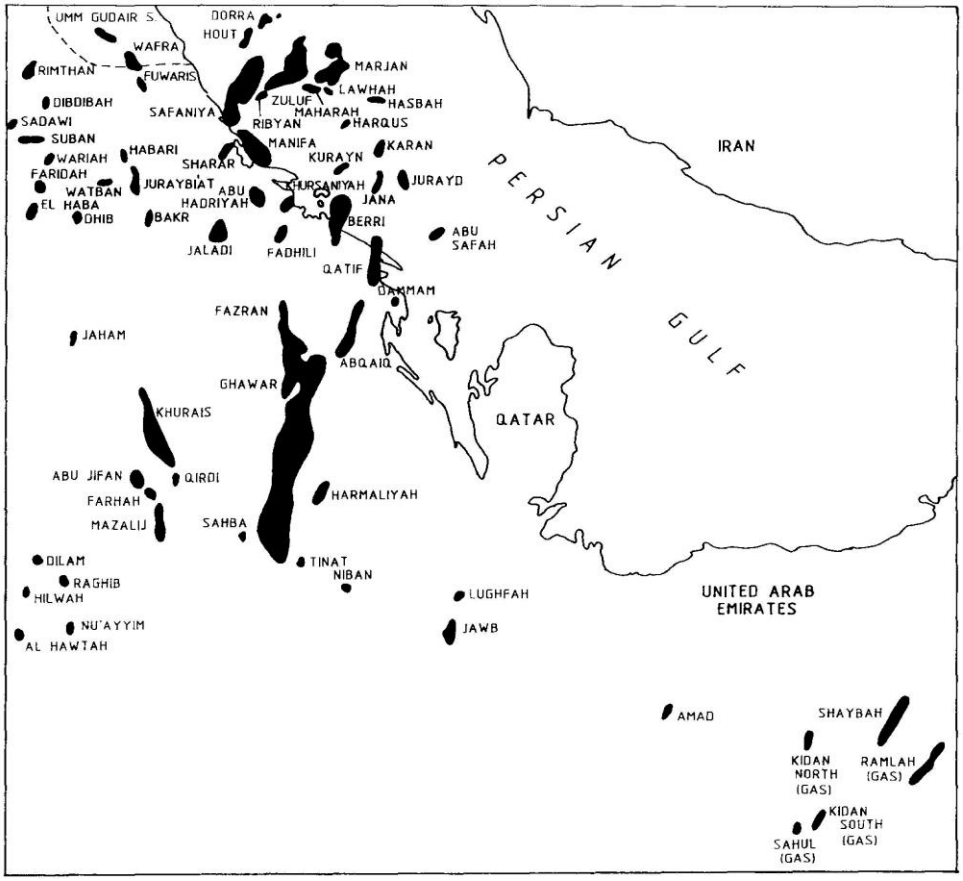

Fig.III.6: Oil and Gas Fields of Saudi Arabia (Edgell, 1992).

III.1.2.3. Geophysical evidence of basement tectonics

Most of the data on geophysics of the basement underlying the Arabian Platform in the Saudi oil-field areas is confidential and restricted by major oil companies. Those which published are from seismic, magnetic or gravity methods. Some magnetic data show a broad, N-S trending belt of magnetic highs, about 100km wide, lies between about longitude 45°E and longitude 46°30'E (Edgell, 1992). Based on gravity evidence(Barnes, 1987), basement shows major trends like N5°E, N20°E, N70°E, N25°W, N80°W. Of course, the N and NNE

trends are most striking, but the presence of basement faults along the other trends is clearly recognizable (Edgell, 1992; McCall, 1996; Bahroudi and Talbot, 2003; Regard et al., 2004).

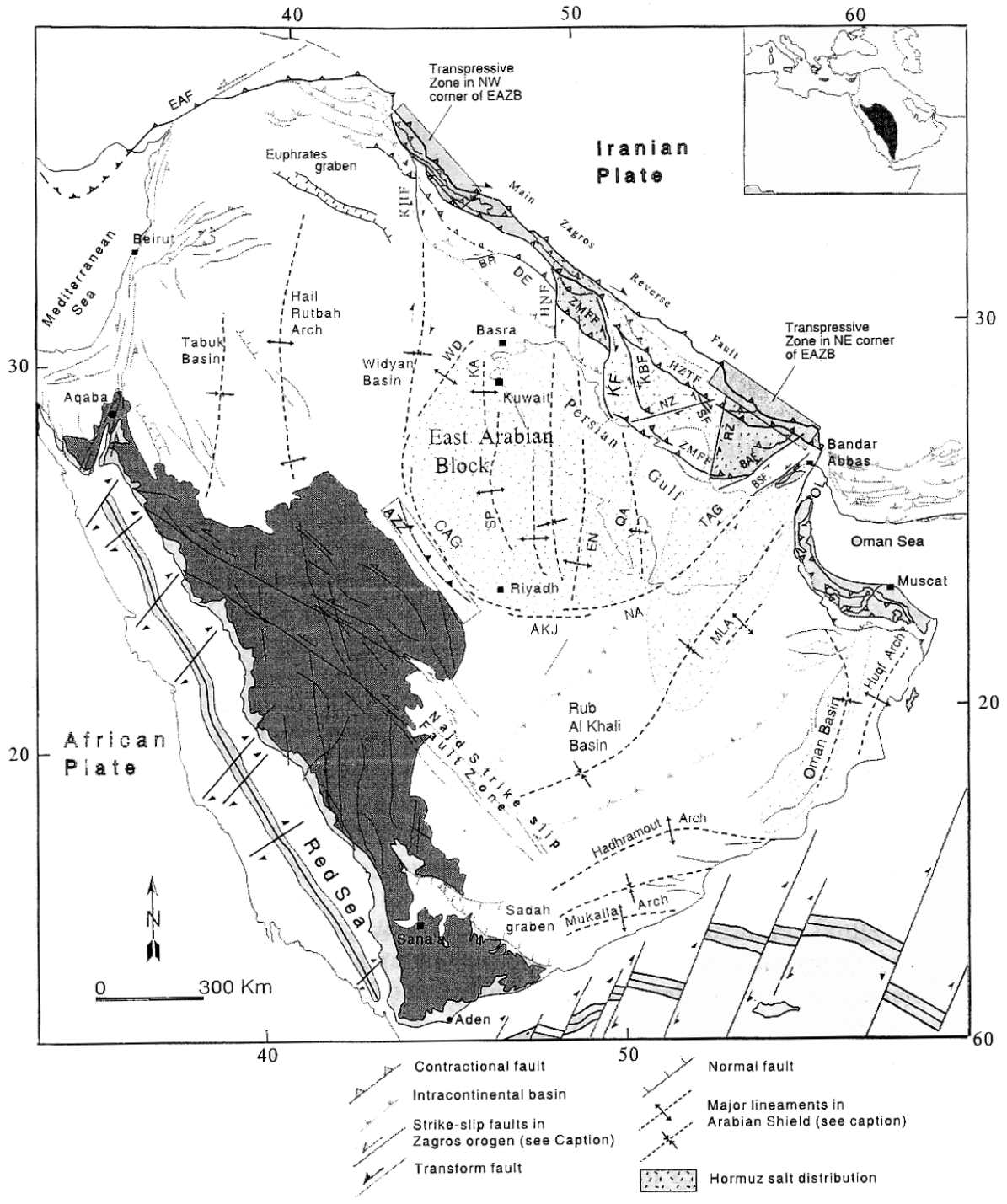

Fig.III.7: Late Precambrian Salt Basin of the Persian Gulf and Arabian Peninsula in addition to the main structural faults and lineaments in the Arabian plate: AKJ, Mughran-Al-Kharj zone; AZZ, A Zilfi lineament; BAF, Bastak fault; BR, Bala Rud fault; BSF, Bostaneh fault; CAG, Central Arabian graben; EG, Euphrates Anah Graben; EN, En Nala Safaniya trend; HNF, Hendijan fault; HRA, Hail Rutbah Arch; KA, Kuwait Arch; KBF, Kareh Bas fault zone; KF, Kazerun fault zone; KH, Khleissia High; KHF, Khanqin fault; MH, Mardin High; ML, Masirah Line; MLA, Mender Lekhwair High; NA, Nisah-sahba lineament; NZ, Nezamabad fault; OA, Oman Basin; ; OL, Oman Line; RZ, Razak fault; SF, Sarvestan fault zone; SP, Summan Platform;TSB, Tabuk basin; WD, Wadi Al-Batin lineament; WSB, Widyan Basin (after Al Laboun, 1986; Beydoun, 1991; Berberian, 1995; Weijermars, 1998; Husseini, 2000; Bahroudi and Talbot, 2003).

III.2. The Zagros belt

III.2.1. The orogenic movements and paleogeography of Zagros

Berberian (1983) has discussed the paleogeography and orogenic movement of Iranian plateau in details. The main orogenic movements of Iranian plateau are summarized hereinafter.

- *Late Palaeozoic and Middle Triassic orogenic movements*

The Late Paleozoic (Hercynian) orogenic belt is presumably associated with the closure of the Hercynian Ocean. The ocean was to the north of Iran (as indicated by the foregoing stratigraphic evidence). The subduction was restricted to the northern side of the ocean in the Middle East region and resulted in prolonged deformation, metamorphism and magmatism.

The deformation apparently started in Carboniferous (around 330 Ma) and finished in Triassic (around 220 Ma). Most of this deformation appears to be associated with intracontinental rifting in the south (during late Paleozoic) and the northward subduction and closure of the Hercynian Ocean in the north. This intracontinental rifting along the present Main-Zagros reverse fault line seems in some way to have prepared the Arabo-Iranian continental crust for the subsequent continental separation. Towards the end of this period, Iran (Central Iran and Alborz) apparently moved as one or a few continental fragments across the Hercynian Ocean leaving new oceanic crust behind to form the High-Zagros Alpine Ocean in the south.

The stratigraphic evidence (continental rift-volcanism, sedimentation consistent with stretching along the Sanandaj-Sirjan belt, regional transgression of the Permian sea with sharp change of sedimentation from lower Paleozoic stable-shelf detritics to Permian shelf carbonates) suggest that Iran and some surrounding countries were becoming detached from Arabia in the Permian (possibly around 240 Ma). However, paleomagnetic poles indicate that Iran remained close to Arabia at least during the early part of this period. The intracontinental rifting and subsequent sea floor spreading process should have thinned the continental crust of the region by crustal extension and by erosion of uplifted crustal blocks. During the passage from Arabia to Eurasia, Central Iran and Alborz should have passed the Equator. The presence of the Laterite Horizons between the Permian and Triassic carbonates in Central Iran may be taken as a paleoclimatic indicator of extensive lateritization in a warm, moist and

tropical climate with seasonal rainfall. Moreover, deposition of extensive shelf carbonate sediments may also support a warm, tropical or subtropical climate (0 to 30° latitude) for this period. The upper Triassic-Jurassic pelagic sediments along the active Central Iran and the passive Zagros continental margins provide the first sedimentary evidence for the appearance of a true oceanic environment in the south.

By Middle to Late Triassic (200 Ma) a major difference in sedimentary environment between Iran (Central Iran and Alborz) and Arabia-Zagros on either sides of the High-Zagros Alpine Ocean is evident. While marine carbonate continued to be deposited in a passive environment on the Arabian foreland (with warm water, tropical-subtropical climate, Tethyan faunas), shallow lagoonal coal-bearing detritial sediments (humid climate) with Asian floras and faunas were deposited in Central Iran and Alborz.

- *Early Alpine orogenic events*

The Early Alpine orogenic events last from 200 Ma to around 65 Ma and apparently represent the period during which the High-Zagros Alpine Ocean in the southern region of Iran closed. Following the Middle Triassic compression phase, the whole region underwent tensional movements characterized by the Upper Triassic continental alkali-rift basalts in the Central Iran and the Alborz.

During the Mesozoic Era two very different environments existed in the Arabian-Zagros foreland and the Iranian unit attached to Asia. The Arabian foreland is subject to progressive subsidence (thinning and extension of the crust) and uniform thick shallow marine sedimentation of shelf carbonates with warm-water Tethyan faunas. There are very striking simple linear facies boundaries parallel to the old continental margin. These were presumably normal faults formed during extensional movement at that time along the passive continental margin. Extension and thinning of the passive margin of the Arabian plate (Zagros belt) was apparently due to the effect of the Permian intra-continental rifting along the Sanandaj-Sirjan belt that proceeded Permian-Triassic rifting.

- *Late Cretaceous orogenic phases*

The Late Cretaceous epoch in Iran is characterized by two episodes of ophiolite emplacement. The emplacement dates and the associated change of sedimentary conditions from oceanic to shallow marine are critical since they may determine the time of ocean closure or collision. The dates of these changes together with the High-Zagros and the Central Iranian ophiolite emplacement seems to be nominally around 75 Ma and 65 Ma. Stratigraphic

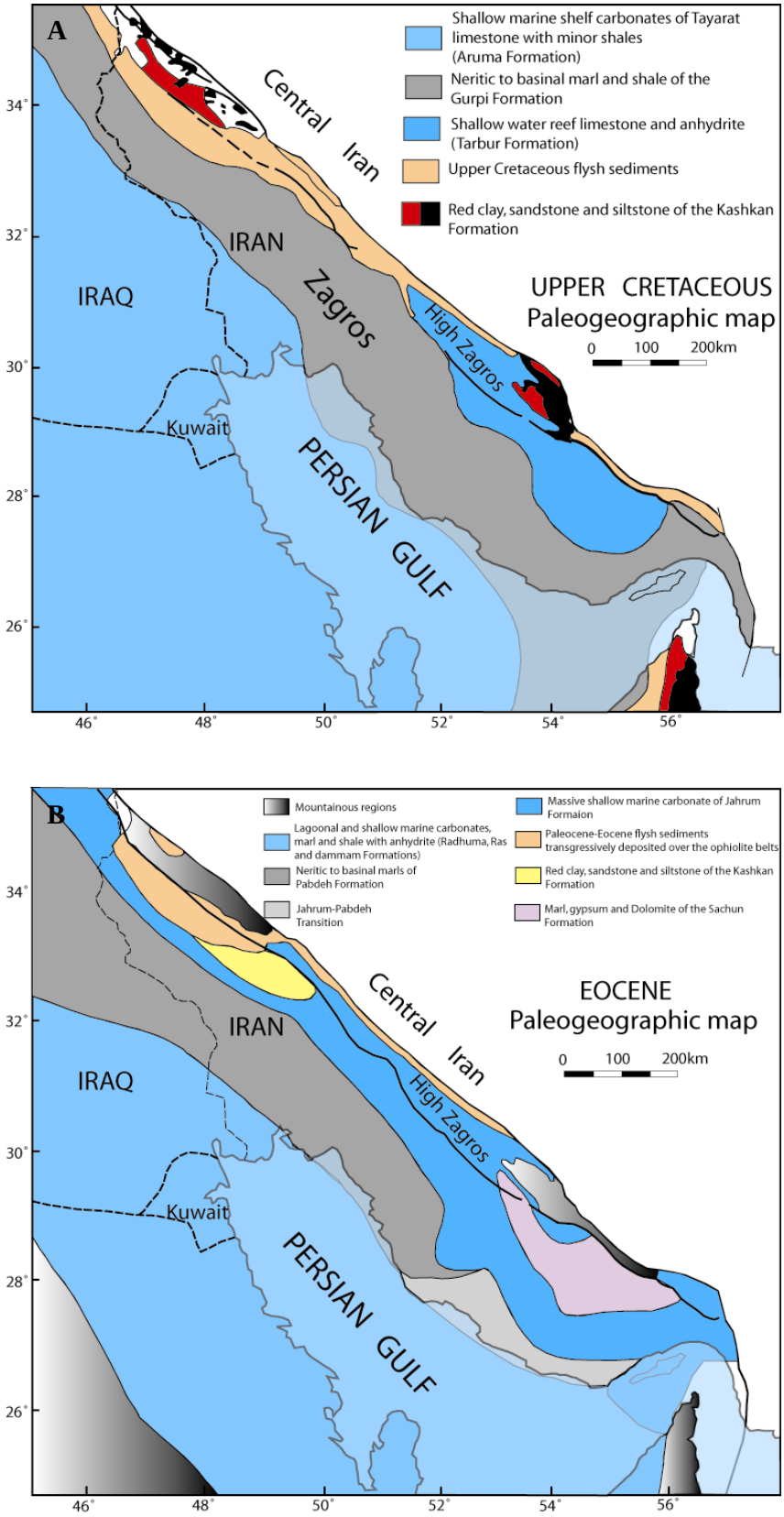

Fig.III.8. Paleogeographic and paleofacies maps during Upper Cretaceous (A) and Eocene time (B).

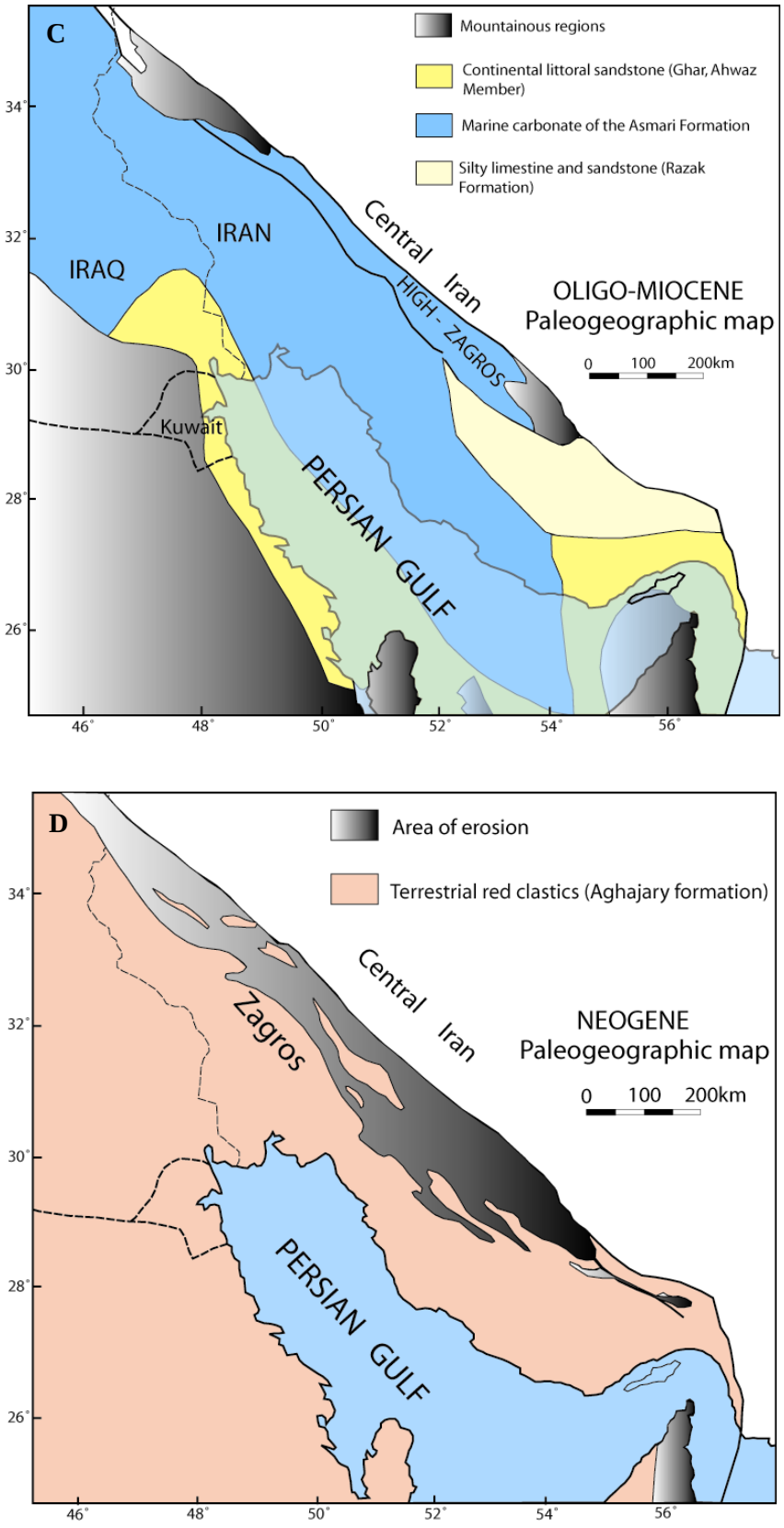

Fig.III.8 (Cont.): Paleogeographic and paleofacies map during Oligo-Miocene (C) and Neogene time (D).

records indicate that during the Santonian-early Campanian (80-75Ma), the High-Zagros and Oman ophiolite-radiolarite belt (Ricou, 1974; Stöcklin, 1977) was apparently emplaced from northeast in the form of a thrust-stack over the Coniacian-Santonian (88-80Ma) shelf carbonates of the Zagros passive margin in the southwest. The fact that the emplaced ophiolite-radiolarite thrust-stack is unconformably covered by the shallow water Maastrichtian sediments (70-65 Ma) provide an upper age limit for ophiolite emplacement along the High-Zagros belt.

- *Middle and Late Alpine events*

The Middle Alpine orogenic events started nearly at the end of the late Cretaceous movements (65 Ma) and ended at about 20 Ma. The Late Cretaceous movements created the main structural features of the present-day Iranian plateau.

The marine carbonate and marl deposition in the narrowing sedimentary basin of the Zagros continued after the Late Cretaceous collisional orogenies. The Late Alpine orogenic events follow continuously from the Middle Alpine and extend to the present. Progressively more of Iran became land with separate mountain-divided narrow basins. By the Neogene time (10 Ma), continental deposits (red beds and conglomerates) supplied from the rising orogenic belts characterize the sedimentation in Iran. The Mesozoic passive continental margin of the Arabian plate (the Zagros belt) underwent considerable amount of shortening and thickening by folding and possibly reversal of motion along the Mesozoic basement normal faults.

During the Middle and Late Alpine orogenic movement, folding and uplift was followed by subsidence in central and north Iran. Thus, although the overall relative motion of Arabia and Asia caused compression and uplift, there are clearly defined diachronous episodes of subsidence and extension. This indicate that the tectonic forces were not supplied from the Asian/Arabian motion alone and presumably must have resulted from motions in the upper mantle or lower crust. However, throughout the period, the major fold belts grow in size with fold axes continuing to form parallel to those initiated during the Late Cretaceous movements. Figures III.8(A-D) show the paleogeography / Paleofacies of Zagros area from Upper Cretaceous to Neogene time.

III.2.2. Stratigraphic and structural division of the Zagros folded belt

In this section different lithostratigraphic and structural divisions of the Zagros area are considered based on different major groups and according to their different deformation

style and mechanical contrasts (Colman-Sadd, 1978). However I tried to pay more attention to the basement especially in the part devoted to its tectonic and related structures because its behavior has not been well understood especially in the Zagros area.

III.2.2.1. Basement Group

Based on Motiei (1993), there is no outcrop from Zagros basement and no oil or gas well has been touched it in this area either. All our information about the Zagros basement is from documents of Arabian Shield, Aeromagnetic Surveys, gravity investigations, stratigraphy investigations, information about central Iran basement and Hormuz cuttings from Salt domes. With regard to all information, the general idea is that Zagros basement is the north-northeast continuation of Arabian-Nubian shield which is entered in Hejaz (Saudi Arabia) from northwest of Africa and crops out in the east of this area and then underlay the east of Saudi Arabia and with a gentle slope, about 15:750 km, underlay the Zagros folded belt. Aeromagnetic surveys (Kugler, 1970; Morris, 1977) and regional facies change shows that the present-day surface topography of the basement is quite complex and its different parts have been affected by various faults whose surface or near surface manifestations are in form of remarkable regional topographic and structural steps (e.g. High Zagros Fault, Mountain Front Fault). The basement surface in areas like the Dezful Embayment is about 15km deep below sea level and in some areas like Lorestan is only 6 km deep below sea level. Toward the Main Zagros Thrust fault, it has come up immediately (Giese et al., 1983).

Based on Aeromagnetic interpretations, it is thought that the basement in the Fars area is not the same as the basement in the Dezful Embayment (Morris, 1977; Kugler, 1970). But there are no strong geological evidence supporting or rejecting of this hypothesis. Lithological composition of the basement is a crystalline granitic-metamorphic complex and possibly it forms from granite, granodiorite, granitoide, schist and maybe ophiolite, marble and slightly methamorphed sediments. Based on isotopic chronology on Hormuz cuttings by Player (1969), Arabian Shield in Saudi Arabia (Alshanti et al., 1983), it is supposed that probably the last plutonic and lithification event has affected the Zagros basement about 800-850 Ma. It is interesting that the granitic basement in southeast of Pakistan has a radiometric age of 870±40 m.y. and granitic basement under Salt Range formation (equivalent to Hormuz formation) of Pinjab in Pakistan has an absolute age of 700 m.y. (Ibrahim-Shah, 1980).

This basement lithification event, which has happened in upper Proterozoic, is related to Assynetic orogeny and is mentioned in different references as Baikaly, Katangai, Arabia and Pan-African events with the age of 950-600 My (Berberian & King, 1981). Based on

Gravity measurements (Dehghani & Makris, 1985), the base of basement in Zagros area has a variable depth between 35 km to 55 km. Combining Aeromagnetic and gravity investigations, a thickness of about 25-50 km can be derived for the Zagros basement.
Based on Zagros basement map of Morris (1977), the thickness of total sedimentary cover may reach to 15Km (Fig.III.10). Figure III.9 shows the stratigraphic and lithologic division of the Zagros folded belt.

III.2.2.2. Lower mobile group

This group consists of the Hormuz salt, which is not exposed in place, but is present as numerous salt diapirs, particularly in Hormuzgan and Fars Provinces. The salt is associated with gypsum, shale, and carbonate rocks, as well as the igneous and metamorphic rocks of the basement. For many years the series was considered to be early Cambrian, but at least part of it is of late Proterozoic age (Stöcklin, 1968b; Kent, 1970). The thickness of this unit has been estimated in a range of 1000m to 4000m (Motiei, 1993).

III.2.2.3. Competent group

The thickest group in the stratigraphic sequence includes sediments ranging from Cambrian to Miocene in age with a comparatively thin development of Cambrian to Carboniferous rocks (in order of 2000m). Carbonate rocks with minor shale, marls, and evaporites dominate the Permian to Upper Cretaceous section (Fig.III.3) with a thickness about 3000 to 4000m. The Upper part of the group consists of Upper Cretaceous to Oligocene shales and limestones, overlain by the massive oil-bearing Asmari limestone. The total thickness of the competent group is 6000 to 7000m.

III.2.2.4. Upper mobile group

Miocene salt, gypsum, anhydrite and marls of the Gachsaran Formation overlie the Competent group with a famous structural mobility and due to this reason, there is no complete type section of this formation on the surface. Based on non-official combined section from different wells in Gachsaran field (Watson, 1962), its thickness is about 1600m.

III.2.2.5. Incompetent group

The remaining part of the stratigraphic sequence consists of a variety of thin-bedded marls, shales, sandstones and conglomerates with minor anhydrite (Lower Miocene to Pliocene), unconformably overlain by the Pliocene to Pleistocene syntectonic conglomerates of the Bakhtyari Formation.

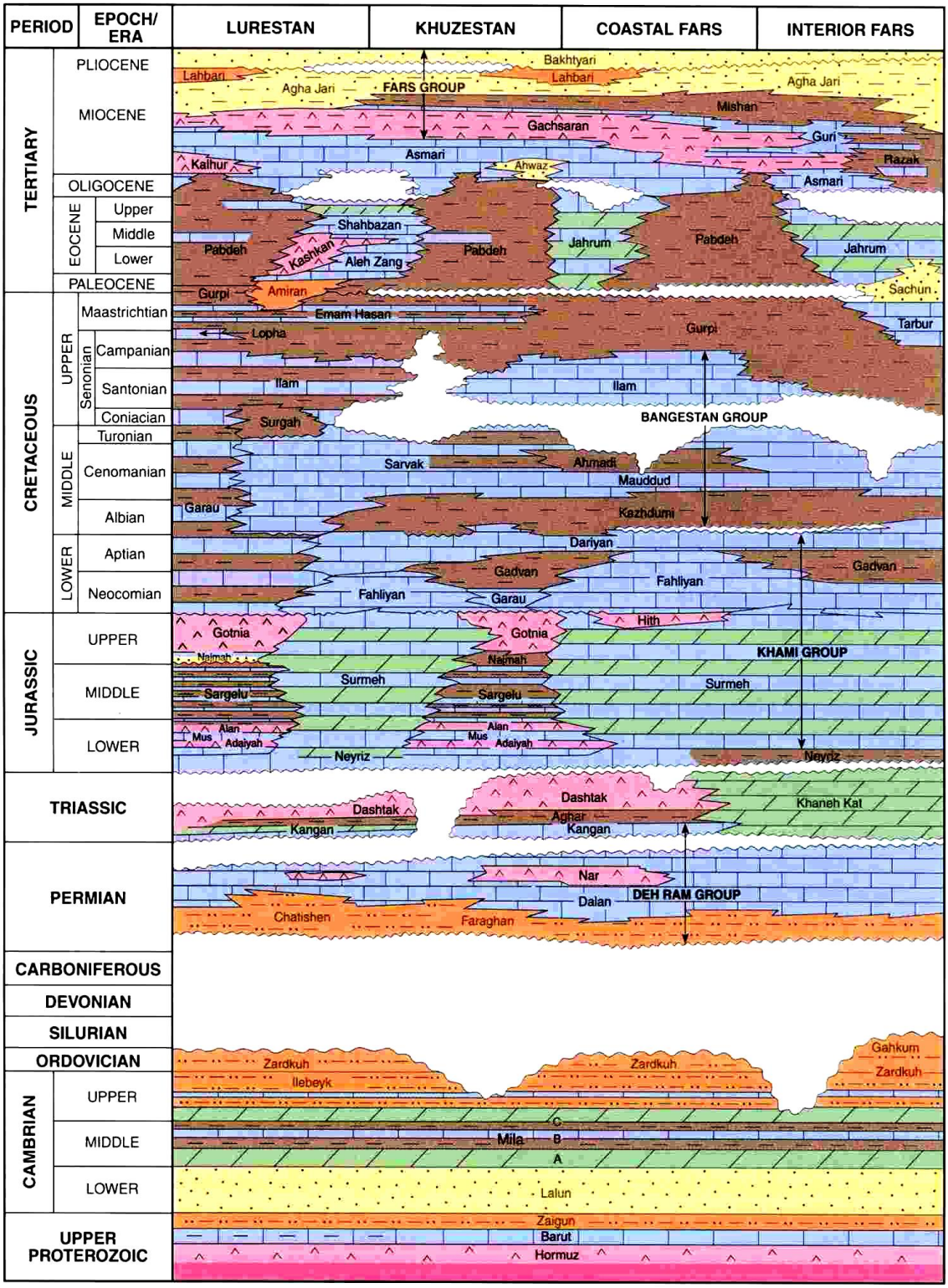

Fig. III.9- Formation correlation chart, southwest Iran. Sources: BP Co. (1956, 1964), James and Wynd (1965), Setudehnia (1972,1975), Szabo and Kheradpir (1978).

III.2.3. Deformation style and kinematic of different groups

Due to the contrast between mechanical properties of the groups mentioned above, during continental collision between Arabian plate and central Iran, they have behaved by various structural style. The basement group is thought either to have remained rigid or to have undergone block faulting (Lees, 1952; Falcon, 1969). The Competent group has become detached from the basement and has been folded independently; the Lower Mobile group forms the zone of detachment (Lees, 1950; O'Brien, 1950). The folds in the Competent group are huge, relatively simple structures. The Incompetent group has been complexly folded and thrust.

Recent developments in geometrical modeling of the folds and balancing software were used by some workers to construct new regional balanced transects across the Zagros (e.g., Blanc et al., 2003, McQuarrie, 2004, Molinaro et al., 2005; Sherkati et al, 2005). One of the main difference among the proposed structural style styles and kinematic in the Zagros folded belt is the role and involvement of the basement in the deformation. Blanc et al. (2003) suggest that the geometries of exposed structures indicate both basement thrust and thin-skinned décollement levels, with major folds possibly nucleated above basement faults. In contrast, McQuarrie (2004) suggest that Lorestan and Fars segments of the Zagros fold and thrust belt are completely detached on lower Cambrian salt and that basement-involved thrusting occurs only in the hinterland of the orogen. Then she concluded that the large-scale geometry of the Zagros orogen may best be explained as a weak salt décollement within the Lorestan and Fars regions that is not present within the Dezful Embayment (Fig.III.10). Molinaro et al. (2005) believe that the involvment of basement faults in deformation of the Zagros, postdated the Zagros fold-thrust belt development occurred late Miocene-Pliocene times (Fig. III.11). Finally, Sherkati et al. (2005) suggest that different final geometries in the Zagros folede belt resulted from activation of intermediate décollement levels in folding and thrusting leading to new thrust faults in shallower levels (Fig.III.12).

III.2.4. General tectonic and morphotectonic features

The active Zagros fold-thrust-belt lies on the northeastern margin of the Arabian plate (Fig.III.10), on Precambrian (Pan-Africa) basement. Shelf sediments laterally equivalent to those in the folded belt are virtually unreformed and overlie the metamorphic rocks of the Arabian shield (Stöklin, 1968a). This is a young (Pliocene) fold-thrust belt currently undergoing 20 mm/yr. shortening (Jackson and McKenzie, 1984; De Mets et al., 1990) and

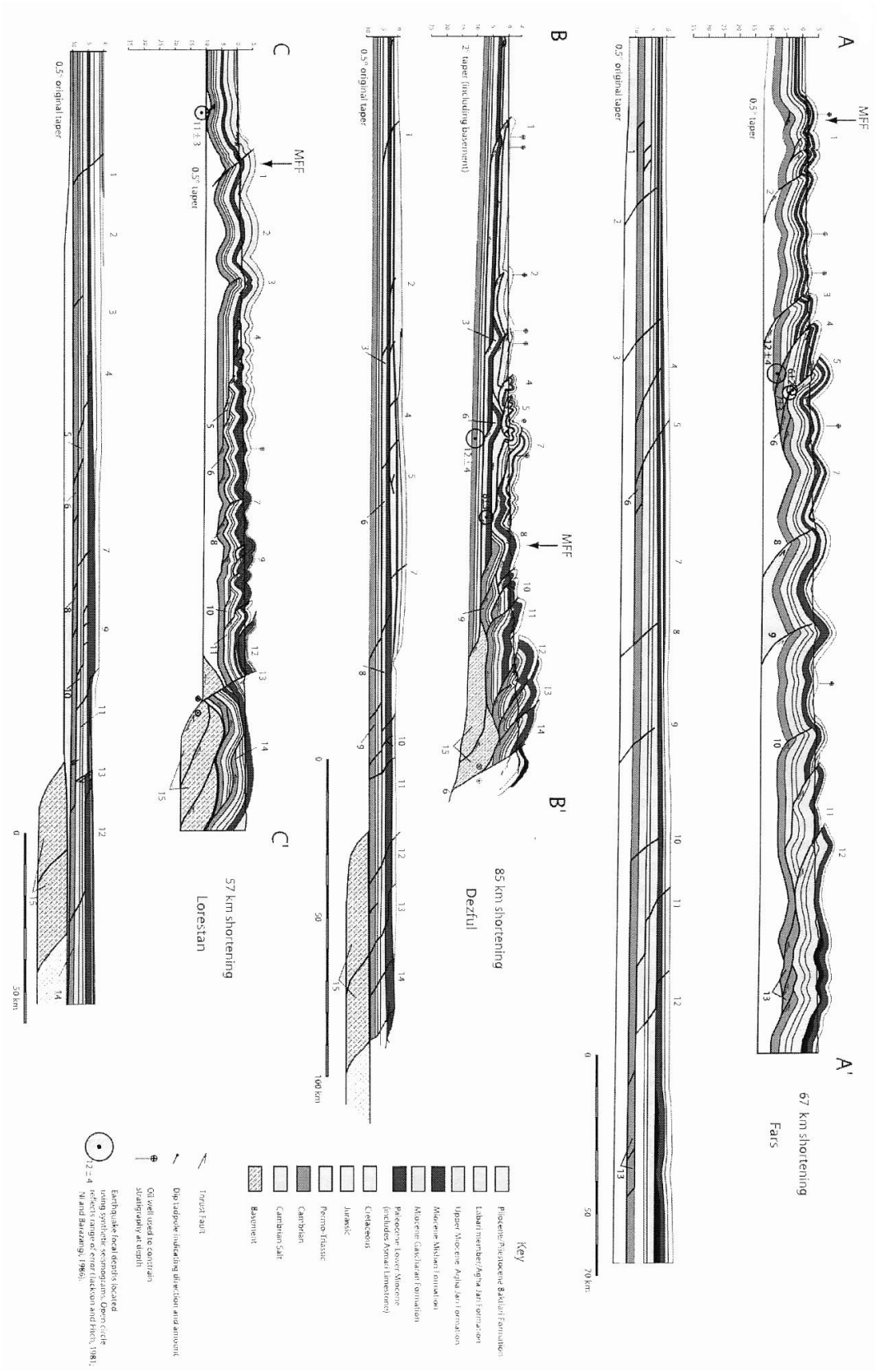

Fig.III.10: Deformation style in the Zagros folded belt (Fars, Dezful, and Lorestan regions); based on McQuarrie (2004); the main shortening was accommodated either by simply buckle folding over a thick basal decollement layer (Fars and Lorestan) or duplex structures (Dezful).

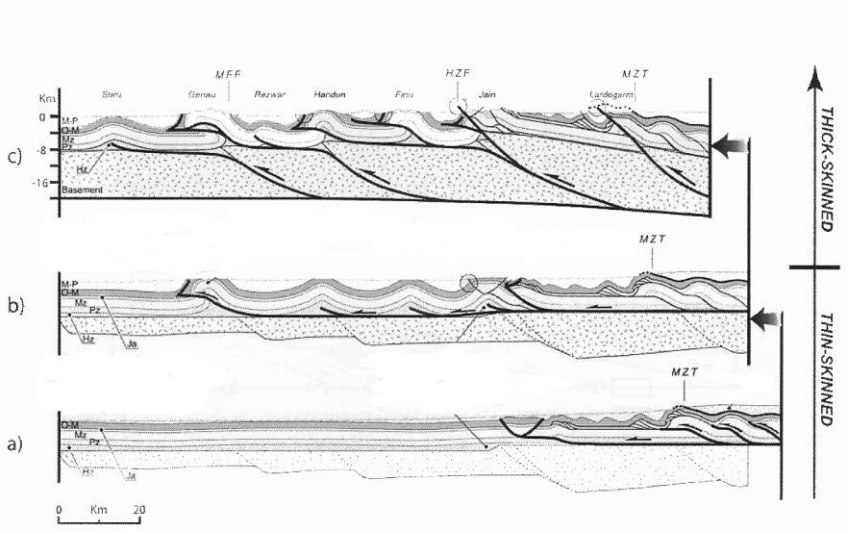

Fig.III.11: Deformation style in the Zagros based on Molinaro et al.(2005); the participation of basement faults in deformation and shortening postdate folding in the cover rocks (thin skinned deformation). (a): middle to late Miocene, (b): late Miocene-Pliocene, (c): Pliocene-recent

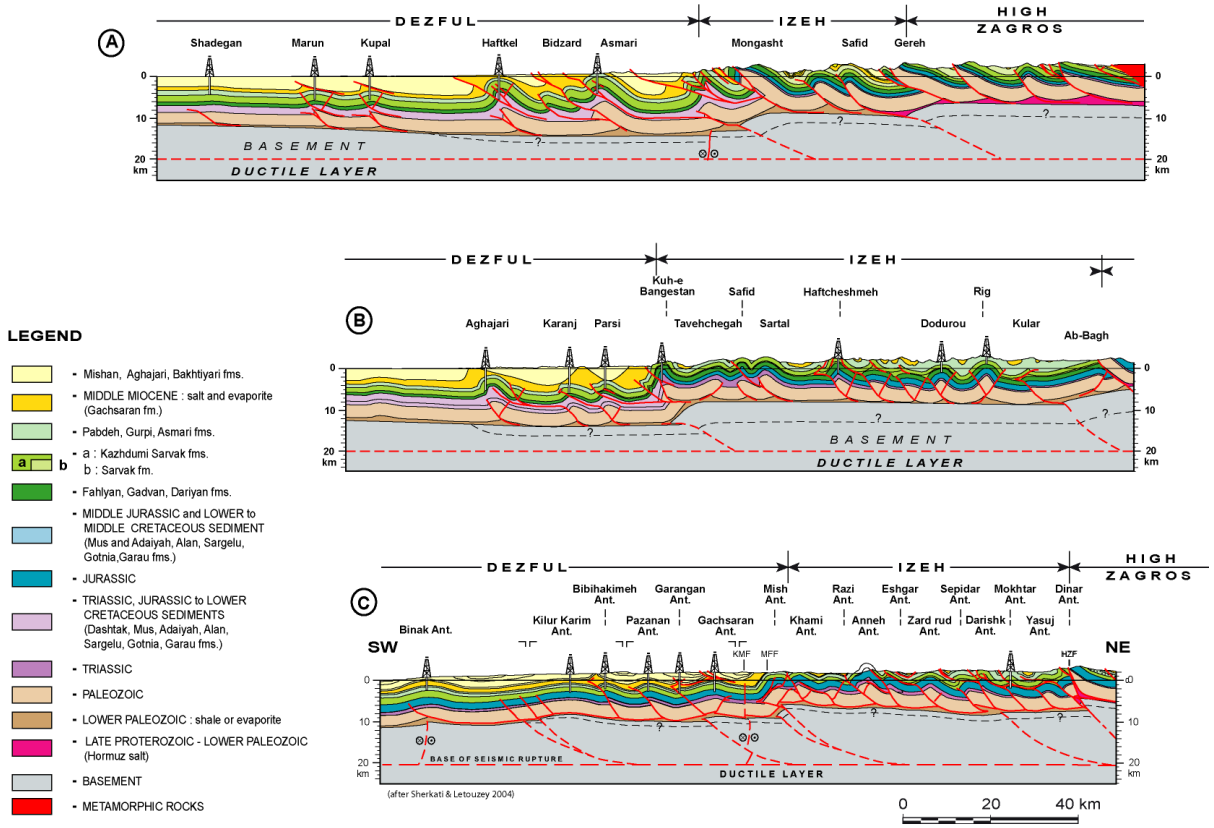

Fig.III.12: Deformation style from NW (A) to SE (C) in the Dezful Embayment and Izeh zone (Sherkati et al., 2005),

thickening as a result of collision of the Arabian and central Iranian plates (Berberian and King, 1981; Berberian et al., 1982; Berberian, 1983).

At the present time, the shortening measured across the Central Zagros by GPS-geodesy is about 1 cm yr^{-1} (Tatar et al., 2002). Jackson (1980) proposed that north-eastward dipping normal faults, postulated to have formed from the rifting of Iran from Arabia during the Mesozoic and located beneath the sedimentary cover, are now reactivated as reverse faults. Most of the large earthquakes (mb>5.0) occur along the southwest Zagros margin, between the coast of the Persian Gulf and the 1500 m topographic contour (Tatar et al., 2004). The focal mechanisms show reverse faulting planes striking parallel to the trend of the fold axes (Jackson, 1980; Jackson et al., 1981; Jackson & McKenzie, 1984; Ni & Barazangi, 1986; Talebian and Jackson, 2004). However, studies of the focal depth of the Zagros earthquakes using body waves modelling show that all of the larger Zagros earthquakes are located at depths less than 20 km (Jackson & Fitch, 1981; Ni & Barazangi, 1986; Baker at la., 1993; Maggi et al., 2000; Talebian & Jackson, 2004). The convergence is still active at the present day, in a roughly N-S direction at a rate of approximately 25-30mm /yr at the eastern edge of the Arabian plate (Sella et al., 2002). This direction is oblique to the NW-SE trend of the orogenic belt. Earthquake focal mechanisms and the GPS velocity field (Talebian and Jackson, 2002) auggest partitioning of this oblique shortening along the faults (MRF) in the Zagros. Recent folding and uplifting of the belt is already evident in the deep river valley cutting the anticlines (Oberlander, 1965), raised beaches, the height of Quaternary alluvial terraces (Berberian, 1995). As an example, uplift of about 1 mm/yr. has occurred in the Shaur anticline (in the Dezful Embayment in the Zagros foredeep) since the late Pliocene (Lees and Falcon, 1952; Lees, 1955; Falcon, 1974; Vita-Finzi, 1979).

III.2.5. Morphotectonic units of the Zagros

The present morphology of the Zagros active fold-thrust belt is the result of its structural evolution and depositional history: a platform phase during the Paleozoic; rifting in the Permian-Triassic; passive continental margin (with sea-floor spreading to the northeast) in the Jurassic-Early Cretaceous; subduction to the north-east and ophiolite-radiolarite emplacement in the Late Cretaceous; and collision-shortening during the Neogene (Falcon, 1974; Berberian and King, 1981; Berberian et al., 1982; Berberian, 1983). (Fig.III.15). The sedimentary column in the belt is estimated to be up to 12km thick (James and Wynd, 1965; Falcon, 1974; Huber, 1977); it includes most of the Phanerozoic without visible angular unconformities (Berberian, 1995).

The Zagros thrust belt is subdivided into five morphotectonic units which step down as five prominent levels to the southwest with different degrees of thrusting, folding, uplift,

erosion and sedimentation (Fig. III.13). These five compressional uplift units which make five parallel trends south of the main Zagros reverse fault line (the Zagros suture) are (M. Berberian, 1995):

(1) the high Zagros thrust belt;
(2) the simple fold belt;
(3) the Zagros foredeep;
(4) the Zagros coastal plain;
(5) the Persian Gulf-Mesopotamian lowland

The deep-seated master thrust faults bordering the morphotectonic units of the Zagros are:

(1) the Main Zagros reverse fault (MZRF: the Zagros suture) and the Main Recent fault(MRF; exposed at the surface);
(2) the High Zagros fault (partly exposed at the surface);
(3) the Zagros Mountain Front fault (MFF);
(4) the Dezful Embayment fault (DEF);
(5) the Zagros Foredeep fault (ZFF);
(6) the Zagros-Arabia boundary (southern limit of the Zagros active fold-thrust belt).

Boundary faults 2 through 5 are master blind thrusts in the Zagros that can be identified at the surface with regard to drastically topographic, thickness and facies changes (M. Berberian, 1995).

One of the most important data sets, pointing to the basement faulting in the Zagros, is the seismic activity. However, a dispersed and poor correlation exists between seismicity at depth and the geological structures on the surface which is due to the presence of ductile layers (Berberian, 1995). Furthermore the instrumental epicentres in the seismic data may be in error by up to 10-20 km (Ambraseys, 1978; Berberian, 1979; Talebian and Jackson, 2004). Berberian (1995) defined the apporoximate location and geometry of the major basement seismogenic faults using geodetic survey, precise epicentre /hypocentre locations and seismic reflections studies in the Zagros, topographic and morphotectonic features, (Fig.III.14).

In spite of that, the interaction between basement faulting and shortening in the sedimentary cover, and whether the shortening is achieved by high angle reverse faulting or low-angle thrusts are not so clear. Jackson et al. (1981) proposed that the current seismicity of the Zagros be explained by the reactivation of older normal faults as high angle thrusts. There

Fig. III.13: Topographic map showing the position of the Zagros folds belt between Arabian plate and central Iran (dark brown color). Down: Simplified transverse cross section of the Zagros active fold-thrust mountain belt. (Falcon, 1974; Hubber, 1977; Berberian; 1995) Abbreviations used: CP = Coastal plain; DFSZ = discontinuous- frictional-seismogenic zone; High Z.T.B = High Zagros Thrust Belt; HZF = High Zagros Fault; K-B = Kazerun-Borazjan active right lateral strike-slip fault; MFF = Mountain Front Fault; MRF = Main Recent active fault; PG = Persian Gulf; ZFF = Zagros Foredeep fault.

is much evidence that during the Mesozoic and early Tertiary the simply folded belt of the Zagros was a subsiding continental margin (e.g. Stocklin, 1968; Haynes & MaQuillan, 1974; Stoneley, 1976). This subsidence began in Permian time (Stocklin, 1968), and it is likely that subsidence was preceded by stretching and thinning of the continental crust by normal faulting, as is the case in intra-continental sedimentary basins (McKenzie, 1978b). The normal faulting was probably listric (Jackson et al., 1981). Thus, the thick sedimentary column of the Zagros was deposited on thinned crystalline basement, which was cut through by normal faults. When lateral compression began in the Tertiary, the listric faults in the basement may have been reactivated as high angle reverse faults, tending to return the basement to its original thickness while causing the younger sedimentary column to take up the shortening by folding (Jackson et al., 1981). Based on Letouzey et al. (2000) the basement thinning by normal faults has occurred in Permian and the inversion and thickening has took place early in

Tertiary (Fig.III.13). Structural-stratigraphic evidence, based on the position of the geologic marker beds (James & wynd, 1965; Falcon, 1961, 1969, 1974), demonstrate the vertical displacements along these faults (thrusts or inverted normal faults) being more than 6 km. Some authors (Molinaro et al., (2005); Sherkati and Letouzey, (2005) suggested that the basement faults only developed at a late stage of the fold evolution.

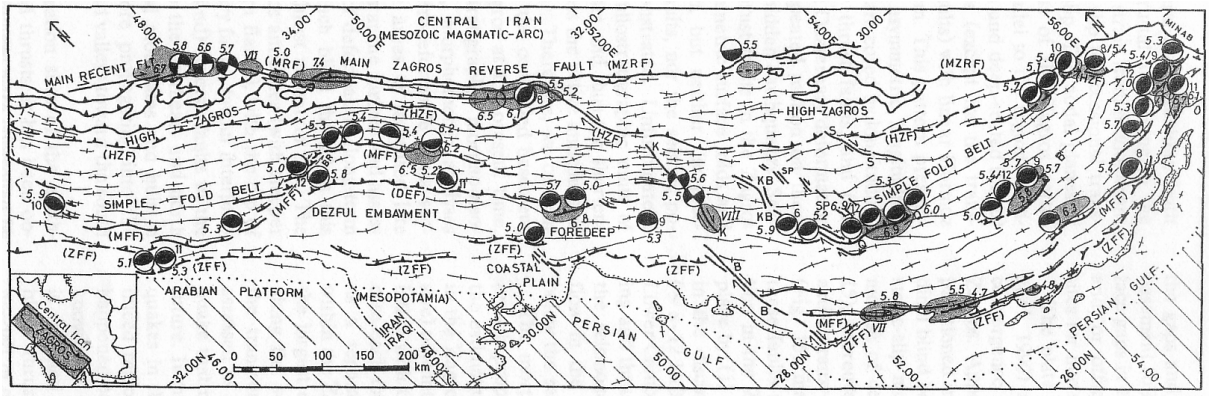

Fig.III.14: Map of the proposed active basement (blind) longitudinal thrust (with sawteeth), the basement-surface transverse active strike slip faults and the longitudinal active Main Recent fault, with some of focal mechanism solutions and macroseismic regions of moderate- to large-magnitude earthquakes in Zagros active fold-thrust mountain belt of southwest Iran. B = Beriz, L = Lar, Q = Qir buried faults. Berberian (1995).

Recent GPS-based estimates of Arabia-Eurasia motion are slower, and suggest a more N-S direction of convergence at ~10-12mm yr $^{-1}$ (Tatar, 2001; Hessami, 2002; Sella et al., 2002). Uncertainty in this direction and rate exist because of ambiguities in the interpretation of sea-floor spreading data in the Red Sea and Gulf od Aden (De Mets et al., 1994; Jestin et al. 1994; Chu and Gordon, 1998; Talebian and Jackson, 2004). Based on Talebian and Jackson (2004), An important change in the fault configuration occurs along strike of the belt. In the NW, overall convergence is oblique to the trend of the belt and the surface anticlines, and is achieved by a spatial separation (partitioning) of the orthogonal strike-slip and shortening components on separate parallel fault systems. The Main Recent Fault (MRF) (Fig.III.12), as a major strike-slip fault system in NW Iran, accommodates the strike-slip component of the N-S convergence between Arabia and Eurasia with ~50 km strike-slip offset (Talebian and Jackson, 2002). By contrast, in the SE, overall convergence is orthogonal to the regional strike and achieved purely by thrusting. In the central Zagros, between these two structural regimes, deformation involves parallel strike-slip faults that rotate about vertical axis, allowing extension along the strike of the belt (Talebian and Jackson, 2004).

III.2.5.1. The High Zagros thrust belt

The High Zagros is a narrow thrust belt up to 80km wide, with a NW-SE trend between the MZRF to the northeast and the High Zagros fault to the southwest. The High Zagros has the highest topography and rainfall in the region. It reaches elevations of 4000m and contains higher mountains and deeper exposures (with lower Paleozoic outcrops in the cores of thrusted anticlines) than the other morphotectonic units of the Zagros Mountains (M, Berberian, 1995). Some shortening occurred in the High Zagros in the Late Cretaceous, at which time ophiolitic rocks and deep sea sediments were emplaced onto the Arabian margin (Stoneley, 1976)

III.2.5.2. The Simple Fold Belt

The Simple Fold Belt of the Zagros is limited to the northeast by the High Zagros Fault (HZF) and to the southwest by the Mountain Front Fault (MFF). It has an average width about 250km to the southeast, 120km to the northwest and a length of 1375 km in Iran. The final saturing of Arabia with Central Iran, probably, began in the Miocene. (Stoneley, 1981) and the main shortening of the Arabian margin in the Zagros, including all of the Simple Fold Belt SW of the High Zagros, began even later, in the Pliocene, probably only 3-5 Ma ago (Falcon, 1974). Thick sequence of late Precambrian to Pliocene shelf sediments, without any visible angular unconformity, has been folded into a series of huge anticlines and synclines (Falcon, 1969). The belt is only 50-60 km wide in the Bakhtiari Mountains with more thrusting and tight folds, shorter wavelengths and steeper surface slops. The simple fold belt contains huge, elongated hogback or box-shaped anticlines, penetrated by salt plugs from the Hormuz Salt in the Zagros Mountains terrain where calcareous ranges of the Eocene-Oligocene Asmari limestone and Mesozoic formations dominate the topography (Fig.III.14). Structures are NW-SE trending in Lurestan, and ENE-WSW trending in northern Bandar Abbas area (Colman-Sadd, 1978). Most of the folds in the simply folded belt are asymmetric and, with a few exceptions, the steepest limbs of the anticlines are on the southwest sides. The mechanism most applicable to the regionally consistent asymmetry of the simply folded belt is shearing in the detachment zone of the Lower Mobile group (Colman-Sadd, 1978). However, this is especially true in the Dezful and Izeh zones but seems not to be applicable in central Fars (Lacombe, personal communication) where the buckle folds are predominant. This term was used for the Zagros folds by Colman-Sadd (1978) and since that time it have been cited by many authors (e.g., Davis and Engelder, 1985; Sattarzadeh et al., 2000; Mitra, 2002; Bonini, 2003; Sherkati et al., 2005) as one of finest examples of large scale detachment

folding. The geometry and kinematics of detachment folds were first discussed in detail by Dahlstrom (1990) and Jamison (1987). The simplest model in a detachment fold consists of a basal incompetent layer acting as a detachment zone, such as shale or salt, overlain by a thick competent unit such as carbonates or sandstones. The basal units responds in a ductile manner to fold growth, with movement of material toward the core of the anticline and descending of the adjacent synclines. Depletion of the ductile layers at the base of the synclines, causing local “touchdown” upon the basement and is followed by the development of the anticline blocks and favors the progressive propagation of a fault through the forelimb (Molinaro et al., 2005).

III.2.5.3. The Zagros Foredeep and the Dezful Embayment

The Zagros Foredeep is bounded to the northeast by the MFF and to the southwest by the Zagros Foredeep Fault (ZFF), which marks the northeastern edge of the alluvial covered Coastal Plain of the Persian Gulf. The formation of the Zagros Foredeep was associated with motion along the MFF and uplift of the simple Fold Belt (Berberian, 1995). There are two regional saddles in the Zagros Foredeep, namely the "Dezful" (in Iran) and the "Karkuk" (in Iraq) Embayments. the Dezful Embayment appears to be a discrete structural unit, with boundaries defined by the Dezful Embayment Fault (DEF) to the north, the Kazerun-Borazjan transverse fault to the east and southeast, segments of the MFF to the northwest and the Zagros Foredeep Fault (ZFF) to the southwest (Fig.III.12). It was a sedimentary basin with pronounced subsidence and thickening of the post-Eocene-Oligocene Asmari deposits in the Zagros Foredeep at the root of the uplifting Simple Fold Belt. The vertical drop of the basin of the Lower Miocene-Pliocene Aghajari Formation (Huber, 1977) is more than 3km in the Dezful Embayment. The anticlinal oil traps of Iran and northeast Iraq are in this belt.

III.2.5.4. The Zagros Coastal Plain

The Zagros Coastal Plain is a narrow feature bounded to the north by the Zagros Foredeep Fault (ZFF) and to the south by Persian Gulf and the Zagros-Arabia boundary, which is the southern edge of the intensely thrusted Zagros folds. The Coastal Plain slopes very gently to the south at a rate of 1m per 5km between Ahwaz and Khoramshahr near the Iraqi border (Berberian, 1995). (Fig.III.14).

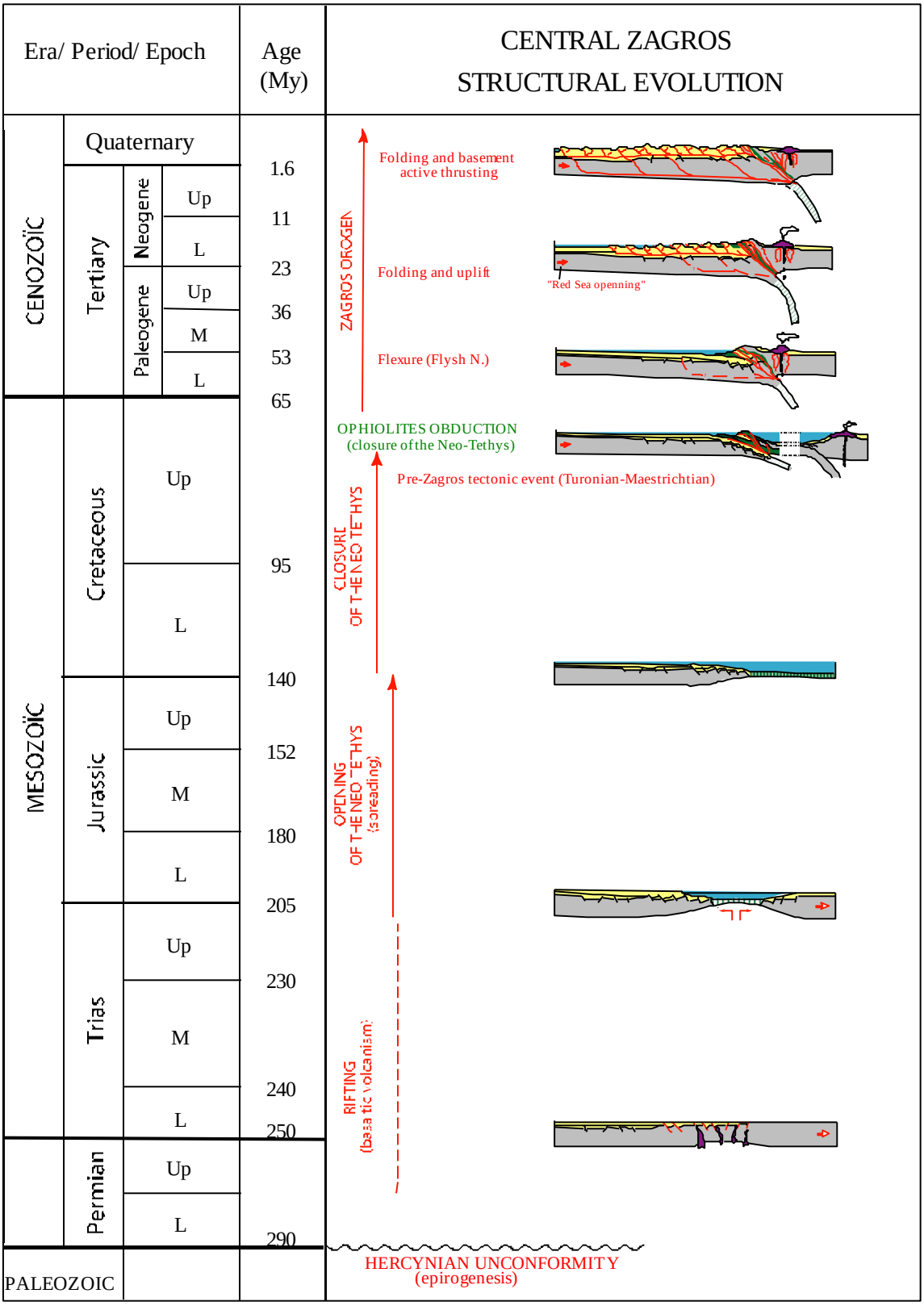

Fig.III.15: Central Zagros structural evolution (after Letouzey et al., 2000)

III.2.5.5. The Persian Gulf-Mesopotamian lowland

This morphotectonic unit lies south and southwest of the Zagros Coastal Plain and is partly covered by the Persian Gulf which is a shallow epicontinental sea with a tectonic origin (a foreland depression) (Berberian, 1995).

III.2.6. Other classification

To cover all the structural and petroleum characteristics of Zagros belt, the following classification is frequently used. It is based on the previous works (Falcon, 1961, Haynes & McQuillan, 1974; Favre, 1975; Berberian, 1995) and is practically used in Iranian Oil companies (Fig.III.16).

III.2.6.1. Complex structural with metamorphic zone

The rocks which have been cropped out in this zone include 1 percent volcanic, 2 percents plutonic, 12 percents metamorphic and finally 85 percents sedimentary rocks (Motiei, 1995). Falcon (1974) has mentioned to four tectonic phases in this zone: The first phase has been occurred before Permian, second phase between Jurassic and Cretaceous, third phase between Middle Cretaceous to Eocene and fourth phase from Miocene to Pleistocene. The most important structural feature in this zone is Zagros Thrust along which, Cretaceous sedimentary series have been thrust over Tertiary.

III.2.6.2. Thrust zone

This zone is equal to High Zagros thrust belt in Berberian's (1995) classification. Falcon (1974), explained the folding in two phases within this zone. First phase in latest Cretaceous and the second phase from near the end of Miocene to recent with the maximum of intensity in Pliocene.

III.2.6.3. Folded belt

Falcon (1974) previously had called this part Simply Folded belt. As the most of known oil fields in Zagros are in this belt, many surface and subsurface studies including seismic and other geophysical methods and drilling of about 2000 exploration and production wells showed that the folding of this belt is not so simple. Participation of basement and its faults, exposure of salt domes, the presence of big faults below the critical points of the folds and the presence of depressions, show the complexity in the folding style of this belt (Motiei, 1995). So the term of “zone” is not used for this belt as there are some big structural zones

within it. In this classification Folded belt is equal to the Simple Fold Belt, Zagros foredeep and Dezful Embayment and the Zagros Coastal Plain in Berberian (1995) classification.
There are different zones in this belt as follows:

- *Lorestan zone*

The part of folded belt in which, north-northwestern boundary is near the political boundary between Iran and Iraq. The East and northeastern boundary is High Zagros Thrust Fault and southern limit is Balaroud flexure.

- *Izeh zone*

The Izeh zone is part of the folded belt delimited to the north-northeastern by the High Zagros Fault (HZF) and to the south-southwestern by the Mountain Front Fault (MFF), and its northwestern limit is along Balaroud flexure.

- *Dezful Embayment*

Dezful Embayment is another structural zone in Folded Belt containing most of Iranian oil fields. Primarily, this name introduce a topographical characteristic but generally it is part of Zagros folded belt in which, there is no outcrop of Sarvak Formation (U. Cretaceous). Dezful Embayment is surrounded by three important structural elements. North-northwestern limit is Balaroud flexure (fault), east-northeastern limit is Mountain Front Fault (MFF) and its south-southeastern limit is Kazeroun Fault (KZ).

- *Abadan Plain*

Abadan plain is a structural zone at the end of southwest of Iran. Its northern and northeastern limit is Zagros Foredeep Fault (ZFF), its southern limit is Persian Gulf and Iraq and its western limit is Iraq-Iran border. There is no seismic activity (seimicity) in this zone. The anticlines in this zone have no surface manifestation in this area and even there is no structural clusure at the top of Asmari Formation within some of these anticlines. And finally, The general trend of these anticlines is north-south, which is different with the general trend in Zagros folded belt.

- Fars zone

Kazeroon fault is western limit of this zone and its eastern limit is Minab fault. Northern limit is thrust zone and its southern limit is almost Persian Gulf coast line. Bandar Abbas Hinterland is suppose to be part of this zone by some authors.

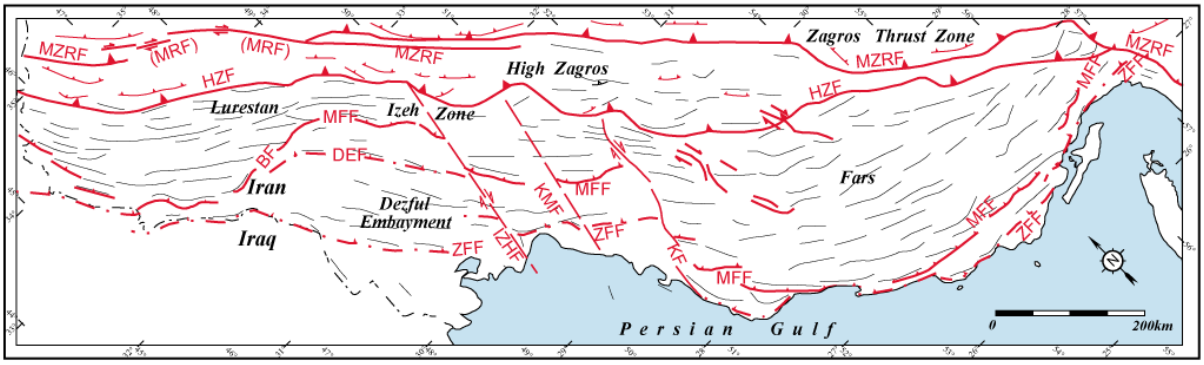

Fig.III.16: Zagros units' classification based on structural and Petroleum characteristics. (modified from Motiei, 1995).

III.2.7. Timing of deformation in the Zagros folded belt

Several local and regional unconformities, in addition to thickness and facies variations have been related to continuous convergence and reactivation of deep seated faults in the Zagros basement between Late Cretaceous and Early Miocene (Berberian and King, 1981 ; Koop and Stoneley, 1982). Hesami et al. (2003), documented local post-Eocene unconformities and attributed them to the beginning of folding and uplift in the NE of the Zagros belt. Homke et al. (2004) defined the beginning of the deformation in part of the Zagros foreland basin (Push-e Kush arc) at 8.1 to 7.2 Ma based on magnetostratigraphy study of Miocene-Pliocene sediments. Agard et al. (2005) documented several major tectonic events taking place at the end of the Cretaceous, of the Eocene and from the Mid-Miocene onwards (ca. <20-15 Ma) and stated that collision must have started before ca. 25-23 Ma. It means that strike-slip mouvements predating Plio-Quaternary (~5 Ma) offsets along the MRF (Talebian and Jackson, 2002), notably between the late Eocene and late Oligocene, and possibly at the end of the Cretaceous.

Conclusion

Arabian Plate tectonics has played an important role in the development and evolution of Zagros basin. However there are still some poorly understood points concerning basement tectonic and its features, which affected by initial rifting phase(s) or later basement fault inversion, and the way in which the sedimentary basin(s) affected by this tectonic.

Although basement and salt tectonic were the main responsible for different oil traps formation in eastern margin of the Arabian plate. The manifestation of such features apparently have been masked and superimposed by Zagros orogeny. It could be one of the reason for some structural complexity within Zagros folded belt. Also to prove the idea concerning the effect of longitudinal and transversal faults of basement on the style of Zagros folds especially in Dezful Embayment, we need more evidence and detailed studies. Regardless of our weak knowledge about these basement faults, they built the main basis for making different morphological classification and subdivision of the Zagros region.

Deformation style in the Zagros folded belt is controlled by the basal and intermediate décollement levels in the cover and also the envolvement of basement faults in deformation. Different ideas exist regarding relative timing of basement/cover in deformation and even the participation of basement in the shortening. Finally the absolute timing for deformation onset and stress partitioning are poorly understood. More evidence and observations are necessary to reduced uncertainties in this regard.

CHAPTER IV: The Asmari Formation

Introduction

The Oligo-Miocene Asmari Formation is significantly present in numerous oil-fields in a belt some 1200km long by 200km wide extending from northeast Iraq to southwest Iran (Beydoun, 1988). This area coincides with the thickest development of Cenozoic sediments, and is thus the optimal area for maturation of underlying Mesozoic source rocks.

Intensive studies were done and still are in progress on typical outcrops to understand dynamic behavior of carbonate fractured reservoirs in this area. The lack of suitable subsurface data, may be one of the reasons for a publication shortage in this domain in Iran. Perhaps long life and high rate production of most carbonate reservoirs by natural depletion without any serious problem related to fractures is a factor for lack of a comprehensive carbonate fractured reservoir study.

The Asmari oil fields of Iran are true giants. Most have recoverable reserves greater than I billion bbl each and many having much more (Hull et al., 1970). The Asmari reservoir is poor in matrix porosity and matrix permeability. Very high production rates are possible because of extensive reservoir fracturing. These rates can be maintained for very long periods because of the great vertical oil columns. The Asmari fields are prime examples of anticlinal traps and of the effect of fracturing on reservoir performance. The lithology and distribution of this Formation are described in this part. Then a review of previous studies follows including fracture studies in Arabian basement and cover rocks in the Asmari Formation.

The information about the Asmari Formation which will be discussed in the following sections is based on the previous studies and published papers which are mostly republished and were discussed by Motiei (1993).

IV.1. Lithology and Distribution

The name of this Formation was taken from Kuh-e Asmari (Asmari anticline), southwest of Masjed-Soleyman City, southwest of Iran. The upper and lower limits of Asmari Formation are in concordance with the Gachsaran and Pabdeh formations in the type section.

Richardson (1924) measured Asmari type section (Fig.IV.1) in Gel-e Torsh valley in Asmari anticline, southwest of Iran. Later on, Thomas (1948) measured and described this type section precisely. He defined a thickness of 314m for this Formation including dense, cream to brown colour limestone with well-developed fractures and some shale beds. In the

type section, lower Asmari does not exist. Based on James and Wynd (1965), this part has been replaced by marl and shale of the Pabdeh Formation.

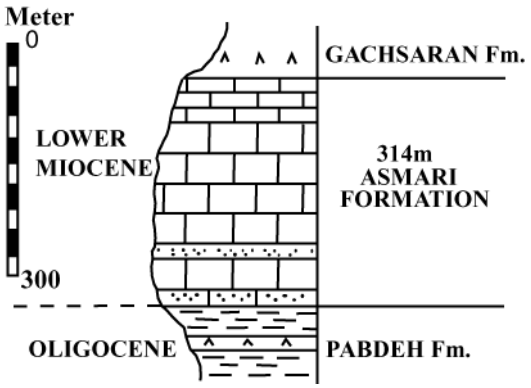

Fig.IV.1: Asmari type section in Gell-e Torsh Valley

- *Complementary section*

As it was mentioned, the lower part of the Asmari Formation doesn't exist in its type section. But considerable thickness of the lower parts of this Formation is seen in southern part of the Dezful embayment, either in outcrops (Takab Valley of Kuh- Khaviz) or subsurface (oil field wells around Gachsaran and Behbahan). A thickness of 420 to 500m has been recognized. So, Stoneley (1975) chose the surface section of Asmari Formation in Takab Valley of Kuh-e Khaviz, 30 km north of Behbahan, as complementary section.

From an age viewpoint, the Asmari Formation starts from Oligocene and continues to Burdigalian of lower Miocene. The base of Asmari Fm. has different ages. Along mountain front and southern oil fields it has been dated Oligocene and in northern oil fields of Dezful embayment, this part is defined by basal anhydrite dated Aquitanian. Upper limit of Asmari Formation above north part of an arbitrary line, which passes from north of Kharg Island to north of Darquain field (Fig.IV.2), is conformable with the Gachsaran Formation. But south of this line, this limit is a transition state from calcareous sandstone to evaporite and sandy limestone, which is taken as marginal facies of the Gachsaran Formation. Owen & Nasr (1958) named this marginal facies as Lower Fars.

In the northern limits of the Asmari basin, like southwest of Sisakht area, only the lower Asmari is seen and its upper limit is called Razak Formation. Razak Formation is seen in northern area of the Gurpi anticline and also Naft anticline in Lurestan as upper limit of the Asmari Formation (Fig.IV.2).

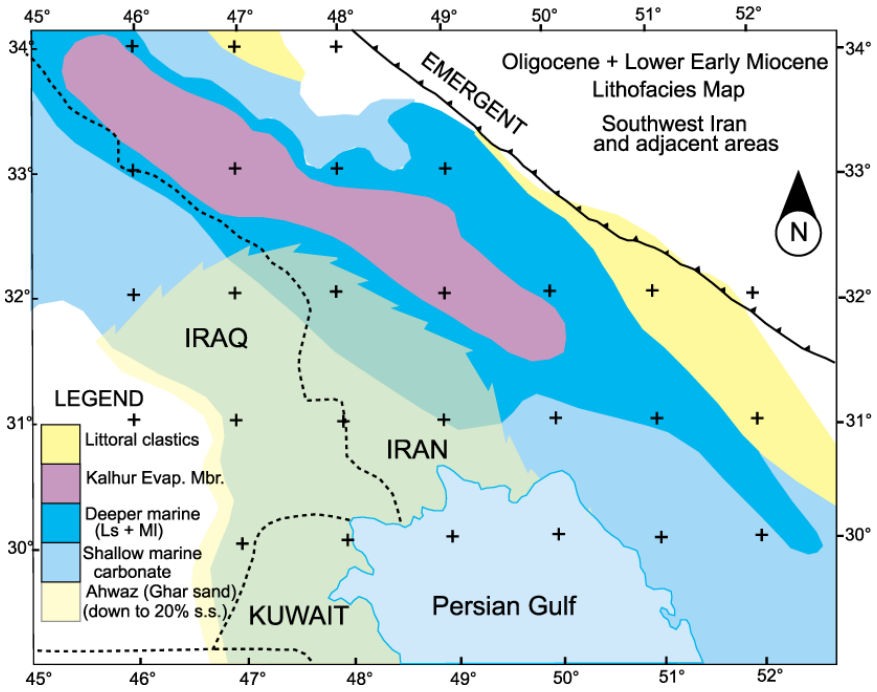

Fig.IV.2: Lithofacies map of Oligocene-lower early Miocene (Asmari Fm.) showing different lithofacies units in Zagros area, Modified from Motiei (1993) See text for details

In Fig.IV.3, the relations of the different Asmari units in Dezful embayment are shown schematically. As it can be seen in this figure, a carbonate shoal occurs on either side of the basin. The Oligocene shallow marine limestone has deposited on either side of deeper Pabdeh basin. Deposition of Aquitanian sediments (lower–middle Asmari) continued up to the disconformity surface. Also, middle Asmari changes facies to anhydrite towards deep part of the basin. In the latest Aquitanian, middle-upper Asmari carbonates was deposited all over the basin. Meanwhile, from upper Eocene, Oligocene, Aquitanian or perhaps Bourdigalian, sandstone has been appeared in southern margin of the basin, which is called Ahwaz sandstone member. The maximum development of this sandstone member is up to the erosional unconformity at the base of upper Asmari. However, local appearance of sandstone has been reported in upper Asmari. However, this figure (IV.3) is quite simplified and does not show lithofacies characteristics of Asmari Formation in details. Different rock units of Asmari Formation have been shown in Fig.IV.4.

IV.2. Bio-chrono facies division of the Asmari Formation

Thomas (1948, 1949), divided the Asmari Formation into three parts of lower, middle and upper Asmari based on fossils and relative chronology. However, the separation of these parts on the outcrops and aerial photos is not possible.

- *Lower Asmari limestone*

Limestone of this part is almost uniform with wackstone and packstone texture and sometimes dolomitic. The lower Asmari limestone in Dezful embayment has been always taken as Oligocene in age. In most of the outcrops in Lurestan, the lower Asmari limestone placed directly on the Shahbazan carbonate (upper Eocene). More towards north in the area, lower Asmari does not exist. Possibly this area was out of the sea from the Upper Eocene to the Oligocene. Towards southern areas, the Oligocene lower Asmari limestone changes its facies to shale of the Pabdeh Formation, which is deep-sea sediment. From Lurestan towards Dezful embayment, the lower Asmari limestone has deposited in the shoal of the Pabdeh basin. In the lower Asmari sedimentary series, no reef has been observed with an exception in Iraq (Henson, 1951, Bellen, 1956).

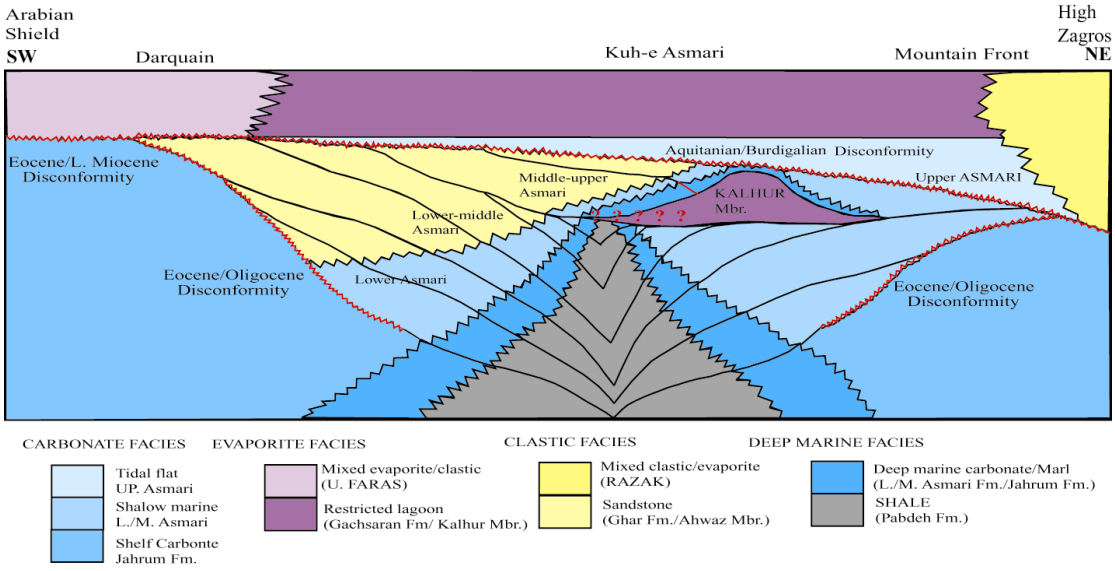

Fig.IV.3: Schematic relations of different Asmari units in the Dezful embayment from high Zagros area towards Arabian shield, modified from Motiei (1993). See text for details.

- *Middle Asmari limestone*

Middle Asmari Formation could be divided into two parts. Lower part, which is lithologically similar to the lower Asmari. Lithology of the upper part has been affected by the development of Sabkha dolomites.

The lower part of the middle Asmari limestone, showing a repetition of shelf-Basin sediments in lower Aquitanian. This limestone has progressively covered disconformity surface of the Eocene carbonate (Shahbazan Formation towards the north and Jahrum Formation towards the south of basin).

Inside the Pabdeh sedimentary basin, the Oligocene marls change their facies vertically and gradually to evaporitic facies of the Kalhur member, the basal anhydrite of the Asmari Formation. These evaporitic sediments are equivalent to lower carbonates of middle Asmari. From lithological viewpoint, lower carbonates of the middle Asmari include severely dolomitized wackstone and packstone, which is uniformly developed in the area. During this period, the Ahwaz sandstone towards south and southwest of the Zagros has considerably developed.

In the upper part of the middle Asmari, Pabdeh-Kalhur basin totally disappeared and with the regression of northern shoreline, the entire basin covered by a shallow shoal environment. In this shoal, carbonates like mudstone, wackstone and fine grain dolomitic carbonates have deposited. With development of the upper part of the middle Asmari, the central trough of the Asmari basin during lower and the middle Asmari is filled and levelled and the Ahwaz sandstone member reaches to maximum state of development.

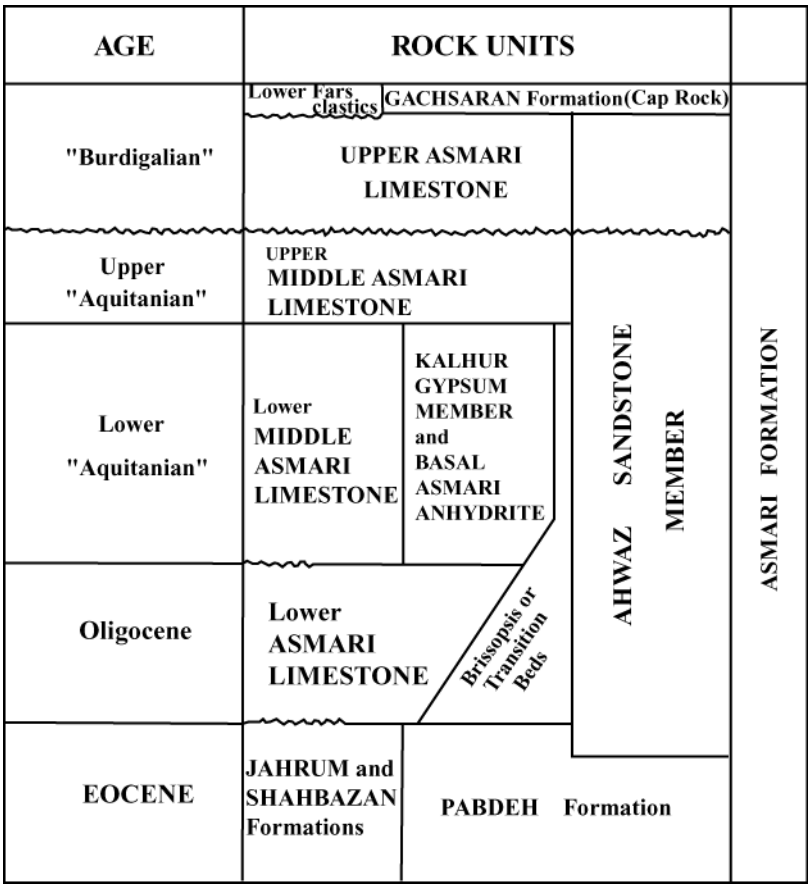

Fig.IV.4: Different rock units of the Asmari Formation . Motiei (1993).

- *Upper Asmari limestone*

From a genesis viewpoint, the upper Asmari limestone is different from the middle and the lower Asmari because upper Asmari limestone deposited in a marine sedimentary environment, which was progradating during the Burdigalian in the region. This limestone, all over the area, has been deposited in the form of alternative wackstone and packstone, which is dolomitized and accompanies anhydrite towards south.

The deposition of the upper Asmari limestone resulted from transgresion of Burdigalian-sea which started from northeast. During the middle Asmari, in the northern regions, a barrier has developed from the Shahbazan Formation sediments, which northern shoreline was on the flank of this barrier within this period. Transgresion in Bourdigalian period covered this barrier and deposited a relatively thick mass of sediments in the south of this ancient barrier.

Southern limit of this progradational basin is an arbitrary line, which passes from north of Kharg Island, south of Binak field and south of Darquain field. In southern areas of Dezful embayment, upper Asmari limestone appears in Sabkha facies form. Beyond northern limit boundaries of Dezful embayment, Asmari has deposited over an unconformity on Shahbazan Formation carbonates. The appearance of conglomerate in the base of upper Asmari in this region has been reported in unpublished technical notes by Slinger and then by Watson (1962). Shepherd et al. (1961) reported this conglomerate at the base of upper Asmari in PoshtKuh and Kuh-e Anaran in Lurestan region. This unconformity has disappeared towards south but its effect in the form of disconformity (erosion) between upper and lower Asmari limestone ,even with the similar lithology, is seen. Probably this disconformity eroded some upper parts of Ahwaz sandstone member.

- *Brissopsis or transition beds in Asmari*

Within oil fields in north of Dezful embayment and also in Kuh-e Asmari, a relatively low thickness series of marl and shale underlay the Asmari carbonate and sit on the basal Asmari anhydrite. These series are called Brissopsis of transition beds.

Bio-stratigraphical characteristics of the Asmari Formation for the first time defined by James and Wynd (1965) and second time they were revised by Adams and Bourgeois (1967) who defined three assemblage zones and two new assemblage sub-zones. As these definitions are frequently used in the region and in all related bio-stratigraphical zonation within the Asmari Formation, they are explained here, upside down within this Formation.

1. Borelis melo group – Meandropsina Iranica assemblage zone, Adams & Bourgeois (1967)

This assemblage zone is defined by the noticeable appearance of following micro-fossils:

Borelis melo curdica, Borelis melo melo, Meandropsina iranica, Valvulinid sp.2, Miogypsina irregularis, Dendritina rangi, Peneroplis farsenis,

The thickness of this assemblage zone near Mountain Front is about 300m. I n this region the upper part of this assemblage zone is changed to deep facies, e.g., near north of DehDez (Kuh-e Razi, see chapter V). The microfossils which could be observed in this deep facies include:

Globorotalia s.s., Tuborotalia s.s., Globogerina spp., Orbulina?? spp.

The age of these microfossil, mentioned above, were defined as Bourdigalian and probably upper Aquitanian and considered as the Upper Asmari.

2. Miogypsinoides – Archaias – Valvulinid sp.1 assemblage zone, Adams & Bourgeois (1967)

This assemblage zone is defined by the appearance of following microfossils:

Archaias Kirkukensis group, Valvulinid sp.1, Miogypsinoides (flood);

Other microfossils that accompany this assemblage zone include:

Kuphus arenarius, Elphidium sp. 14, Archaias asmaricus, Archaias hensoni, Miogypsinoides complanatous, Astroterillina asmariensis, Spiroclypeus blankenhorni, Pseudolitionella reicheli;

The age of this assemblage zone defined as Aquitanian which is equivalent to Middle Asmari.

3. Eulipidina spp., Nephrolepidina spp. Nummulites assemblage zone, Adams & Bourgeois (1967)

This assemblage zone is defined based on following microfossils;

Eulepidina spp., Nephrolepidina spp., Nummlites spp.

Other index microfossils which could be seen in this assemblage zone include;

Eulipidina elephantina, Eulipidina dilitata, Nummulites fichteli – intermedius group, Nummulites vascus – incrassatus group, Nepherolepidina tournoueri Lepidocyclina sp. 1, Heterostegina costata, Heterostegina praecursor, Spiroclypeus ranjanae, Subterranophylum thomasi, Archaias operculiniformis, Astrotrillina paucialveolata.

The age of this assemblage zone is generally defined as Oligocene but the related stages (Lattorfian, Rupelian, and Chattian) within the Lower Asmari series, belonging to Oligocene times can not be distinguished.

IV.3. The members of the Asmari Formation

There are two members in this Formation: Ahwaz sandstone member, which is seen in southern areas of the Dezful embayment; and evaporitic Kalhur member in northwestern of the Dezful embayment and southwestern of Lurestan region.

- *The Ahwaz sandstone member*

In Ahwaz, Mansouri, Ab-Teimour, Cheshmeh-Khosh and some other oil fields, Asmari Formation consists of the series of limestone, limy sandstone and sandy limestone with some shale interbeds. This sandstone is called Ahwaz sandstone member. Initially, this sandstone was divided in to upper and lower parts. The upper part is correlated as the wedge-edge of the Ghar Formation of Kuwait and southern Iraq and this relation is quite clear in Jufair, Darquain and Khuramshar wells. The lower part of this sandstone has developed in the fields like Ahwaz and Maroun in the form of tongue, interfinger and lens bodies within Asmari Formation. There is no equivalent Formation in Iraq for this part. So, the name of Ahwaz sandstone Member is more suitable for this part.

James & Wynd (1965) chose the interval, 2455.5-2668.8m as the type section for Ahwaz sandstone Member (Fig.IV.5). Here sandstone directly overlies the Pabdeh and at Mansouri, just south of Ahwaz, limestone is found both above and below the Ahwaz Member. Ahwaz sandstone Member ranges in age from Oligocene to Early Miocene.

Watson (1962) divided the Asmari Formation of Ahwaz oil field into 10 parts. He called the fourth part as superior sandstone and the third part as inferior sandstone. Walker (1969) divided the Asmari Formation of Maroun field to four layers or sedimentary period, in which each layer consists of two carbonate and sand sub-layers. Also, he defined a fifth layer, which chronologically reaches to Eocene and has been seen just in a few oil wells.

Adams (1969) studied the stratigraphy of the Ahwaz sandstone Member and defined its upper limit as the base of the upper Asmari. He took in to account the lower limit as a diachronous surface. Using stratigraphic features, he showed that the Ahwaz sandstone in Kharg and Darquain fields belongs to Aquitanian in age and overlay the Jahrum Formation (middle Eocene) by a disconformity equivalent to the one between Ghar and Damam formations in south of Iraq and Kuwait. He believed that this disconformity disappeared towards north regions and the Ahwaz sandstone overlay the Pabdeh Formation concordant. Also, he defined the age of the Ahwaz sandstone from Oligocene to Aquitanian.

Mc. Coard (1974) classified the Asmari Formation of Ahwaz field, with special regards to the Ahwaz sandstone Member, as follows (Fig.IV.6):

- Upper Asmari; including A1and A2 layers in Ahwaz field equivalent to first layer in Maroun field.
- Middle Asmari; including A3, A4 and A5 layers in the Ahwaz field equivalent to second layer in the Maroun field and A6 layer in the Ahwaz field equivalent to third layer in the Maroun field.
- Lower Asmari; including M2 and A7 layers in the Ahwaz field equivalent to forth layer in the Maroun field.

Wlaker (1969) introduced the fifth layer of the Maroun field at the base of the Asmari and in part of the Pabdeh Formation top and considered it as equivalent of A10 and A11 in Ahwaz field.

The thickness of Ahwaz sandstone Member is quite variable and its changes does not follow a specific trend. Regarding chrono-stratigraphy, there are considerable differences. For example, the Eocene and the Oligocene sandstones which are seen in Ahwaz and Maroun fields, are absent in Mansouri and Ab-Teimour fields or earliest sandstone which is seen in these two later fields, belongs to Aquitanian. So, Mc. Coard (1974) divided the Ahwaz sandstone Member into two more general parts; the lower and the upper sandstone. He called the sandstone of upper and middle Asmari as the upper sandstone and the sandstone of lower Asmari and the upper Pabdeh as the lower sandstone. But generally, it is supposed that, firstly, the development of the upper sandstone is quite less than the lower sandstone and secondly, the total volume of lower sandstone is less than that of upper sandstone. FiguresIV.7(a-e) show the development of the Ahwas sandstone Member based on the percentage of sand within five different layers from top to the base of Asmari Formation in Zagros area.

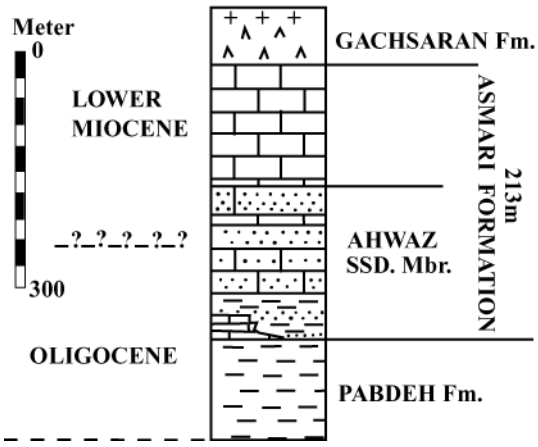

Fig.IV.5: A schema of Ahwaz sandstone Member type-section within the Asmari Formation.

- *The Kalhur evaporate Member*

The Kalhur member of the Asmari Formation was previously treated as a Formation called the Kalhur Anhydrite or Kalhur Gypsum. The type section was measured on the southern flank of Kuh-e Anaran, 2 miles southeast of where the road passing along the southwestern flank of Kuh-e Anaran crosses the Changuleh River (James & Wynd, 1965). It is composed of three units: a basal gypsum 4.5 m thick, 42.6 m of marl and thin bedded marly limestone, and 82.3m of massive gypsum (Fig.IV.8). This Member conformably overlies the marls of the Pabdeh Formation and is conformably overlain by the Asmari limestone. Elsewhere, the Member may be present as a tongue within the Asmari Formation limestone.

New studies show that the basal anhydrite of the Asmari which is seen in northern fields of Dezful embayment like Lali, Masjed-Soleyman, Haftkel and Naft-Sefid, is a continuation of the Kalhur evaporate member. This Member has formed in a narrow depression in front of mountain front (Fig.IV.2). In north of Dezful embayment, from Changuleh to Danan and Dalpari field and following the Anaran bending, it follows the Balaroud fault and then along the continuation of the Mountain Front Fault, it passes from Ghale-Nar, Kaboud, Ziluee, Naft-Sefid, Haftkel and Parsi fields. Along this axis, the Kalhur evaporate Member Includes anhydrite and sometimes halite. From northeast to southwest direction, along this axis, the thickness of this Member decreases and reaches to zero. In the places where halite is found, as we keep away from this axis, first halite disappeared and then anhydrite become thin and then disappeared.

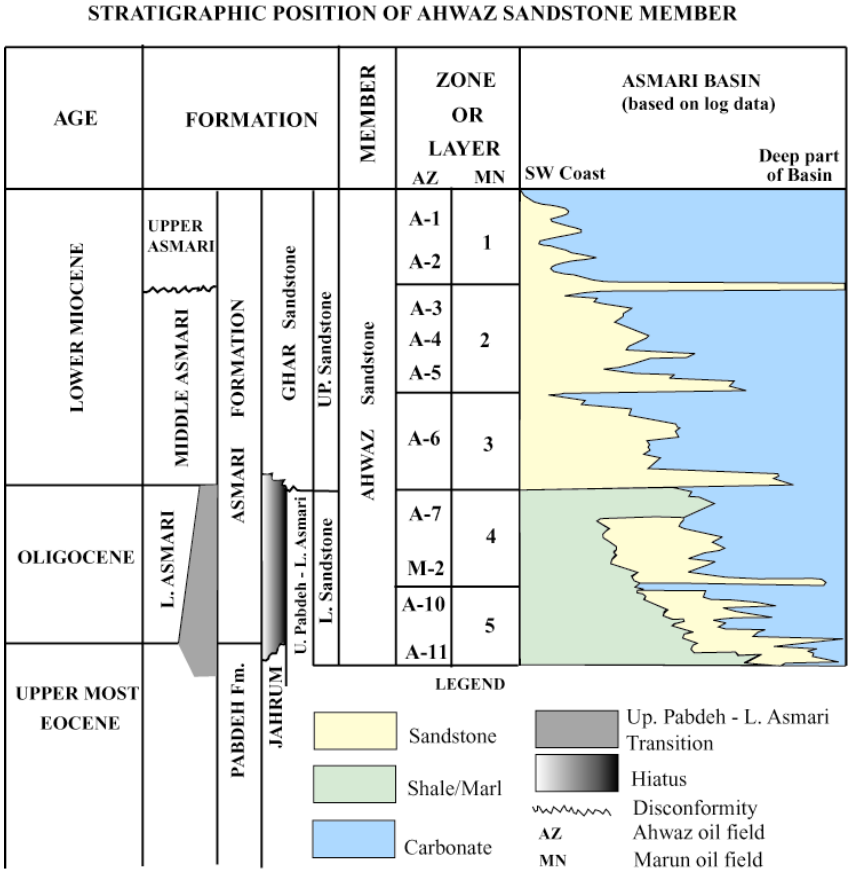

Fig.IV.6: Stratigraphic position of Ahwaz sandstone Member with special regards into Ahwaz and Maroun oil fields, modified from Motiei (1993).

The thickness of the Kalhur Member in the Anaran type section reaches to 129.5m whereas in Changuleh well No.1 its thickness reaches to 275.8m. This subsurface interval shows a relatively complete evaporitic series including anhydrite, halite and rarely sylvite. This series is not comparable with surface type section. It means that surface type section has been chosen near the margin of the Kalhur basin. So, subsurface section of Changuleh No.1 is introduced as Reference section as it bears more complete and correct information of Kalhur evaporate Member. The location of this well is 32km southeast of Mehran City and 80km northwest of Dehluran City and 14km west-southwest of surface type section. The interval of 2593.87-2871.86m (275.8m corrected thickness) was selected as Reference section for the Kalhur evaporitic Member (Fig.IV.9).

The lithology of this part could be divided to three parts from the top to the base. Firstly, the upper part including 75m alternative beds of anhydrite, limestone and grey marl in which towards the base the thickness of anhydrite increased. Second, middle section including a halite bed with 135m thickness on above and 28m anhydrite on below. Finally, third part including 30m marl and dark green to gray shale on above and two anhydrite beds on below with 7.8m thickness.

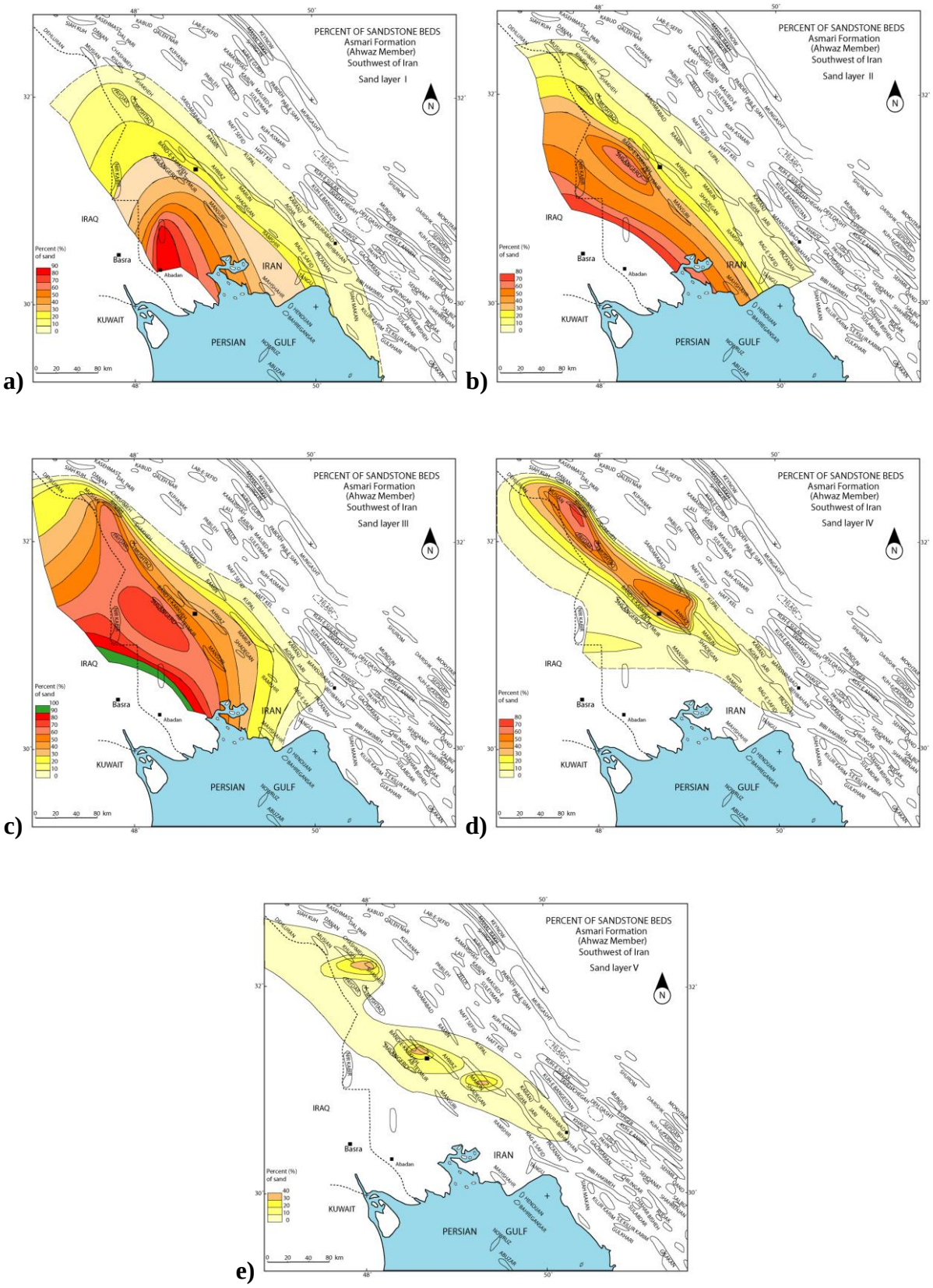

Fig.IV.7: Percentage of sandstone beds in Asmari Formation; a)Sand layer 1; b) Sand layer 2; c) Sand layer 3; d) Sand layer 4; e) Sand layer 5. Motiei (1993).

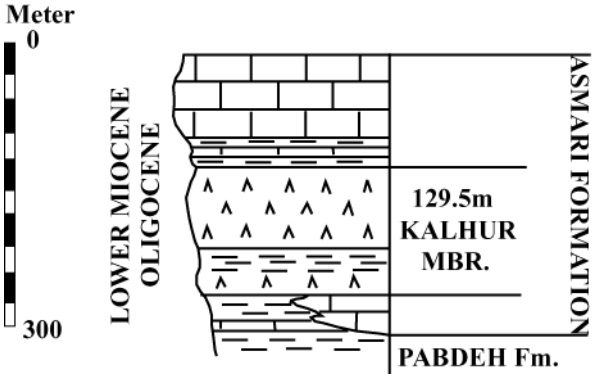

Fig.IV.8: A schema of Kalhur type section within Asmari Formation (James & Wynd 1965).

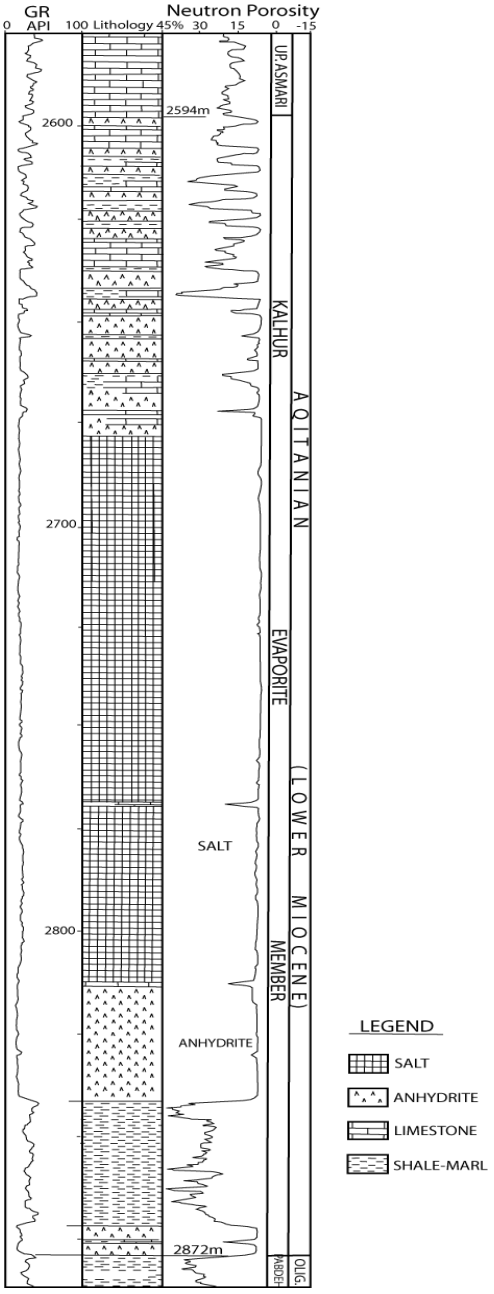

Fig.IV.9: Complementary section of Kalhur anhydrite Member in Changuleh No. 1 Well

Conclusion

Three main different lithofacies including clastic, carbonate, evaporite, and shale can be found within the Asmari Formation. These facies deposited in the Zagros basin during Oligocene to Lower Miocene times. Clastic facies developed importantly within the Dezful Embayment where evaporitic facies cover a limited zone in this region and can be found on neritic to deep basinal facies of the Asmari Formation. Carbonates form the main lithofacies of the outcrops within the Izeh zone and the northern part of the Dezful Embayment.

PART 3
Fracture development and its relation with large scale deformation in the Central Zagros

CHAPTER V
Previous studies of fracture development in the Arabian plate / Zagros

Introduction

It is important to devote a section to stress evolution in the Arabian platform and related features of brittle deformation in its sedimentary cover rocks. As a great part of these rocks have not been affected by Zagros orogeny, the local or regional fracture patterns may correlate with those which could be seen in Zagros folds and apparently show no relation with general stress state developed by Zagros orogeny. Furthermore to look for the evidence of regional fracture patterns, unfolded area beyond Zagros folds in Arabian plate, could be helpful. Then fracture pattern in the Asmari Formation based on previous studies is discussed in the chapter.

V.1. Regional fracture sets in Arabian cover rocks

V.1.1. Stress conditions

During the Mesozoic, and especially in the Triassic and Late Cretaceous, and even probably during the Permian, the N-S uplifts and basins of the Arabian Trend were intermittently reactivated, as seen in the Ghawar Anticline, Dibdibah Trough and Qatar Arch (Fig.V.1). There is even evidence in the Ma'aqala Arch, and by truncation of the Lower Eocene, Rus Formation in Ghawar, that tectonism along the Arabian Trend extended to at least Mid Tertiary times. The prominence of the Hofuf Formation, and its topographic expression over the Ghawar Anticline, indicates that intermittent reactivation of these N-S trends probably continued until the end of the Pliocene. With the NNE drift of the Arabian Plate, and its separation from the African Plate from Oligocene onward (McKenzie 1972), a new set of stress conditions prevailed in basement beneath the Saudi oil fields. In this movement, the Arabian Plate was not only pushed north-northeast but was also stressed between two shear zones formed by the left-lateral, Aqaba- Dead Sea Fault (Freund et al. 1970) and the right-lateral Masirah Fault and Owen Fracture Zone (Jackson et al. 1981)(Fig.V.1).

With the greatest principal-stress axis directed NNE towards the Zagros Ranges of southern Iran, two major vertical shears were produced at about N 36° E and N 20° W. The NW direction of vertical shear stress has produced right-lateral, strike-slip faults in the

basement parallel to the shoreline of northeastern Saudi Arabia, and roughly parallel to the Najd Fault Zone (Agar, 1985) and the axis of the Red Sea. This basement fault trend offsets the axial trace of the Safaniya Anticline in a right-lateral fashion, as shown from running difference gravity survey (Edgell, 1992).

A whole series of left-lateral, strike-slip faults were also produced in the basement along the N 36° E trend (i.e. Aualitic Trend), as can be clearly seen in southern Iran, where rows of Hormuz Series salt-piercement structures are aligned along this trend (Fürst 1970). An interpretation of the evolution of the stress field in northeastern Saudi Arabia and the Persian Gulf from Late Proterozoic to Late Cenozoic is shown in Fig.V.2.

V.1.2. Lineament trends in the east Arabian platform

Lineaments represent failure zones that involve at least a significant portion of the upper crust. They may mark vertical movement, tilting or horizontal displacements. Sometimes they are associated with structural features such as faults and joints. As an examples of systems of lineaments is in Saudi Arabia where they generally consists of numerous lineaments of about 400 km in length, spaced about 40 km apart with occasional parallel but closer-spaced examples (Onyedim & Norman, 1986). The age of aligned plutonic intrusives in the Central Arabia shows that the system is at least 500m.y. old, but where rocks of Phanerozoic are affected, the lineaments have presumably propagated from below by later movements. The lineaments in Nigeria and Saudi Arabia are remarkable for their North-South alignment (Oneydim & Norman, 1986).

Concerning the association of lineaments with petroleum traps perhaps the best example is in Saudi Arabia (Fig.V.3), (Al Khatieb and Norman, 1982) where the displacement of adjacent faults have created conditions for "giant" oilfields. If the subsurface contours are studied, it will be seen that the effect in the North creates conditions for oil reservoirs as far away as Kuwait.

According to Hancock et al. (1984), an important Neogene response in the Arabian platform to NE-SW shortening in the Zagros ranges was the Formation of a swarm of NE striking master joints and lineaments. These structures reflect the diffuse and peripheral expansion of the foreland beyond the Zagros deformation front.

In general four lineament trends are identifiable in the eastern part of the platform underlain by Neogene rocks. These trends are (Fig.V.4):

(1) E-W, e.g., Al Wari'ah,

(2) NE-SW, e.g., Al Musannah, Wadi Al Batin,

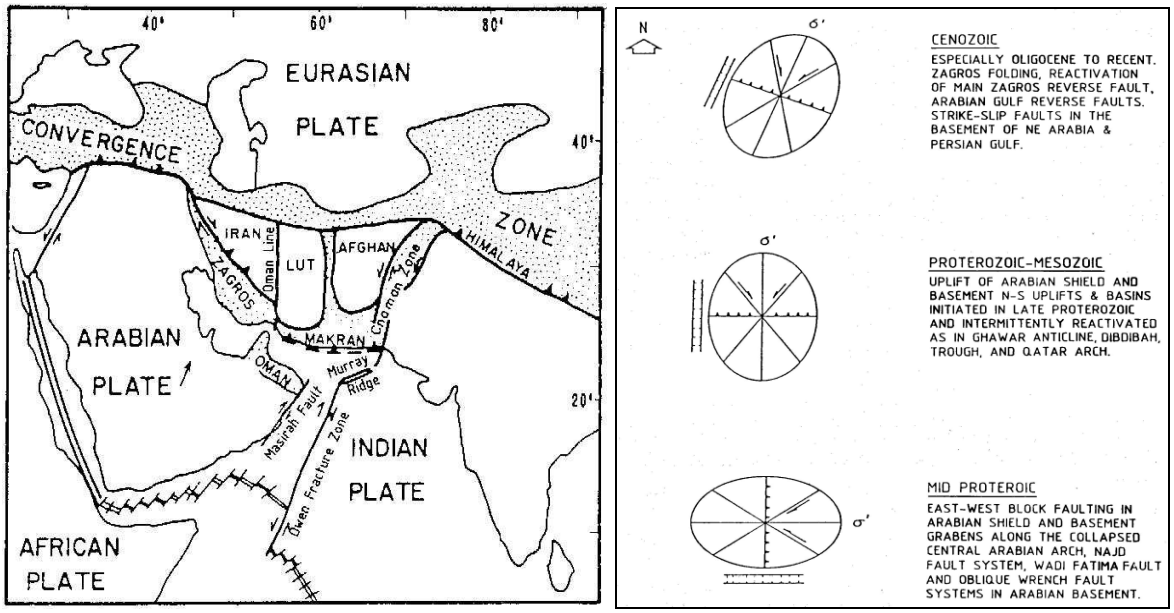

Fig.V.1: (left) Plate tectonic setting of Arabia, Shear couple stress in Arabian plate, produced by left-lateral Dead Sea fault (northwest) and the right-lateral Owen fracture zone (southeast) (Edgell, 1992).
Fig.V.2: (right) Evolution of the Stress Field in the basement of the Saudi Arabia oilfields areas as indicated by the Stress Ellipse (Edgell, 1992).

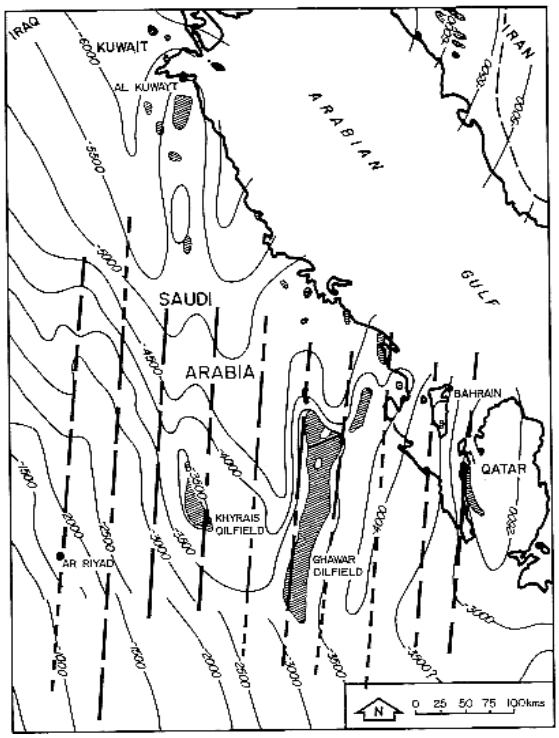

Fig.V.3. The dotted lines are part of an old parallel system of lineaments in Saudi Arabia that have controlled movements creating large petroleum reservoirs (Al Khatieb and Norman, 1982). The subsurface contours show the approximate base of the Mesozoic.

(3) NW-SE, subparallel to the Gulf coast and recognized on color satellite images by Halbuty (1980).
(4) N-S, the so-called Arabian trend (De Jong, 1982) represented by the hydrocarbon-bearing structures, the axial traces of which locally range from NNW, through N-S to NNE.

V.1.3. Macro-fractures (map scale fractures) and regional joint sets in Arabian basement-cover rocks

Maybe one of the best places to see those fracture patterns, especially regional fractures, which have not affected by folding due to Zagros orogeny, is the eastern Arabian foreland platform. More than 90% of mesofractures in Arabian platform are systematic joints, the remainder being calcite veins or, more rarely, mesofaults (Hancock et. al., 1984). The latter are mainly associated with the central Arabian graben system, or they occur in sand-dominated Formations elsewhere in the platform. Macrostructures, which disturb the Phanerozoic sedimentary sequences of the east Arabian foreland platform, are few, subdued and simple. Those of Mesozoic-Palaeogene age are the central Arabian arch, the central Arabian graben system and major N-S growth folds (Fig.V.4) (Powers et al. 1966; Hancock et al. 1984).

Superimposed obliquely on these older structures is a group of NE-trending lineaments, fault belts and mesofractures that are especially well expressed in the Neogene-Quaternary covers. The principal element is Wadi Al Batin (Fig.V.4), a rectilinear gentle-sided relief, eroded in Neogene rocks except in the SW where it crosses outcrops of Cretaceous and Palaeogene Formations. NE-trending normal faults offset Palaeogene and Neogene sediments beneath and immediately to the east of the Kuwaiti sector of the Wadi (Al Sawari, 1980). The Wadi extends over a distance of 75 km in the state of Kuwait and can be traced for another 700-km westward as the great Wadi Ar-Rimah in Saudi Arabia. The greater part of Wadi Al-Batin's course has a direction of N35°E. Faults and fracture systems affect Eocene, Miocene and possibly Pliocene sedimentary strata in the Wadi Al-Batin region. The trends of both the major and secondary faults in the area are northeast-southwest, similar to that of a large part of the Saudi Arabia fault system (Al-Sayari and Zotl, 1978).

Hancock et al. (1984) have argued that the large dimensions and straightness of Wadi Al Batin favor a tectonic control along its entire length. It is noteworthy that Wadi Al Batin, the longest and widest of the NE-trending lineaments, is directed towards the Khuzestan topographic embayment of the Zagros mountain front. Within the east Arabian foreland platform it is possible to recognize three suites of mesofractures (Hancock et al. 1984). Two

of the suites are restricted to Mesozoic-Palaeogene Formations and are genetically related to the development of the central Arabian arch and graben system, while the third is superimposed obliquely on them and is called Wadi Al Batin trend. NE-SW striking mesofractures in the third suite also cut the previously unfractured Miocene-early Pliocene sequence, although they do not cut the overlying duricrust layer, dated by Chapman (in Al Sayari & Zotl 1978) as of latest Pliocene-Pleistocene age, equivalent to Bakhtiyari conglomerates in the Dezful embayment region in Iran. It follows, therefore that they were initiated during a Miocene-medial Pliocene interval, that is, during the earlier part of the neotectonic history of the gulf region. Thus the Batin-trend mesofractures are interpreted here as being related to the Miocene (Berberian et al. 1982) collision in the Zagros domain with most of them probably being formed before the late Pleistocene (Berberian & King 1981).

Mesofractures in the neotectonic suite either strike NE-SW (the Batin trend) or they enclose an acute bisector about that direction. The following classes of structure are present (Hancock et al., 1984):

(i) Vertical NE-striking joints;

(ii) Vertical NE-striking veins;

(iii) Steeply inclined, NE-striking conjugate hybrid (transitional tensile) joints enclosing an average acute dihedral angle (2θ) of 35°;

(iv) Steeply inclined, planar NE-striking conjugate normal mesofaults;

(v) Vertical NNE- and ENE-striking conjugate hybrid joints? (or possibly two separate joint sets) enclosing a 2θ angle of 31° about a NE-trending acute bisector.

This suite is mainly represented by a set of joints, conjugate sets of hybrid fractures (or joints) being rare and restricted to sites in Mesozoic-Palaeogene rocks north of the crest of the central Arabian arch. Because the Palaeogene direction of stretching north of the arch crest was also NW-SE, some of the conjugate structures in that area may be older than those of the neotectonic suite (Hancock et al. 1984).

Because lineaments and fractures of Batin-trend are uniformly oriented throughout at least 750,000 km² and because they are superimposed obliquely on older structures they are interpreted as the products of a regional strain field (Hancock et al., 1984). The direction of horizontal extension derived from the normal to extension fractures, or the obtuse bisector between conjugate hybrid fractures, is everywhere orientated NW-SE, sub-parallel to the Zagros deformation front.

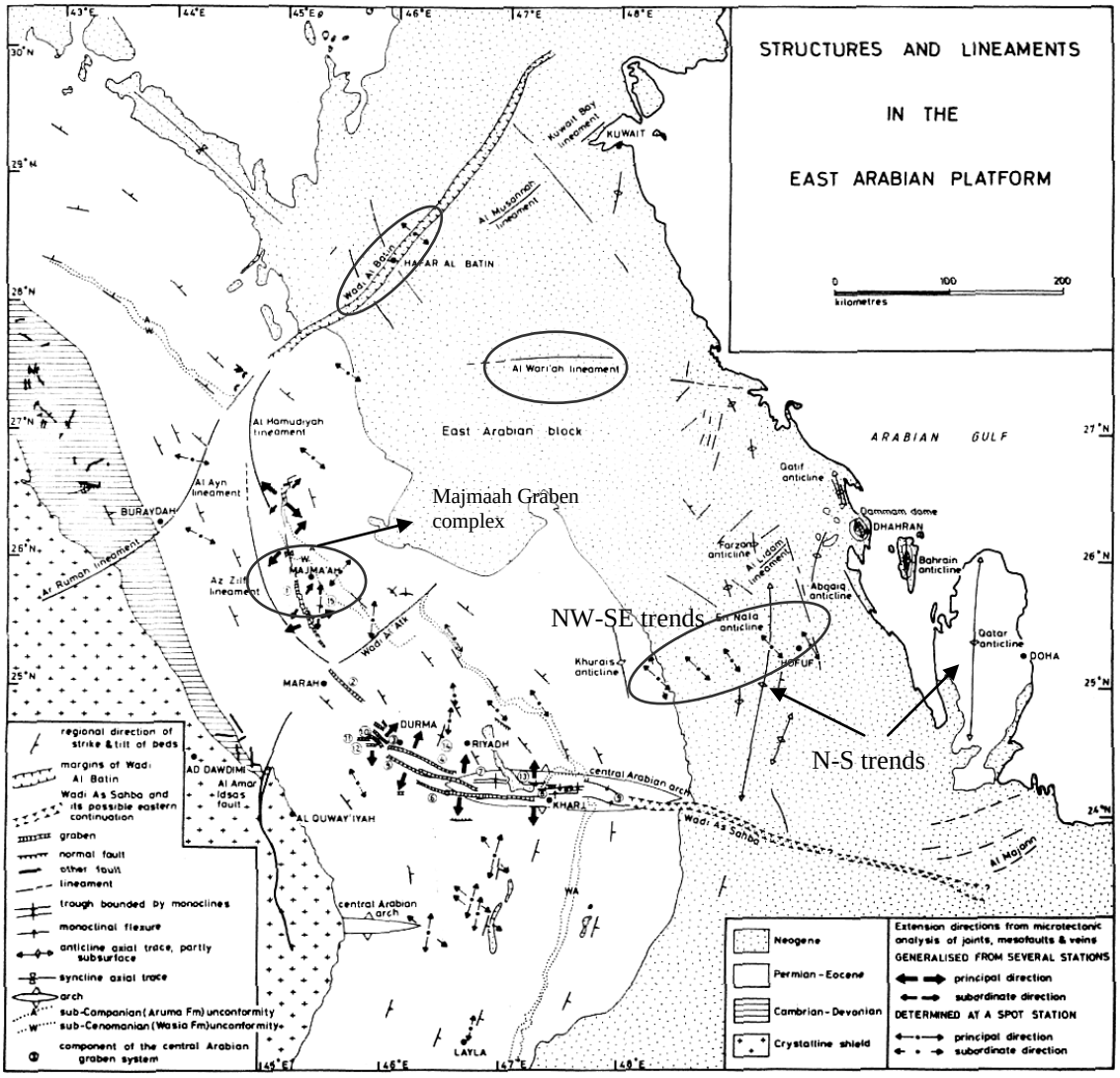

Fig.V.4: Structures, lineaments, and directions of extension inferred from mesofracture systems in the eastern Saudi Arabian platform (Hancock et al. 1981).

Hancock (1984) recognized three types of microtectonic scale dominant fracture sets (Fig.V.5). They can be interpreted as follows.

- *Type I:* comprises a single vertical set of surfaces interpreted as joints initiated normal to a principal extension direction.
- *Type II:* consists of vertical conjugate sets enclosing a small dihedral angle (2θ) about a horizontal acute bisector parallel to the strike of type I fractures. Because 2θ is less than 45°, they are interpreted as hybrid fractures (i.e., oblique joints)
- *Type III:* steeply to moderately inclined fractures strike parallel to those of type I but they enclose an acute dihedral angle symmetrically about the vertical. Conjugate type III fractures are interpreted as hybrid joints where they enclose 2θ angles of less than 45°, as hybrid shear

fractures where 2θ is 45° to 59°, and as shear fractures where 2θ is 60° or greater (Hancock et al., 1984).

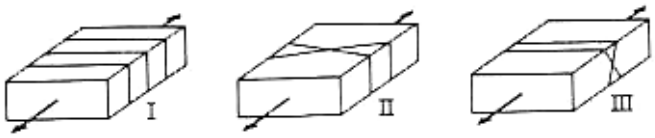

Fig.V.5: Brittle macrofracture sets from which extension directions in the Arabian platform are inferred (Hancock et. al., 1984). See text for details

The observation that at some places the single vertical set strikes parallel to the steep fractures reinforces the interpretation of the former, because it is difficult to envisage the steep fractures developing in a regime other than an extensional one (Hancock et. al., 1984). Neogene rocks are commonly cut by only a single set of systematic extension joints and a single set of non-systematic cross-joints, giving rise to a simple orthogonal fracture pattern (Hancock et. al., 1984).

V.1.4. Age of the mesofractures

Because in the arch and graben system domains the mesofracture pattern persists through Formations from Triassic to late Cretaceous, it is concluded that the fracture probably date from the end of the Cretaceous or early Palaeogene. Furthermore, since the boundaries between the domains are transitional and there is no evidence for one domain overprinting the other, they are probably of the same age.

Mesofractures with the Batin trend (Fig.V.4), which cut Formations from the Triassic to Early Miocene, are interpreted as Neotectonic structures. In pre-Neogene rocks they have been superimposed on fractures in the arch and graben system domains. Some of the NE striking Batin domain joints in the Hofuf area pass upward into the lower layers of the overlaying duricrust, which Chapman (in the work of Al-Sayari & Zötl, 1978) thinks started to form in the latest Pliocene (Hancock et. al., 1984).

V.1.5. Integration and interpretation of megatectonic and microtectonic

Where the northward motion of the east Arabian block or sheet was normal to the separation zone it give rise to a broad belt of E-W grabens and troughs, and a mesofracture system symmetrically arranged about the N-S extension direction.

In the Wadi Al Batin, the lineaments parallel to the Wadi, and the NE striking extension and hybrid joints of the Batin domain are interpreted as foreland responses to Neogene collision which, on the leading edge of the subplate, gave rise to the Zagros Simple folded Zone. The neotectonic horizontal direction of compression external to the fold belt would be approximately NE-SW, while the complementary direction of extension would be NW-SE, that is parallel to the extension direction determined from the dominant joints in the Neogene sediments. The geophysical evidence (Al Sawari, 1980) for NE trending normal faults cutting Palaeogene rocks beneath and to the east of the Kuwaiti sector of Wadi Al Batin introduces the possibility of the entire 300-Km length of the Wadi being fault-controlled.

The Ar Rumah, Al Ayn, and parallel lineaments may mark the sites of other late Palaeogene-Neogene fault zones, guided perhaps by basement faults rejuvenated during collision. The NE trending lineaments and the superimposed NE striking extension joints in the northern sector of the Majma'ah graben complex (Fig.V.4) and the southern part of the central Arabian arch were also probably formed at the same time and in response to the same direction of NW-SE extension. The structures of the Batin domain are those, which might be expected in a zone of peripheral expansion external to a belt of NE-SW collisional shortening as in the Zagros ranges (Hancock et. al., 1984).

V.2. Fracture patterns in the Asmari Formation in the Zagros; previous studies

Concerning the studies on fractured reservoirs in Iran, specially, the geological analysis of fractures, there are not many papers. Maybe, one of the most quantitative investigation on fracturing in Asmari Formation, belongs to McQuillan (1973, 1974). He had a detailed investigation on fracture orientation, distribution, density and its relation to bed thickness on different structural realms. His investigation was based on three outcrops, namely, Kuh-e Pahn, Kuh-e Asmari, and Kuh-e Pabdeh-Gurpi of southwest Iran (Fig.V.6). The summary of his results is as follows:

No trend in fracture density variation (on 1D scanned lines) is apparent either locally on individual structures, parallel with or normal to the regional strike, or associated with major fault systems. For a given bed thickness in the Asmari limestone the fracture density is constant and independent of the structural position in an anticline. Moreover, for structural realms considered, there is a relatively uniform distribution of fracture density over all azimuth classes. In the random spread of fracture orientation McQuillan suggested that there

is an influence of late Tertiary folding affecting the development of, or exploiting pre-existing fractures in the sense of an orthogonal conjugate system.

V.2.1. Bedding-Plane Distribution

In the Asmari limestone, bedding is defined by thin shaly partings, sharp changes in lithology, and possibly by stylolites. To predict fracture densities, and hence block dimensions within an Asmari reservoir, knowledge of the bedding-plane distribution is required. This can be established by examination of nearby surface outcrops of the reservoir rock or, better still, from subsurface cores.

V.2.2. Origin of Fractures

The orientations and distributions of the fractures have been related to tectonic style, and variations have been explained by appealing to local complexities of stress field, rate of change of the curvature of the rocks, proximity to fault planes, and so on.

In keeping with Cook and Johnson's (1970) findings, McQuillan (1973) suggested that fractures in the Asmari limestones are not necessarily due only to Zagros tectonics. Regionally well-defined fracture sets related to the major stress axis are not present alone, but rather a wide spread of fracture azimuths is evident. A uniform fracture density is associated with a limestone bed of given thickness and lithology regardless of its structural position. The origin of fractures is not necessarily related to folding.

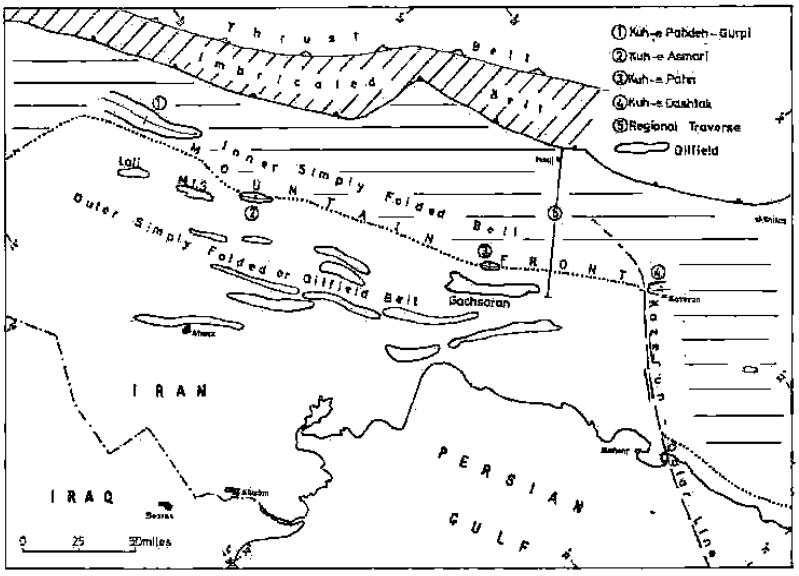

Fig.V.6: Map showing general structural features of southwest Iran and location of individual structures studied by McQuillan (McQuillan, 1973, BP Co., Ltd., 1956, 1: 1 million).

Figures V.7 show McQuillan's (1973) result on fracture density and their relation with bed thickness on several structural realms of Kuh-e Asmari anticline. The main conclusion drawn from this study of small-scale fractures in the Asmari limestones is that fracture density is, within limits, constant in beds of given thickness and lithology (Fig.V.7). This applies not only to individual anticlines but also regionally over a great variety of structural settings. The thickness of a limestone bed has a direct relation to the density of fracturing. The density varies as an inverse logarithmic function of bed thickness.

Over the structural realms considered, fractures show a widespread distribution of orientations and the densities for all azimuth classes are comparable for a given bed-thickness class. Within the spread of fracture azimuths there is a suggestion of a preference for azimuth classes corresponding to regional tension (NW-SE) associated with late Tertiary folding (McQuillan, 1973).

"Photo scale investigation of Kuh-e Asmari fracture patterns, in contrast, shows a simple pattern of fracturing which is, in the main, related to the major lines of extension normal to and parallel with structural axis. Plunging noses exhibit a high density of fracturing, center realm exhibit the second greatest fracture density, and flank densities are lower. The fracture density in latter structural position consequent on the degree of flank curvature (Fig.V.8). The wide diversification of ground-observed fracture orientations and their independence, in term of density, with respect to folding intensity can mean only that they were formed much earlier than the main Zagros folding phase. The north-south trend over the eastern part of the structure suggests the presence of the lineament of older structural affinity (McQuillan, 1974)."

V.2.3. Fracturing and Dynamic Data in Asmari Reservoirs

Dynamic data, here, refer to well test and production data. High initial well productions from low porosity limestones, often in excess of 80,000 bbls/day, were explained by appealing to the presence of fractures (O'Brien, 1953). The mechanism of production is related mainly to fracturing, and variations in productivity across oil fields within which lithologies are relatively constant have been interpreted to be due to variations in fracture density or spacing (Lees, 1948; O'Brien, 1953). Studies of fracturing over surface anticlines in the foothills and in more tightly folded structures to the northeast have provided results that, instead of revealing a relationship between structural position and fracture density, have shown that their fracture density is constant. It has been suggested (McQuillan, 1973a) that small-scale fractures were initiated prior to folding, as a partial response to the diagenetic

process. Then fracture-plane orientations were related to the morphology of the depositional surface.

Based on McQuillan (1985), the indication of a constantly oriented three-set pattern with trends of N10°-20°W, N20°-30°E, and N80°E, in surface photo-scale fracture patterns, bears no relation to the folds resulting from the late Tertiary Zagros orogeny. It means that the pattern is related to features reflecting basement discontinuities (McQuillan, 1985), which are manifest in southeast Iran as abrupt strike changes along large-scale features such as the Kazerun and Oman lines (Falcon, 1969; McQuillan, 1973a).

Examinations of surface linear densities along the field (based on McQuillan, 1985 over Gachsaran and Bibihakimeh fields) reveals an obvious relationship between fracture density and production potential. Moreover, areas of comparable productivities on the two fields lie along the N20°E major fracture trend (Fig.V.19). The alignments of trends exhibiting high surface linear fracture densities with zones of high production potential along N20°E trend are most significant. It suggests that over such zones, the small-scale fractures, which have been present in the rock since early in its diagenetic history, have been subjected to renewed movements. These movements have been propagated upward from deep seated adjustments along basement features.

In contrast with McQuillan (1985), Gholipour (1998), in a qualitative fracture study, stated that fractures in Asmari reservoirs, southwest Iran, are associated with vertical and axial growth of concentric folding, which means they are mainly fold-related fractures (Figs.V.10&11). His assumption was based on the investigation that has been done on the dynamic data. He supposed that the birth of folding took place in the central portion of the present reservoir structures, where high production rate, productivity indices, sever mud losses, and faulted well assemblages are rare due to cementation phenomena in developed reservoir fractures in water saturated reservoir rocks during the early folding phase in the Miocene and before the oil migration. Again, based on these dynamic data, he also found out that the greatest fracture intensity is associated with the plunges of the Asmari anticlines, which indicate this part as an intense open fractured portion of the anticlines and concluded that productive fractures were found to be associated mainly with the plunges and bends of the Asmari reservoir structures.

The conclusion which was taken by McQuillan (1985) regarding the production variation in two giant fields, Gachsaran and Bibi Hakimeh, is based on the distribution of wrench faults in the region. On this map (Fig.V.12) the positions and orientations of two

indicated wrench faults are almost matched with the area of enhanced fracture, production zone (Fig.V.9).

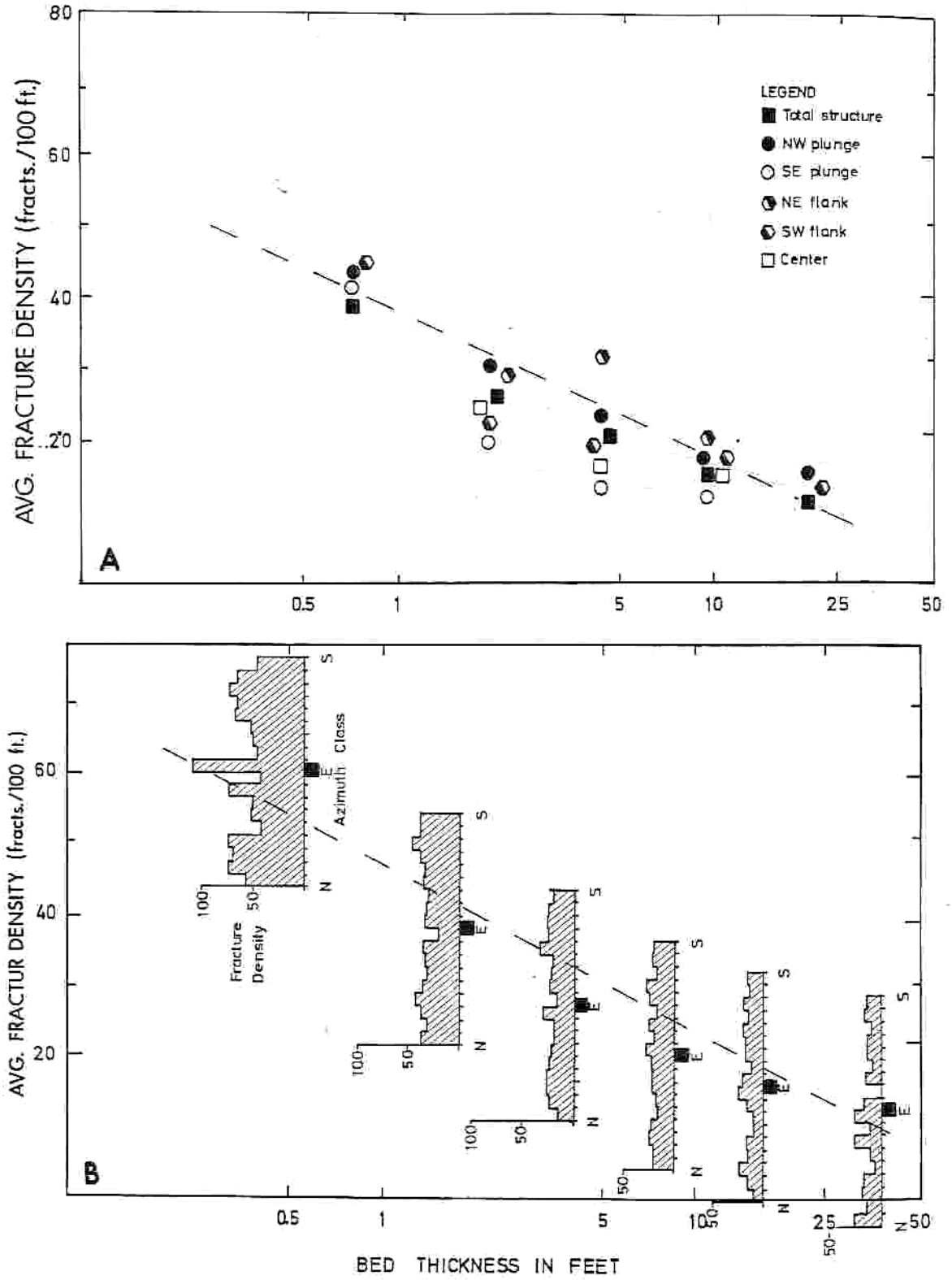

Fig.V.7: A. Graph showing the relationship between bed thickness and density of small-scale fractures in various structural depositions and for the overall structure of Kuh-e Asmari anticline; B. Graph showing the relation

between bed thickness and density of small-scale fractures from anticlines selected from a large area of the Zagros foothills. Histograms show fracture-density distributions by azimuth classes.

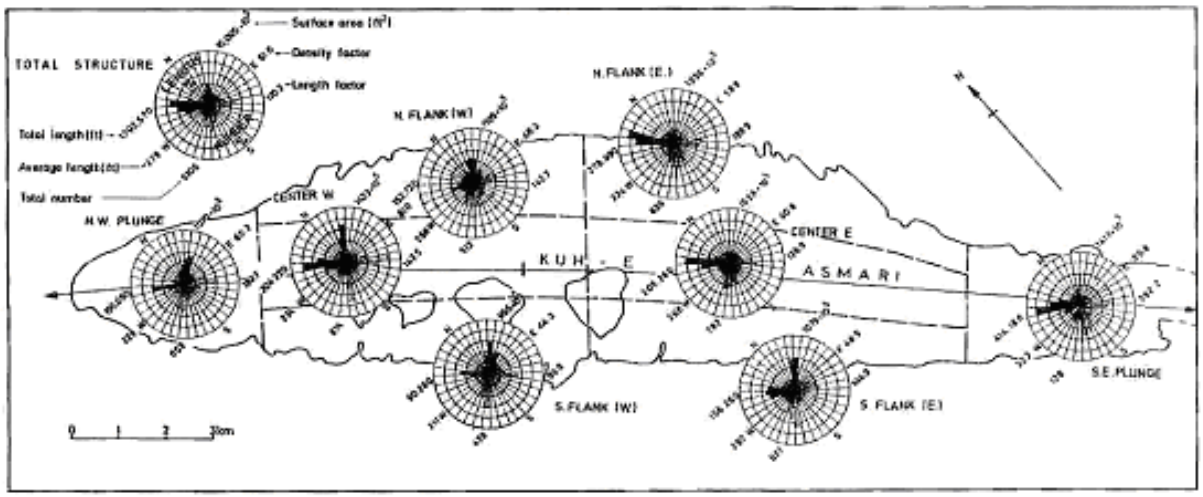

Fig.V.8: Map of Kuh-e Asmari anticline showing structural realms and their associated polar diagrams indicating fracture-length and number percentages; Total-structure diagram is also key to figures associated with other diagrams.

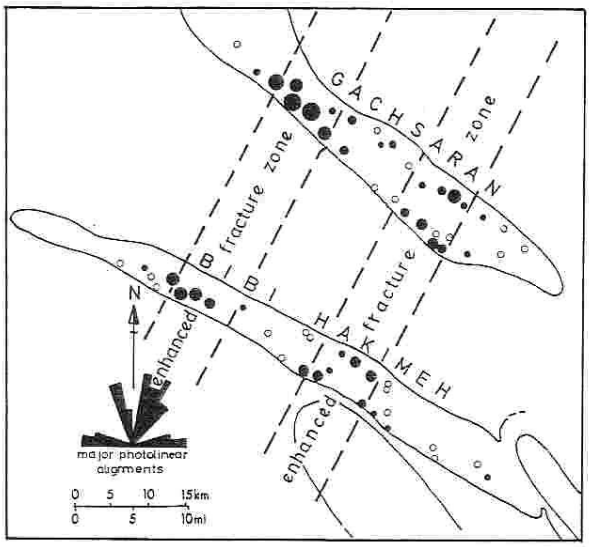

Fig.V.9: Form-line map of Gachsaran and Bibi Hakimeh oil fields. Areas of solid circles are proportional to maximum allowed production rates. Open circles are non-commercial or non-producing wells. High-production wells lie in zones of enhanced fracturing related to trends of basement features.

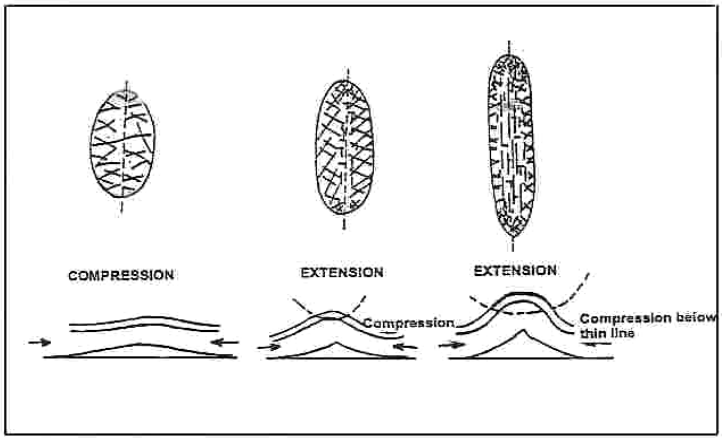

Fig.V.10: Three stages in development of a concentric fold (plan view above and cross section below)(A. M. Gholipour, 1998).

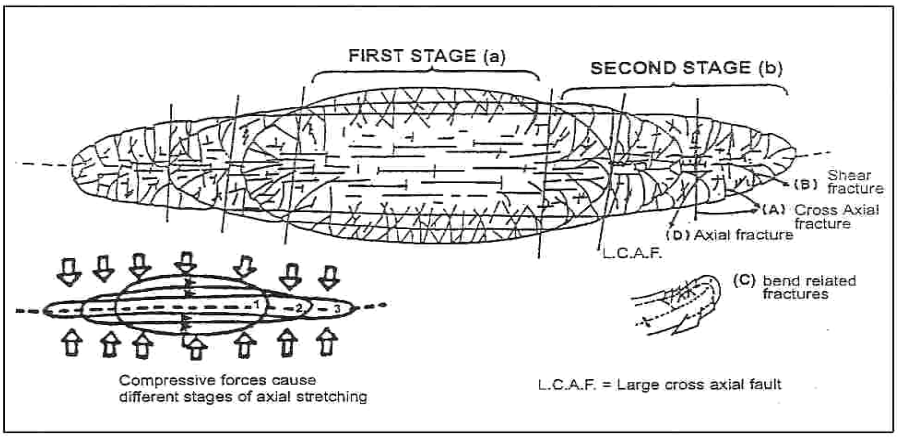

Fig.V.11: Schematic illustration of axial folding development of a concentric fold (Gholipour, 1998): a) First stage shortened area by flextural slip mechanism. b) Second stage shortened area with stretching by axial growth of the fold as well.

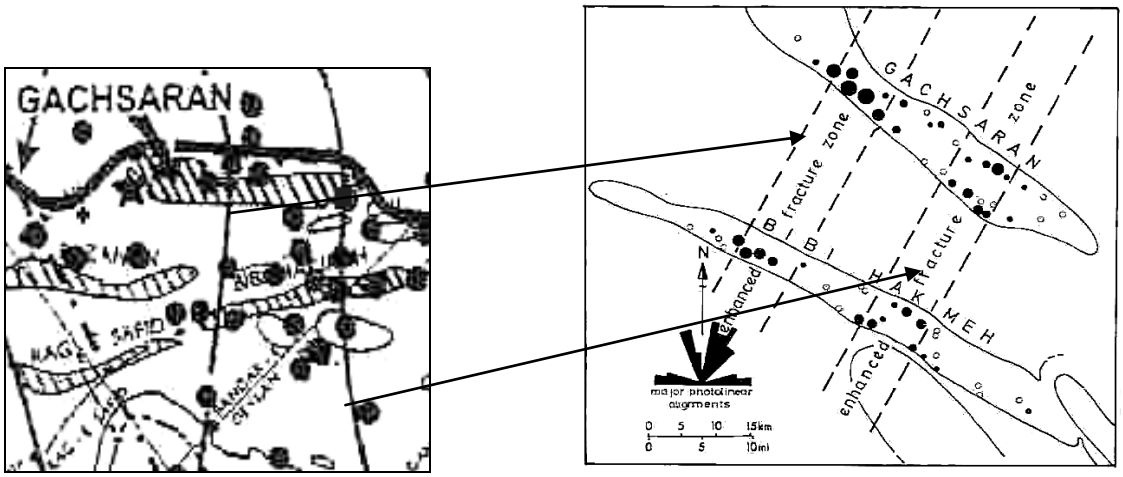

Fig.V.12: Comparison between the conclusion of McQuillan and Wrench Fault map of Ironmagnetic study (1969).

Conclusion

Beyond Zagros folded belt and within the east Arabian foreland platform, three suites of mesofractures exist. Two of them are restricted to Mesozoic-Palaeogene Formations and are related to the development of the central Arabian arch and graben system, trending east-west and north-south. The third is superimposed obliquely on them and is called Wadi Al Batin trend (NE-SW) and presumably reflects far-field effects of the Zagros collision.

Fracturing in the Asmari Formation, in other side, may be resulted of different mechanisms and tectonic events. Different fracture sets have been defined in the Asmari Formation as a well-known fractured reservoir. There are many attempts to find a logical relation between fracture sets and general folding mechanism and related stress distribution in Zagros area. However in photo-geology scale it may possible to find a coherency between Zagros orogeny event and fracturing but it is quite difficult to generalize it to small-scale fractures collected by field survey. It seems to be not easy to distinguish regional fractures from those which are only related to fold Formation. However, in general, two major sets (parallel and perpendicular to fold axis) are the best developed at least in the Asmari outcrops. Those fractures striking N-S and E-W seems to be older than the major sets (parallel and perpendicular to fold axis) and are in minor priority. On the other hand, fracture propagation and mechanisms controlling orientation are still a controversial subject. Apparently, the impact of fractures on fluid flow doesn't follow a general rule and it could vary from one field to another. Almost, all studies on fracture in the Zagros area (and typically Asmari Formation) were based on old technology. New progress and methodology in fractured reservoir characterization using more advance tools and data could help in better understanding of fracture pattern and its impacts in fluid flow. It may solve some enigmas and decrease some uncertainties in fracture characterization of Iranian fields not only in Asmari but also in Cretaceous reservoirs as well.

The previous fracture studies which were done in the Zagros folded belt, did not fully integrate all aspects which should be taken into account in some of Asmari fracture. Among them we may mention lineament study, fracture chronology (including fracture and stylolites), local/regional stress analysis (using fault-slip data, stylolitic peak directions, calcite twins and their relative chronology), macro-faults and their relationships with other farctures, fold/fracture relationship, the effect of lithology and diagenesis on fracturing, microscopic fracture study (chronology, cement filling, diagenesis), mechanical aspects including analogical and numerical modeling. Each one of these aspects, itself, requires an intensive work both in local and regional scale.

Following the recent progress in high resolution satellite imagery, it is possible now to have a precise and detailed image of the surface fold geometry, faults and other large scale fractures. These sort of data should systematically use as the base of any regional fracture study. Using these data, in addition to large scale fracture and lineament mapping, any local anomalies which may affect field data could be distinguished. Detecting fracture chronology at the outcrops is an important and sometimes difficult task which should be carried out patiently. Different fracture filling phases, cross-cutting relationships and fracture reactivations should be fully taken into consideration. Micro-tectonic studies including micro-faults and tectonic stylolitic peaks analysis in addition to their chronology should be an essential part of any fracture analysis in a region. Finding different phases of tectonic events and related stress fields orientation serve us valuable information to interpret spatial distribution of the fractures. Finding the effect of diagenesis and lithology on fracturing needs a collaboration between structuralists and sedimentologists. Diagenesis was mentioned as one of the main reasons of fracturing in the Asmari Formation by McQuillan (1973, 1974). The effect of dolomitization on fracturing were discussed by many authors (see Nelson, 2001), but there is no systematic and detailed study on this important diagenetic feature in the Asmari reservoir.

Part of the aspects mentioned above could be performed in microscopic-scale to completely analyse the main factors controlling the fracturing process in a fold or in a region. The field scale observations and kinematics aspects of fracturing should be tested via analogue or numerical modeling to be confirmed and explained by physical laws. For example, the initiation and reactivation of different fracture sets in the Asmari Formation may be modeled numerically and compared to field observations.

All above need planning, organization and time. In this thesis, I tried, at least, to touch all these aspects and to learn, first, the theoretical background and to see what are the main drawbacks in the previous studies, how to approach and what is the difficulties in this way. The stress and strain state constitute the mechanical aspects of the fracturing. Fracture is a general term which may be applied for joint, vein, fault, shear fracture, and even stylolite. Each of them has different mechanical origin and has specific characteristics which should be carefully considered during field study. Furthermore, in a regional scale fracture study, our tasks will be multiple because different observations on individual structures should be compared and carefully treated without ignoring the tectonic evolution and deformation history of the region.

CHAPTER VI: A new study of regional fracture pattern in the Asmari Formation

VI.A. Fracture patterns within Oligo-Miocene Asmari Formation in the Central Zagros folded belt, SW of Iran; evidence for pre-folding joint development (Pre-Publication)

Faram Ahmadhadi[1], Jean-Marc Daniel[2], Olivier Lacombe[3].

[1]Iranian Offshore Oil Company (IOOC), IOOC Tower - 12th Floor, Geology & Petrophysics Department, # 38, Tooraj St., Vali-e-asr Ave., Chamran Crossing (Park-vey), Tehran, Iran, Post code: 19395
[2]Institut Français de Pétrole (IFP), Division Geologie et Geochimie, 1 et 4, Rue de Bois-Préau, 92506 Rueil-Malmaison Cedex, France
[3]Université P. & M. Curie - Paris VI, Laboratoire de Tectonique, UMR 7072 CNRS, T46-45, E2, Case 129, 4 place Jessieu, F- 75252 Paris Cedex 05 France

Abstract

Regional fracture patterns in the Asmari Formation, one of the most famous petroleum reservoirs in Iran, have been investigated in several anticlines in the central part of the Zagros folded belt. The principal lithology of this Formation in the studied outcrops is carbonate (mostly mudstone and wackstone and rarely gainstone). In addition to fracture orientations and chronology, attention was paid to regional deformation scheme, folding style and local stress state.

Combining fracture chronology observation based on calcite-filling phases and cross-cutting relationships, fault-slip data analysis and aerial/satellite image interpretation on several anticlines in the region allowed us to propose a tectonic model involving pre-folding fracture development in the Central Zagros folded belt. Most of the fractures in the Asmari carbonate predated folding of the sedimentary cover which occurred in Miocene-Pliocene times. An early regional joint set striking ≈N40°-50°, presumably marked the onset of far-field compression in the region, followed by the development of N20°-30° reflecting a slight change in the regional compressional trend. In response to the early reactivation of the main Zagros basement faults (e.g. HZF, MFF, DEF, ZFF, IZHF, KMF) under the mean NE compressional stress trend , ≈N140° and N-S trending joint sets were initiated as second and third early fracture families. At the onset and during the main Miocene-Pliocene folding phase in the sedimentary cover, early formed fractures were reactivated (reopened and/or sheared) while shear fractures including duplexes, low angle reverse faults and thrusts newly formed, as more classical fold-related fracture sets.

This study puts emphasis on the need of carefully considering regional/local fracture development predating folding of the cover in models of fractured reservoirs as well as influence of possible underlying basement faults. In the Asmari carbonate reservoir in the Central Zagros, the complex fracture pattern include both classical fold-related fractures as well as prefolding joint sets, some of them being related to early reactivation of underlying basement faults.

Key words: Zagros, fold, stress, fracture, fault, fault-slip, basement fault.

Introduction

The understanding of the factors that control the characteristics of fracture patterns such as orientation distribution, density spatial variation and chronology is fundamental to improve the methods used to characterized fractured reservoirs. Furthermore, from a regional-scale point of view, this understanding is of major interest for development plans of these reservoirs, which can constitute petroleum provinces like the Southwest Zagros. Fold geometry and kinematics are well known to be important factors that control fracturing. Therefore many studies have tried to relate fracture development to fold geometrical elements such as fold axis, forelimb, backlimb and termination. Reviewing the list of the published literature on this topic is beyond the scope of this introduction. However the paper published by Stearns in 1968 should be mentioned as the synthesis of the pioneering work done in the first half the 20^{th} century on this topic. This synthesis is presented in the form of a classification of fractures (including joints and faults) based on their position with respect to the characteristic geometrical elements of folds. This famous scheme of fractures pattern in a typical anticline including axial, transversal and oblique fractures, was essentially static and trying to emphasize the relationship between typical fracture patterns and their location in a fold according to the present day shape of the fold. Then It was followed by the definition of quantitative characterization of fold geometry using curvature (Lisle, 1994; Lisle 2000). That is why today, curvature is still used frequently as a tool to define fractures direction and intensity (Bergbauer and Pollard, 2004). However, in the recent years due to the development of kinematics models of folding, several attempts have been made to relate fracturing to the kinematic of folds instead of looking simply the final shape of the folds. This type of work still represents an active research area evolving with our understanding of folding mechanisms. Providing new data to challenge these models is the motivation of the present study.

Due to the important role of the fractures in the hydrocarbon production from the Dezful Embayment (South West Zagros) oil fields, many studies have been done in this area to describe the fracture pattern within carbonate reservoirs since 1940 (see Motiei, 1995 for a review). Among the studied formations, the Asmari Formation is quite famous with regards to fracture studies. This Oligo-Miocene Formation is present in numerous outcrops in a 1200km long by 200km wide belt extending from northeast Iraq to southwest Iran (Beydoun, 1988). A lot of these fields are truly giants. Most of them have recoverable reserves greater than 1 billion bbl each and many have much more (Hull et al., 1970). The Asmari reservoir is poor in porosity and matrix permeability. Very high production rates are possible because of extensive reservoir fracturing. These rates can be maintained for very long periods because of the great vertical extent of the oil columns. Therefore, the Asmari fields are prime examples of the effect of fracturing on reservoir performance and the term fractured reservoir was defined to emphasize the production characteristics of these reservoirs. The Asmari type section was described initially by R.K. Richardson (1924) and Thomas (1948) in Gel-e Torsh valley in the Asmari anticline. This type section is 314m thick and is mainly made by dense, cream to brown colour limestones with well-developed fractures and some shaly beds. One of the most detailed investigations on fracturing in the Asmari Formation belongs to McQuillan (1973, 1974). He carried out a systematic study of fracture orientation, distribution, density and their relation to bed thickness on different structural settings in few anticlines of southwest Iran. Using aerial photos, McQuillan demonstrated that fracture patterns in this area are consistently defined by three fracture sets trending N10°-20°W, N20°-30°E, and N80°E. These sets bear no relation to the fold geometry resulting from the late Tertiary Zagros orogeny (McQuillan, 1985). In contrast with McQuillan, Gholipour (1998) claimed that fractures in the Asmari reservoirs are associated with vertical and axial growth of concentric folding, which means that joints are mainly fold-related fractures. This conclusion was however mainly based on the study of well data (well-tests, production logs, mud losses) in some of the Asmari reservoirs.

The aim of this paper is first to present new outcrop observations concerning fracture network growth in the Asmari formation. Special attention is paid to the chronology of fracturing with respect to fold in order to test various existing models of relationship between fracturing and folding and to establish a link between this chronology and the regional structural evolution. Toward this end, the variation of fracture orientations was taken into consideration from a regional-scale point of view. Local stress analysis using fault-slip data, and high resolution satellite and aerial images were used as complementary tools. These

observation are synthesized, in our conclusion, in form of a conceptual model that highlight the fact that a lot of fractures predate folding and were reactivated during folding.

VI.A.1. Geological setting

VI.A.1.1. Tectonic setting

The Zagros is a young (Mio-Pliocene) NW-SE to nearly E-W (in its SE part) trending fold-thrust belt located along the eastern margin of the Arabian Plate. This belt is currently undergoing 20-25mm/yr shortening (Jackson and McKenzie, 1984; De Mets et al., 1990, McClusky et al., 2003, Vernant et al., 2004) and thickening as a result of collision of the Arabian and central Iranian plates (Berberian and King, 1981; Berberian et al., 1982; Berberian, 1983). The present morphology of the Zagros is the result of a geological history including a platform phase during the Paleozoic; a Tethysian rifting phase in the Permian-Triassic; a passive continental margin phase (with sea-floor spreading to the northeast) in the Jurassic-Early Cretaceous; subduction to the north-east and obduction in the Late Cretaceous; and finally collision during the Neogene (Falcon, 1974; M. Berberian and King, 1981; F. Berberian et al., 1982; M. Berberian, 1983). The Zagros folded belt has been divided into several morphotectonic regions (Falcon, 1961, Haynes & McQuillan, 1974; Favre, 1975; Berberian, 1995) (Fig.VI.1b). These main morphotectonic regions are limited by deep-seated basement faults (Berberian, 1995). Despite the lack of detailed deep crustal knowledge in the Zagros, the approximate location and geometry of these faults have been defined using geodetic survey, precise epicenter/hypocenter locations, seismic reflections studies, topographic and morphotectonic features in the Zagros (M. Berberian, 1995).

As shown in Fig.VI.1b, the Izeh zone is part of the Zagros folded belt: it is limited to north-northeast by the High Zagros Fault (HZF), to the south-southwest by the Mountain Front Fault (MFF), and to the northwest by the Balaroud flexure (BF). The Dezful Embayment is another structural zone in the Zagros region containing most of the Iranian oil fields. It primarily corresponds to a topographical characteristic but generally it is part of the Zagros folded belt with a few outcrops of the Asmari Formation. The Dezful Embayment is surrounded by three important structural elements. The north-northwestern limit is the Balaroud flexure, the east-northeastern limit is the Mountain Front Fault (MFF) and its south-southeastern limit is the Kazerun Fault (e.g. Sepehr and Cosgrove, 2004). The area studied in

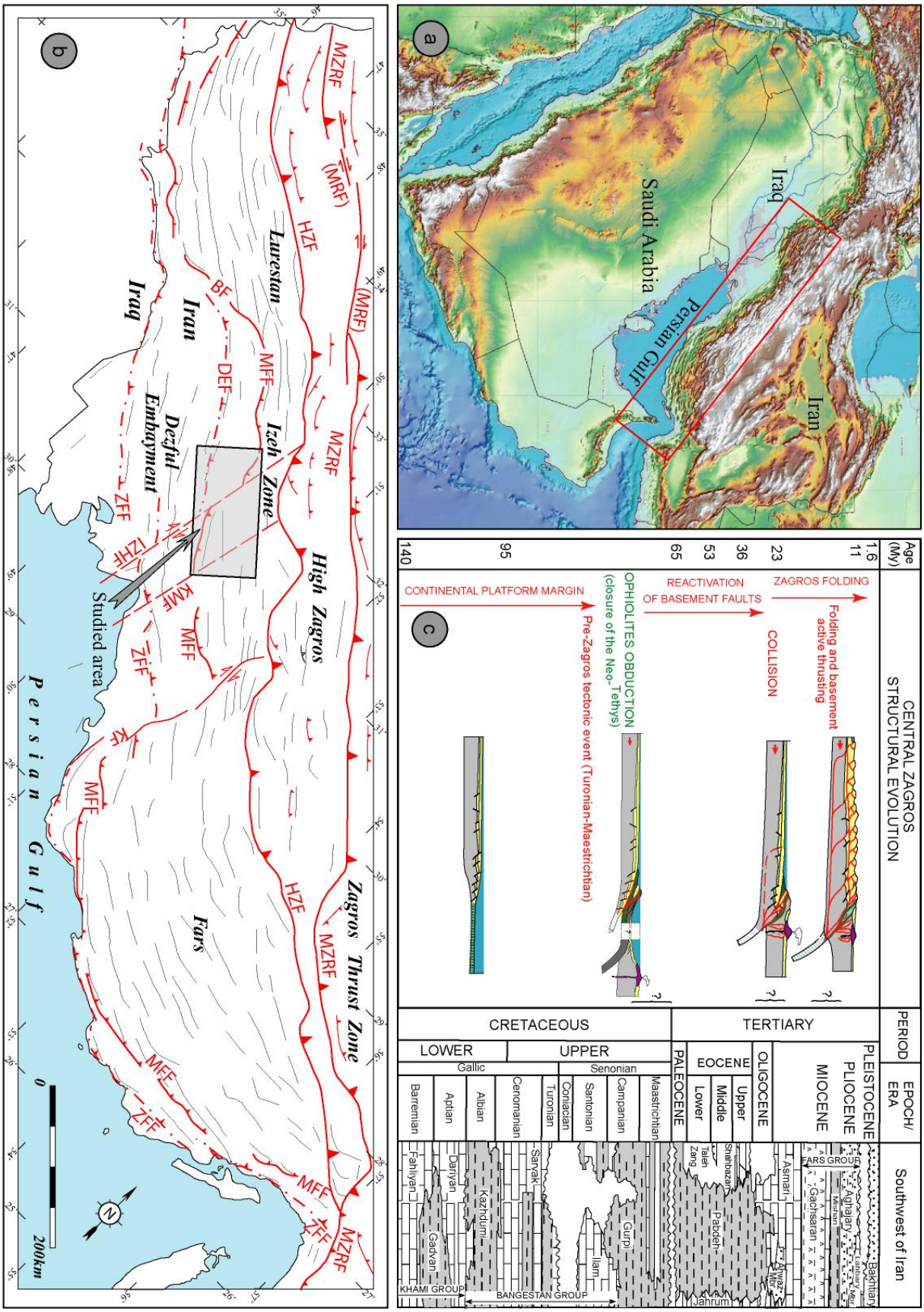

Fig.VI.1: Location map (a), main morphotectonical divisions (b) (Falcon, 1961; Haynes & McQuillan, 1974; Favre, 1975; Berberian, 1995; Motiei, 1993) and structural evolution (modified after Letouzey et al., 2000) and lithostratigraphical divisions of the sedimentary series in the studied area since Lower Cretaceous (modified from James and Wynd, 1965; Setudehnia, 1972, 1975; Szabo and Kheradpir, 1978) (c).

this paper covers part of the southwestern margin of the Izeh zone and the northeastern margin of the Dezful Embayment (Fig.VI.1b).

VI.A.1.2.Lithostratigraphy

Generally three main lithological series could be found exposed in this area from Lower Cretaceous up to Pliocene (Fig.VI.1c); (i) Carbonate series, including part of the Khami Group (Fahliyan and Dariyan Formations, of Neocomian and Aptian age respectively), Ilam and Sarvak Formations (Cenomanian to Santonian) and the Asmari Formation (Oligocene-Lower Miocene). They form the main reservoir rocks in the southwest of Iran. (ii) Clastic and argillaceous series, including the Gadvan Formation of the Khami Group (Neocomian-Aptian), Kazhdumi (Albian), Gurpi (Campanian-Maastrichtian), Pabdeh (Paleocene-Oligocene), Mishan, Agha-Jari and Bakhtiary Formations (Upper Miocene-Lower Pleistocene). Kazhdumi and Pabdeh Formations are well known as petroleum source rocks in the region. (iii) Evaporitic series, including the Kalhur member (Lower Miocene?) within the Asmari Formation and the Gachsaran Formation (Middle Miocene), which is the main cap-rock of the Asmari reservoirs in Iran. All the above sedimentary series, more or less, crop out in the Izeh part of studied area whereas the most part of the Dezful Embayment is covered by Middle Miocene to Recent sediments. However, near the north-north-eastern margin of the Dezful embayment and south of the Mountain Front Fault, the Asmari Formation crops out in anticlines that are sometimes cored by the Pabdeh Formation (e.g. Asmari, Khaviz, Dil and Pahn anticlines). Fig.VI.2 shows the geological map of the studied area (see Fig 1b for location).

VI.A.1.3. Structural style

The sedimentary column in the Zagros is estimated to be up to 12km thick and a great part of this column was supposed to be folded as a single competent group (James and Wynd, 1965; Falcon, 1974; Huber, 1977). This competent group includes sediments ranging from Cambrian to Miocene. It is embedded between two main detachment levels (mobile groups): the Hormuz Salt Formation (Infra-Cambrian) at the base and the Gachsaran Formation (Lower Miocene) at the top (Lees and O'Brien, 1950, Falcon, 1969, Colman-Sadd, 1978). The basement is thought either to have remained rigid or, more likely, to have undergone block

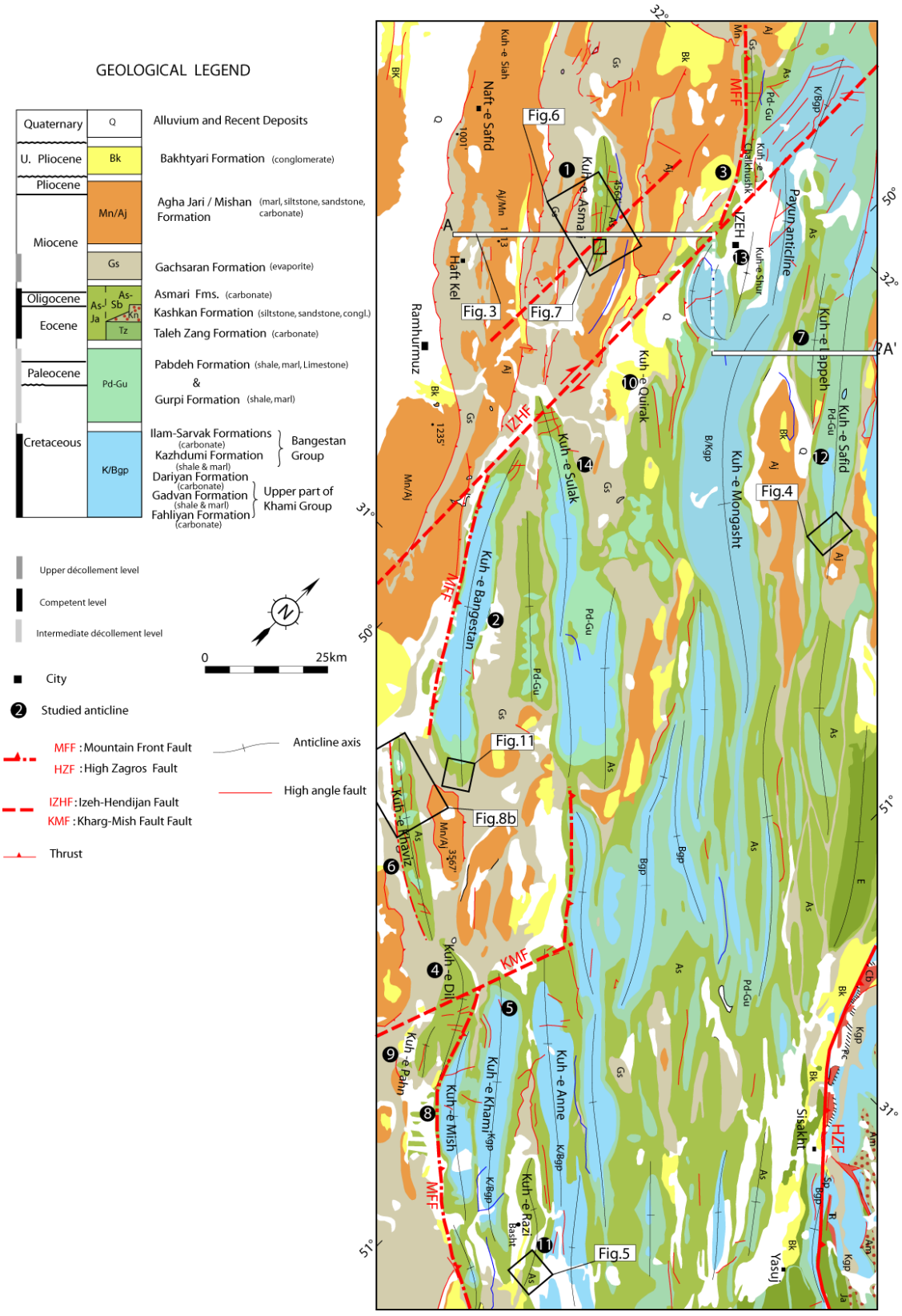

Fig.VI.2: Simplified geological map of the studied area (modified from NIOC 1/1000,000 scale geological map of south-west Iran). The locations of a structural transect, along the line AA' (Fig.VI.3), aerial/satellite images, and zoomed geological maps have been reported.

faulting (Lees, 1952; Falcon, 1969; Talebian and Jackson, 2004). From a geometrical point of view, most of the folds in the Central Zagros are asymmetric and, with a few exceptions, the steepest limbs of the anticlines are on the southwest sides. The most likely mechanism to explain this regionally consistent asymmetry is shearing in the detachment zone of the lower mobile group (Colman-Sadd, 1978). The depth of this basal decollement is not clear through seismic data within Izeh zone and Dezful Embayment. It has been considered to be at a minimum of 9000-10,000m below see level in the Dezful Embayment based on the thickness of the sedimentary sequence and the largest wavelength of the folds (Letouzey et al. 2002). In this context, parallel (buckle) folding in the Zagros have been introduced as essential fold geometry based on mechanical stratigraphy of the area (Colman-Sadd, 1978), folds aspect ratio (half wavelength to axial length ratio) and spatial organization (Price & Cosgrove, 1990). In the competent group, flexural slip has been described as associated to buckling (Colman-Sadd, 1978). In addition to buckle folds, forced folds have been described in the Zagros fold belt and many of them are linked to underlying thrusts. These (often high angle) thrusts are thought to develop in response to the reactivation of basement normal faults during (and subsequent to) the major plate collision in the Miocene-Pliocene (Sattarzadeh et al., 2000).

Recent studies have revealed that a single basal detachment is not sufficient to explain the shape of the Zagros folds. Consequently, the presence of intermediate incompetent layers within the sedimentary succession and their role on folding style have been discussed by different authors (Sherkati & Letouzey, 2004; Sepehr & Cosgrove, 2003; Blanc et al., 2003). Short wavelength anticlines in the Oligo-Miocene Asmari Formation in the Izeh zone shows for example that Pabdeh and Gurpi formations are efficient intermediate décollement levels in this area whereas this role is played by the Albian shales of the Kazhdumi Formation in the southeast of the Izeh zone and parts of the northeast Dezful Embayment (Sherkati et al., 2005 in press). These intermediate décollements strongly influence the kinematics of folding with a progressive thrust propagation into upper décollement levels through time inducing successive reduction in the anticline wavelength. These observations are in line with numerical and analogue models showing how multiple detachments, their spatial distributions, their thickness and their competency relative to the competence of rigid layers can affect this kinematics (Curie et al., 1962; Dahlstrom, 1990; Couzens-Schults at al., 2003; Koyi and Sans, 2003, Sherkati et al., 2005 in press). Furthermore, the geometry of footwall synclines, of thrusts and the amount of limb rotation are best explained by a transition from detachment folding to fault-related folding (Sherkati & Letouzey, 2004).

At regional scale, the amount of shortening and inter-limb angle in the folds decreases from NE to SW within Izeh zone (with an average of shortening about 16%) and Dezful Embayment (with an average of shortening about 6%)(Sherkati and Letouzey, 2004). Figure 3 shows the typical deformation style at basin (Fig.VI.3a) and fold scale (Fig.VI.3b). As shown on this figure, thrusts and detachment levels play an important role in controlling structural evolution and fault geometry.

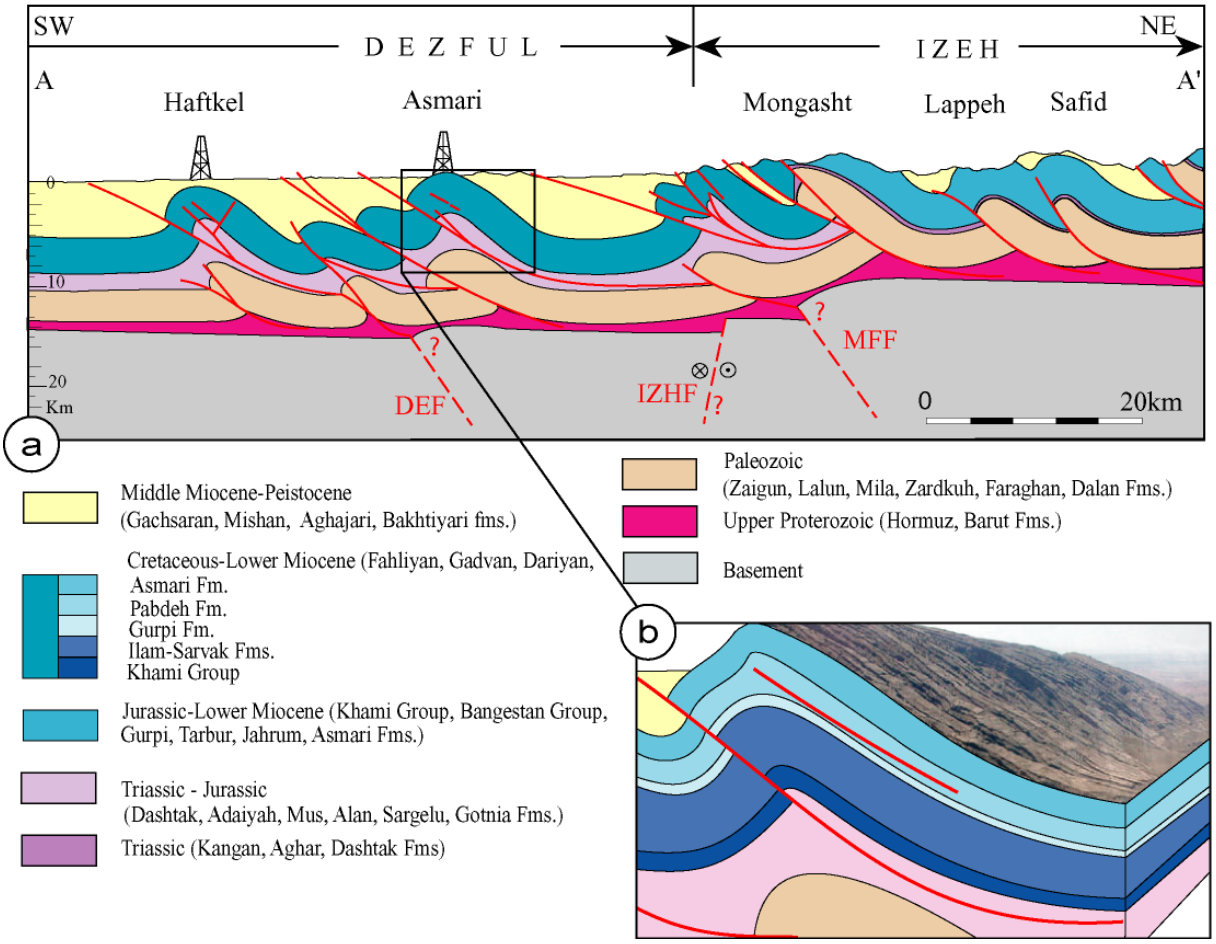

Fig.VI.3: Structural style of the studied area. a) Regional transect through the studied area showing regional deformation style in the Izeh zone and the north of Dezful Embayment (line AA' in Fig.VI.2). Important basement features, Mountain Front Fault (MFF), Dezful Embayment Fault (DEF), and dextral strike-slip Izeh-Hendijan Fault (IZHF) are seen in this transect (modified from Sherkati et al., 2005). b) Zoom into one of typical fold (Asmari anticline) along the regional transect, which shows the effect of intermediate decollement levels and thrust propagation as two principal elements that control fold evolution in the Zagros folded belt.

In addition to thrusts and décollement levels, N-S striking transfer faults (i.e. IZHF, KMF) significantly control the deformation pattern at large scale. These lineaments are strongly oblique to the Zagros trend and they directly or indirectly affect the axial trends of the overlying folds (e.g. Bangestan anticline, Fig.VI.2). These lineaments correspond to linear uplifts along pre-existing basement trends (Motiei, 1995). The IZHF (Izeh-Hendijan Fault) is

seismically active at the present day, with right-lateral movement (Berberian, 1995). The activity of Kharg-Mish fault (KMF), based on thickness and facies variations seen in wells, started after Lower Aptian time (Motiei, 1994). Structural information derived from seismicity within the Zagros belt (see e.g. Jackson & McKenzie, 1984; Ni & Barazangi, 1986; Berberian, 1995; Talebian and Jackson, 2002, 2004) proves the existence of these strike-slip faults in the basement underlying the folded cover.

VI.A.2. Data collection and analysis

VI.A.2.1. Sampling strategy and type of collected outcrop data

Data gathering was organized to cover a large area in order to be able to differentiate regional trends from fold related fractures and local complexity. With this objective in mind, several anticlines were selected throughout the Izeh zone and Dezful Embayment (Fig.VI.2). Table 1 shows the list of the studied folds, their structural position, the number of measurement stations per structure and the type of microstructures which were measured in these stations. Among the studied outcrops, five anticlines are presented in more detail in this paper. In the Asmari anticline fracture measurements were carried out on different structural positions, including SE nose, crest and SW flank. In the Bangestan and Khaviz anticlines, the fracture measurements were restricted on their SE noses and in the Safid and Razi anticlines, fracture orientations were measured in their NE and SW flanks, respectively. The choice of sampling a significant number of anticlines located in a large area forced us to focus on the description of the following major characteristics of the fracture networks: number and types of fracture sets, orientation and detailed observations of fracture cross-cutting relationships, cement filling, and reactivation. Though fracture density data or abutting probabilities on beds and other fracture sets were not acquired, the large size of the surveyed area and the variety of structural positions surveyed, allows us to discuss in detail (i) the relationship between fracture sets occurrence and regional structural trends, (ii) the effect of the structural position in the folds and (iii) the influence of local and/or regional faults on the fracture network characteristics. The detailed observations made on fracture sets chronology provide key input to this discussion and new findings.

In order to speed up the measurement of fracture orientations, all acquisitions were done using electronic compasses (TECTRONIC 4000) except for fault-slip measurements that were acquired with standard compasses. The measurement sites were carried out either along an entire section of the Asmari Formation, on structural surfaces at the top of the Asmari Formation, or in a single position where it was possible to limit the bias due to outcrop

orientation. In most of the measurement stations, the bedding thickness was in the range of 20cm to 200cm. Each station corresponds in average to a 50 by 50 m2 area in which 50 to 200 fractures with a length greater than 50 cm where measured surveying randomly the area. In the presentation of the results, fracture sets are coloured according to the number of fractures in each sets. As the fracture sampling is not systematic along scanlines or surfaces, we are aware that this colour code should be interpreted with caution. However, when a set is clearly oversampled with respect to the others, there is a high probability that it corresponds to the denser one, especially if this is consistently observed in nearby sites.

VI.A.3.2. Orientation measurements analysis

In the following, fracture orientations data are presented in form of lower hemisphere stereodiagrams using Schmidt projection. Measurement locations, sometimes, includes several measurement sites to reduce the number of diagrams on regional map (Fig.VI.10). In this case, fracture orientations data coming from sites located close together in the same structural position (fold location, bedding dip) were gathered in one single diagram.

No.	Structure name	Structural position	Total site No.*	Measured elements**
1	Asmari	SW. flank, Crest, SE plunge & flank	13	1, 3, 4
2	Bangestan	SW plunge & flank	6	1, 4
3	Chalkhushk (Izeh)	NE flank	2	1, 4
4	Dil	NE flank	7	1,3, 4
5	Khami	NW plunge	4	1, 4
6	Khaviz	SE plunge	10+1	1, 2, 4
7	Lappeh	SW flank	7	1, 4
8	Mish	SW flank	3	1, 4
9	Pahn	SW flank	2	1, 4
10	Quirak	NE plunge	4+1	1, 2, 4
11	Razi	NE & SW plunge	8	1, 4
12	Sefid	NE & SW flank	6+1	1, 2, 4
13	Shur (Izeh)	NE flank	1	1, 4
14	Sulak	NE flank of W plunge	2+1	1, 2, 3, 4

Table1: Main studied anticlines and measured structural elements. * the number +1 in total site No. indicates a complementary site for fault-slip data measurement in the studied anticline. ** measured structures include 1= fracture, 2= fault-slip, 3= stylolite, and 4= bedding.

In each surveyed site, bedding planes were measured in order to represent the collected fracture orientation data in their present day or in their unfolded attitude. To unfold the orientation data, we assumed that the sites did not suffer any rotation around a vertical axis and that the local fold axis is horizontal. If the later is a reasonable hypothesis in view of

the structural setting of each site, the former could be discussed for some of the sites, especially for those located along the NS trending lineaments. Following these hypothesis, the fracture data were unfolded using the rotation necessary to bring the average bedding dip to a horizontal attitude. Maps of "folded" and "unfolded" fracture orientation data will be presented to discuss the chronological relationship between folding and fracturing.

VI.A.3.3. Fault-slip data

Fault slip data measurements always provide key constraints on the tectonic evolution. Unfortunately, as Asmari carbonates are very sensitive to weathering, it was difficult to find fresh exposures suitable for such measurements. Despite this difficulty, they have been collected in a few sites (Khaviz, Sulak, Safid and Quirak anticlines, Fig.VI.10) where civilian construction like dams and roads have recently refresh the outcrops. In those sites, paleostress directions were calculated using fault slip data inversion (Angelier, 1990). Faults with sense of slip ranked as doubtful on the field were not used in the inversion process. The result of the inversion is presented in form of the principal stress axes orientations on the stereographic projection of the raw data. In addition, the stress ellipsoid shape ratio, "Φ" =[$(\sigma2-\sigma3)/(\sigma1-\sigma3)$, $0\leq\Phi\leq1$, with compression in positive sign] is shown for each analysis using the dimensionless Mohr diagram. Finally, these tensors are compared with other fracture data to constrain the chronology of different faulting events and to define the possible paleostress history of the studied area.

VI.A.2.4. Satellite and aerial images

In addition to the outcrop scale study where direct fracture observation can be made, satellite (60 x 60 km SPOT 5 scene, HRG instrument, resolution 2.5 meters/pixel) and aerial images (from standard 1/50^{e}000 plane surveys and helicopter) were used as complementary information to define properly the structural context of the observations made at smaller scale. Furthermore, this gives us the opportunity to compare fracturing at different scales. In our data set, part of the Khaviz and Asmari anticlines in the Dezful Embayment and the SE plunge of the Bangestan anticline in southwestern margin of the Izeh zone were selected for analysis based on the quality of the available aerial and outcrop data. The structural maps drawn from the images are used to define the general orientation of major structural lineaments, faults and fracture network. It should be underlined that the objective of the photo

interpretation was to define the location and the orientation of the main lineaments and not to precisely map them.

VI.A.3. Observations

VI.A.3.1. Structural types

Any naturally occurring macroscopic surface discontinuity in a rock due to deformation or diagenesis is called *fracture* (Nelson, 2001). This term will be used in this paper, instead of genetic terms like joint, crack, fissure, vein, and fault when the mechanical origin of a described fracture is not clear.

The most represented fractures on the outcrop are rectilinear fractures, with quite a regular spacing and a significant length (3 to a few tens of meter). These fractures show no evidence of offset across the fracture plane. They are generally perpendicular to major bedding surfaces and often show plumose structures, a common and characteristic feature of mode I fractures based on Pollard and Aydin (1988), Engelder et al. (1993), Kulander and Dean (1985). Though fractographic structures (plumose structure, arrest lines ...) are easily weathered due to the delicate Asmari carbonate lithology, but in the case of their presence, fractures can confidently be called "systematic joints" (Price, 1959, 1966, 1974; Hodgson, 1961a; Ziony, 1966), "regional joints" (Babcock, 1973, 1974a, 1974b) or simply "joints" following standard fracture genetic classifications. At least two sets of joints are found generally within the outcrops of the Asmari Formation.

Stratigraphic stylolites are also frequently observed. Tectonic stylolites (oblique or perpendicular to bedding plane) are less frequent but the orientations of their peaks are used to improve the definition of paleostress orientation.

Finally, faults have been observed in all surveyed sites. At outcrop scale, the more frequent are normal faults, followed by strike slip ones that are themselves more frequent that reverse faults. The two criteria that were used to determine the sense of motion along fault planes were calcite steps and stylolite striations. Slip along bed boundaries is also frequently seen demonstrating that flexural slip is one of important deformation mechanisms in Zagros folds.

VI.A.3.2. Examples of simple fracture patterns: Safid and Razi anticlines

Safid anticline is located in the Izeh zone, in the northern part of the studied area (Figure 2, site 12). This anticline provides an example of a very simple fracture pattern that

can be easily related to the fold geometry. Fracture orientations were measured in the NE flank through six sites from the base to the top of the Asmari Formation (Fig.VI.4a). Two main fracture families striking N50° and N140°±10°, in form of systematic joints, are well developed in this anticline. They show well preserved fractographic structures (Fig.VI.4b). These two sets respectively correspond to fold parallel and fold perpendicular joints. In addition, the analysis of fault and bedding slip kinematics constrains a compressive state of stress with an N40° compression direction (Fig.VI.15C).

The Razi anticline, located in the southeast corner of the studied area, shows a similar fracture pattern (Fig.VI.5a). It is noteworthy that this anticline is a gentle fold whose dips in the exposed flanks poorly reach to 10°. Despite this weak deformation intensity, fracture density seems quite high on the outcrop (Fig.VI.5b).

In the other surveyed anticlines (Fig.VI.10), the observed fracture patterns are generally more complex. They are made of at least three fractures sets that do not necessarily show clear relationship with the fold geometry. Two of these anticlines, which are described hereinafter in detail, include the Asmari and Khaviz anticlines.

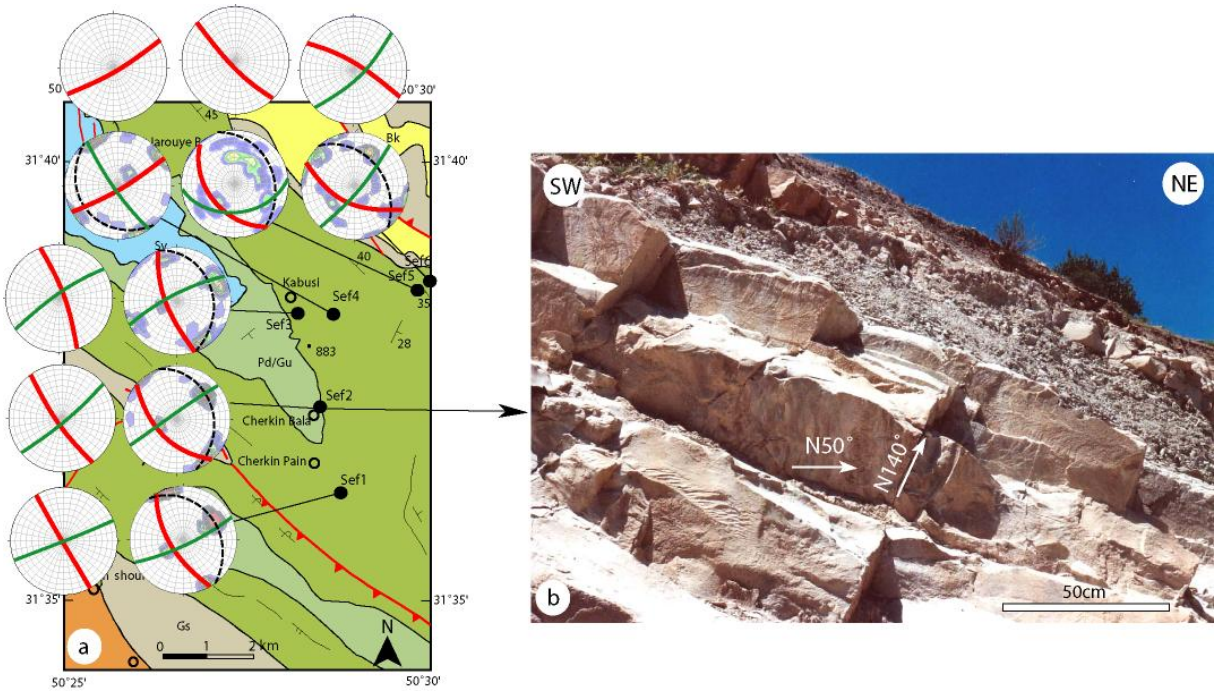

Fig.VI.4: Fracture orientations in the Safid anticline (a), two main fracture sets strike N40° to N50° and N140° to 160°; Plumose structure on the ≈N50° trending fractures suggest their initiations in form of mode I (joint) (b); red, green, and black dashed lines on the diagrams represent the first, second prominent fracture sets and bedding plane respectively (see VI.2.1)

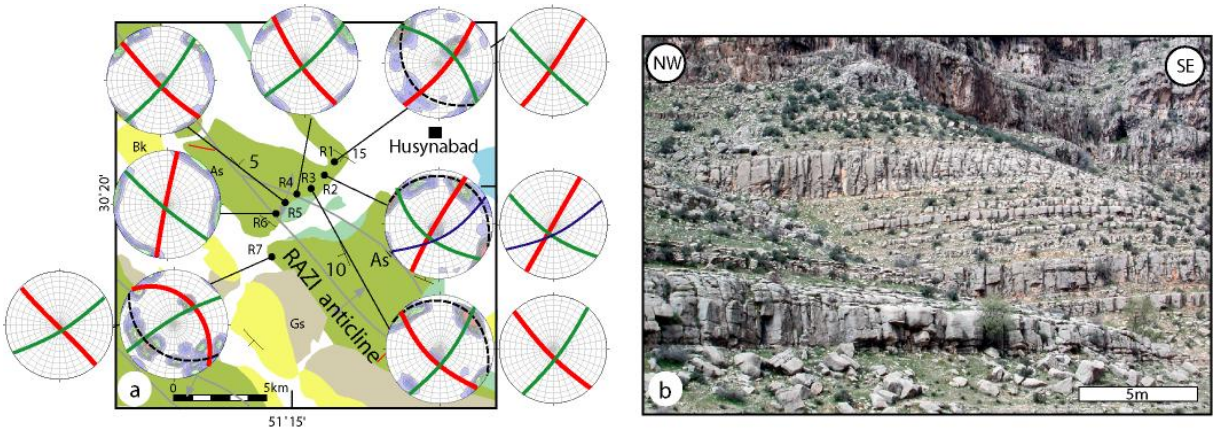

Fig.VI.5: Fracture orientations in the Razi anticline. Sites R1, R2, with the fracture set parallel to the fold axis are located in the syncline (a) red, green, and black dashed lines on the diagrams represent the first, second prominent fracture sets and bedding plane respectively (see VI.2.1); intensive fracturing within different horizontal beds having different thickness suggest the lack of relationship between apparent fracture intensity and the degree of deformation (b).

VI.A.3.3. Asmari anticline

The well-known Asmari anticline (Fig.VI.2, site 1) is located towards the northwest of the Dezful Embayment and west of the IZHF. We measured fracture orientations (mostly joints) in 13 sites selected in the south-western flank, the crest, the north-eastern flank and the south-western plunge of this anticline. These fractures are normal or slightly inclined with respect to bedding planes. Based on orientation (Fig.VI.6a), these fractures can be sorted in three major sets, (i) N40°±10°, (ii) N140°±10°, (iii) N20°±10° and two minor ones (N-S and E-W). Lineament directions (Fig.VI.6b), provided by aerial photos interpretation, can also be classified according to these trends. Bedding strike in the SW flank, where most of the measurement sites are located, varied between N120° to N150°.

From the orientation map (Fig.VI.6a), it appears that the N140° set is best expressed in the southwest flank of the anticline. This can be due either to outcropping condition (the valley in which the measurements was carried out, is perpendicular to this set), or a real increase in the fracturing intensity for this set. Such a density increase is weakly observed on the lineament map. The N20° set seems to be more represented in the south-eastern part of the Asmari anticline even at large scale on aerial photos and can be correlated with the presence of dextral N-S trending faults observed on aerial photos on this anticline as previously mentioned by McQuillan (1973).

The observation of the fractures geometry from helicopter photos taken on the crest of the anticline towards its south-eastern nose provides key constraints on the chronology among these fracture sets (Fig.VI.7 a & b). In this area, structural dip is quite gentle, near horizontal and the trend of the fold axis is about N130°. Figure 5 shows that the N40° fracture set (N50°

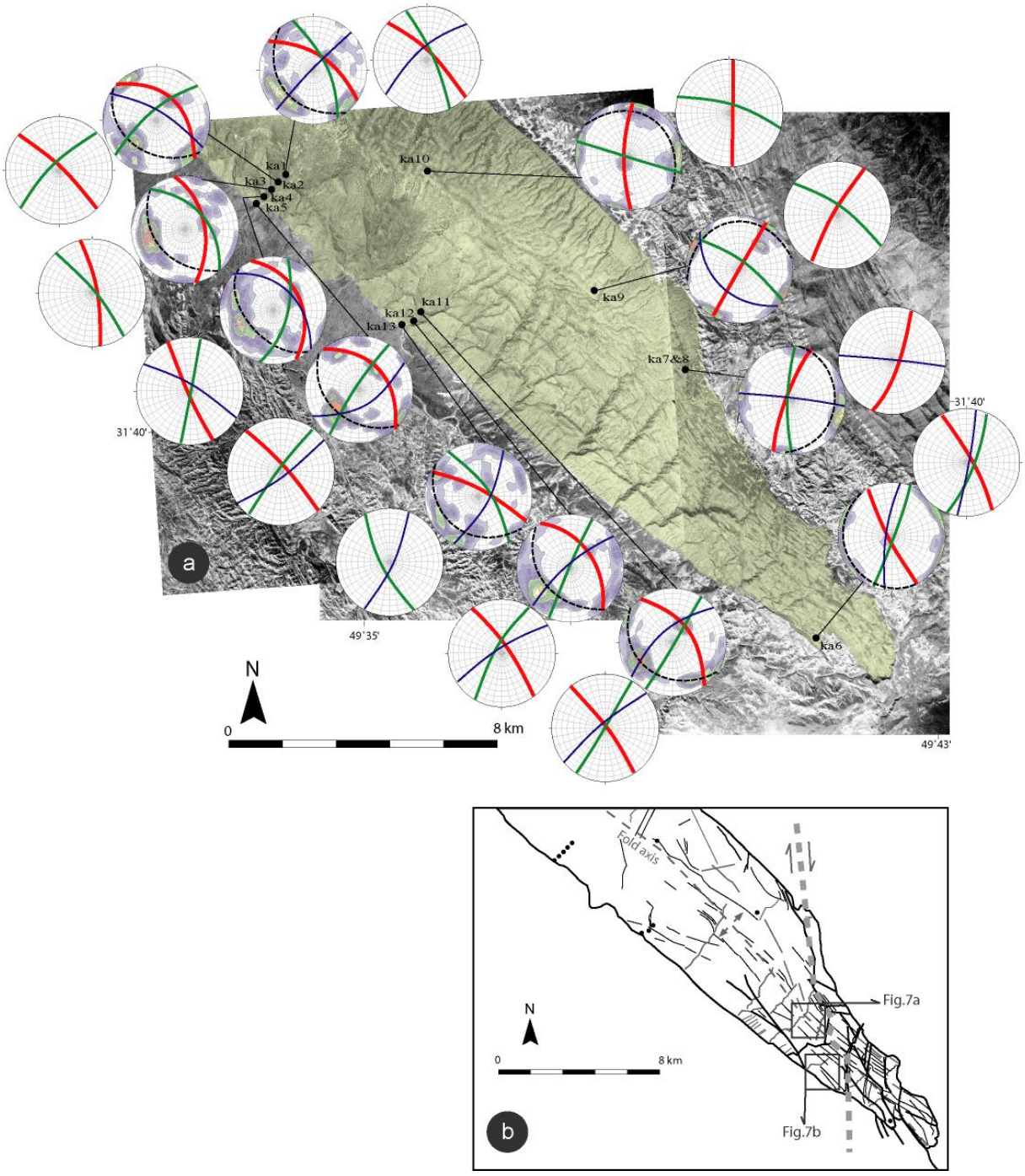

Fig.VI.6: (a) Fracture orientation diagrams from 13 sites on a aerial photo from part of the Asmari anticline, lower hemisphere projection; red, green, and blue solid semicircles are first, second, and third prominent fracture sets respectively (see VI.2.1); black dashed semicircle is bedding plane. Both measured data sets (with fracture density diagram at the background) and back-tilted data sets (without density diagram at the background) were reported on the figure (b): Lineament interpretation, derived from aerial photo, the trend of the main lineaments are compatible with the trend of principal fracture sets recognized in the field.

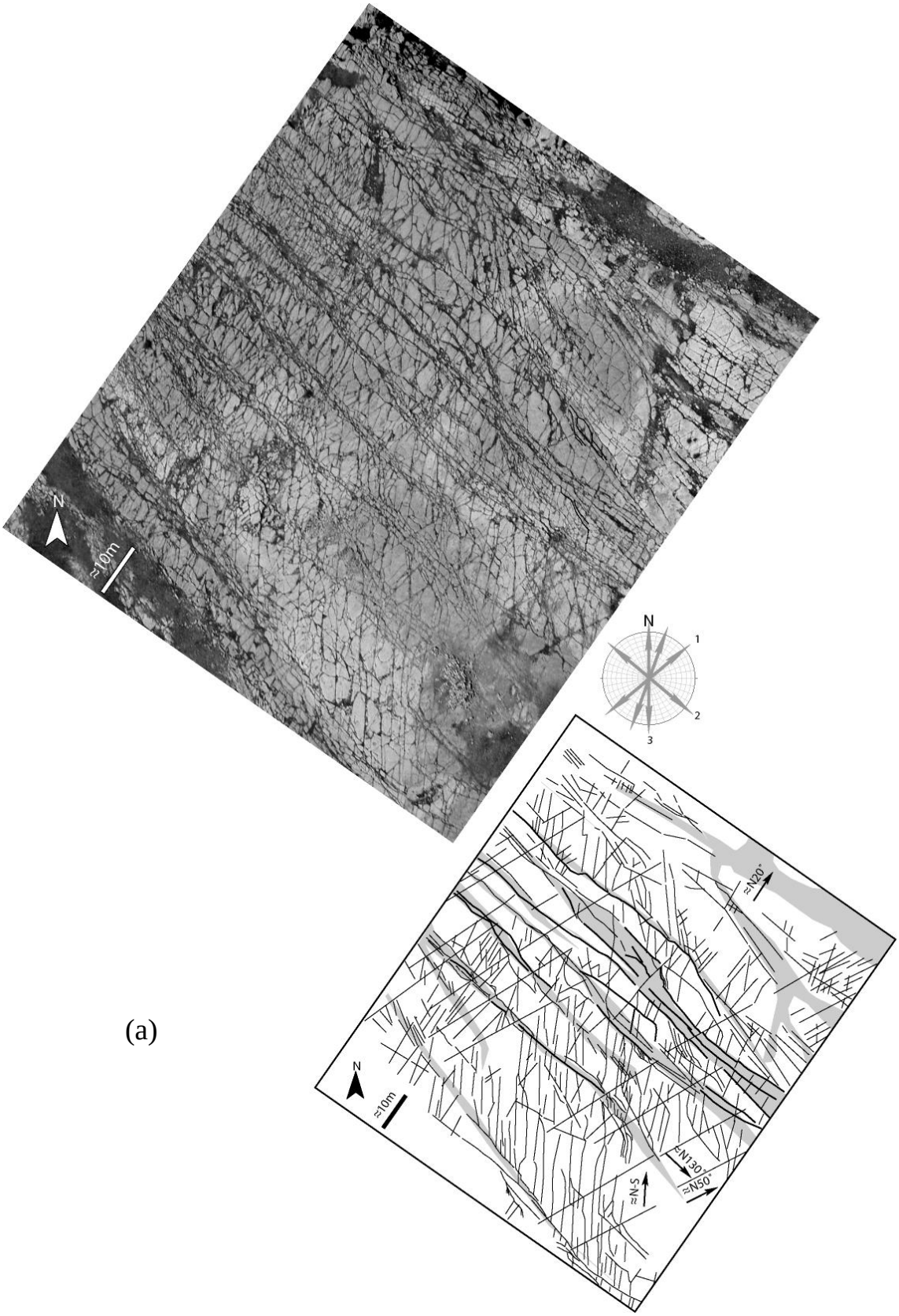

(a)

Fig.VI.7: Four main fracture sets, observed on the southern plunge of the Asmari anticline (a); regular, non-disturbed fracture network with an azimuth of about N50° is considered as the first fracture set, N130° formed a series of fracture swarms are almost parallel to the fold axis, N20°-30° and also N-S fracture sets were abutted to the previous sets. (b) Regular N50°, N20° and N-S fracture sets on the flank position near the location of Fig.VI.7a; 1, 2, 3: chronology of the fracture development.

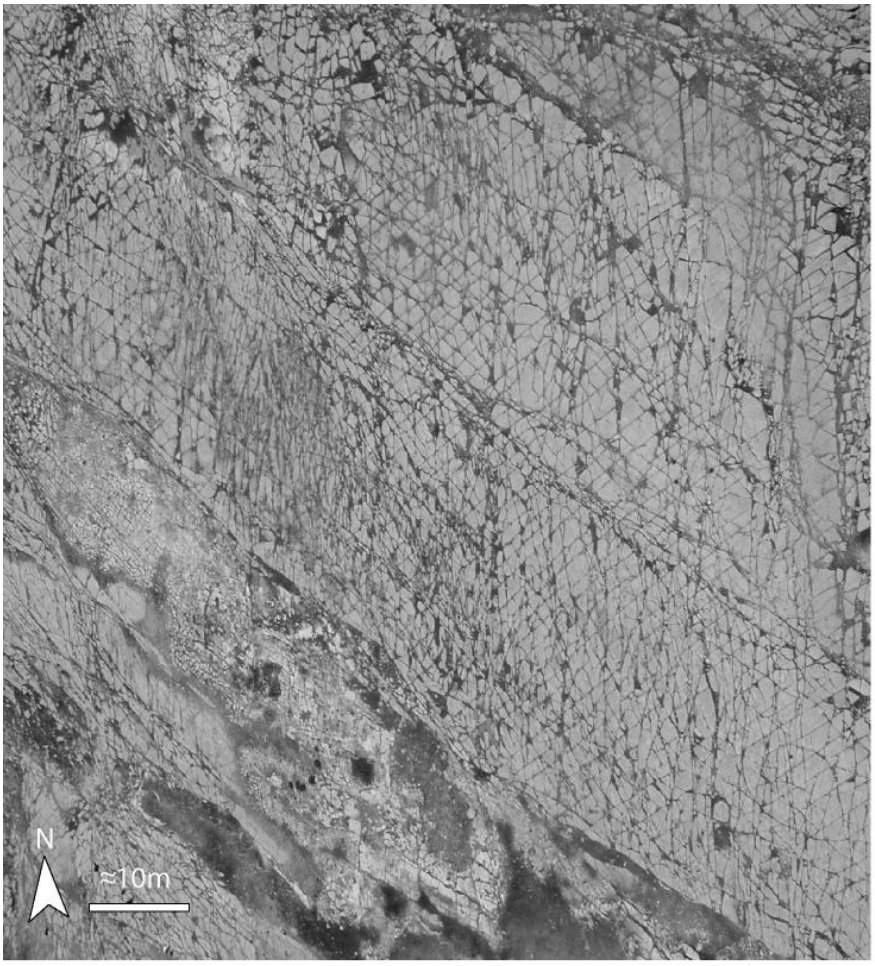

(b)

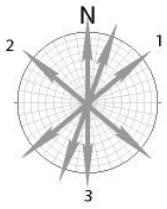

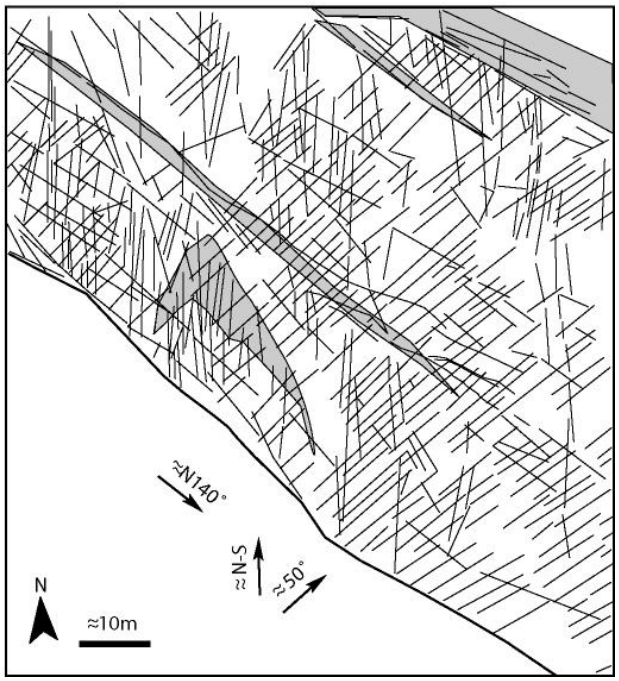

Fig.VI.7 (continued).

at this site) is neither parallel nor perpendicular to fold axis. It corresponds to a very regular systematic joints pattern without any directional perturbation. At the same location, longitudinal lineaments in form of NW-SE trending fracture swarms (Fig.VI.7a) are almost parallel to the fold axis. These lineaments correspond to the N140° fracture set. As some of these fractures abut on fractures belonging to the N40° fracture set this suggest that the latter developed first. Such a chronology is further compatible with the fact that the N40° fracture set forms a very regular fracture pattern when compared to the N140° set. Finally, the N-S minor set corresponds to relatively short rectilinear fractures generally abut on the two previous fracture families. In addition, some of these N-S fractures are branching on the N140° forming dextral horsetail structures (Fig.VI.7a). These observations demonstrate that the N-S fractures postdate N40° and N140° fractures and that these fractures were reactivated during the growth of the N-S ones.

In conclusion, three main fracturing episodes are observed on the Asmari anticline: (i) first, a N50° systematic joint set was formed and (ii) followed by the development of a N140° set, almost parallel to the fold axis. (iii) Finally, an N-S fracture set developed at the vicinity of N-S dextral strike-slip faults strongly controlled by the pre-existing ones.

VI.A.3.4. Khaviz anticline

The Khaviz anticline is located between IZHF and KMF (Fig.VI.2, site 6). This anticline has a quite rectilinear geometry with a general structural trend of about 115° and average dips in the flanks in the range of 30°.

The fracture orientations have been measured in ten sites around the south-eastern nose of this anticline (Fig.VI.8), in an area where bedding-strike covers a wide range of values. Four sets observed on the map (Fig.VI.8a) include: N150°±10°; N50°, N10±10°; N90°±10°. It is worthy to note that large scale lineaments observed on a satellite image from western part of the anticline can be sorted according to the same directional sets (Fig.VI.8b).With this four sets, the observed fracture network is very similar to the one observed in the Asmari Anticline located 150 kilometers away. Despite bedding strike variability, the prominent fracture set does not show significant strike rotation, staying confined between N140° and N160°. The N90° set is very well developed in the southern part of the anticline termination. Numerous small scale normal faults with a variable amount of strike slip movement strike parallel to this set.

The chronology between the fracture sets is well constrained by geometrical relationships between fractures and the history of fracture fillings. The N30° fracture set is

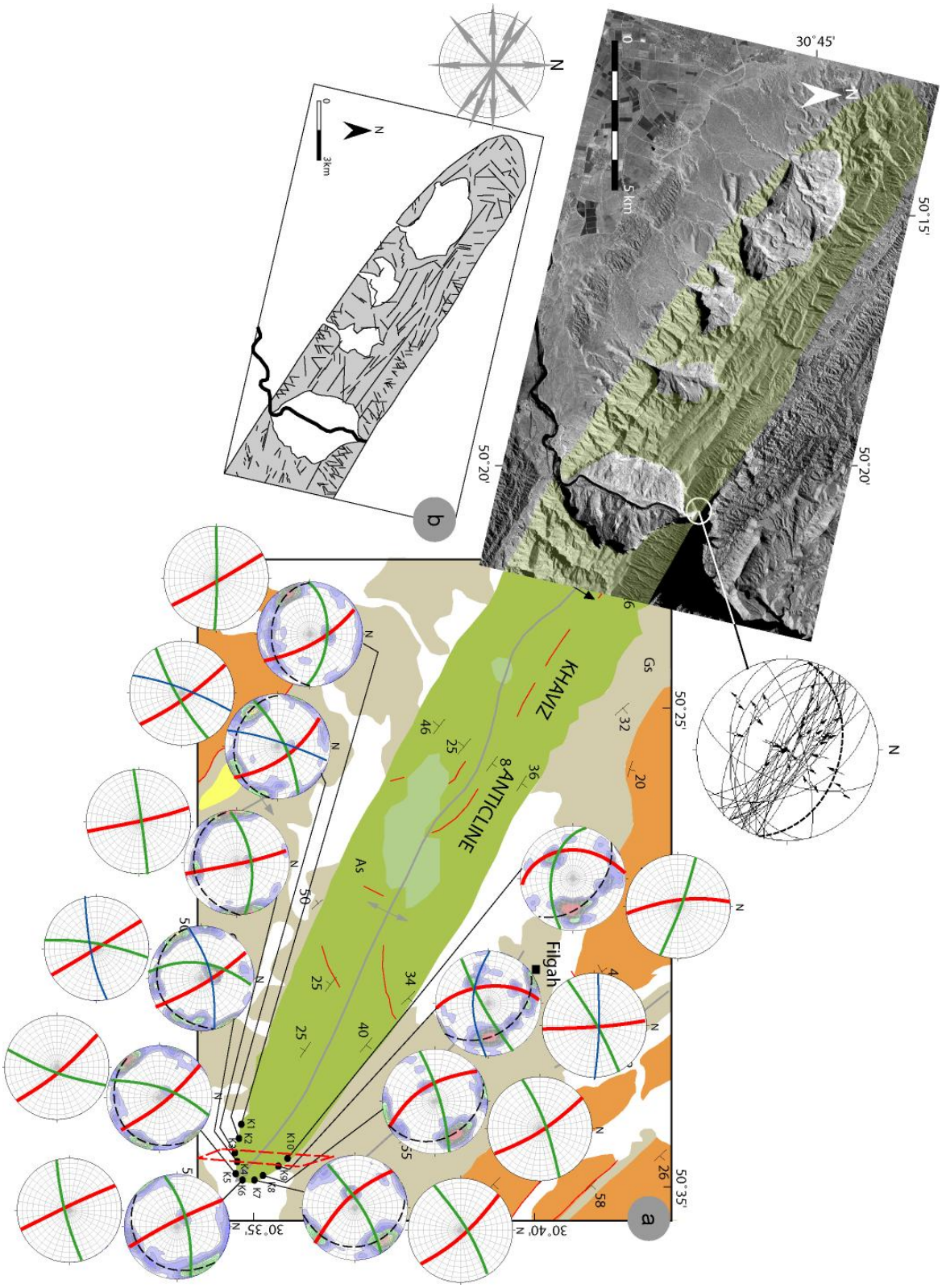

Fig.VI.8: (a) Fracture orientation on the SE termination of the Khaviz anticline, the prominent fracture set, striking N140° to N160° is persistently observed around anticline termination regardless of bedding attitude. The prominent N-S fracture trend, observed in the sites K3, K4, K9, and K10, is likely the effect of a N-S trending fault zone, indicated by a dashed line; lower hemisphere projection; red, green, and blue solid semicircles are first, second, and third prominent fracture sets respectively (see VI.2.1); black dashed semicircle is bedding plane. (b) lineaments on a SPOT5 satellite image on the western part of Khaviz anticline. The main trends which observed in the field, including the fracture sets on the SE nose of this anticline and also the trend of fault-slip data, could be distinguished among interpreted lineament trends in the western part of this anticline.

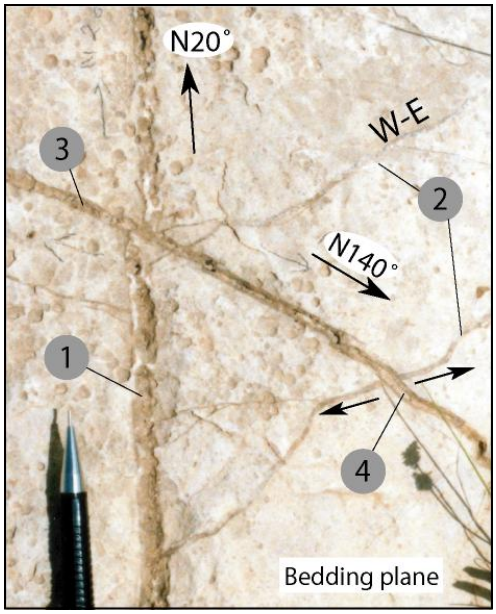

Fig.9: Definition of N20°, N140° and E-W fractures chronologies in the SE nose of the Khaviz anticline. Based on cross-cutting relationships and opening phases, N20° fractures set is likely the first fracture family, while E-W and N140° fracture sets comprise the second and the third fracture generations respectively.

filled by white calcite, with a fresh appearance. The E-W fractures have been filled with two types of calcite: (i) a white calcite similar to the one filling the N30° fracture is observed at the margin of the fractures, (ii) a brown calcite occupies the center of these fractures. N140° to N160° fracture sets are filled by a brown calcite only. As an example repeatedly observed in the southern part of the nose, Figure 9 demonstrates that N20° fractures formed first, then followed by E-W fractures and finally N140° were created and locally sheared and displaced pre-existing ones (Fig.VI.9). In addition, dextral strike-slip movements are observed along E-W fractures where they are widely open and filled by the brown calcite.

Fault slip-data in the Khaviz anticline were collected from the NE flank of this anticline (Fig.VI.8a). An important point at first glance is that most of the fault-plane strikes slightly obliquely to the local bedding strike (N130°-N°140 vs. N110°) though the local fold axis is very rectilinear nearby the measurement site (Fig.VI.8). The data set contains three populations of faults. These three populations are respectively characterized mainly by: (i): dip-slip normal faults indicating a N30° extension with a maximum stress axis perpendicular to bedding (Fig 15A.a), (ii) dip-slip reverse faults that can be interpreted by a poorly constrained N40° compression with a vertical minimum principal stress axis (Fig 15A.b) and finally (iii) sinistral normal faults that may be created by N20° extension applied with a vertical maximum stress axis (15 A.c). Though no direct fault-slip chronology was found on the outcrop, the relationship between the principal stress axis and bedding suggests that the

N30° extension was active before or at the very early stage of folding. The faults defining this extension appear newly formed (and not reactivated fractures) as they have a dip at 30° from the maximum compressive stress axis. In the two other families, faults lying parallel to those associated with the N30° extension are found. This suggests that the two other tectonic events are partly marked by the reactivation of pre-existing normal faults. Concerning the last two faulting events and according to a simple flexural model of folding, we can propose the following chronology: first N40° compression corresponding to the state of stress necessary to create the fold, followed by reactivation of pre-existing faults by extension at the fold extrados.

To summarize, the Khaviz anticline shows the successive development of N50°, N90°, N150° fractures. A fourth fracture set, N10°, is observed, but can not be tied to the others in term of chronology. In addition, fault kinematics indicates the following stress evolution: pre-folding N30° extension, N40° compression and N20° post-folding extension. The relationship between fracturing and this stress evolution and the source of early extension in an overall compressional setting is discussed after the presentation of other key outcrops.

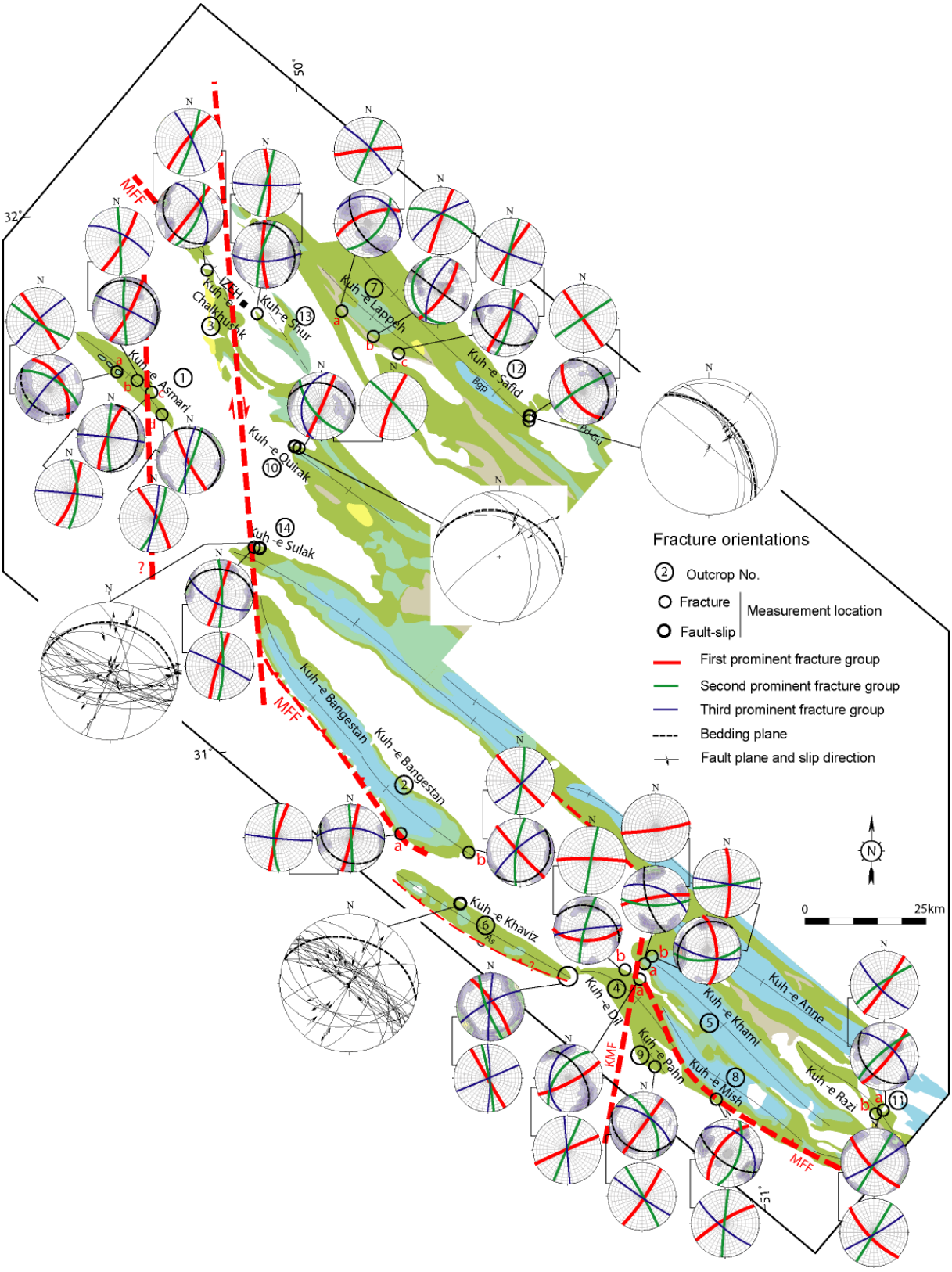

Fig.VI.10: Fracture orientation diagrams (lower hemisphere) and fault-slip data in the studied area. Each circle is representative of a prominent fracture set (generally, two to three fracture families are presented). Measured data were shown by fracture density et the background of the diagram; diagrams with simple white background are unfolded data.

VI.A.3.5. Supplementary fracture data

As shown, in Figure 10, fracture orientation and characteristics were also investigated in other anticlines of the Dezful Embayment. Some of the important observations made in these anticlines are summarized below.

The Bangestan anticline is one of the giant folds in the Izeh zone. The SE nose of this anticline shows a fracture pattern similar to the southern nose of Khaviz and Asmari anticlines with fold parallel and perpendicular fracture sets (N140° and N50°) similar to those observed in the Safid and Razi anticline plus N20° fractures. All these fracture sets are also observed at large scale as lineaments on the SPOT 5 image (Fig.VI.11). Though the chronology between the formation of N140° and N20° fractures is not clear, there is no doubt that the shearing of N50° fractures post date the large opening of N140° ones (Fig.VI.12). This demonstrates that, as in Asmari and Khaviz anticline, a sub-meridian compressive stress was active after a sub-meridian extension.

The Dil anticline (Fig.VI.10, site 4) provides interesting observations to analyze the relationship between folding and fracturing because its axis turns from nearly E-W towards SSE when the axis is followed from West to East. This change can be related to the influence of the nearly N-S trending Kharg-Mish basement fault (KMF). On Figure 10, two sites are presented in the northern flank of this anticline where the average structural dip is close to 40° with a strike changing from N120° to N150°. This figure shows that whatever the dip is, the fracture pattern is made by two major fracture sets perpendicular to bedding: a nearly E-W striking one (N90° to N70°) and a sub-meridian one (N10° to N20°). This suggests that these two fracture sets were created independently from folding. Evidence of shear movements postdating the opening of these fractures demonstrates that they have reactivated many times.

Finally, the analysis of Figure 10 demonstrates that anticlines located at the vicinity of the Izeh-Hendijan fault (IZHF) are dominated by N-S and E-W fractures. This is the case for Shur, Chalkhushk, Sulak, and Lappeh anticlines. Interestingly these fracture sets stay dominant in these anticlines whatever the local trend of the fold axis is. While N-S fracture set is oblique to local bedding azimuth in Chalkhushk and Shur anticlines (Fig.VI.10, sites 13&3), it is perpendicular to local fold axis in the Quirak and Sulak anticlines (Fig.VI.10, sites 10&14). It is noteworthy that similar fracture pattern is observed in the NW nose of the Khami anticline (Fig.VI.10, site 5a&b) located close to the KMF.

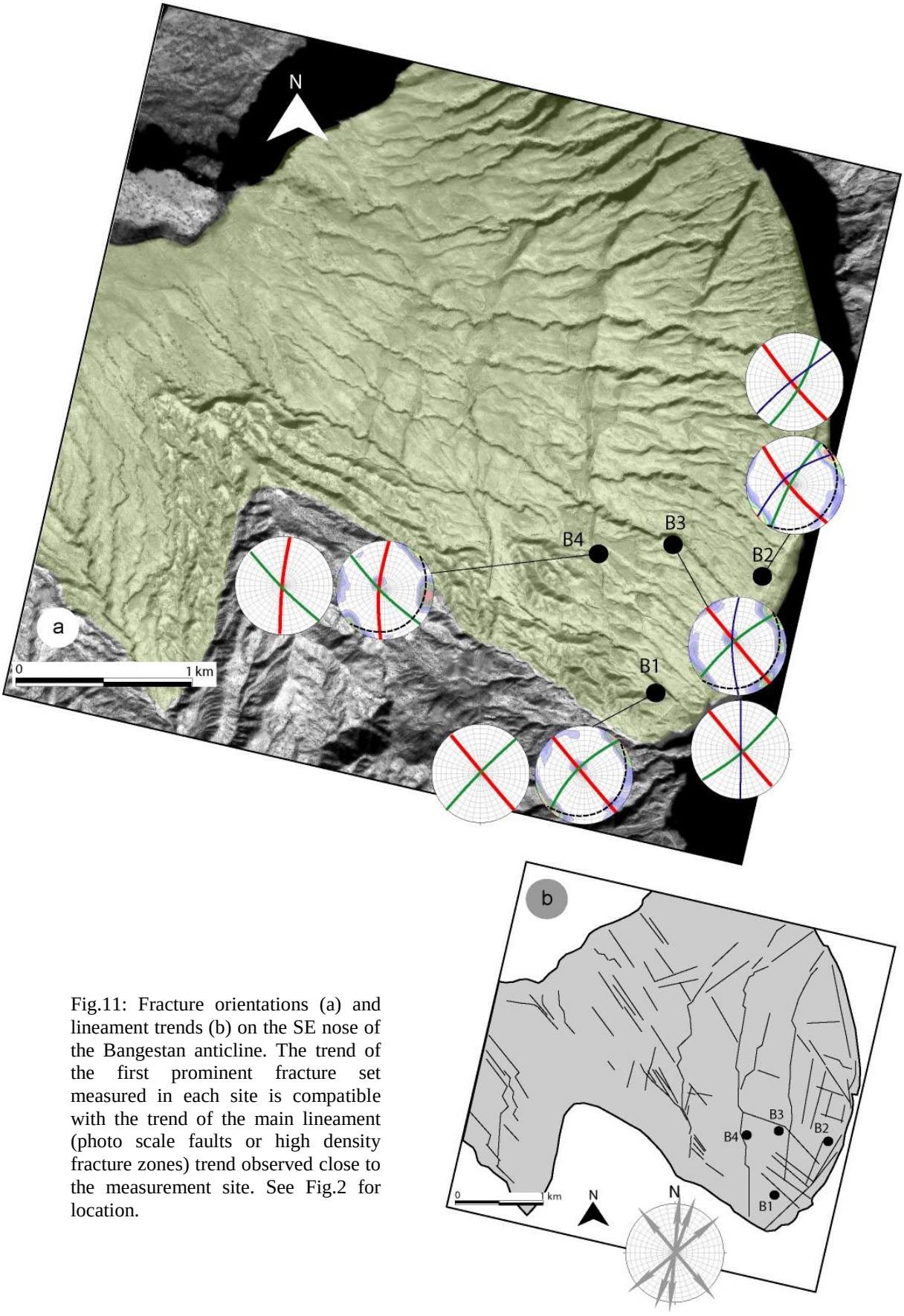

Fig.11: Fracture orientations (a) and lineament trends (b) on the SE nose of the Bangestan anticline. The trend of the first prominent fracture set measured in each site is compatible with the trend of the main lineament (photo scale faults or high density fracture zones) trend observed close to the measurement site. See Fig.2 for location.

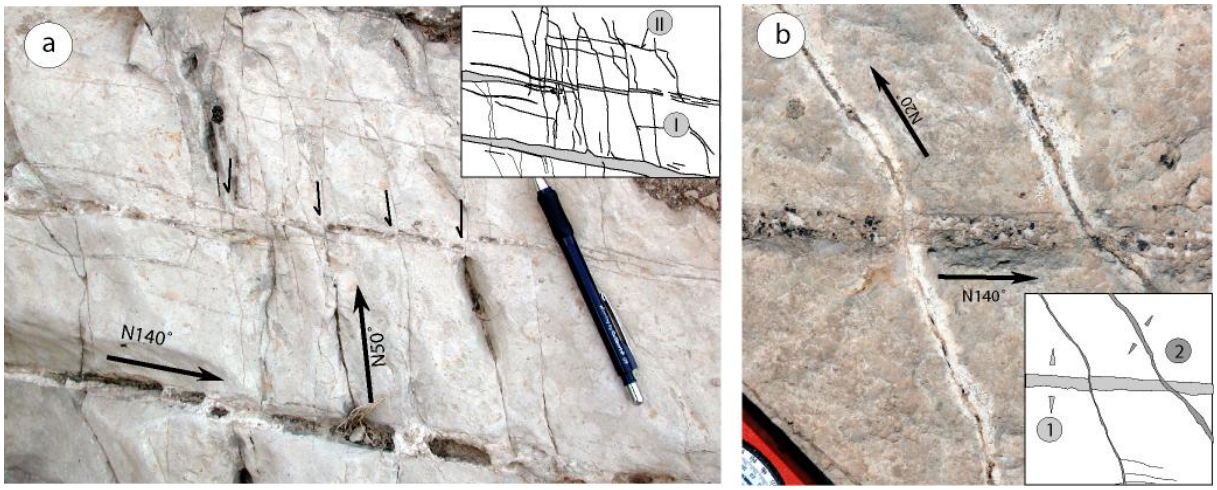

Fig.VI.12: Fracture chronology on the SE nose of the Bangestan anticline; (a) N50° fracture set considered as the first fractures; they underwent a late sinistral shearing associated with offset of the N140° veins. (b) N20° veins likely postdated N140° vein.

These supplementary observations demonstrate that a large population of fractures appears to be independent from the fold geometry, being partly controlled by the location of the sites with respect to basement trends. Furthermore, in the Quirak anticline (Fig.VI.10, site 10) the second prominent fracture set strikes about N140° but in contrast with the SW flank of the Asmari anticline this set appears to be strongly oblique to the axis of the anticline.

VI.A.3.6. Supplementary fault-slip data

The NW nose of the Sulak anticline (Fig.VI.10, site 14) provides an example of paleostress tensor at the vicinity of a major basement fault (IZHF). From the analysis of the stress tensor inversion, three states of stress can be described (Fig.VI.11B): (i) an N25° extension with a maximum principal stress axis perpendicular to bedding and corresponding to the development of N120° normal faults (oblique to local bedding strike), (ii) an N-S compression controlled by flexural slip observation and reverse movements on steeply dipping faults, (iii) an N30° extension with a vertical maximum principal stress. The N25° extension could be attributed to an early tensional stress state as suggested by a maximum principal stress axis lying perpendicular to bedding and by the purely dip-slip movement on normal faults dipping at 65° when unfolded. Such a tensile state of stress is similar to the one described in the Khaviz anticline in term of fault characteristics and chronology. As in the Khaviz, the other stress states seem to reactivate joints or faults inherited form this initial tensile regime as the steeply reverse faults and the oblique slip normal ones. Unfortunately no

direct constraints on the chronology between the N-S compression and the N30° extension were found.

Finally, in the Quirak anticline located a little bit farther from the IZHF, a compressive stress regime similar to the ones described in the Safid and Khaviz is found (Fig.VI.15D).

VI.A.4. Interpretation of the results and discussion

In this section we interpret and discuss our observations taking into account the scale of our observations in the light of the Zagros orogeny. Fold/fracture relationships, fracture relative chronologies and local paleostress orientations derived from inversion of fault-slip data are combined in order to derive a conceptual fracturing model in the Central Zagros. We discuss the evolution of the stress field based on our fault-slip data set and try to find a relation between the stress field and the different observed fracture families.

The fold-related fracture models (Price, 1966; Ramsay, 1967; Stearns and Friedman, 1972; Price and Cosgrove, 1990) are widely accepted by structural geologists to explain fracture patterns in a typical fold. However, relative chronology of different sets and also reactivation and possible effect of inherited fractures on fold geometry are sometimes overwhelmed in most of these models, and only few models attempt at including prefolding joints (e.g., Bergbauer and Pollard, 2004). The fold/fracture relationship involved in most of these models is in poor agreement with fracture patterns observed in anticlines described in this paper: NS fractures are consistently observed in the eastern of Asmari Anticline, N40 to N50 joints predates all the other joint sets whatever the location within fold, fold parallel joint are observe in the flanks quite far from the crest of the anticlines, in Kuh-e Khaviz the orientation of the N140 fracture set in the nose in constant whatever the bedding direction, in Kuh-e Dil the fracture strike is independent of fold axis orientation. In addition, we described a clear chronology between the various fractures sets, demonstrating that they do formed synchronously. Therefore, the progressive deformation of Asmari from the onset of collision should be taken into account to explain the observed fracture pattern.

Furthermore, the geometry of some folds is more complicated than the general trend of the Zagros fold belt. Some examples in this complexity are provided by the axial rotation of Mongasht, Bangestan, and Dil anticlines in the studied area (Fig.VI.2). These local rotations of fold axis are located above well known basement structures (Motiei, 1993). These rotations can be due either to movement at depth along these structures as suggested by the seismicity recorded along these basement faults either to the changes in the depth of decollement level

across these lineaments described by Sherkati et al. (2005). Unfortunately, the geometry of these structures and the timing of their activity during the tertiary are still weakly constrained precise influence of these two mechanisms. However, it is difficult to explain the observed complexities in fracture development and more generally in the deformation pattern of the Zagros sedimentary cover without taking into account basement tectonics.

In order to explain the fracture sets chronology described in this paper together with the role of basement faults, we proposed a conceptual model in the Central Zagros (Fig.VI.13) based on our field observations. This model includes the following two major steps: (i) development of joint sets predating folding, related to the onset of stress loading / layer-parallel shortening of the Zagros sedimentary cover and/or early reactivation of basement faults, (ii) reactivation of the early fracture sets and development of classical fold-related fractures during the main Mio-Pliocene folding event.

VI.A.4.1. Pre-folding fracture patterns in the central Zagros

Hereinafter, the general terms of fold, folding and fold-related fractures in the Zagros will be used for the final orogenic event, leading to the development of folds and thrusts in the Zagros belt during Miocene-Pliocene time (Stöklin, 1968; Falcon, 1969, 1974; Huber, 1977; Stoneley, 1981; Berberian, 1981), together with the general involvement of the basement in shortening. To this respect, fractures which possibly developed in association with large wavelength forced-folds or flexures related to reactivation of N-S and N140° -trending basement features before the main Mio-Pliocene shortening event will be referred to as prefolding fractures.

VI.A.4.1.1. Fracture set I and II: prefolding joints related to the onset of stress loading

Fracture set I (N40°-50° joints): Based on our observations in the field and aerial photos, N40°-50° trending, regularly spaced, joints are considered as the first fracture group which developed in the Central Zagros (Fig.VI.13a). The strike of this joint set is related to the orientation of the regional stress field. It is therefore not necessarily perpendicular to present day fold axis or to the local bedding strike (e.g. in Asmari, Khaviz, and Bangestan anticlines). Development of this joint set could be synchronous with the formation of stylolitic

peaks parallel to this direction. We proposed that this fracture-stylolite association marks the earliest stress loading in the cover

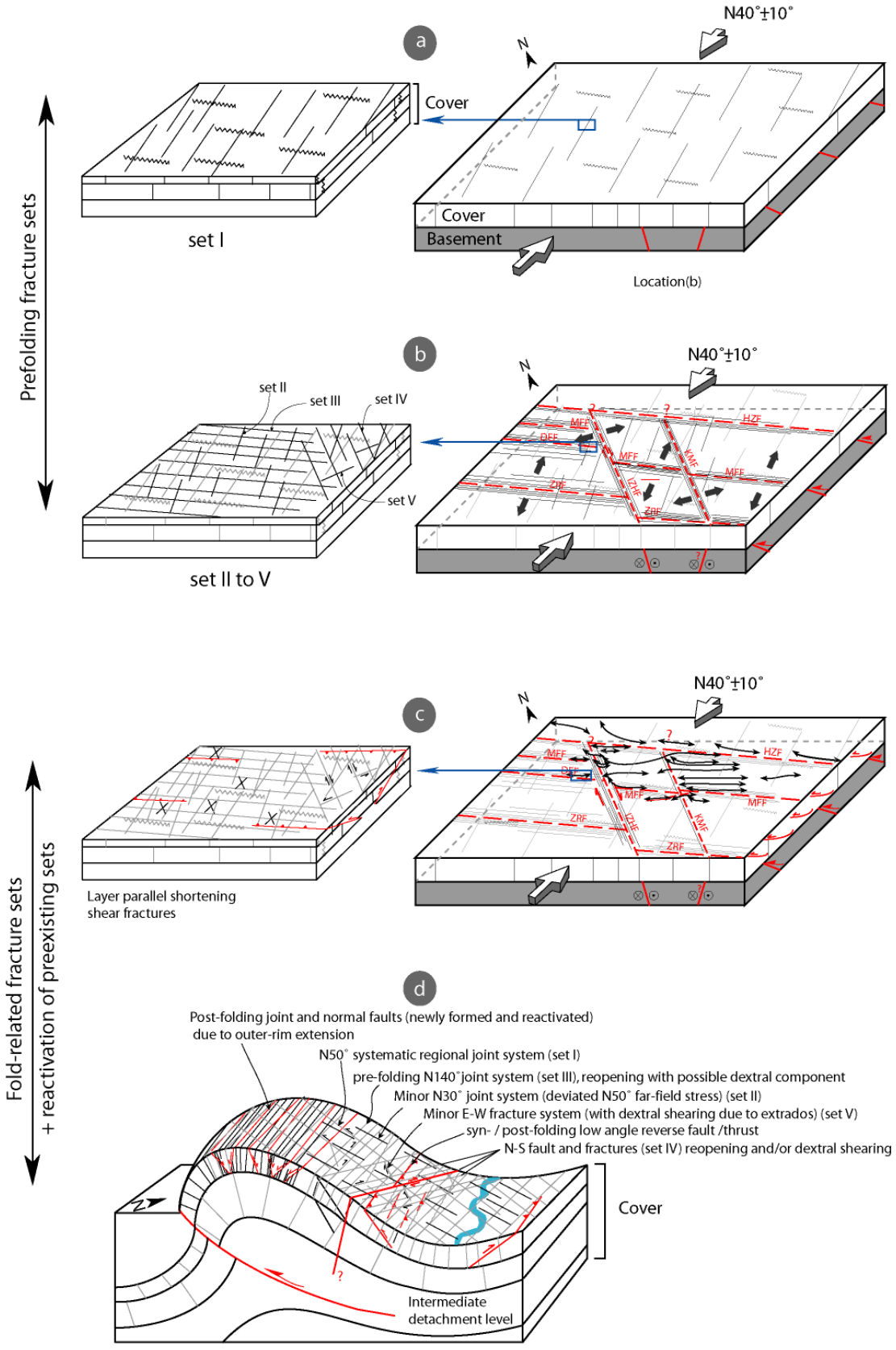

Fig.VI.13: Conceptual model for fracture development within Asmari Formation in the central Zagros folded-belt (see text for more details), putting emphasis on prefolding, regional joint development.

in response to the orogenic far-field stress. Defining the absolute age of this earliest fracture set could be a key point towards the determination of deformation onset within the Zagros basin. They are considered as the first fracture set developed within the Asmari Formation after (or during) its deposition. Development of this joint set presumably predated reactivation of basement faults as proposed in the conceptual model and deformation scenario. If the timing of the early basement fault reactivation can be defined by any means, it may lead to definition of the absolute age of onset of deformation.

Fracture set II (N20°-30°) joints: The second minor group of fractures comprises N20° to N30° joints (e.g. in Asmari, Khaviz, Bangestan). In Kuh-e Bangestan, they postdated the development of set I joints, but show conflicting chronological relationships with N140° fractures. They likely reflect a slight evolution of the compressional trend from N40°-50° to N20°-30°, also marked by the change in trends of stylolitic peaks.

During this pre-folding evolution, the compressional trend defined from joint orientation, stylolites did not change significantly: it evolved from N40°-50° to N20°-30°, and then back to N40°-50°, either in response to a slight rotation of the far-field orogenic stress or as a result of reorientation of the N40°-50° compression within the pattern of N-S trending basement faults, reactivated as right-lateral strike-slip faults.

VI.A.4.1.2. Fracture set III and IV: prefolding joints related to early reactivation of NW-SE and N-S trending basement faults and related flexure/forced folding

Fracture set III (N140°±10° joints): These fractures were identified by their consistent direction and opening mode I. Their strike, more or less parallel to the overall mean tend of fold axes, makes them mimic those of fold-related fractures which are parallel with the fold axis and developed in response to local outer rim extensional stress field at fold hinge (set 3 of Stearns, 1968). Based on our observation in the central Zagros anticlines, however, fracture set III and those lineaments which are parallel to them do not follow exactly fold axis trend or may depart slightly from local bedding azimuth within each individual studied fold. N140-N160° fracture and lineaments directions in Khaviz, Pahn, Quirak, Lappeh, and Asmari anticlines (Fig.VI.10) do not always follow local bedding attitude. In the Lappeh anticline, in spite of important variations in structural dip along measurement sites, these, apparent, axial fractures are rarely seen whereas they are frequent in other anticlines within the same

structural position. In contrast, in the Razi anticline (Fig.VI.9), with a much more flat-lying bedding attitude compare to the other studied anticline set III is prominent. In agreement with McQuillan (1973), concerning the lack of relation between deformation intensity and fracturing within Asmari Formation, we suggest that, at least for this fracture group, local bedding flexure related to folding seems not to have played an important role in their initiation. There are two points to this regard which argue against a simple fold-related nature for set III, even though a late, syn-folding reopening of these early fractures is likely. In the Razi anticline, the measured stations, R1, R2, are located in a gentle syncline, where set III is observed. In these stations, outer rim extension is unlikely. Another evidence of prefolding development of set III is provided by fracture distribution around the terminations (periclinals) of the folds. If one supposes that fold-related joints usually propagate normal to the maximum extensional stress, their trends should change around the periclinal regions of the folds (whatever the model retained, Stearns and Friedman, 1972 or Gholipour, 1998). It means that their trend should change with respect to the mean fold-axis or local bedding trend variations. Periclinal regions of the folds in the studied area, however, do not show such an agreement between fracture and local bedding trend and the same fracture trend can be observed in the limbs and the periclinal parts of the folds. In the SE nose of the Bangestan anticline, set III fractures form the prominent fracture set but the local bedding azimuth is not parallel with this fracture set (Fig.VI.8). Many long valleys on the SE plunge of the Bangestan anticline have developed parallel to this prominent fracture direction. Accordingly, lineament directions parallel to this fracture set on the satellite image on the nose of the Bangestan anticline do not follow bedding attitude changes in the pericline (Fig.VI.8b). Almost the same situation is observed on the SE nose of the Khaviz anticline, where N140°-160° trending fractures are again a prominent fracture set. In this anticline, the model of fold-related fracture pattern can not explain the relative orientation stability of N140°-160° fractures around periclinal area and even of faults and lineaments parallel to this direction, on the NE limb of this fold (Fig.VI.6b).

From the observations and examples mentioned above, a model of fold-related fractures does not apply to set III because the same fracture set could be found in different structural positions with different attitudes and even within different folds. The N140°±10°-oriented fracture set III likely developed early, before the main folding phase of the cover rocks in the studied area. We suggest that set III initially formed in response to a local extensional stress above the main NW-SE trending basement faults like HZF, MFF, DEF and ZFF (Fig.VI.13b). These basement faults, which are almost parallel to the general axial trend

of the Zagros folded belt, might have played an important role in supplying the necessary stress field for development of this extensional fracture set and even associated normal faults (e.g. Khaviz anticline). This role, either in form of inverted pre-existing normal faults (Jackson, 1980, Hessami et al, 2001) or high angle reverse faults (Falcon, 1974; Hubber, 1977; Berberian 1995), should not be overwhelmed in the initiation of the fractures within sedimentary strata. Even, thrust faulting and folding within the sedimentary cover are often triggered and controlled by these basement faults. This could be one of the main reasons for the lack (or weak evidence) of fold/fracture symmetrical relation in some folds in the studied area.

This extensional stress over major basement structures can be responsible for the prefolding extension state of stress measured in Kuh-e Khaviz and Sulak.

Fracture set IV (N-S joints): Another group of fractures, which do not follow fold geometry, are N-S trending fracture system (set IV). They are even observed as faults or lineaments on aerial photos or satellite images (e.g. Asmari, Khaviz, and Bangestan anticlines). In Dil and Mish anticlines (Fig.VI.10, sites 4&5) this fracture set has been recognized as a systematic joint set. Set IV has been mostly identified in the vicinity of N-S trending basement faults (e.g. IZHF and KMF). In the Asmari anticline this set has been observed next to an N-S trending faults in the eastern part of the fold (Fig.VI.4), where likely underlain by a N-S trending basement fault. Koop and Stoneley (1982) show that these basement trends were strongly reactivated as soon as the late Cretaceous in response to ophiolite obduction. Early compressional-wrench reactivation of these N-S trending basement faults could have occurred more or less contemporaneously with those of the basement faults which are parallel to the Zagros trend (e.g. HZF, MFF, DEF, and ZFF), in Oligo-Miocene times. There is no sufficient evidence to suggest a relative priority of reactivation between the two. We suppose that local joints of the set IV have direct relation with underlying basement faults and may have developed with the same forced-folding mechanism and synchronously with set III fractures (Fig.VI.13b). Beyond the Zagros deformation front and Zagros Foredeep fault (ZFF), there are many folds with N-S to NNE-SSW axial trend. This trend is one of the main prominent trends within Arabian sedimentary cover and the related folds are supposed to have formed either directly by the reactivation of N-S trending basement faults in form of horst and graben system (giant fields e.g. Ghawar, Bourgan,…), by salt movements along these faults (see Edgell, 1992 for more details) or due to compression in the cover, induced by shear along a basement wrench fault (Sattarzadeh et al., 2000). Such a fold/flexure trend and related fractures are supposed to have existed locally along the main N-S trending basement

faults (e.g. IZHF, KMF) in the studied area before the Zagros underwent general Mio-Pliocene shortening and fold-thrust belt evolution. It means that NW-SE trending Mio-Pliocene Zagros folds possibly superimposed onto ancient N-S trending folds or flexures in the area. Some sigmoidal-shaped and axially-deviated folds of the Zagros folds could be due to this superimposition of two different deformation trends.

VI.A.4.I.3. Fracture set V: prefolding local minor E-W joints

In the studied area some E-W fracture trends show generally no symmetrical relationship with fold axis. Thus, they are supposed to be pre-folding fractures. Like set IV, set V is restricted to the places where an underlying N-S trending fault is encountered (e.g. Dil, Khami, and Sulak anticlines, Fig.VI.10), and both set IV and V are commonly observed with N-S trending fractures. In the Asmari anticline and near an N-S trending fault, they accompany N-S trending fractures (Fig.VI.6, site ka7&8). There is little evidence for any regional or local E-W trending compression or N-S trending extensional stress; but the close association of fractures of set V with fractures of set IV suggests that they also developed in relation to deep-seated faults. However, some observations of en echelon fracture patterns along an E-W trend could also suggest that some initiated as shear fractures, under a N50° or even N30° local compressional trend.

VI.A.4.2. Fold-related fractures in the Central Zagros

In addition to prefolding sets I to V fractures, fractures unambiguously related to folding could also been observed. Among them are those, initiated as shear fractures. They could be divided into two principal categories (Fig.VI.13c): (1) low-angle (compare to bedding plane) shear fractures, some reverse faults, thrust faults and duplexes (set 4 of Stearns, 1968), which are normally seen near synclines axes (e.g., Safid, Quirak and Dil anticlines, Fig.VI.14), and (2) conjugate shear fractures with the bisector of their acute angles normal to the fold axis or parallel to the maximum compression direction (set 1 of Stearns, 1968). From a geometrical point of view, most of these fractures have formed consistently with the compressional stress field responsible for the main deformation event in the Zagros area. These new shear fractures developed together with faults during the early stage of folding (e.g. Safid, Quirak, and Dil anticlines, Fig.VI.14). The reactivation of preexisting fractures likely happened in this stage as well. As examples, we can mention the observed (i)

dextral shearing along N-S fractures, (ii) sinistral and dextral shearing along E-W fractures, due to local compressional then outer arc extensional stress

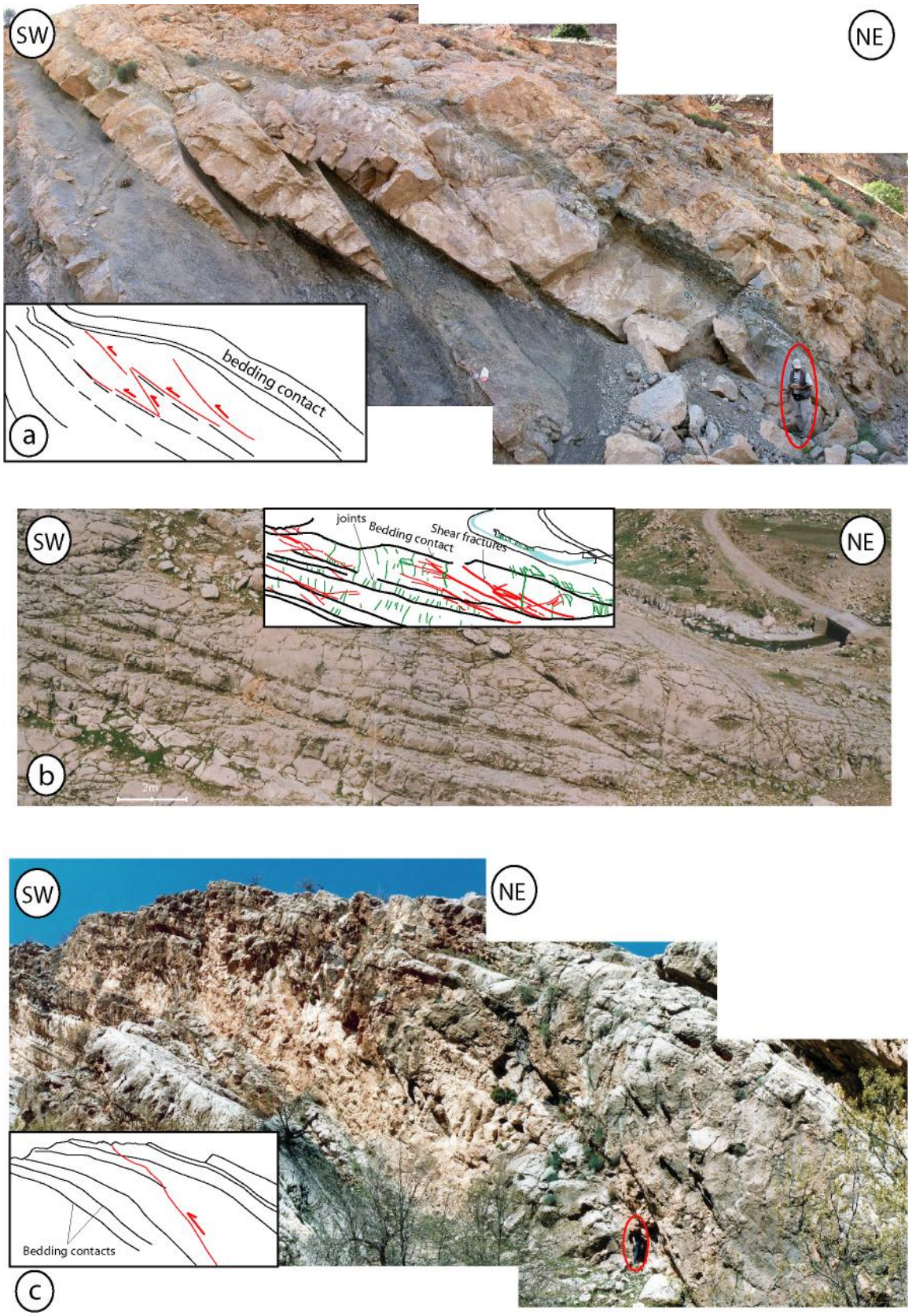

Fig.VI.14: Duplex and reverse faults in the Asmari Formation near the syncline axes. (a) Safid anticline; (b) Quirak anticline; (c) Dil anticline.

field, respectively, and also (iii) sinistral shearing along N50° trending fractures (Fig.VI.12a). This shearing was even observed along NW-SE trending fracture set in form of branched or horsetail fracture pattern towards N-S direction (e.g. the Asmari anticline, Fig.VI.7a). So, the main Miocene-Pliocene folding/thrusting event in the Zagros folded belt is accommodated through both reactivation of previously formed joint sets and new fold-related fractures (Fig.VI.13d). Other forms of fracture reactivations, including fracture intensifying and reorientation under local stress field perturbation related to fold, likely occurred in this phase. So, in the final fold geometry, and based on its location in the studied area, different fracture trends are observed (Fig.VI.13d). Even, we suspect that fold axial-trend variations in the Central Zagros could have been partly controlled by pre-folding, intense fractured zones (e.g., Dil and Bangestan anticlines) in addition to the effect of possible preexisting folds at the vicinity of N-S trending basement faults in the Zagros area.

This deformation stage corresponds well with the second state of stress defined form fault kinematics as a syn-folding reverse faulting event in Kuh-e Khaviz, Sulak, Sefid and Quirak (Fig.VI.15). This compression created new fault-planes (Kuh-e Sefid VI.15C) or reactivated existing fractures (Kuh-e Khaviz and Sulak in Fig. 15). The maximum horizontal stress direction in this phase is consistent with the main folding event. Folding could be responsible for the late-folding normal faulting episode (Fig.VI.15Ac) and for the reopening of the pre-existing ≈N140° fracture and shearing (dextral)-opening reactivation of E-W factures seen in Kuh-e Khaviz and Dil. This last event could be the result of the outer rim extension triggering a state of stress characterized by a minimum principal stress perpendicular to the fold axis.

Conclusion

Fold-fracture relationship and fracture patterns in the Asmari carbonate within central part of the Zagros folded belt, southwest of Iran, were described at different scales (field observation aerial and satellite images) in this paper. Our observations on fold geometries, deformation styles and fracture patterns indicate that the Central Zagros anticlines are not compatible with cylindrical fold model and conventional fold-related fracture patterns may not fully explain their fracturing style. The most important result of this study is the early, prefolding development of most joint sets, which were later reactivated during folding. To this end, this study supports the need of carefully considering prefolding joint sets in realistic conceptual fold-fracture models as pointed out by Bergbauer and Pollard (2004).

The second important result is the demonstration of the role of basement faults on fracturing. The fracture sets striking N040°-050°, N020-030° and N140°±10° are widespread

over studied area and while the former presumably initiated during the earliest stage of the far-field stress loading, the latter developed in the studied area in response to flexure (forced-folding) above NW-SE trending reactivated basement faults. The absolute fracture dating for these earlier sets could be a key point towards a better definition of deformation timing and will allow discussion of the model of partitioning of the Arabia-Eurasia convergence in relation to the onset of motion of the MRF (e.g. the model of Talebian and Jackson, 2004) in the NW Zagros basin. The N-S and E-W fracture (joint) systems show a local concentration near the other major tectonic elements like N-S trending Izeh-Hendijan (IZHF) and Kharg-Mish (KMF) basement faults. Apparently, the occurrence of these fracture trends was controlled either directly by underlying deep-seated basement faults and/or N-S trending preexisting fold in the Zagros region like the ones which exist beyond the Zagros deformation front.

Development of the low angle reverse faults and thrusts in the sedimentary cover is considered as the latest newly-fracturing episode in the Central Zagros based on proposed conceptual model in this paper. Shearing and re-opening of pre-existing fracture sets appears finally to be a very important mechanism to control the deformation within folds. In the present-day folds of the Central Zagros, the observed different fracture sets are the products of a long deformation history which started before the onset of the final stage folding of cover rocks.

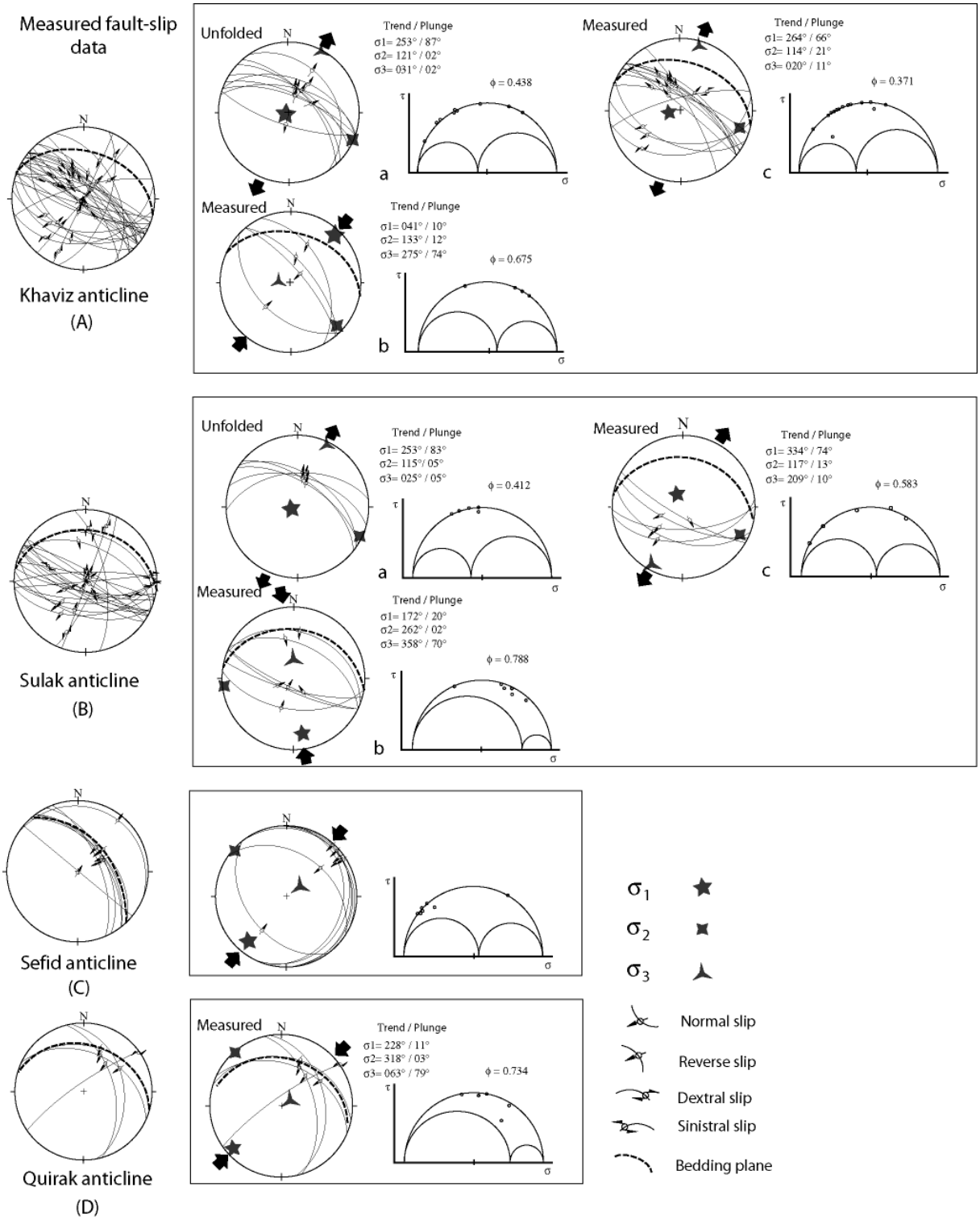

Fig.VI.15: Fault-slip data interpretation in four anticlines including (a) Khaviz, (b) Sulak, (c) Sefid, and (d) Quirak (se text for more details).

VI.B. Supplementary results on fracture study

The aim of this chapter is to provide some complementary remarks and additional explanations in order to complete the previous chapter which was written in a framework to be submitted as a paper. The remarks which are given in this chapter cover different aspects including N-S and E-W fractures, diagenesis, fracturing in the Upper Cretaceous Sarvak carbonates, tectonic stylolites in the Asmari Formation, and some results from paleostress analysis using calcite twins in a few anticlines in the Dezful Embayment.

VI.B.1. Second-order early fracture patterns (N-S and E-W) in the anticlines of Izeh zone in the Asmari Fm.

An important group of oblique fractures within the Asmari Formation are those which are seen either in form of systematic joints, e.g. in the Dil, Khami, and Bangestan anticlines (Fig.VI.16a-c), or near a local fault (Fig.VI.6a, site ka7&8). Presumably, a local E-W direction extensional stress field in the sedimentary cover due to the reactivation of these basement faults, induced N-S trending joint system around the zone of its reactivation within the Asmari Formation. This could be achieved by two mechanisms: (1) they either formed due to oblique-slip reactivation of N-S basement faults, similar to the one proposed for NW-SE trending basement faults, or (2) this reactivation has been almost purely strike-slip, in this case local buckling of sedimentary strata above these strike-slip basement faults is more probable (see, for example, Richard, 1990; Richard et al., 1990; Cosgrove and Ameen, 2000). To be more precise, the observed fractures with trends between ≈N355° to N20° could be gathered in this group. The Shur anticline (Fig.VI.10, site 13), the NW nose of Sulak (Fig.VI.10, site 14), Khami (Fig.VI.10, site 5) and Bangestan (Fig.VI.10, site 2a&b) anticlines and the northern flank of the Dil anticline (Fig.VI.10, site 4a&b) are the locations in which such N-S trending fractures are observed locally as the predominant fracture set. In a photo scale, also, large-scale N-S and E-W fractures and lineaments are observed remarkably near N-S trending basement fault. An example in this regard is the NW plunge of the Bangestan anticline (Fig.VI.17).

E-W joint set in the Dil anticline as a prominent fracture family has a weak relation with structural geometry. A series of E-W calcite seams within uppermost part of the Asmari Formation in Dil anticline is shown in Fig.3a. Their arrangement relating to bedding and their cross-cutting relationship with sedimentary stylolite in this figure show that they should have

formed during certain stage of diagenesis and compaction phase. On the contrary, the reactivation of these E-W fractures in form of sinistral shearing in this anticline is observed, which is compatible with an NE directed local compression stress. Nevertheless, shearing and displacement along E-W directions sometimes show some conflicting features in this regard. E-W sinistral shear bands, echelon, and horsetail fractures (Fig.VI.18a-b) are sometimes seen near the same features in form of dextral shearing along E-W direction (Fig.VI.18c-d).

Such a strange feature is even seen on the SE plunge of the Khaviz anticline, where an E-W directed local shear zone has shifted N30° and N165° fractures dextrally (Fig.VI.19a). Furthermore, based on cement filling of the fractures, two relative period of filling could be distinguished (Fig.VI.19b). A white calcite cement has filled essentially N30° fractures and is also seen along the marginal zone of quite open E-W fractures. Then a brown calcite cement has filled a great part of E-W fractures (Fig.VI.19b). This brown calcite, as was shown in the previous chapter, is seen within ~N140° striking fractures as well.

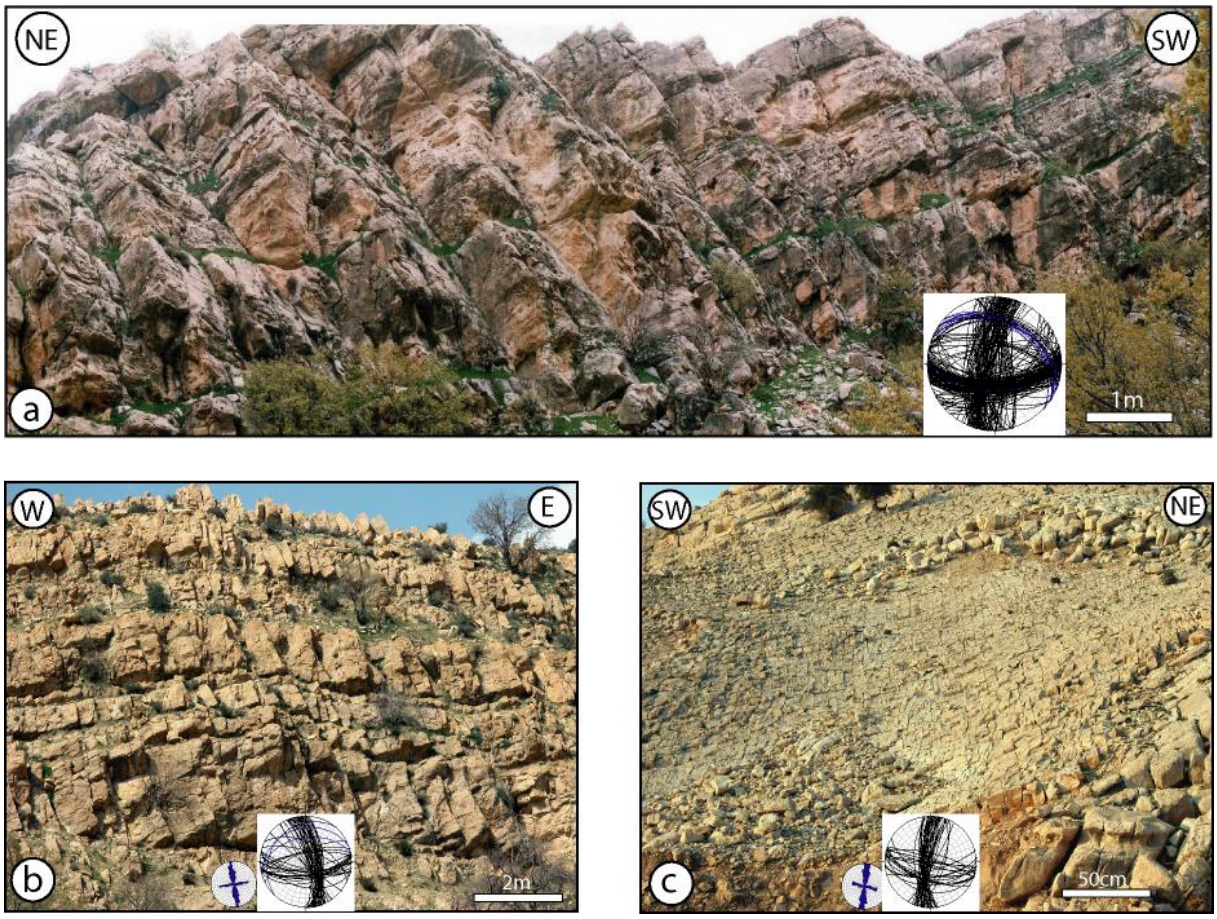

Fig.VI.16: Systematic N-S and E-W trending joint sets in Dil (a), Khami (b), and Bangestan anticline (c).

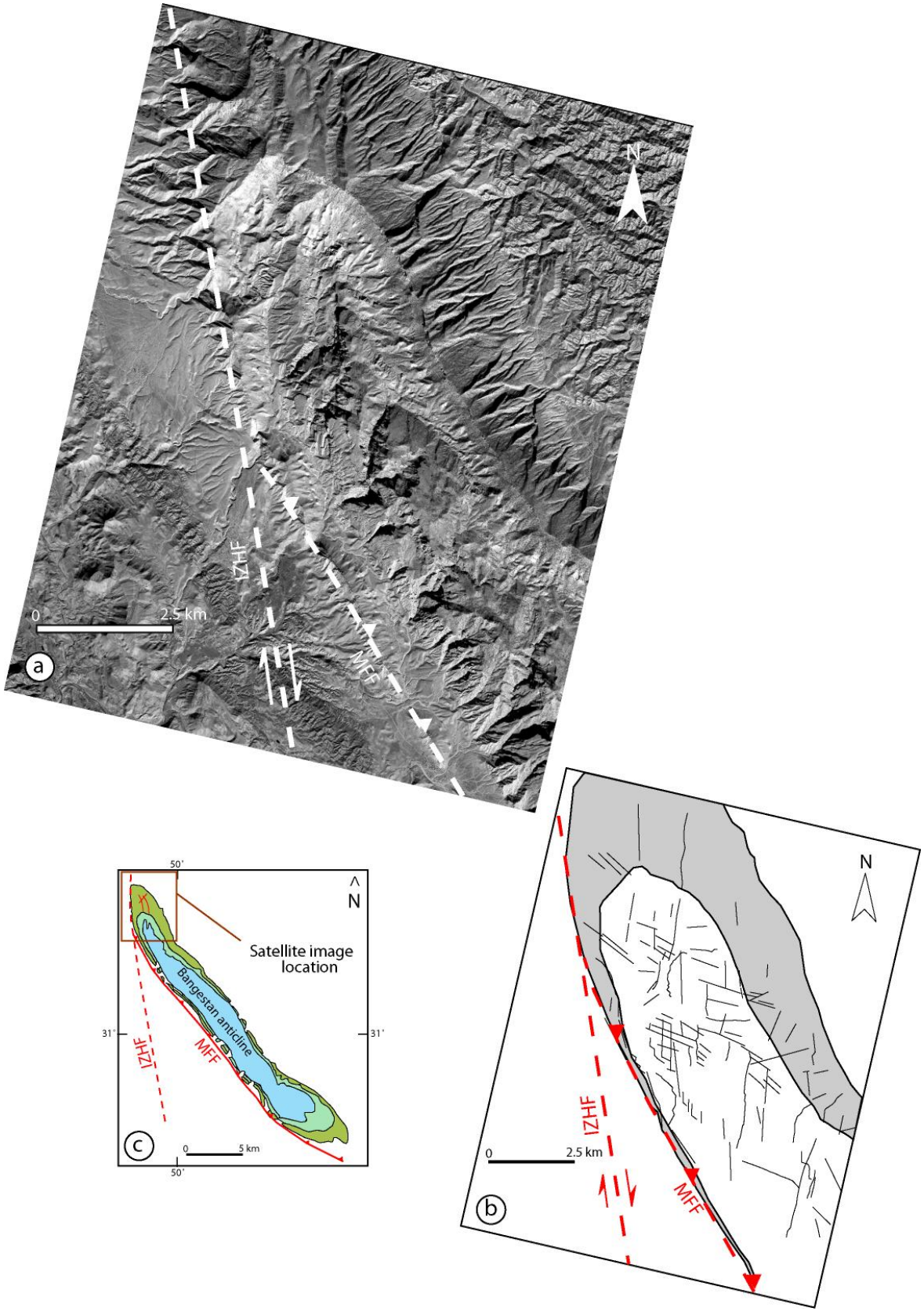

Fig.VI.17: Photo scale N-S and E-W trending lineaments on the NW plunge of the Bangestan anticline (a & b), almost the entire length of the SW limb is delimited by the MFF (Mountain Front Fault) while western limb near the NW termination is bordered by an N-S trending basement fault (i.e., Izeh Fault or IZHF).

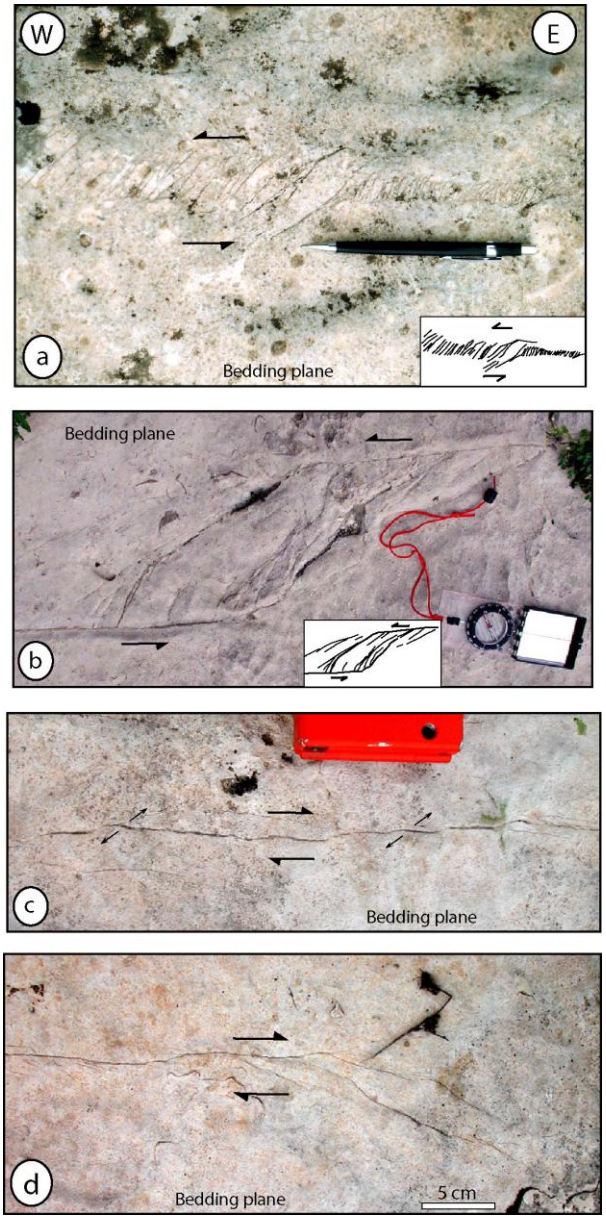

Fig.VI.18: conflicting sense of shearing along E-W direction in the Dil anticline; (a) & (b) sinistral echelon and horsetail fractures; (c) & (d) dextral left-stepping and horsetail fractures.

From the observations mentioned above, we supposed that E-W joint set and calcite veins are presumably local preexisting fracture family in the studied outcrops. Their sinistral shearing and also those minor fractures formed as shear bands and sinistral echelon fractures plus dextral shearing along N-S fracture set should be due to a local compressional stress field. Then dextral shearing while opening, like those observed on the Khaviz plunge and also other dextral echelon and horsetail fractures, e.g., in the Dil anticline, likely formed under a local extensional stress field during folding phase on the uppermost part of the structures (outer rim extension).

Our observations can not support relative chronology of N-S vs. E-W fracture group compared to the other fracture sets. The only place in which a relative chronology between these two fracture sets was observed is the Sulak anticline. As shown in Fig.VI.20a E-W fractures predated N-S fracture set. Furthermore, second generation of small echelon N-S fractures along NNW-SSE direction likely formed due to shearing along this direction (Fig.VI.20b). It is noteworthy to mention that the N-S trending IZHF basement fault is underneath the NW nose of the Sulak anticline.

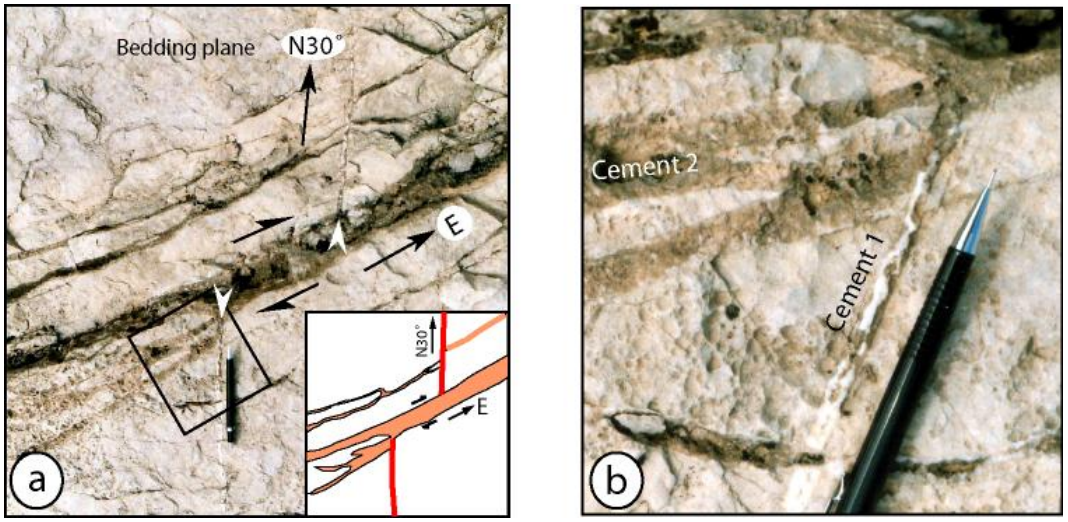

Fig.VI.19: Dextral sense of shearing along E-W direction on the SE nose of the Khaviz anticline (a); two generations of calcite cements are observed (b, zoom of area shown by rectangle in "a"), a with calcite within ~N30° fractures and along margins of E-W fractures and a brown calcite which filled in the middle of E-W fractures.

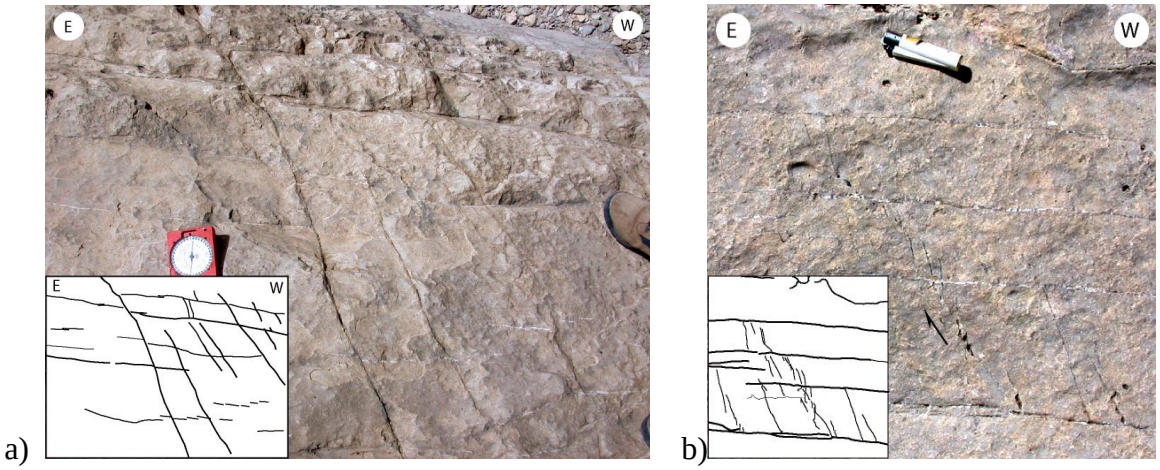

Fig.VI.20: (a) abutting relationship between N-S and E-W fracture sets on the NW nose of the Sulak anticline suggest that E-W fractures predated N-S fracture set, (b) second generation of N-S fractures following a NNW-ward shearing.

VI.B.2. Tectonic stylolites in the Central Zagros folds and their relations to extensional fractures

Tectonic stylolites are other structural elements from which the direction of maximum compressional stress, applied to a fold, may be deduced. Based on Nelson (1981), stylolite zones in outcrops or in cores commonly have a variety of associated natural and induced fractures. It is postulated that the fractures which are directly associated with the stylolite zone originate from the same stress state that caused the stylolite. The fractures have a distinct morphology and can, like the stylolites, be used as paleostress indicators. Not all stylolites have so-called extension gashes associated with them. The presence of extension gashes must, therefore, indicate something unique about the origin of the stylolite zones which have them. A stylolite without fractures shows the rock deformation by uniaxial compaction (all strain or displacement and section loss are parallel with the maximum stress direction). The deformation of stylolite zones with associated extension gashes is, on the other hand, quite different from those without fractures. In this case, there is not only a compaction parallel with the maximum principal stress direction, but there is also an extension parallel with the minimum principal stress direction (Nelson, 1981). Readers can refer to chapter IV for more details.

In the southern flank of the Asmari anticline a system of parallel stylolites with N130° strike are observed. This strike is almost parallel with the general trend of the fold axis. The fractures (extension gashes) accompanied these stylolites abut on the plane of these stylolites and therefore likely postdate them (Fig.VI.21a). The stylolitic peaks were not measured in this anticline, so coincidence of stylolitic plane with general trend of the fold makes it difficult to judge about the relative chronology of stylolitic planes compared to folding event. However, stylolitic planes, with almost the same orientation, were observed in other studied anticlines which show quite weak relation with fold geometry or local bedding azimuth (e.g. Dil and Sulak anticline, Fig.VI.21b&c). These observation suggest that NW-SE trending stylolite planes presumably predated folding phase in these anticlines. In the Dil anticline a group of E-W fractures cross-cut these stylolites (Fig.VI.21d) and confirm the relative fold/stylolite chronology as the E-W fractures, themselves, were argued to predate present folds. On the northern limb of the Khaviz anticline three directions for a series of stylolite peaks were measured, including N020°, N040°, and N060°. All of these direction are compatible with a general NE-ward shortening in the Central Zagros. One of the ambiguities regarding derived

local shortening direction in the studied area is the presence of E-W trending stylolitic planes in the Sarvak Formation (Payun anticline) which suggest an N-S trending shortening. But as a detailed microtectonic study on stylolitic peak directions was not performed and, on the other hand, E-W fracture set in the Payun anticline (Sarvak Formation) is also one of the prominent fracture sets, these E-W trending stylolite planes are likely preexisting reactivated discontinuities in form of antifractures (or stylolites) under a general NE trending compressional direction.

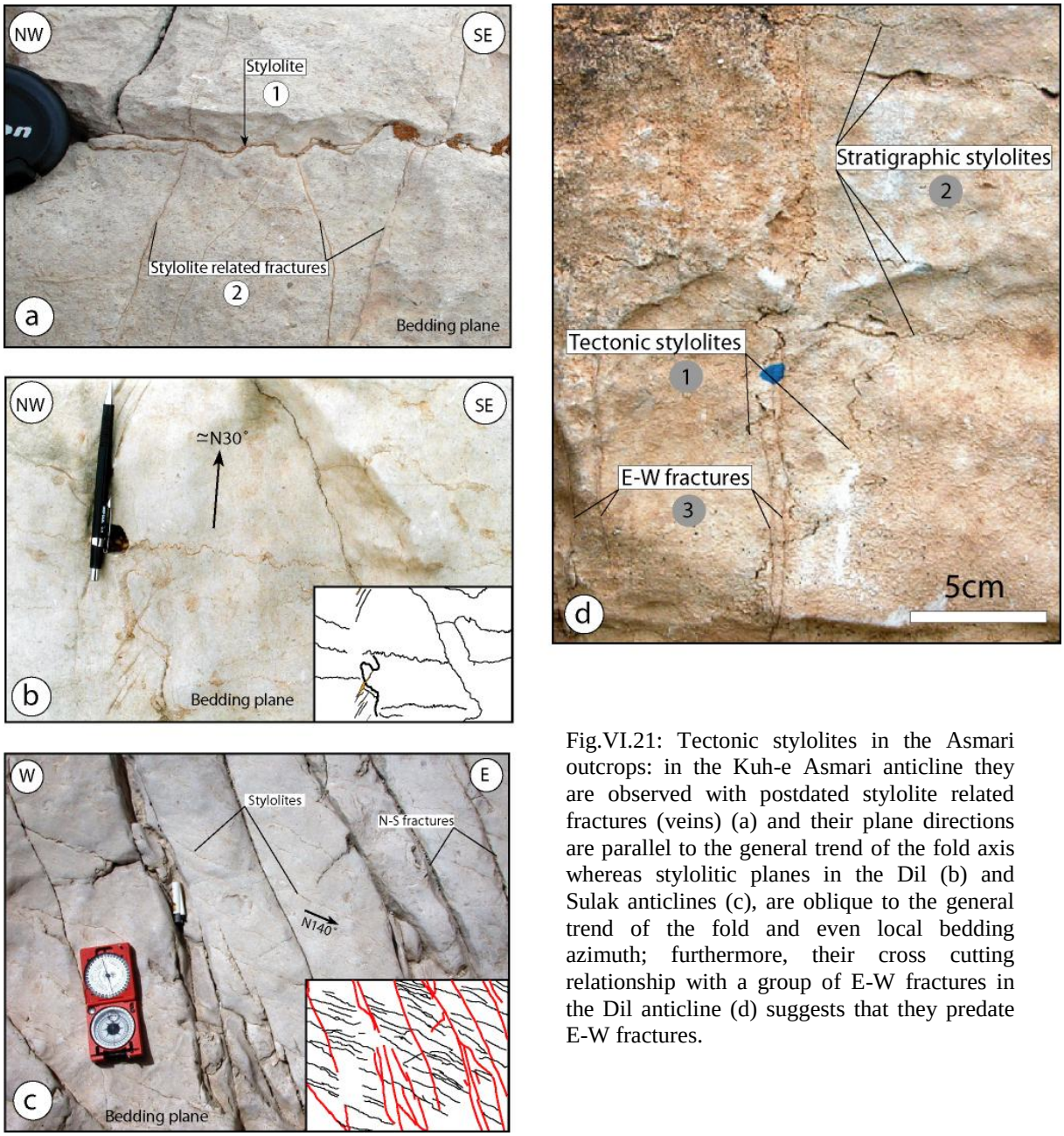

Fig.VI.21: Tectonic stylolites in the Asmari outcrops: in the Kuh-e Asmari anticline they are observed with postdated stylolite related fractures (veins) (a) and their plane directions are parallel to the general trend of the fold axis whereas stylolitic planes in the Dil (b) and Sulak anticlines (c), are oblique to the general trend of the fold and even local bedding azimuth; furthermore, their cross cutting relationship with a group of E-W fractures in the Dil anticline (d) suggests that they predate E-W fractures.

VI.B.3. Comparison of the results of paleostress analysis using fault-slip data and calcite twins in veins from Khaviz and Dil anticlines

(This part summarizes the main results obtained by K. Amrouch on calcite twinning in the Khaviz and Dil anticlines during his stay at IFP (summer 2005) under the supervision of J.M. Daniel and O. Lacombe)

As was mentioned in chapter III, in addition to fault-slip data, calcite twins were introduced for paleostress analysis by some authors (e.g., Lacombe et al., 1990, 1992, 1994). The application of this method in the Asmari carbonate was tested in the Khaviz and Dil anticlines (Amrouch, 2005). In both anticlines, an N-S (~N170°) extensional stress direction was calculated (Fig.VI.22) which is compatible with observed E-W trending joints in these anticlines. This joint set is oblique to the general axial trend in and shows no symmetrical relationship with the fold geometry. In both anticlines, this joint set is perpendicular to the bedding plane and stratigraphic stylolites (Fig.VI.23a&b) and presumably predate Mio-Pliocene folding phase. This joint set and related minimum stress direction has been labeled as no.1 in Fig.VI.22. The second calculated stress tensor in the Dil anticline shows an NE-SW direction for the minimum stress axis which is similar to the stress direction derived from fault-slip data in the Khaviz anticline (Fig.VI.15Aa).

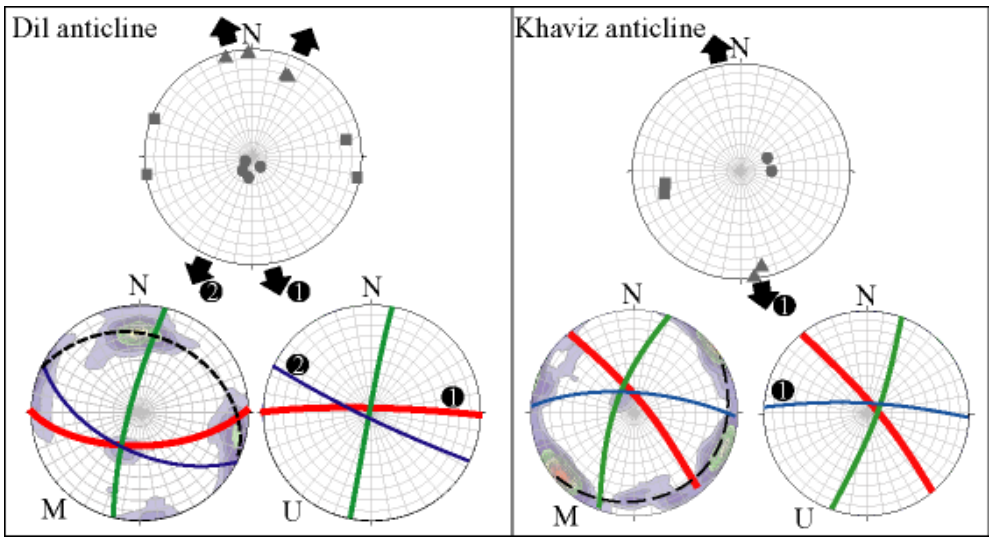

Fig.VI.22: Stress tensors derived from calcite twins analysis (top diagrams, modified from Amrouch, 2005), and comparison with the prominent joint sets in the Khavis and Dil anticlines. Gray color filled circles, squares, and triangles are the maximum, intermediate and minimum stress axis respectively ($\sigma_1, \sigma_2, \sigma_3$). Red, green, and blue color lines are the first, second and third prominent fracture set respectively. see text for more details.

This extensional stress direction predated folding event in the Khaviz anticline (see chapter V for more details). This interpretation for the Dil anticline is applicable as well because the measurement and sampling location was in a syncline (Fig.VI.24), so this stress field and limitedly developed NW-SE trending joint set (Fig.VI.22) in this anticline (as in the Razi

anticline, see chapter VII for more details) can not be interpreted as outer rim (extrados) type joint set and likely predated the present-day fold.

a) 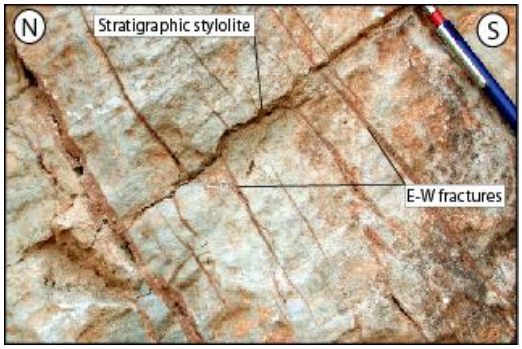

b) 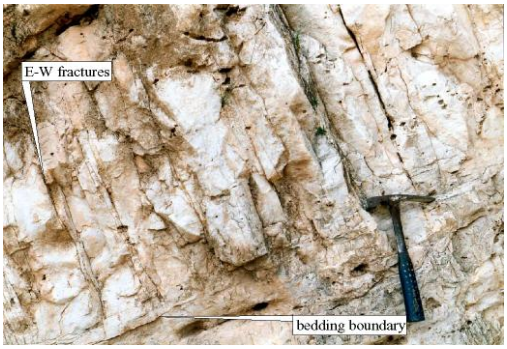

Fig.VI.23: Calcite filled E-W veins in the Dil (a) and Khaviz (b) anticlines perpendicular to the bedding plane and stratigraphic stylolites.

Fig.VI.24: One of the fracture measurement and sampling site (shown by an arrow) is located in a syncline between the Dil and Mish anticlines.

VI.B.4. Diagenesis and fracturing

Diagenetic aspects of the Asmari Formation were poorly covered in this study. It is worthy to deal with this part through a detailed study, applying sedimentary and diagenetic characterizations of the Asmari Formation both on a fold and basin scale. But, in this study , to get a better idea about the possible relationship between fracturing and diagenesis in the Asmari Formation, a few plugs were taken in some sites. Among diagenetic phenomena within the Asmari carbonate, dolomitization and dedolomitization are more important. Our observations show that the effects of these types of diagenesis in fracture and/or stylolite development are noticeable within those anticlines, where the fracturing is remarkable (Khaviz, Dil, Bangestan… anticlines) compare to those with quite low fracturing and high stylolitization process (Mish anticline).

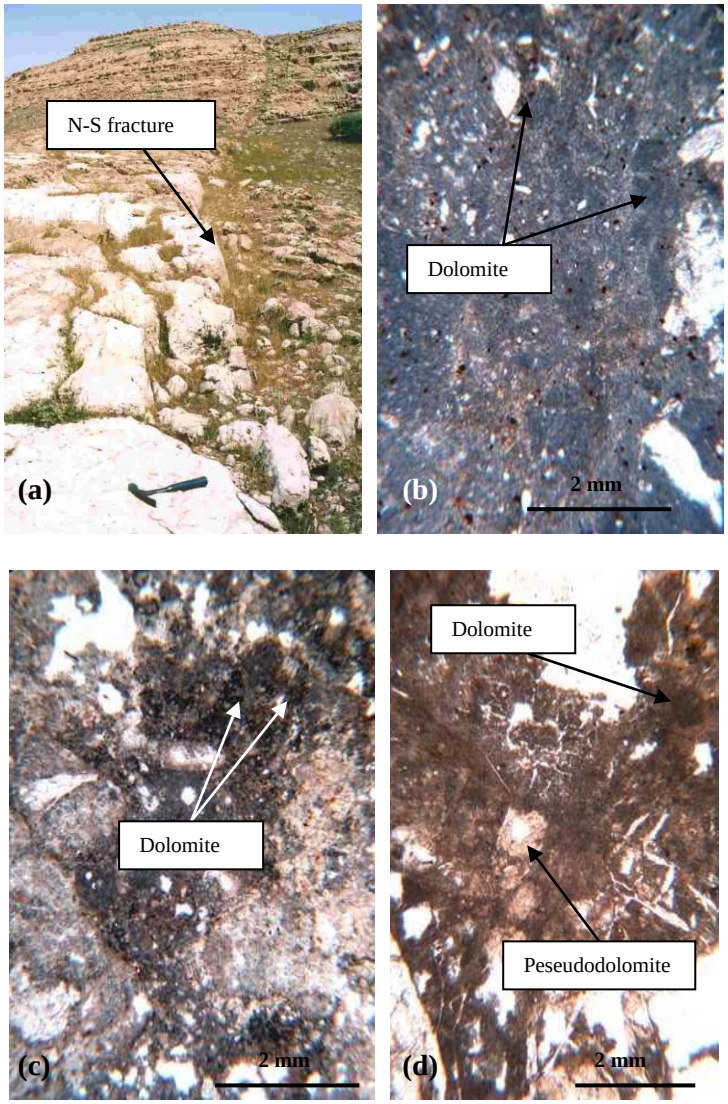

Fig.VI.25: The effect of diagenesis in the Asmari carbonate either side of a large scale fracture (A); B to D: Thin section photos from the samples which were taken from either side of the fracture. Note the effect of diagenesis in the form of dedolomitization, dissolution and evelopment of vugy porosity.

Normally, meteoric diagenesis is more important in the outcrops as they are on the surface and near surface (Vadose and phreatic zones), so the features of this kind of diagenesis is more evident in outcrops. Based on James and Choquette (1988), the wide variety of limestones that result from meteoric diagenesis, are the end result of several reactions, governed by intrinsic and extrinsic factors that may proceed at different rates for varying lengths of time. The most important intrinsic factor is original *mineralogy*: sediments composed of several $CaCo_3$ minerals, dominated by aragonite and magnesium rich calcite (Mg-calcite), which are metastable with respect to fresh water, alter most; and those sediments composed only of various calcite minerals alter least. *Grain size* controls the rate at which these components change; fine-grained sediments and finely crystalline particles, because of their large ratio of surface area to particle size, change most rapidly, whereas large

skeletons of the same mineralogy change more slowly. Individual grains will also alter at different rates, depending upon the crystal size and relative amount of organic material. Finally, *porosity* and *permeability* of the sediment, which govern the rate at which fluids flow through and the length of *time* they are in contact with the sediment or rock, affect the speed at which changes take place. The effect of large scale fractures in local dedolomitization and dissolution seems to be important. An example in this regard was observed on the SE plunge of the Asmari anticline where an N-S fracture (or fault) likely controlled a local alteration and diagenesis in form of dissolution and dedolomitization (Fig.VI.25a-d).

- *Dolomitization and dedolomitization processes*

Two types of dolomites may observed in the outcrops; First, what we may call it as early diagenetic dolomite. This kind of dolomite could be generated under a favorable physico-chemical conditions of pores fluid during a specific stage of diagenesis. It should not be taken as primary dolomite which forms under a suitable chemical condition of sedimentary basin during the main phase of sedimentation. As it is seen in Fig.VI.26a, this early diagnetic dolomite has quite small rhomb crystal with a homogeneous matrix texture appearance.
Second type of observed dolomite is the late dolomite, which is formed under overburden pressure or burial effect. In this case dolomite rhombs are scattered and are bigger than early diagenetic dolomite. Fig.VI.26b shows an example of late dolomite in the Asmari limestone in a sample from Mish anticline. In this anticline, dolomitization is quite poor, someting in the range of a few percent to zero. The interesting point is that, fracturing in this anticline is quite poor too. It means that, presumably, due to the lack of suitable diagenetic process like dolomitization, fracturing is weak in this anticline. Instead of fractures, stylolites are widely developed in the Mish anticline.

Dedolomitization as a retrograde or reverse diagenetic process is also seen in the Asmari carbonate. This process could be observed by two forms; (1) Formation of calcite rhombs as pseudo-dolomite (Fig.VI.26c), and (2) Dissolution of either dolomite or pseudo-dolomite (calcite) rhombs, and development of moldic porosity (dolomolds).

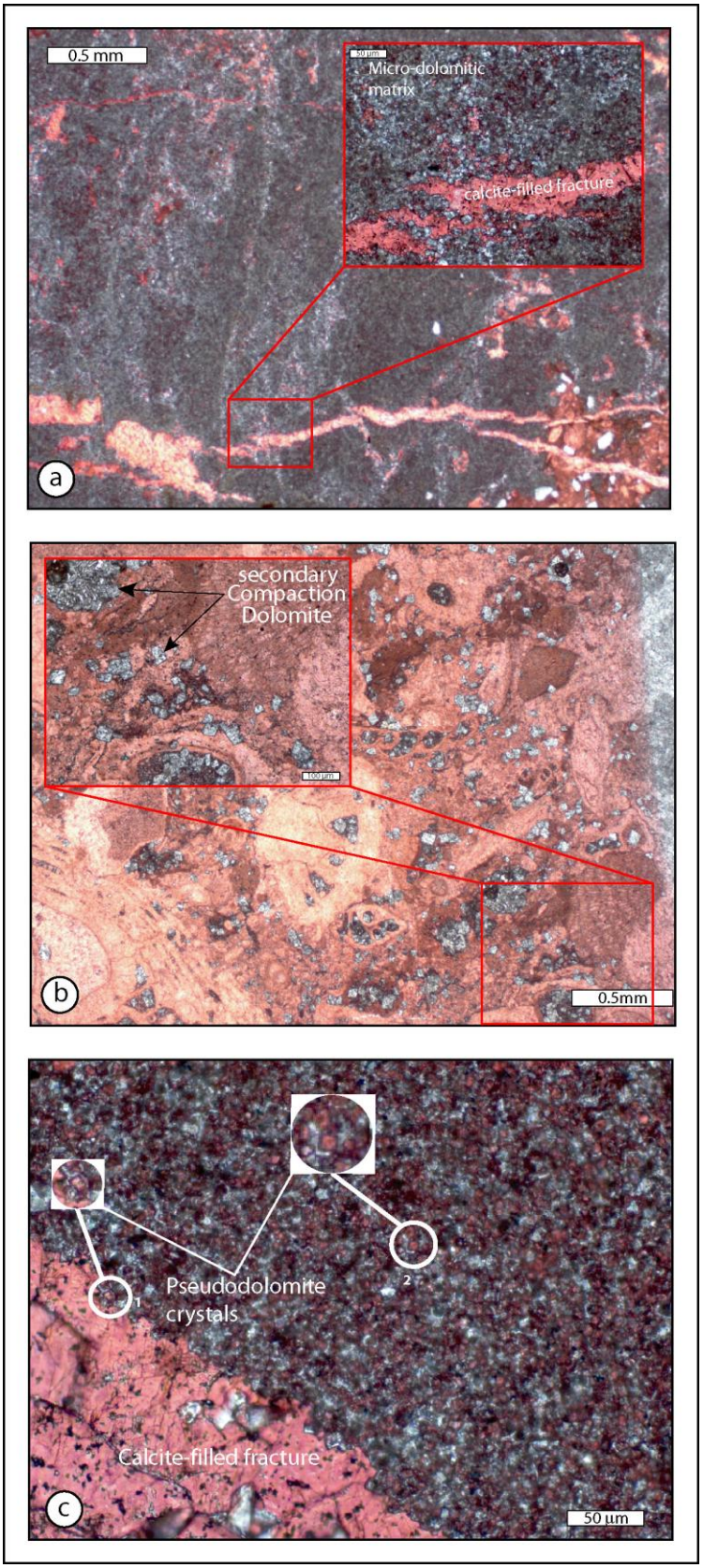

Fig.VI.26: Diagenetic features in the Asmari carbonates, (a) early dolomites, in form of micro-size dolomitic rhombs; (b) late dolomite rhombs, scattered and bigger than early dolomite crystals, (d) pseudo-dolomites as indicators of dedolomitization in the Asmari carbonates, see text for more details.

VI.B.5. Fractures in Upper Cretaceous carbonate of the Sarvak Formation, a preliminary observation

Fracture study in the Sarvak carbonates was not an objective in this thesis, but preliminary observations were carried out in one of the outcrop (Payun anticline, Fig.VI.27) of this Formation in the Izeh area. The aim of this observation was to see if the fracture pattern in both carbonate formations (Asmari and Sarvak) are comparable. Furthermore, fracture study in the Sarvak carbonates is another prospective in the Central Zagros (see General Conclusion) as this Formation is one of the main hydrocarbon reservoirs after Asmari Formation and exploration and development programs are more and more concentrated on this Formation.

The Sarvak Formation generally appears in two major facies (Motiei, 1993): (i) a massive limestone deposited in a neritic environment, and containing rudists, gastropods, pelecypods, and a rich microfauna; and (ii) the other is a deep water facies of thinner-bedded, fine-grained, dark-colored, argillaceous, "Oligostegina" limestones with pelagic microfauna. The first facies in the Izeh area, in form of massive or thick-bedded limestone containing micro and macro faunas has a more development than the second one. Regarding micro-fabric and grain size, like the Asmari carbonate, mudstones and wackstones are frequently seen in the samples which have been taken from this Formation in the studied area. The main studied structure of Sarvak Formation (Payun anticline) in the Izeh area is located in the northeast of the Izeh city. Axial trend of this structure follows the general NW-SE trend of the Zagros, but its NW termination (like in the case of the Bangestan anticline) gradually turns towards the north near N-S trending IZHF. Fracture orientations were measured in several stations in northern part of the NE flank (near IZHF) and also the SW flank of this anticline.

The main fracture orientations measured in this anticline include, orthogonal N-S and E-W trending fractures, N040°-050°, and N150°-160° fracture sets (Fig.VI.27). These are the main fracture families which were observed in the outcrops of the Asmari Formation in the studied area. Almost all fracture directions are oblique to the local bedding trend and show no symmetrical relationship with fold geometry, as observed in most of studied Asmari outcrops. One of the main differences in fracturing style between the Sarvak and Asmari formations is (qualitative) fracture intensity. While intensive fracturing is remarkable in most of the studied outcrops, the Sarvak carbonates are weakly fractured in spite of almost the same rock fabrics and facies (mudstone to wakestone) as the Asmari Formation (Fig.VI.28). However, systematic joints are rarely developed within the outcrops of both formations, where thick, massive carbonates (with mostly reefal facies) are present.

Furthermore, mechanical properties of both formations should be defined by laboratory experiments to see if fracture intensity variations is controlled by mechanical rock properties. The problem which may be encountered in this case is that rock properties change through geological time. What may be suggested as one of the reasons of this difference in fracture intensity between the Sarvak and Asmari anticline is presumably the timing of fracturing in the Central Zagros. As it was explained in the previous chapter and will be argued in the next chapter, most of the fractures (joints) predated Miocene-Pliocene folding

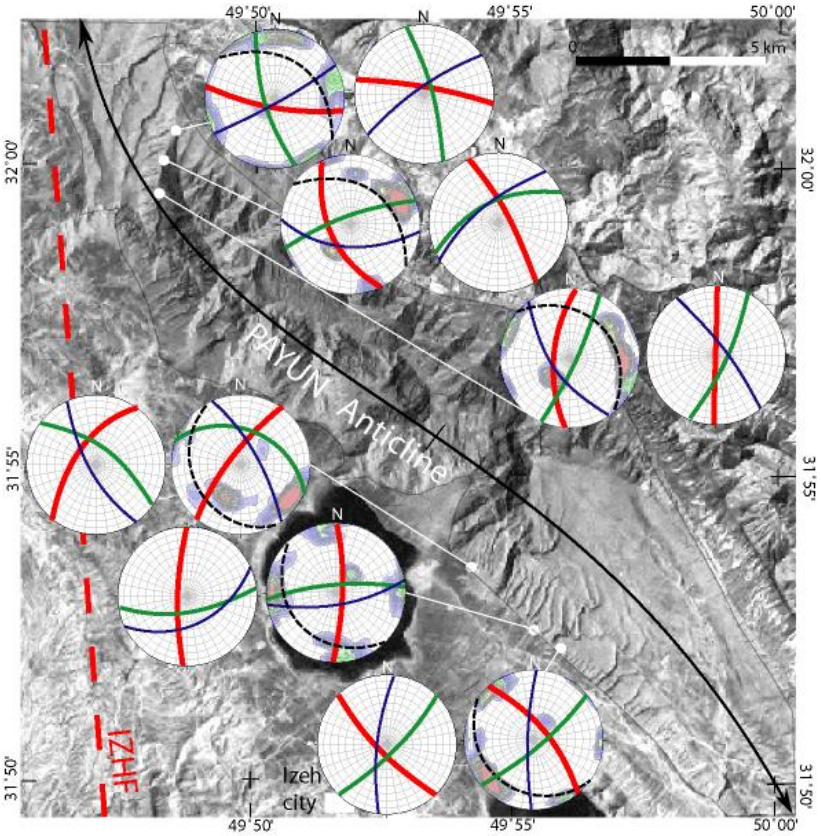

Fig.VI.27: Fracture orientation in the Payun anticline (Sarvak Fm.), north of Izeh city, for the location of the anticline, see geological map of Fig.VI.2. Orientations of the main fracture sets are, more or less, similar to what observed in the Asmari outcrops in the studied area (see text for more details).

phase in the Zagros. Different joint sets were formed during the sedimentation of the Asmari carbonate when it had not been still deeply affected by diagenesis and compaction process in the basin. At this time the Sarvak Formation were quite lithified and therefore displays the mechanical properties different from those of the fresh carbonate sediments of the Asmari Formation. In this case, joints can easily initiate in the Asmari rather than the Sarvak carbonates even in form of well oriented hairline discontinuities or micro-fractures and then they gradually developed and reactivated during the burial diagenesis and later tectonic events including folding. This scenario is compatible with the proposed conceptual model of fracturing in the Central Zagros (part VI.A) and the difference of fracture intensity in the

these carbonate formations can be tentatively explained by absolute timing of fracturing (see chapter VII).

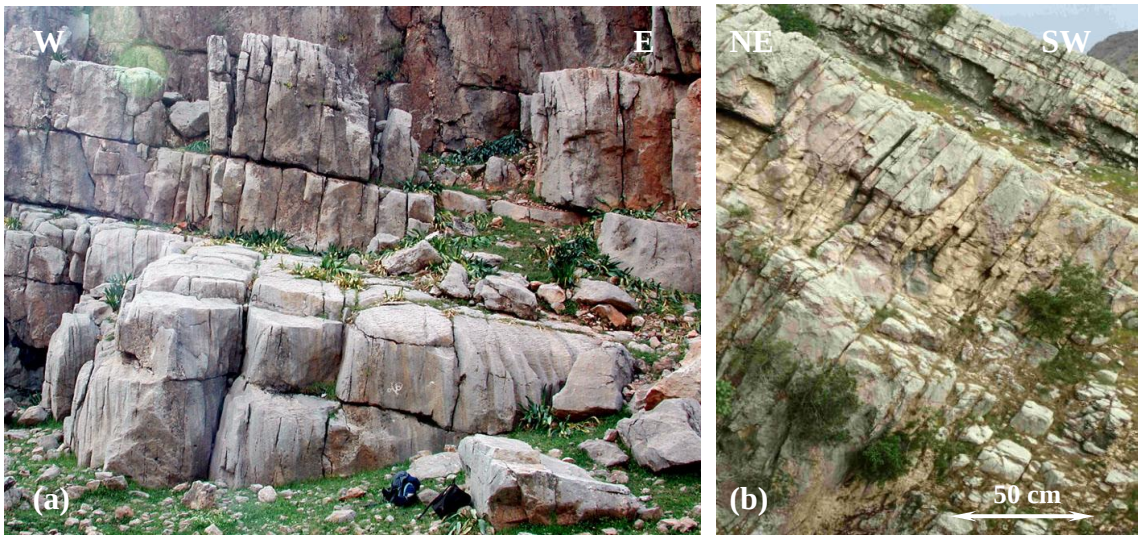

Fig.VI.28: Systematic joint sets in the Sarvak (a), and (b) Asmari formations. Note the different fracture intensities in these carbonate formations.

Another typical difference between the Asmari and Sarvak formations is the presence of fracture swarms (Fig.VI.29) which are more developed in the Sarvak than in the Asmari outcrops. Furthermore, observed fracture swarms in the Sarvak Formation have no symetrical relationship with the fold geometry. As the fractures are less in the Sarvak carbonates than the Asmari carbonates, characteristic and relationships of these fracture swarms with the main structure (anticline) are important in the field development plans of the Sarvak reservoirs.

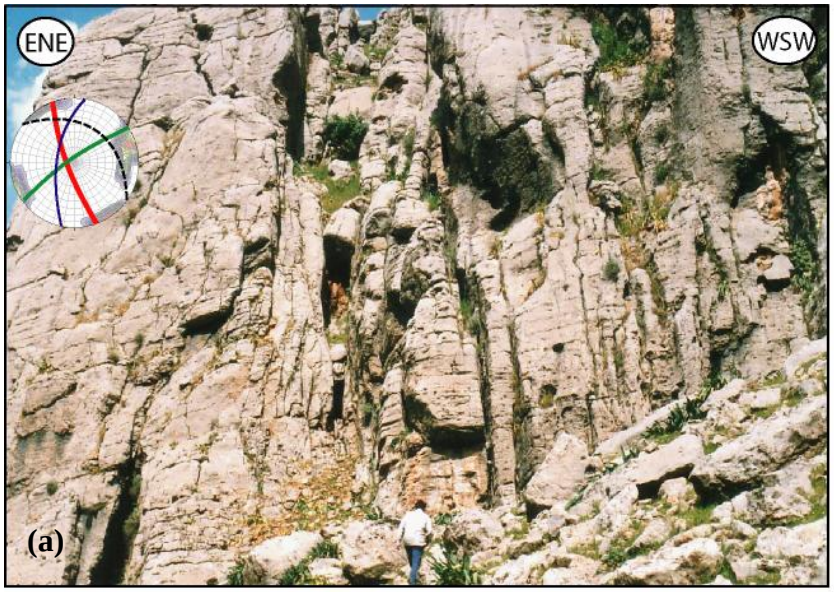

Fig.VI.29. Fracture swarms in the Sarvak (a), and the Asmari formations (b). Fracture swarm in the Sarvak (Payun anticline) is oblique to the general trend of the fold whereas observed fracture swarm in the Asmari anticline is parallel with the general trend of the fold.

CHAPTER VII: Early fracture development within Asmari carbonates: role of basement faults on Lower Tertiary facies changes and possible forced-folding

Introduction

Different fracture patterns in the Central Zagros were introduced and interpreted in chapter (V). A simplified conceptual evolutionary tectonic model was proposed based on field observations, fracture chronologies, reconstruction of local stress-field using fault-slip data, and aerial and satellite image interpretation. Then, it was concluded that most of these fractures are likely pre-folding fracture sets (i.e. formed before the main Miocene-Pliocene folding phase) and presumably formed due to early reactivation of the main Zagros basement faults. For the N140°±10° set, the main arguments in this regard were its directional stability in the studied area and also the anomalous presence of this set within synclines, where outer rim extension is unlikely. This set, therefore, shows no symmetrical relationship with the fold as implied by most fold-related fracture models (e.g. Stearns 1968). Another fracture group, discussed in the previous chapter, was N-S trending fracture. This set is strongly oblique to the studied fold axes and is especially encountered near N-S trending basement faults (e.g. IZHF and KMF). Furthermore, they possibly formed synchronously with previous set (~N140°).

In this chapter, the previously proposed fold-related fracture model is reminded. Then this model is briefly compared with part of our observations in a few anticlines presented in the previous chapter. Then, the proposed hypothesis about the reactivation of the main Zagros basement faults and development of forced folds are discussed not only using fracture patterns, but also on the basis of paleogeography and facies changes in the Oligocene-Miocene Asmari basin. Development of a lithospheric bulge in the Central Zagros is discussed as an alternative hypothesis regarding extensional stress development within the Asmari basin and its effect on possible triggering of motion along the pre-existing main basement faults (as a short note at the end of this chapter). Finally, a possible absolute timing for the onset of deformation in the Central Zagros is proposed.

VII.1. Possible links between prefolding fracture development in the Asmari Fm. and forced folding/flexure related to basement fault reactivation

VII.1.1. Early fracture patterns in the Asmari Formation

The Asmari Formation is one of the main reservoir rocks in southwest of Iran. This Formation crops out along the Zagros folded belt and is well-known as carbonate fractured reservoir. Many studies dealing with the fracture pattern of the Asmari carbonate have been carried out and are still in progress. While McQuillan (1973, 1974, and 1985) stated that some of the fracture orientation bears no relation to the folds, Gholipour (1998) believes that the Asmari fractures are associated with vertical and axial growth of concentric folding. Furthermore, the relative chronologies of different fracture sets with folding are still controversial.

Fracture patterns within different anticlines in the Central Zagros were studied (see chapter VI.A for more details). Fracture orientation and chronology, local stress field definition using fault-slip data and aerial and satellite images interpretations were used to interpret fracture pattern through different scales in the region. Among the fracture sets introduced in previous chapter, a set striking N140°±10° (set III, see chapter VI.A) was suggested to be in direct relation with deep-seated basement faults and presumably formed above flexures or forced folds in the Central Zagros. So, from a point of view, this fracture family is a fold-related fracture set but neither chronologically nor through its creative mechanism, this pattern is related to the Miocene-Pliocene folds in the Zagros folded belt. The trend of this fracture family is, more or less, parallel to the general trend of the Zagros folds. It means that, at the first glance, it seems to be difficult to differentiate, genetically, between axial fractures within two types of the folds (i.e. buckle folds and forced folds). One of the main points which should be coherent with fold/fracture symmetry, as it was presented by the model of Stearns (1968), is the effect of bedding attitude on fracture orientation. Based on this model, fracture orientation in the periclinal part of the folds follows the bedding curvature. If these fracture sets are projected on a horizontal plane, one of the patterns shown in Fig.VII.1 should be obtained. These patterns, especially in the periclinal part of the fold, are not similar to those observed in the studied anticlines (e.g. Khaviz and Bangestan). Directional stability of N140°-150° fractures in the Khaviz nose (Fig.VI.8, chapter VI) is not compatible with the proposed fold-related model.

Another incompatibility between NW-SE trending fractures and fold geometry is their presence within the layers with quite low structural dip and near horizontal attitude. Even these fractures are observed in the synclinal position of some of studied folds (e.g. Razi, Safid, Dil, and Quirak anticlines, see chapter VI.A for more details). In the fold-related fracture pattern, the axial fracture set is formed above neutral surface of a fold and under a local extensional stress field at the outer arc. Such a condition is unlikely within synclines or even flat-lying beds. However, when this fracture set observed on the hinge or in more generally in a place where extension is a likely effective local stress in a fold, it seems to be difficult to differentiate between those formed during former large scale forced folding episode and those formed later during smaller scale episode of generalized cover folding. Even in this case both of them form two azimuthal fracture families making an acute angle in range of 10 to 30° (see fracture diagrams in the Asmari anticline, Fig.VI.6). But one of the most practical solutions in this regard (which was not covered in this study) is the microscopic and cathodo-luminescence study of their cement fillings.

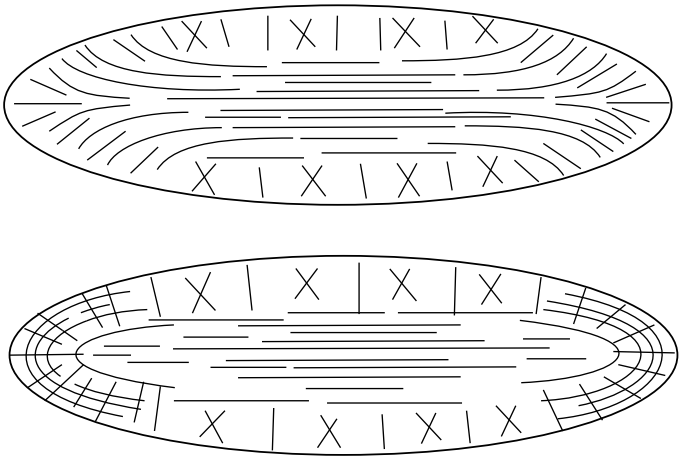

Fig.VII.1: Possible patterns of different fold-related fracture sets on a horizontal surface, combining conceptual fracture models of Stearns (1968, 1978) in cylindrical and pericline parts of a fold.

N-S and E-W fracture sets (sets IV & V, see chapter VI) are other fracture families which proposed, in previous chapter, to be in direct relation with N-S trending basement faults. Their distribution in the studied area and their relationships with the fold geometry were argued. Then, it was suggested that these fracture sets formed with the same mechanism proposed for NW-SE fractures in the Central Zagros, above basement faults. Unfortunately, there are not enough evidence for the kinematic and the role of N-S (and even E-W) trending

basement faults during the evolution of the basin in the studied area but paleogegraphic and isothickness show some evidence of their reactivation since Upper Cretaceous times.

Discrepancies between fracture orientation and fold geometry in the Central Zagros were discussed previously. In addition to lack of fold/fracture relationship, there are some structural macro-features that are not so compatible either with local stress in a fold or fold evolution. This kind of structures may be considered as inherited structures. The Central Zagros folds are asymmetric and their northeastern limbs have less structural dip than their southwestern limbs. Most of them are characterized by hinge migration and limb rotation suggesting local compressive and extensional stresses on the northeastern and southwestern limbs respectively. This is in contrast with the extensional structures on the NE flanks of these folds. Fig.VII.2 shows a graben located on the NE flank of the Asmari anticline. The position of this graben on the northern limb where structural dip is quite low (just near the foothills) suggest that its development unlikely happened during folding phase in response to an outer rim extensional stress field.

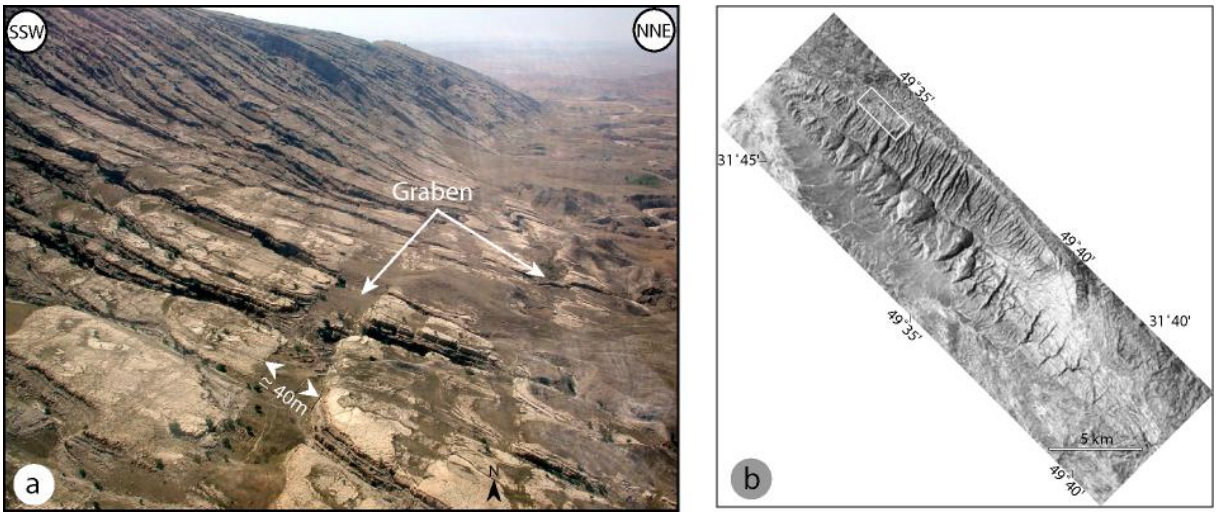

Fig.VII.2: A series of grabens just at the foothill of the Asmari anticline may be considered as inherited structures which predate folding, (b) the location of these grabens on a satellite image (Mr SID).

Based on Colman-Sadd (1978), indication of movement between the layers of the Competent group are provided by numerous bedding-plane slickensides on fold limbs which are normal to the fold axes and has been considered as "flexural-slip" mechanism of parallel folding in the Zagros folded belt. In agreement with Colman-Sadd and based on our observations in the Central Zagros, flexural slip mechanism of folding or simply parallel bedding gliding is frequent in the studied area. On the other hand, chronological evidence based on parallel-bedding slipping shows that some fractures, which are thought to be syn-

folding, in fact have been reactivated during folding phase. What is seen in Fig.VII.3 is a reactivation of a segmented pre-existing fracture by flexural-slip. It is difficult to suppose a governing compression stress during early stage of folding could create such a fracture, normal to bedding and almost parallel to fold axis.

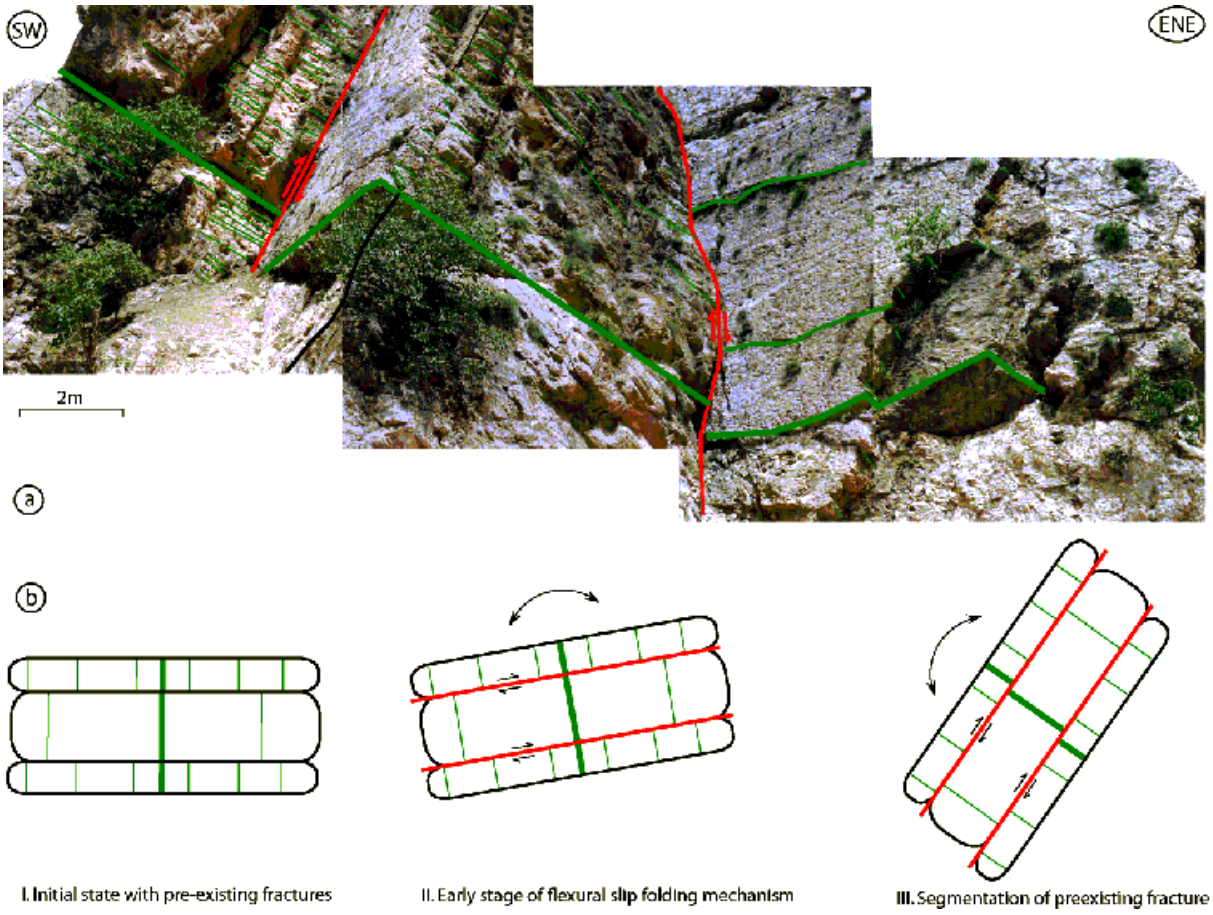

Fig.VII.3: segmentation and displacement of a pre-existing fracture by flexural slip mechanism, southern flank of the Lappeh anticline, Izeh zone.

VII.1.2. Fold-related fracture pattern; reminder

Fractures in folded sedimentary rocks are usually interpreted as the result of folding (de Sitter, 1956; Harris et al., 1960; Price, 1966; Price, 1967; Stearns, 1968; Cooper, 1992; Nelson and Serra, 1995; Jamison, 1997; Fischer and Wilkerson, 2000; Hennings et al., 2000; Stewarts and Wynn, 2000). Among different groups of so called fold-related fractures, axial fractures (including joints and faults) are supposed to result from local extension in the folds. Furthermore, based on consistent relation of the fractures to bedding orientation, even on the noses of folds, they are supposed to be in direct relation with folds geometry and especially bedding attitude (Stearns and Friedman, 1972; Stearns, 1978; Ameen, 1990; Price and Cosgrove, 1990; Nelson and Serra, 1995; Gholipour, 1998; Nelson, 2001, Bergbauer and

Pollard, 2004). Generally, fold-related fractures may be divided into two categories: first, those are associated with buckle folds and, second, those related to forced-folds above basement faults. For more information on buckle folds and their related fracture patterns, readers can refer to chapter II and III.

VII.1.2.1. Fold-related fractures associated with buckle folds

Stearns (1968) suggested that there are 11 common fracture orientations in folded strata comprising five fracture sets that form systematically with respect to the fold axis and bedding (Fig.VII.4a). Based on Bergbauer and Pollard (2004), and comparing with the pure bending of an elastic plate (e.g., Timoshenko and Woinowsky-Krieger, 1959) fracture set 1, in this figure, could form below the neutral surface of a convex-upward bent plate and be genetically related to set 2, which could form above neutral surface. Furthermore, fracture pattern are specifically related to bending in this model and their attitude is expected to change spatially, for example, at the nose of a plunging anticline (e.g. Stearns, 1968; Cosgrove and Ameen, 2000; Bergbauer and Pollard, 2004) (Fig.VII.4b) where the direction of greatest curvature changes. Because of the very different stress field in which these fracture sets form, Stearns (1968) suggested that set 1 forms early during folding, set 2 forms when extension normal to the folds becomes "large," and set 3 and 4 "reflect locally developed bending or buckling."

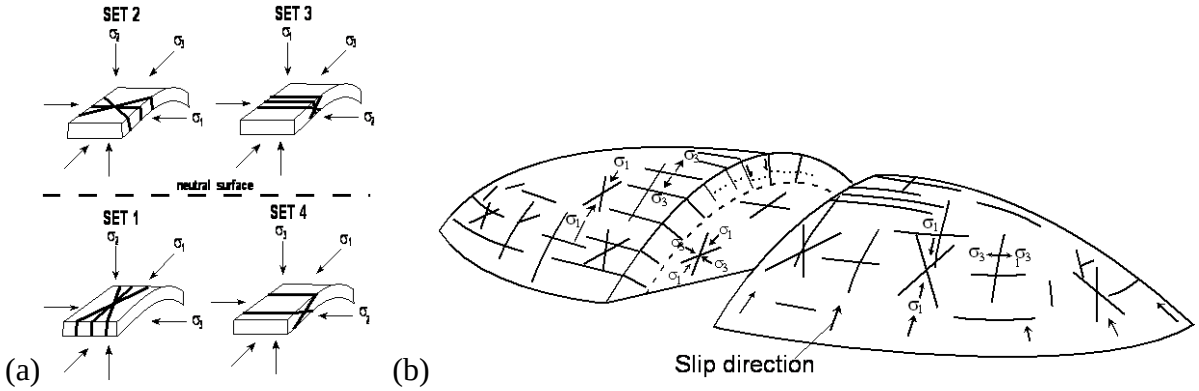

Fig.VII.4: (a) Conceptual model of Stearns (1968), in which multiple fracture sets are assumed to form symmetrically to fold axis (cylindrical part of the fold); (b) Various fractures associated with a pericline (after Stearns, 1978).

Gholipour (1998) suggested that all fracture sets within the Asmari reservoirs are related to different phases of concentric fold growth and using the production data, and mud

losses in drilled wells, he concluded that productive fractures were found to be associated mainly with the plunges and bends (Fig.VII.5) of the Asmari reservoir structures.

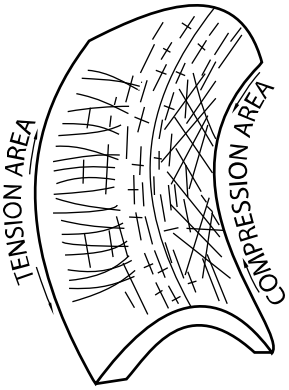

Fig.VII.5: Bend related fractures pattern in a bent concentric fold (Gholipour, 1998).

VII.1.2.2. Fold-related fractures associated with forced folds above basement faults

The geometry of forced folds (formed above a basement faults) and their related fractures were discussed in Cosgrove and Ameen (2000). Fold and fault initiation and development above pure dip-slip, oblique-slip, and wrench basement faults were shown through analogue modelling and discussed by some authors (e.g. Richard, 1991; Richard et al., 1991). Among different kinds of forced folds, those formed above dip-slip and strike-slip basement faults are of particular interest in our study. First, the geometry of this kind of folds is briefly presented and then fracturing style in this type of folds is discussed.

- *The geometry of forced folds*

Stearns (1978) defined that the final overall shape and trend of a forced fold are dominated by the shape of some forcing member below. One of the most common geological situations where such folds develop is within cover above a fault-scarp in a more rigid basement. Such folds can form above pure dip-slip and oblique-slip basement faults. These faults form over the fault scarps that fault movements generate. The geometry of the produced folds is generally controlled by the geometry of the scarps. As a result, they are often long, linear structure, and have a much higher aspect ratio than buckle folds (Cosgrove and Ameen, 2000). The orientations of a deep seated basement faults could determine the spatial organization of the related fold in the cover. This spatial organization and large aspect ratio contrast sharply with the shorter, more uniformly distributed buckle folds.

Analogue models (e.g. Ameen, 1988, 1992; Richard, 1990, 1991; Richard and Krantz, 1991) and finite element studies (e.g. Nino et al., 1998) suggest that the profile geometry of forced folds is controlled both the type of movement (i.e. reverse or normal dip-slip, reverse or normal oblique-slip, etc.) and the amount of slip on the basement fault. Folding of cover rocks above pure reverse dip-slip and reverse oblique-slip faults will involve some layer parallel shortening of the cover rocks. In contrast, those folds are formed in the cover above strike-slip basement faults have the aspect ratio similar to that of a classical buckle fold, because no fault scarp develops at the basement-cover contact during pure strike-slip faulting in the basement. However they do differ from buckle folds in their spatial organization and in details of their profile geometry (see chapter I for more details). They generally form a linear en echelon array above the basement fault, with the folds being consistently offset either to the right or left depending on whether the basement fault is dextral or sinistral, respectively (Cosgrove and Ameen, 2000). However, analogical experiments (Richard, 1990) show that the thickness of the weak layer at the boundary between the basement and the cover (basal décollement layer) and the dip's amount of basement fault can severely control fold/fault patterns and their offsets. Furthermore the presence of any dip-slip component, even weak, in the fault-slip may affect resulted fold/fault pattern and related aspect ration in the cover. Some of N-S trending oil fields (e.g., Azadegan, Khoramshahr, Tangu, Hendijan), in the coastal plain and Persian Gulf are likely formed above a strike-slip basement fault.

- *Associated fractures*

There are some experimental works based on analogue modeling (Ameen, 1988) in which the initiation and growth of forced folds above dip-slip basement faults were investigated. The models consist of two basic parts, the 'basement' which was simulated by wooden blocks and the 'cover' which was simulated by layered wax. Variations in competence between different layers within a sedimentary cover were modeled using waxes of different theologies. The layers were imprinted with strain marker grids both in the profile section of the fold and on the surface of the layer. These experiments enabled the progressive development of the forced folds to be studied. In particular, they allowed the strain field and associated fracture patterns to be determined at various stages during fold amplification and, thus gave a clear indication of how these strain fields and fracture patterns changed as the folds grew. Analysis of the results shows that the cover accommodated, itself, faulting in the basement by two main mechanisms, namely rigid body rotation and internal deformation. The

deformation was highly concentrated in the vicinity of the basement fault and died out away from these areas. Having determined the extension normal and parallel to the layering (in directions parallel and normal to the strike of the basement fault) using the strain marker grids, these values were then contoured and their evolution tracked during the course of the experiment. Two examples of strain distribution around forced folds are shown in Fig.VII.6a for a fold formed over a normal dip-slip fault and a fold formed over a reverse dip-slip fault. The models have been divided into different strain fields on the basis of the values of the three principal stresses. These fields are numbered and the magnitudes of the three principal strains in each field given in the accompanying tables.

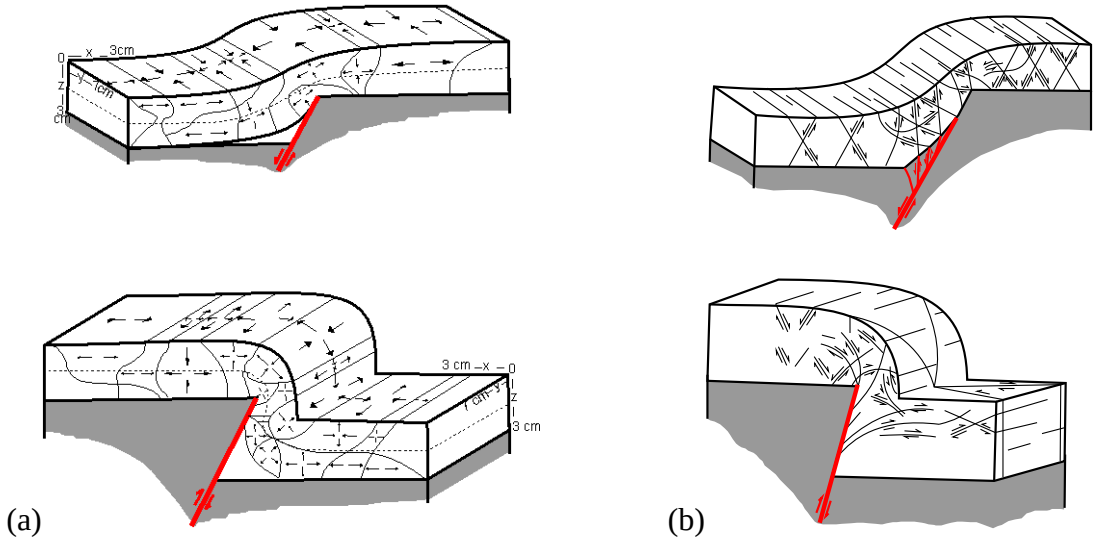

Fig.VII.6: (a) block diagrams of forced fold models formed over a planar normal (top) and reverse (bottom) basement fault (Cosgrove and Ameen, 2000). (b) Schematic block diagram showing potential geometry and sense of movement of macrofaults in experimentally produced forced folds above normal (top) and reverse (bottom) basement faults (after Ameen, 1990)

These experiments show that the strain fields and associated fractures around forced folds formed in cover rocks as a result of dip-slip movement on basement faults are very sensitive to the sense of movement, i.e. either normal or reverse. In extensional forced folding (i.e. where the causative basement faults are normal dip-slip faults) the strain patterns generated in the folded layers are characterized by layer perpendicular shortening and layer parallel extension in the direction normal to the strike of fault, regardless of the amount of movement on the fault (Fig.VII.6b, top). Thus, an extensional strain field forms throughout the fold and, although the fracture density is predicted to increase with increasing movement on the fault, the fracture type will remain the same. This is in marked contrast to the fracture

patterns generated during the forced folding of a cover sequence above a basement dip-slip fault reactivated with a reverse movement. Whereas basement normal faults cause strain patterns in the cover that are homogeneous in both time and space, the strain pattern and associated fracture pattern formed in the cover above a reverse dip-slip basement fault are found to vary both in time and space (Fig.6b, bottom). The result is that one set of fractures, characteristic of a particular strain field, may subsequently be overprinted by another set characteristic of different strain field. In this way extensional fractures can be cut by compressional fractures and visa versa. Field studies of compressional forced folds show this superposition of different fracture patterns very clearly (Ameen, 1992). This feature in the Zagros folded belt is more complicated. First, the main NW-SE trending basement faults in the Zagros, at least since lower Cretaceous, seem not to be active as normal faults. Because (i) the Zagros basin with an almost uniform carbonate platform established during this period of time; (ii) based on well data no considerable thickness variations in the area, relating to any normal activation of these basement faults are observed; (iii) following the ophiolite obduction, the Zagros basin entered in a compressional system of Alpine orogeny in late Cretaceous-Tertiary times (Stoklin, 1968, Berberian and King, 1981); (iv) this Alpine orogeny in the Zagros range caused shortening in the basement by reverse faulting or inversion of pre-existing extensional faults (Jackson et al., 1981; Ni and Barazangi, 1986, Ameen, 1991); (v) seismotectonic data within Zagros folded belt show a compressional faulting mechanisms, and mostly in form of reverse and thrust faulting (Berberian, 1995; Talebian and Jackson, 2002, 2004); (vi) more than 6 km vertical displacement on the top of the Asmari Formation (e.g., Berberian, 1995) in the Zagros belt was likely accommodated by the reverse faulting mechanism of the main basement faults. Therefore, those fracture patterns which are proposed to be related to dip-slip basement faults within Asmari Formation, are considered to have formed above reverse dip-slip basement faults in our studied area. Fig.VII.6b shows schematic block diagrams, illustrating the geometry and the potential orientation of macrofaults and fractures in experimentally produced forced folds formed above basement dip-slip faults. The overlapping of different strain fields during fold amplification is a characteristic feature of forced folds form over reverse dip-slip basement faults. The neutral surface, which separates extensional and compressional strain fields, migrates through the layer. This migration is much less in buckle folds than in forced folds (Cosgrove and Ameen, 2000). In case of the Zagros sedimentary cover with more than 10 km thickness below the Asmari Formation (with about 300m thickness), neutral surface migration in the forced fold toward the superficial part of the force-fold (taking into account total sedimentary thickness)

within the Asmari Formation may not be occurred. It means than in the Asmari Formation which form the upper most part of the sedimentary cover above the forced folds, fracture complexities due to overlapping of different strain fields during forced fold amplification unlikely happened and the main governing local stress field presumably remained always extensional. But the overlapping of different strain fields in the Asmari Formation exists due to different folding mechanisms. As it was discussed in the previous chapter, most of the compressional fracture sets (e.g., low angle reverse faults and thrust, conjugate shear fractures) formed during the main folding episode of the cover rocks (Mio-Pliocene orogenic movements) and both types of fractures (extensional and compressional) could be seen with together in a fold.

VII.1.3. Our knowledge about the Zagros basement faults

The main morphotectonical regions in the Zagros fold belt in the studied area are bordered by major deep-seated basement faults (Fig.VII.7). There is no published information on basement depths from seismic refraction or reflection and without such knowledge it is difficult to give a clear image of basement faults pattern and their role in geodynamic evolution of the Zagros folded belt. But it was stated that two dominant tectonic trends exist in the Arabian Shield (Stern, 1985; Stacey et al., 1984). The older one, trends north-south and is generally steeply-dipping; the younger trend, strikes NW-SE and is related to the left-lateral strike-slip Najd fault system parallel to the trend of the Zagros folded belt (Fig.III.5). There is evidence for the continuation of several structures in the Arabian Shield, northwards, into the Zagros Basin before their reactivation and deformation during the Cenozoic Zagros orogeny (Berberian, 1976, 1981, 1995; Talbot and Alavi, 1996; Hessami et al., 2001, Bahroudi and Talbot, 2003).

Berberian (1995) introduced two groups of major basement faults in the Zagros (Fig.VII.7). The first group are major reverse faults including the Main Zagros Reverse fault (the geosuture, MZRF) with a strike-slip segment of Main Recent fault (MRF) towards the northwest part of the fold-belt, the High Zagros fault (HZF), the Mountain Front fault (MFF), the Dezful Embayment fault (DEF), and finally, the Zagros Foredeep fault (ZFF). Fault plane solutions for earthquakes along these faults indicate that they all dip about 60° NE (Bahroudi and Talbot, 2003), suggesting that they now act as reverse faults although they may have been activated as normal faults during the Permo-Triassic opening of Neo-Tethys (e.g. Jackson, 1980; Berberian, 1995). The second group are major right-lateral strike-slip faults. Some of them are located in the studied area including the Izeh Fault (IZHF), the Kharg-Mish Fault

(right lateral reactivation in this fault has not been well documented), the Kazerun Fault (KZ). The Balarud Fault (BR) is an E-W left-lateral shear zone northwest of the Dezful Embayment. These N-S faults in the Zagros belt are steep to vertical with significant strike-slip displacements (Kent, 1958, 1979; Barzegar, 1994; Baker et al., 1993; Berberian, 1995; Sepehr, 2001; Hessami et al., 2001). The reactivation and the related block rotations along these faults is thought to have deviated the general NW-SE trend of the former major group through east-west to NE-SW trend to the SE of the Kazerun fault (KZ) (Hessami et al., 2001; Bahroudi and Talbot, 2003).

North-northeast, east, south, and north-northwest boundaries of the studied area coincide with High Zagros, Kazerun, south of Zagros Foredeep, and Balarud faults respectively. Here, briefly the characteristics of the main basement faults in the studied area are discussed based on Berberian (1995).

- *The Zagros Foredeep fault (ZFF)*

The ZFF separate the Zagros Foredeep (to the north and northeast) from the Zagros Coastal Plain (in the south and southwest) (see chapter I). It forms the north-eastern edge of the alluvial covered Coastal Plain of the Persian Gulf and is principally a reverse-slip system. The ZFF is a discontinuous line and is roughly parallel to the MFF at an altitude of a few hundred meters above sea level. The anticlines associated with the Zagros Foredeep are still growing (Lees and Falcon, 1952; Falcon, 1961; Berberian, 1995) which indicate that, presumably, this fault is still active.

- *The Dezful Embayment fault (DEF)*

The DEF which forms the northern boundary of the Dezful Embayment (foreland basin of the Neogene molasses of the Agha-Jari-Bakhtiari formations), is located in the area between the MFF and the Zagros Foredeep fault (ZFF). Based on geological evidence of the top of the Miocene Gachsaran Formation (Huber, 1977), the vertical displacement along the DEF is more than 3000 m. Two earthquakes of 1977 (Ms = 5.8, h = 12km) and 1985 (Mb = 5.2) with thrust mechanism seem to be associated with reactivation of the DEF at depth (Berberian, 1995).

- *The Mountain Front fault (MFF)*

The MFF, which delimits the Zagros Simple Fold Belt and the Eocene-Oligocene Asmari limestone outcrops to the south and southwest, is a segmented master blind thrust

fault with important structural, topographic, geomorphic and seismotectonic characteristics. Pronounced subsidence of the Zagros Foredeep and the Dezful Embayment with thickening of the post-Asmari deposits (Neogene Gachsaran Evaporites and the Agha-Jari-Bakhtiari synorogenic molasses) provides evidence of relative motion along the MFF and the Dezful Embayment fault since Early Miocene times. The geological evidence, based on the present position of the top of the Oligocene-Lower Miocene Asmari Formation, from stratigraphic, seismic and borehole data (Falcon, 1974; Huber, 1977; Berberian, 1995), demonstrates the vertical displacement along this fault is more than 6 km. This fault is composed of discontinuous, complex thrust segments of 15-115 km long, with a total length of more than 1350 km in Iran.

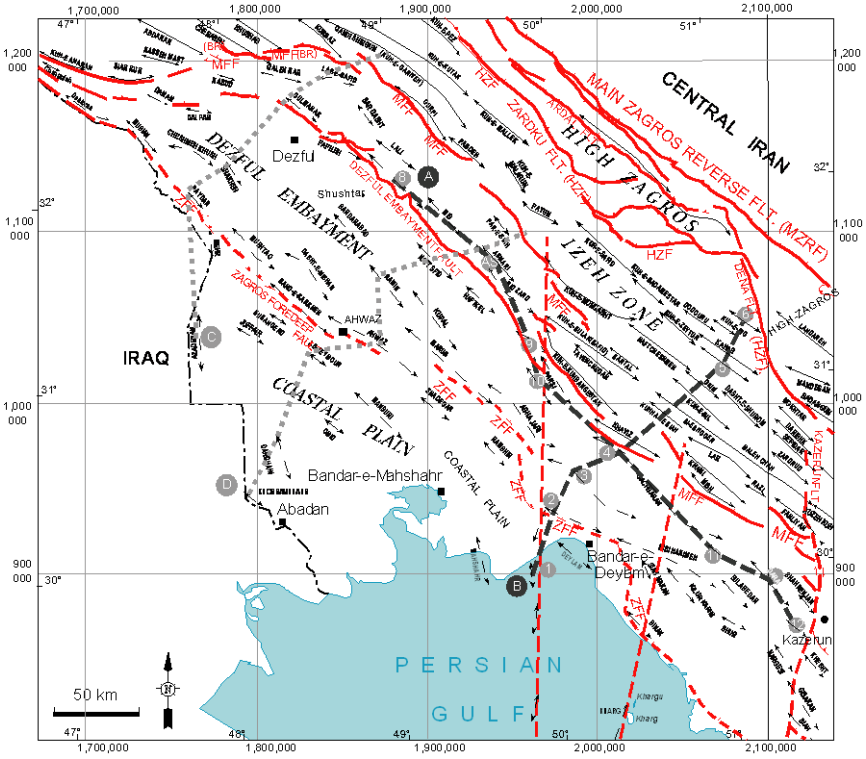

Fig.VII.7: The main morphotectonical regions of the Zagros folded belt in the studied area. Deep-seated basement faults are shown in red lines (see text for more details). The locations of transects, mentioned in this text, are shown in dashed grey-coloured lines.

- The High Zagros fault (HZF)

The HZF separates the thrust belt of the High Zagros (in the northeast) from the Simple Folded belt (in the southwest). The High Zagros is upthrusted to the southwest along discontinuous different segment of the HZF (Berberian, 1995). Geological evidence such as the present position of the Palaeozoic rocks (Huber, 1977) demonstrates the vertical displacement along the HZF to be more than 6 km. Wedging of the post-Asmari deposits (Miocene Gachsaran evaporites together with the Lower Miocene to Pleistocene Agha-Jari-

Bakhtiari syn-orogenic molasses) towards the High Zagros (James and Wynd, 1965; Falcon, 1974; Huber, 1977), suggest uplift of the High Zagros along the HZF since the Early Miocene, contemporaneous with the relative subsidence of the Zagros Foredeep and southward migration of the Zagros basin and deformation.

- *N-S trending faults*

The Kazerun (KZ), Kharg-Mish (KMF), and Izeh (IZHF) faults correspond to a series of roughly N-S striking linear uplifts along pre-existing basement trends (Motiei, 1995). Koop and Stoneley (1982) show that these trends were strongly reactivated in response to the ophiolite obduction at late Cretaceous. Izeh and Kazerun faults are seismically active at present day, with right lateral movement in the Precambrian basement (Berberian, 1995; Hessami et al., 2001; Sherkati and Letouzey, 2004). The peak of activity along the Izeh and Kazerun fault zones took place in the Mid-Cretaceous (Sepehr and Cosgrove, 2004, 2005). Seismic activity along the Kharg-Mish fault (KMF) has not been documented, but Motiei (1994) suggested that the activity of the Kharg-Mish fault, based on thickness and facies variations seen in drilled well, started after Lower Aptian times. During the Albian, the activity of this fault increased remarkably and caused clear thickness variations (Sherkati and Letouzey, 2004).

VII.2. Paleogeographic evidence of early basement fault reactivation

We saw that lineament patterns on aerial/satellite images (e.g. Asmari, Khaviz, and Bangestan anticline), strong obliquity of NW-SE trending fracture set to folds axis (e.g. Quirak anticline), and an NE-SW directed, pre-folding local stress field, derived from fault-slip data (e.g. Khaviz and Sulak anticlines) suggest that this fracture set unlikely has direct relation with the present folds. If we suppose that basement faults played an effective role in fracturing within sedimentary cover, their reactivation likely affected sedimentary basin in form of facies changes and/or local unconformities. As our knowledge about basement faults and their kinematics is quite poor, it may be possible to deduce, indirectly, kinematic information about basement faults reactivation at the time when this reactivation presumably controlled sedimentary basin evolution (Ahmadhadi et al., 2005), at least before the main folding phase of the cover which occurred in Miocene-Pliocene times (Stöcklin, 1968; Falcon, 1969, 1974; Huber, 1977; Stoneley, 1981; Berberian, 1981). In this approach, facies variations and paleogeography of the studied area from Lower Cretaceous to Lower Miocene will be discussed using different constructed transects and maps, using documented paleologs

and surface sections. This time period covers the time interval time in which deformation signals were documented by some authors (e.g., Agard et al., 2005; Allen et al., 2003; Hessami et al., 2003), which should help providing time constraints on fracture development.

VII.2.1. Constraints from paleofacies evolution from Upper Cretaceous to Lower Tertiary

In order to provide time constraints on the age of fracture initiation within the Asmari Formation, paleofacies evolution of the central part of the Zagros, a region between Bala-Rud (BR) Fault to the northwest and Kazerun Fault to the east, during Lower Cretaceous to Lower Tertiary was carefully re-analyzed based on previous studies (James and Wynd, 1965; Berberian and King, 1981; Motiei, 1993) and paleologs of drilled wells in the Dezful Embayment. I especially focus on Oligocene and Lower Miocene facies variations within the Asmari basin. In addition to paleogeographic maps, two stratigraphical transects of the studied area were prepared using combined GR/Neutron and/or GR/SONIC with paleontological data based on microfossils (Paleologs) in order to identify facies variations and basin geometry in its third dimension (depth). Furthermore, a few transects were provided to show the possible basinal scale effects of the main basement faults on structural and thickness variation of different formations in the region.

VII.2.1.1. Stratigraphical transects

Fig.VII.7 shows the studied area and the location of constructed longitudinal (parallel to the Zagros trend) and transversal (perpendicular to the Zagros trend) transects (transects "A" and "B"). These transects (Figs. VII.8&9) cover the latest Cretaceous (Maastrichtian) up to Lower Miocene (Burdigalian) times. The boundary between Upper and Middle Asmari Formation (the boundary between assemblage zone 1 and 2, see bio-zonation of the Asmari Formation, Chapter IV), was taken as a reference horizon.

The first transect (Fig.VII.8) is located in the northern part of the DEF and south of the MFF. As is shown in this transect, the Asmari carbonate basin is located on the basinal facies of the Pabdeh Formation indicating an important upward swallowing since lower Oligocene time. The basinal facies of the Lower Asmari, west of the IZHF and north of DEF, changed to carbonate platform towards the east of the IZHF during Oligocene. Furthermore the presence

of some anhydritic beds during Oligocene times indicates the development of a limited restricted lagoonal facies during this time. The middle part of the Asmari Formation corresponds to the evaporitic part of the Kalhur Member which gradually disappears near the middle part of the transect, near the N-S trending IZHF. Towards the east of this fault, the middle part of the Asmari Formation shows a remarkable thickness which gradually decreases towards the east of KMF. This thickness variation could be due to the presence of a trough between two N-S trending basement faults; i.e. IZHF and KMF. The facies of the Upper Asmari remained, more or less, without any specific change. However towards the east of the transect and near Kazerun Fault the thickness of the Upper Asmari is reduced.

The second transect (Fig.VII.9) is perpendicular to the general trend of the Zagros folded belt. Maastrichtian Gurpi/Tarbour Formation and Paleocene-Eocene Pabdeh/Jahrum formations form the basinal facies in the middle of the transect whereas carbonate platform facies in the NE and SW parts of the transect through the latest Cretaceous to the Upper Eocene are more predominant. The lower Asmari is almost uniformly developed in the region. The middle part of the Asmari Fm. is thicker at the middle of the transect and gradually its facies become deeper (hemipelagic) towards the north of the MFF. The upper part of the Asmari Fm. shows a clastic facies (Ahwaz/Ghar Member) toward the southern part of the region. However, this clastic facies towards the northwest and near the ZFF could be observed since Oligocene times. Towards the northeast and south of HZF the hemipelagic facies of the Upper Asmari locally developed during Lower Miocene times. This facies has been observed also in the Lappeh anticline which indicates that the area between HZF and MFF was located in a deeper part of the Upper Asmari basin.

VII.2.1.2. Paleogeographical maps

A few paleogeographic maps were constructed based on the information of previous works (e.g. James and Wynd, 1965; Berberian and King, 1981; Motiei, 1993) as well as the constructed transects and some other paleologs in the studied area.

The Zagros basin with marine carbonate platform sedimentation became established from early Jurassic and continued until Miocene time with the greatest subsidence being in the northeast, possibly along several faults (Berberian and King, 1981). The Lower Cretaceous is represented by an almost uniform continental margin carbonate platform in most part of the Zagros basin (Fig.VII.10a). The apparent trend of this basin seems not to be

affected by the main NW-SE or even N-S trending crustal-scale faults. It rather shows a general E-W trend in the studied area. During the Middle Cretaceous (Cenomanian-Turonian) vertical movements likely produced NNE-SSW trending anomalies in form of highs and troughs as indicated by sedimentary thickness variations during that time (Fig.VII.11). The locations on these local anomalies coincide with the main N-S trending basement faults (e.g. IZHF and KMF) in the region. Following the obduction of the ophiolites during late Santonian-early Campanian time (80-75 Ma) along the High Zagros belt (Berberian and King, 1981), neritic carbonates of Ilam Formation and deeper water marl and shales of Gurpi Formation (Campanian-Maastrichtian) were deposited in most part of the Zagros basin (Fig.VII.10b). Apparently the vertical movements along N-S basement structures in the studied region were still in progress. Some parts have been emerged during Maastrichtian. Also, reef over flysh sediments and marls formed a narrow neritic facies along the NE margin of basinal facies of the Gurpi Formation at this time (Fig.VII.10b).

During Palaeocene and Eocene times the closure of Neo-Tethys Ocean was completed and Pabdeh (neritic to basinal marls and argillaceous limestones) and Jahrum (massive shallow marine carbonates) formations deposited in the middle and both sides of the Zagros basinal axis respectively (Fig.VII.10c). This basin was gradually restricted by Lower Oligocene times and the Lower Asmari Fm., including the carbonate, deeper marine marl, and sandy limestone (Ahwaz Member) deposited (Fig.VII.10d). The localization of the sandy carbonate lens border (with about 30% sand) almost coincides with the location of ZFF (Zagros Frontal fault) in the studied area (Fig.VII.10d). Progressively, different intra-basins and facies including clastic facies (Ahwaz/Ghar sandstone Member), carbonate and evaporites (Kalhur Member), presumably, developed during Upper Oligocene-early Miocene times (Chattian-Aquitranian) (Fig.VII.10e). The important feature at this time is the coincidence of these intra-basins with the main NW-SE trending master basement faults (i.e. MFF and DEF). Just in the center of the basin, basinal facies (marl and shale) of the Pabdeh (Lower Asmari ?) Formation is superimposed by an evaporitic facies. No intermediate facies variation and transition is observed from marls and shales to evaporites. This narrow basin is limited to the north and northeast by MFF and BF and to the south and to the east by DEF and IZHF. Farther south, the Ahwaz/Ghar Member delta front, indicated by more than 30% of the sand content of the Asmari carbonate, formed just along the south of ZFF. This sand content gradually increases southward (Fig.VII.10e). During Burdigalian times, the carbonates of Upper Asmari covered the entire basin with a hemipelagic facies toward the northern part of Mountain Front fault (Fig.VII.10f).

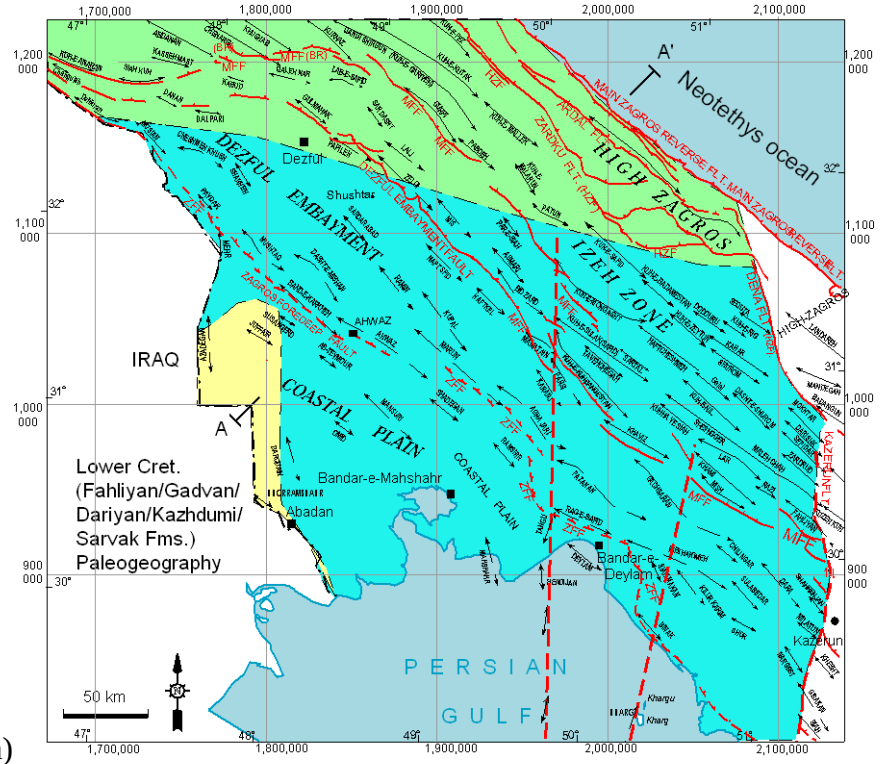
A'
Neotethys ocean
DEZFUL EMBAYMENT
HIGH ZAGROS
IZEH ZONE
IRAQ
A
COASTAL PLAIN
Lower Cret.
(Fahliyan/Gadvan/
Dariyan/Kazhdumi/
Sarvak Fms.)
Paleogeography
Dezful
Shushtar
AHWAZ
Bandar-e-Mahshahr
Abadan
Bandar-e-Deylam
Kazerun
PERSIAN
GULF
50 km

(a)

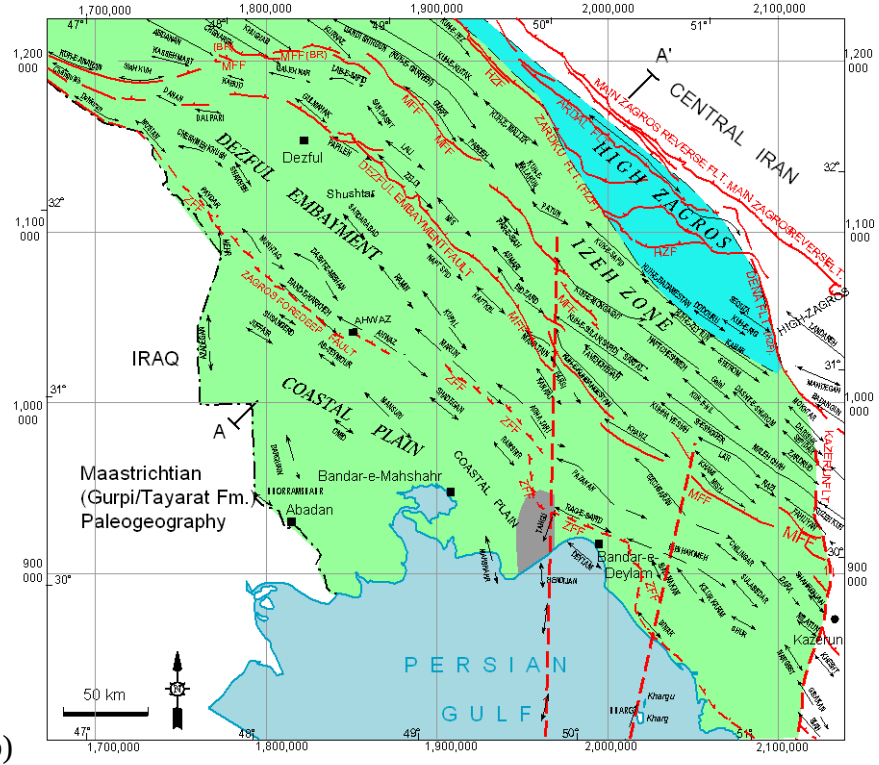
A'
CENTRAL IRAN
DEZFUL EMBAYMENT
HIGH ZAGROS
IZEH ZONE
IRAQ
A
COASTAL PLAIN
Maastrichtian
(Gurpi/Tayarat Fm.)
Paleogeography
Dezful
Shushtar
AHWAZ
Bandar-e-Mahshahr
Abadan
Bandar-e-Deylam
Kazerun
PERSIAN
GULF
50 km

(b)

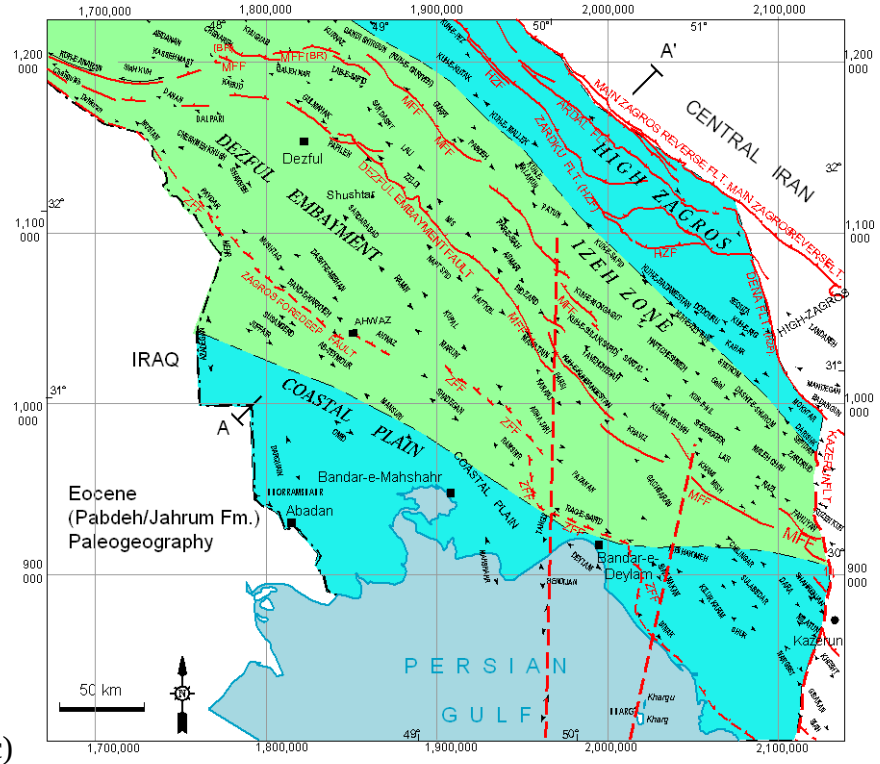
Eocene
(Pabdeh/Jahrum Fm.)
Paleogeography
IRAQ
DEZFUL EMBAYMENT
HIGH ZAGROS
IZEH ZONE
CENTRAL IRAN
COASTAL PLAIN
PERSIAN GULF
Dezful
Shushtar
AHWAZ
Bandar-e-Mahshahr
Abadan
Bandar-e-Deylam
Kazhun
MFF
HZF
ZFF
50 km

(c)

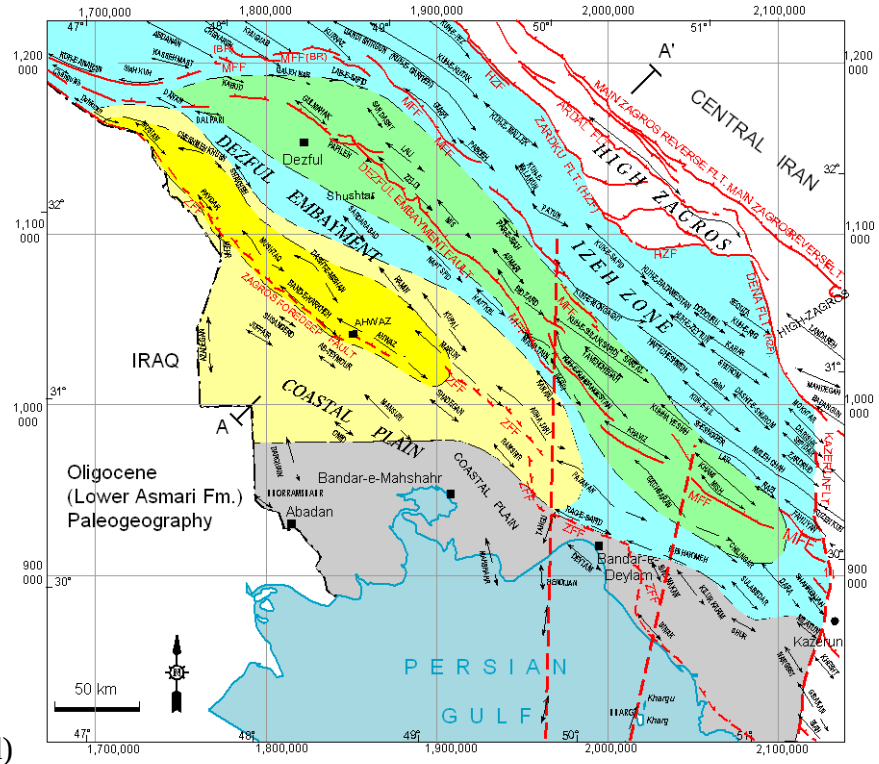
Oligocene
(Lower Asmari Fm.)
Paleogeography
IRAQ
DEZFUL EMBAYMENT
HIGH ZAGROS
IZEH ZONE
CENTRAL IRAN
COASTAL PLAIN
PERSIAN GULF
Dezful
Shushtar
AHWAZ
Bandar-e-Mahshahr
Abadan
Bandar-e-Deylam
Kazhun
MFF
HZF
ZFF
50 km

(d)

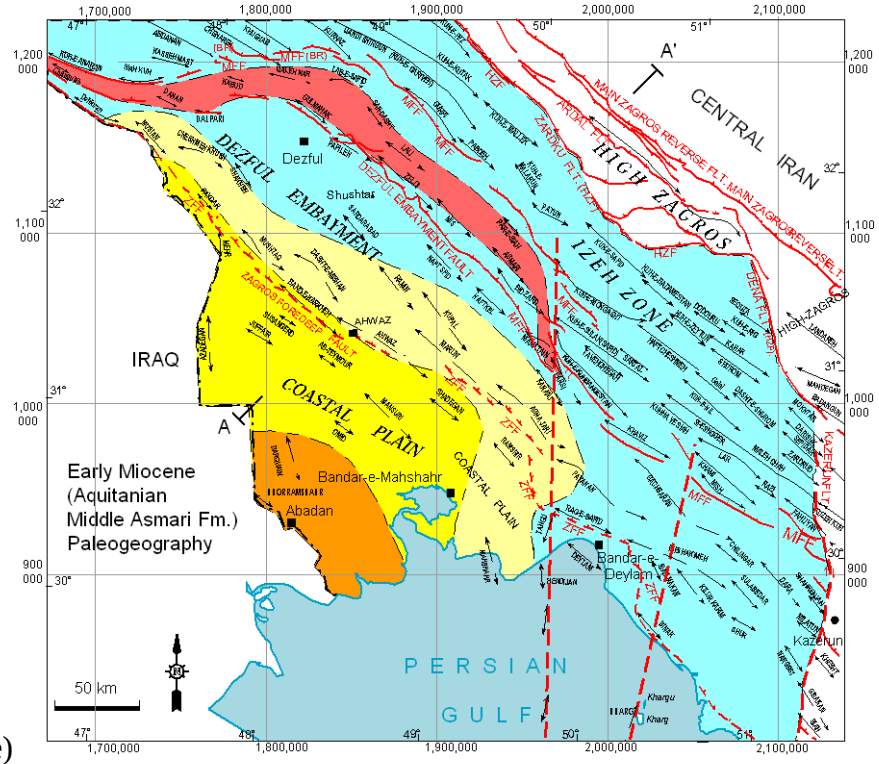

(e)

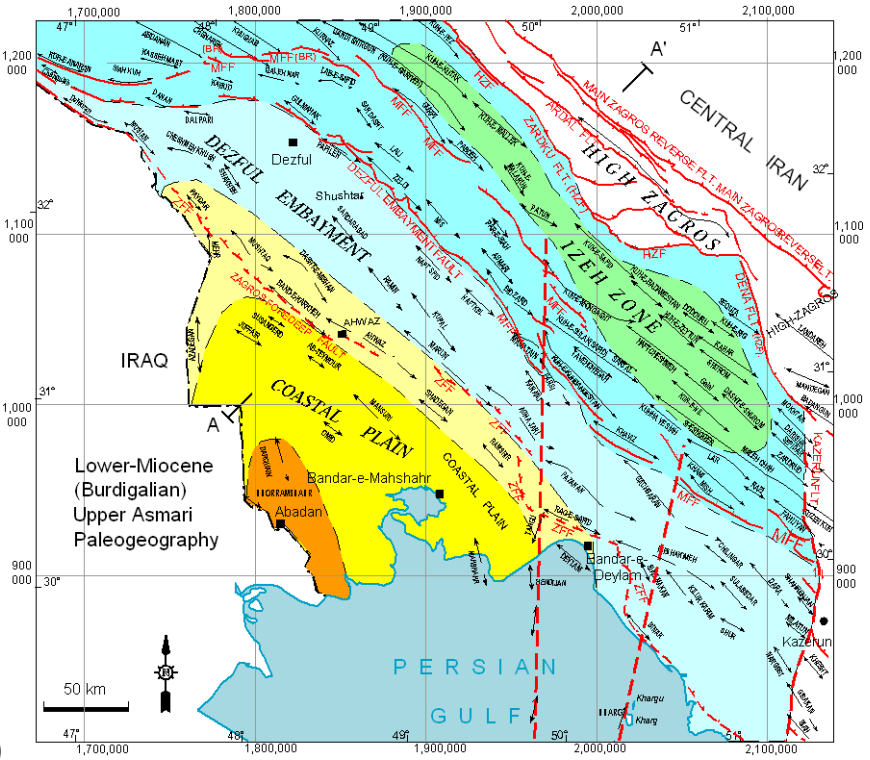

(f)

Fig.VII.10: Lower Cretaceous (Gallic) – Lower Miocene (Burdigalian) paleogeography. See text for details.

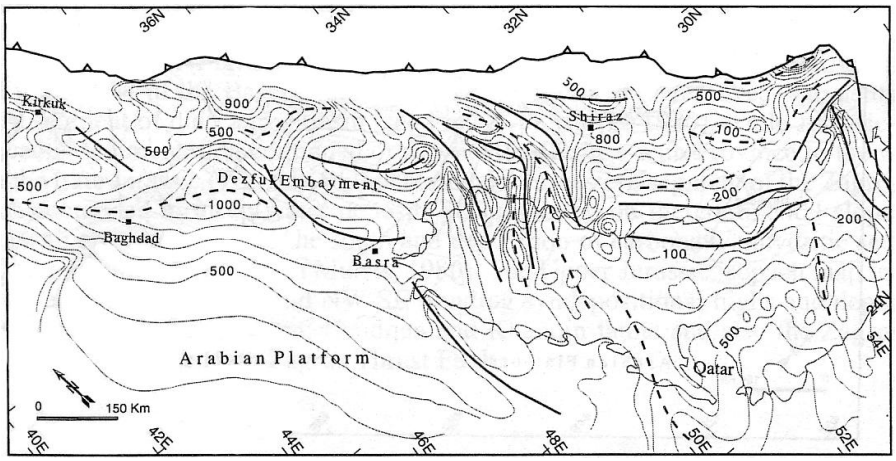

Fig.VII.11: Isothickness map of the Zagros sediments during Middle Cretaceous times. The locations of roughly N-S trending basement faults (Fig.VII.5) coincide with the locations of troughs (solid lines) and highs (dashed lines) during this period. This suggest that they likely reactivated at that time (after Koop and Stoneley, 1982; Motiei, 1993, Bahrudi and Talbot, 2003).

During the evolution of the Asmari basin, development of a narrow, elongate evaporitic sub-basin and its coincidence with the main basement faults (i.e. MFF and DEF) in the region is remarkable. Such a restricted narrow basin is supposed to have formed due to the reactivation of the main basement faults in the region. Description of the different Asmari members was given in chapter IV. As the evaporitic Kalhur Member is supposed to be a stratigraphical key point towards the timing of the Zagros deformation within the Asmari basin and development of the forced folds and related fractures, it will be discussed in more detailed hereafter.

VII.2.1.3. The Kalhur Member: geographical development and timing

As mentioned above, the intra-basin Kalhur Member is located somewhere between MFF and DEF and west of IZHF. This restricted intra-basin, still extends towards southwest of Lurestan area and in the northern part of Iraq and Syria (Motiei, 1993). This Member conformably overlies the Pabdeh Formation and underlies dolomitic limestone of the Upper Asmari Formation. Sometimes a basal conglomerate locally appears on the Kalhur Member (Shepherd et al., 1961). Adams (1969) described the most complete evaporitic Kalhur Member bearing series of the Asmari Formation within the outcrops, upward down, as follows (Motiei, 1993) (Fig.VII.12):

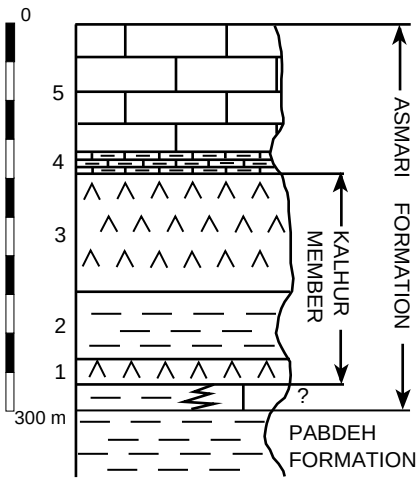

Fig.VII.12: Kalhur Member type section

- *Upper and Middle Asmari limestones*

These limestones were previously called Kalhur limestones. These thin bedded dolomitic limestones have characteristics compatible with Upper and Middle Asmari in the Dezful Embayment.

- *Brissopsis transition beds*

They include thin beds, interfering with marly limestones and gypsiferous marls. Siltstone, sandstone and sometimes conglomerate were sometimes reported in this part. The thickness of this series is between zero to 65.5 m.

- *Upper Kalhur anhydrite*

This part includes massive and thick bedded anhydrite in which crushed, clastic limestones are observed. The thickness of this part is quite variable from 49m to 152m.

- *Internal beds*

This part mostly includes the alternative of well bedded green marls in which thin bedded grey colour marly limestones are seen. Near the top of this part a one meter thick marl horizon separates this part from Upper anhydrite. There is a porous limestone in this part in which Operculina spp., fossils are seen abundantly (see Asmari bio-zonation, Chapter IV).

This limestone is very important on a biostratigraphical correlation point of view . Internal beds thickness is between 15 to 67 meters.

- *Lower Kalhur anhydrite and the Kalhur Member dating*

This part includes a series of thick gypsum beds with 3 to 18m thickness. Based on stratigraphical chart, prepared by Adams (1969), the Kalhur evaporitic Member can be correlated with gypsiferous Dhiban Formation in Iraq. The difference between the two is that the Dhiban Formation is separated from the upper part, the Jarib Formation, by a unconformity. Probably part of the upper part of Dhiban Formation disappeared through this unconformity. The same observations in the southwest of the Lurestan were reported by Shepherd et al. (1961).

As the evaporitic Kalhur Member is located below the dolomitic limestone, belonging to the Elphidium sp. 14 - Miogypsina sub-zone, the age of the Kalhur Member is considered to be Aquitanian. In the Haftkel field well, Aquitanian planktons were identified in the Pabdeh marls and beneath the basal anhydrite. Also, the limestones over the basal anhydrite belong to Ephidium sp. 14 –Miogypsina assemblage zone (see the Asmari bio-zonation, Chapter IV), so the age of basal anhydrite is considered to be Aquitanian. In some of the oil-fields, located in the northern part of the Dezful Embayment, this basal anhydrite is located on a zone of Operculina. On the other hand, Operculina spp. was reported in the middle layers of the Kalhur Member in the Lurestan. So, possibly the basal anhydrite of the Asmari Formation in the Dezful Embayment is equivalent of the upper layers of the Kalhur Member in the Lurestan area.

VII.2.2. Possible control of basement fault reactivation on Intra-basins geometries

If we suppose that the basement faults were reactivated in the region, this reactivation should have influenced accommodation space for the sedimentation especially for those areas above basement faults. To test this idea, a few transects based on the thickness variations of the main lithostratigraphical units (formations) with definite time lines (top and bottom) and data accessibility in the region were prepared. The direction of these transects were chosen somehow to cut the main NW-SE trending basement faults in the studied area (Fig.VII.7). Two types of information are shown by these transects: (i) structural formation tops for different formations including Ilam/Sarvak (Upper. Cretaceous) Gurpi (late Cretaceous,

Maastrichtian), Pabdeh/Jahrum (Eocene), Asmari (Oligocene-Lower Miocene), Gachsaran formations; (ii) Formation thickness variations along these transect.

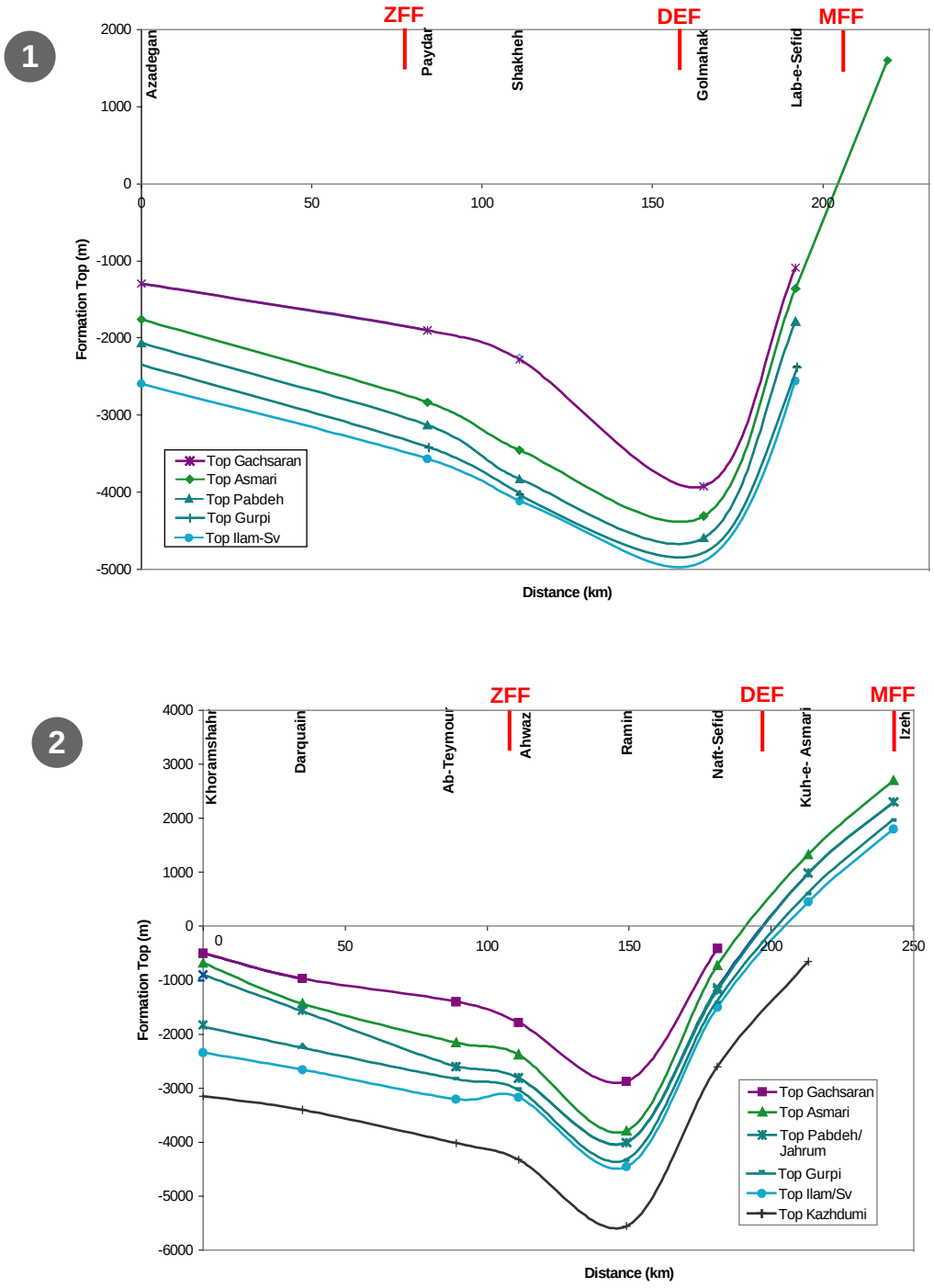

Fig.VII.13: Structural transects (see figure VII.4, for location map) showing present-day situation of Ilam-Sarvak to Gachsaran formation tops in the studied area. See text for more details.

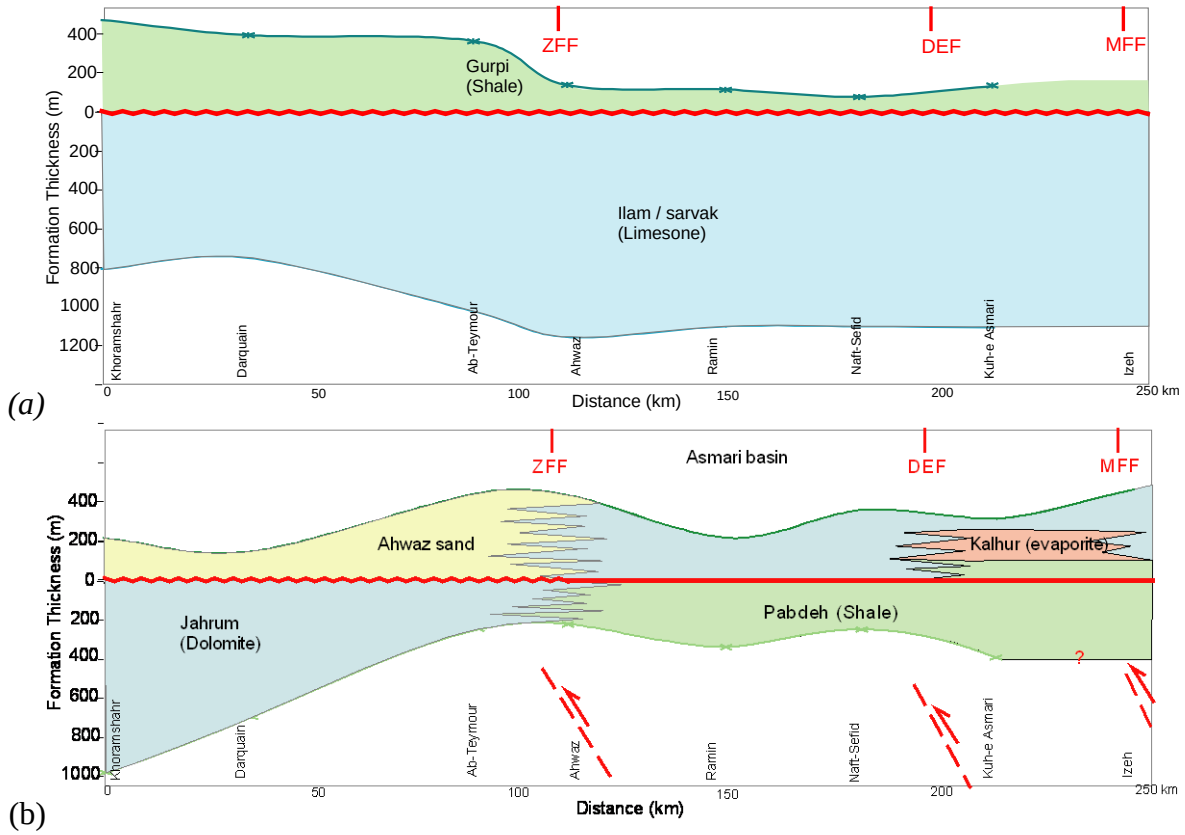

Fig.VII.14: Thickness variations within Ilam/Sarvak and Gurpi formations (a) and Pabdeh/Jahrum and Asmari formations (b) along transect No.2 of Fig.VII.10. (location map in Fig.VII.5); reference horizon selected as top Ilam/Sarvak and Eocene-Oligocene unconformities for both transect respectively (red lines).

As is seen in Fig.VII.13 a depression is seen in front of ZFF, forming the molassic basin filled with syntectonic sediments of the Agha-Jari Formation (Upper Miocene). The vertical offset which affected the top of different formations is near 6000 m, and was presumably accommodated by the main basement faults movements. Thickness variation along one of these transects, with the maximum control point (well data), is shown in Fig.VII.14. Sarvak and Gurpi formations (Fig.14a) as Upper Cretaceous sedimentary series seem not to be affected by the NW-SE trending basement faults. Both of them show almost a uniform variations in their thickness between ZFF and MFF while the important fluctuations appear within Pabdeh/Jahrum and Asmari formations (Fig.VII.14b) which could be related to early vertical movements along the main basement faults.

VII.3. Nature of vertical motion along reactivated basement faults : compressional or extensional ?

In the previous discussion it was supposed that the reactivation of the basement faults was affected the facies distribution in the Central Zagros. This reactivation can be considered

in form of normal or inverse dip-slip motions of deep-seated basement faults. These two hypotheses are discussed in more details hereinafter.

VII.3.1 Early fracturing in the Asmari carbonates and extension due to lithospheric foreland flexure

(This part was written following a collaboration with F. Mouthereau and J. Tensi on lithospheric bulge development in the Central Zagros, Pierre and Marie Curie University, Paris)

In this part, we test lithospheric flexure of the eastern continental margin of the Arabian plate as a mechanism for development of a larger scale extensional stress field and related fracture set (set III). This hypothesis is based on proposed conceptual geodynamical models of the Arabian and Eurasian collision by different authors (e.g. Hayens and McQuillan, 1974; Berberian, 1981; Berberian and King, 1981; Alavi, 1980; 2004). The age of the collision onset is still controversial.

The accretion of thrust nappes following the ophiolitic units obduction onto the Arabian margin has resulted in shortening and thickening of the Zagros mountain belt and presumably produced the tectonic load required to flex the Arabian lithosphere. The subsidence history of the Central Zagros basin was analyzed by the backstripping procedure in which a progressive reversal of the depositional process is modeled. The sedimentary sequences and timing information were derived from well data (paleologs) in the studied area. Then, the foreland basin geometry for any time step (or time line) along a profile, defined by the geometry of decompacted depth to the basement (or any reference sedimentary horizon, e.g. Sarvak in this case), is searched to fit by a theoretical (flexural) profile using a numerical approach.

VII.3.1.1 Theoretical background and methodology

- Airy-type (1D) backstripping

The backstripping procedure consists first of removing stratigraphical units from the top downwards (hence backstripping). Correction must also be made for sediment compaction in response to burial and for subsidence arising from the isostatic response to sediment loading. Paleobathymetry estimates are needed in order to constrain or calibrate earlier stages of basin bathymetry. The isostatic response to loading is commonly calculated assuming Airy

isostasy in which 1D stratigraphic data, obtained from a well or a point sample of a cross-section, is used. The Airy backstripping process which produces the history of water-loaded basement (or T_0 surface) driving subsidence, consists of the following steps (Fig.VII.15):

(1) A sediment-loaded basement subsidence curve is constructed from the initial stratigraphic data by removing each layer in the sequence in turn (Fig.VII.15a),
(2) The remaining underlying sediment units are then decompacted (Fig.VII.15b),
(3) As each layer is removed, the new sediment surface is set to a prescribed datum by assuming a depth of deposition for each stratigraphic interval, and, if desired, correcting sea-level for eustatic changes (Fig.VII.15c).
(4) The sediment-loaded subsidence curve is corrected to an equivalent water-loaded subsidence curve (Fig.VII.15d). The loading correction from sediment to water is performed assuming 1D Airy (local) isostasy.

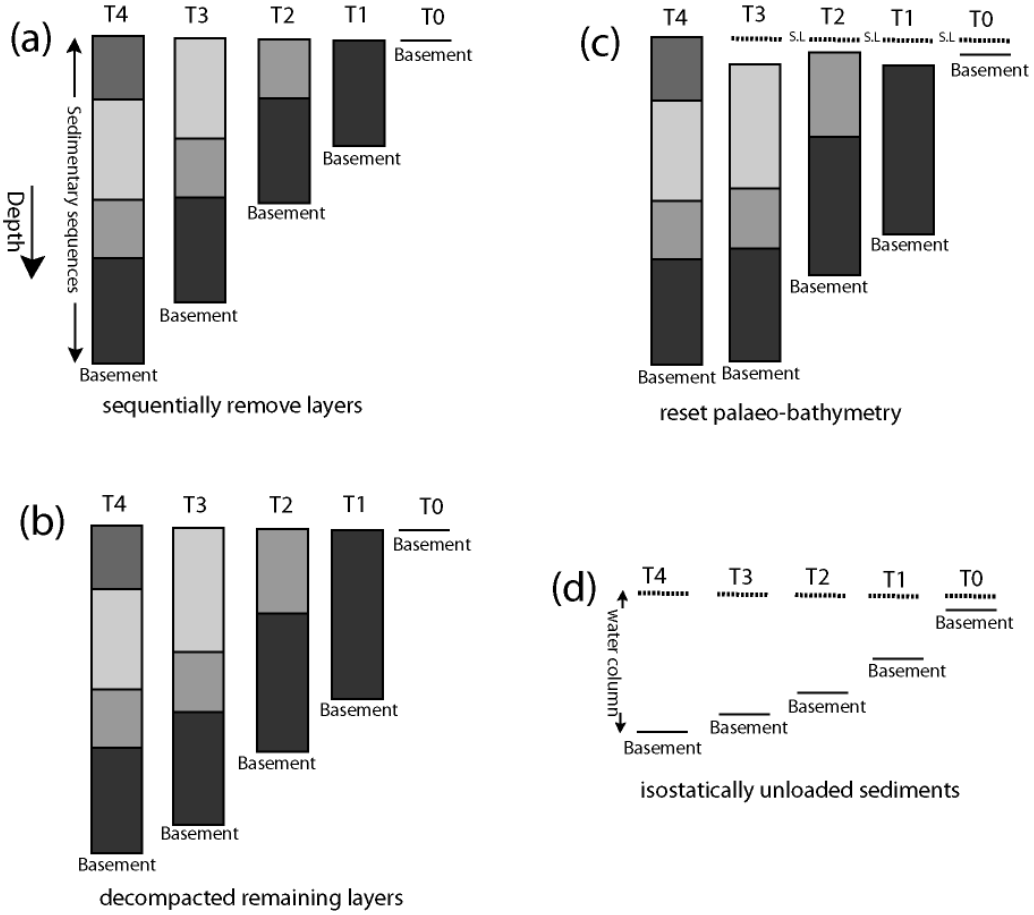

Fig.VII.15: Schematic illustration of the 1D Airy backstripping technique: (a) stratigraphic layers are progressively removed (top first); (b) remaining sedimentary layers are decompacted; (c) the top of the remaining decompacted section is reset to observed palaeobathymetry at each time stage; (d) the effects of sediment loading are removed using 1D local (Airy) isostasy in order to produce water-loaded basement-driving subsidence, S.L.=sea level, (modified from Roberts et al., 1998).

As is mentioned above, decompaction is one of the main steps in backstripping because of the loss of water during sediment burial. For decompaction, the empirical porosity-depth curves for different lithologies are usually employed (Bond and Kominz, 1984). Taking into account the uncertainties of porosity for a single lithology it is usually reasonable to decompact the sedimentary column using a simple averaged depth-porosity curve regardless of lithologies. The evolution of the rock porosity, φ, with depth, z, follows an exponential law (Athy, 1930) $\varphi = \varphi_0 e^{-cz}$, where φ_0 describes the surface porosity of rocks. In the limestone (mudstone) this value may be in a range of 0.40 to 45%. *c* is the coefficient of compaction and was considered about $0.4km^{-1}$ in this calculation. Then, decompacted thickness and the average porosity of the sedimentary column over time are calculated using the simplified method of Angevine et al. (1990) based on the method of Van Hinte (1978) as follow:

$$T_{i,t-1} = T_{i,t} \cdot \left(\frac{1-\phi_{i,t-1}}{1-\phi_{i,t}} \right)$$

where $T_{i,t-1}$ / $T_{i,t}$, and $\varphi_{i,t-1}$ / $\varphi_{i,t}$ are the thickness and the porosity respectively of layer *i* at the time *t-1* and *t* with $\varphi_{i,t}$ estimated by the porosity-depth law. After the removal of the top layer, we obtain new porosity values for the decompacted underlying layers following the exponential porosity-depth profile. We assumed that the porosity of a given layer is constant at a depth which is taken as the half of the layer thickness. Finally, applying the effect of eustasy and paleo-bathymetry the total subsidence is obtained.

If this method applied for a cross-section composed of several sample points (e.g. well data) then at each well location and in the absence of sedimentary loading, the depth at which the basement (or any reference) horizon is located, i.e. the tectonic subsidence, is obtained (Watts and Ryan, 1976). In addition to the effects of the sedimentary load, paleo-bathymetry and eustasy should be taken into account. Tectonic subsidence, Z, for local isostasy is given by Watts (2001), Allen and Allen (2005):

$$Z = S^* \frac{(\rho_m - \rho_{si})}{(\rho_m - \rho_w)} + W + \frac{\Delta_{abs}\rho_m}{(\rho_m - \rho_w)} \quad \text{with} \quad \rho_{si} = \frac{\sum_{i=1}^{n} (\rho_w \phi_i + \rho_i (1-\phi_i)).S_i^*}{S^*} \qquad (1)$$

where;

*S** is the decompacted thickness of sedimentary column,

W is the paleobathymetry at which the sediment was deposited in the time interval considered,

ρ_m and ρ_w are the densities of mantle and water, respectively,

ρ_{si} the average density of the i_{th} column,

Δ_{abs} is the eustatic correction which refers to the global oscillations of sea level based on the chart proposed, e.g., by Haq et al. (1987).

So far, the flexural rigidity of the lithosphere has been neglected. It can roughly estimated using the solution of a simple elastic case. The 2D deflection *w* of a chosen reference layer that is downflexed under a distributed vertical load *q(x)* is given by a fourth-order differential equation given by :

$$\underbrace{\frac{d^2}{dx^2}\left(D(x)\frac{d^2w}{dx^2}\right)}_{\text{flexural resistance}} + \underbrace{F\frac{\partial^2 w}{dx^2}}_{\text{end load}} + \underbrace{\Delta\rho g w}_{\text{restoring force}} = \underbrace{q(x)}_{\text{vertical load}} \qquad (2)$$

where *D* is the rigidity of the plate related to the effective elastic thickness (Te) by

$$D = \frac{ET_e^3}{12(1-\nu^2)}.$$

Te is the elastic thickness of the lithosphere which is defined as the thickness of an equivalent elastic plate which, under applied loads, would have the same deflection as that of the real (anelastic) lithosphere (Wang and Mareschal, 1999), *E* and *v* are the Young and Poisson coefficients respectively. F represents the horizontal forces applied at the plate end, $\Delta\rho g w$ is the restoring forces proportional to the difference between mantle and infill densities, *x* the horizontal distance along the coordinates axis. As the horizontal forces F have generally little effects on the first-order evolution of the flexure F and it is set to zero in all models. *w* is deflection of plate, *q* and F are vertical and horizontal (end) loads respectively and $\Delta\rho$ is density contrast (Fig.VII.16).

One simple analytical solution of equation (2) is obtained by replacing the distributed load by a line load V_0 and bending moment M_0 at origin x=0 respectively (Turcotte and Schubert, 1982) :

$$w = \frac{\alpha^2 e^{-\left(\frac{x}{\alpha}\right)}}{2D}\left\{-M_0.\sin\frac{x}{\alpha} + (V_0\alpha + M_0).\cos\frac{x}{\alpha}\right\} \quad \text{with} \quad \alpha = \left[\frac{4D}{(\rho_m - \rho_w)g}\right] \qquad (3)$$

α is the flexural parameter as defined in a equation above (see Turcotte and Schubert (1982), equation (3-127)), g is the gravity acceleration, ρ_m and ρ_w are the gravity of mantle and water respectively.

The solution of equation (2) is obtained numerically using central finite differences and back substitution in a five-band matrix (Sheffels and McNutt, 1986; Tensi et al., submitted).

At x=0, the bending moment applied to the plate end is $M=-D(\partial^2 w/\partial x^2)_{x=0}$ and $D(\partial^3 w/\partial x^3)_{x=0}=T(\partial w/\partial w)_{x=0}$. At the opposite side of the plate we set $w(\infty)=0$ and $\partial w/\partial x=0$. These boundary conditions follow that of a plate broken at x=0, typically found in subduction/collision setting where one plate is overthrusted onto another. The plate deflection and distributed load is discretized into nodes spaced every 5 km. Erosion of the growing orogen and sedimentation in the basin are included in the algorithm following studies of (Flemings and Jordan, 1989; Sinclair et al., 1991) but this possibility was not required in the present study.

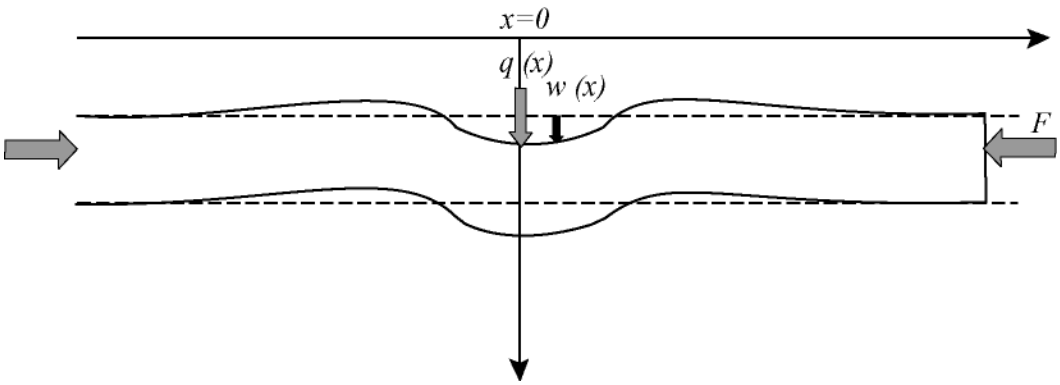

Fig.VII.16: Lithospheric deflection (*w*) under vertical (*q*) and horizontal or end (*F*) loads.

- Geometrical fitting of decompacted depths by a deflection profile

The main goal is to fit, geometrically, the decompacted depths of the base of the foreland obtained from the subsidence analysis with the numerically solved theoretical deflection profile. This requires (1) the choice of a reference isochronous horizons belonging to the sequence contacts whose deflection should be modelled, and, (2) an estimate of the elastic thickness, Te, of the continental lithosphere.

VII.3.1.2. Application of the method in the Central Zagros

Subsidence curves in the Dezful Embayment (Fig.VII.17) were constructed using well data (paleologs) and the procedure explained above. Airy-type backstripping applied in the sedimentary sequences of a cross-section comprising of 8 well data (table 1). The timing information, furnished by the paleologs and micropaleontological data, was constrained the sequence contacts (time lines) in the transect (Fig.VII.17). It means that, each resulted subsidence curve is considered to be isochronous in the transect. The Upper Cretaceous Sarvak Formation was selected as the basal reference depth at T_{95} (as an initially flat geometry and zero subsidence line) as based on the thickness variations in this period the Central Zagros basin was almost stable. Then, the subsidence history was constructed for the overlain younger sequences (Fig.VII.18a). The paleobathymetry values for the carbonate and marly sequences were considered around 50m and 100m respectively. Finally, forebulge rise was numerically modelled by fitting the basin deflection profile at the time of the Asmari deposition (T_{23}) by a calculated deflection profile (Fig.VII.18b).

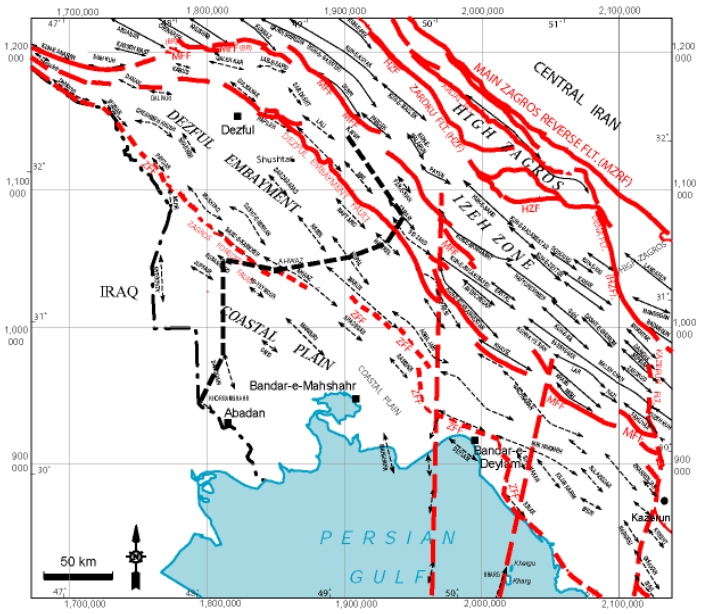

Fig.VII.17: The location of the selected cross-section in the Dezful Embayment for subsidence history analysis and lithospheric deflection modelling.

VII.3.1.3. Interpretation of the results and discussion

As is shown in Fig.4, subsidence history from Upper Cretaceous to Mio-Pliocene times along the selected transect is irregular. While during a period from 95 to 83.5 Ma,

almost a uniform subsidence is observed along the transect, the main fluctuations appear since about 70 Ma and subsidence significantly increased since that time in the SW part and NE margin of the transect. One of the main limitations in this analysis is the number of data points which do not fully cover whole the deflected lithosphere of Arabian plate's margin. So an important part towards the crush zone (or the MZRF) which may supply the main sedimentary charge for the plate deflection, does not exist in the transect.

Based on resulted subsidence curves it is almost impossible to fit the results with a simple elastic model. Such anomalies in the subsidence curves (Fig.VII.18) may be either due to basement faults reactivation or lateral variation of the lithosphere elastic thickness or even a combination of both. In this case, the basement faults (e.g. HZF, MFF, DEF, and ZFF) reactivation should be taken into account or different elastic thickness should be introduce in the model. For this reason, the resulted subsidence in the SW part of the transect may not be argued by a simple flexed model of lithosphere with the main load in the northeast. Therefore, to reduce and compensate this drawback and to fit the obtained basin geometry from the subsidence analysis with an universal deflection profile, part of the transect near NE margin, comprising of the last four well data, was used for lithospheric flexural modelling (Fig.VII.18b). This modelling was performed uniquely for the Asmari subsidence curve (~ 23Ma) (Fig.VII.19).

This model is a first attempt to describe the state of stress in the continental lithosphere of the Arabian plate which is approximated by an elastic broken plate. The choice of a broken plate is justified by the presence of one plate (Iran block) overriding another one (Arabian plate). Because the model considers the flexed plate as an elastic beam the stresses are not realistic in yield parts of the crust. But it gives reliable information about the type of far-field state of stress (extensive or compressive) in the flexed plate.

The best fitting plate deflection (Fig.VII.19) is obtained for an elastic plate thickness (Te) of 20 km. This value is low regarding the old and cold lithosphere. This results may be a consequence of (1) the poor horizontal distribution of the data available to constrain the observed plate deflection at 23 Ma; only 4 wells provide information; (2) the lack of information about deformation at depths; (3) and errors on age estimates. Some well like KN-10 does not fit with the modelled plate flexure. We infer that this is due to the presence of a thrust ramp at depths beneath the fold that accommodated displacement of 10 km southward.

well name	Time (Ma)	0	11	16	23,03	33,9	35	37,2	48,6	55,8	60	65,5	70,6	83,5	85,8	89,3	93,5	95
KM_1	0,00	1723,37	1726,25	1697,97	1658,20	1596,71	1566,73	1506,77	1196,06	1067,33	992,24	893,91	765,29	439,94	361,34	241,72	213,86	0,00
DN_1	31030,23	1601,28	1602,79	1580,77	1426,15	1187,07	1166,76	1126,12	915,57	782,59	615,07	557,84	465,00	230,17	188,30	124,59	48,13	0,00
SD_2	80304,93	984,92	985,30	986,15	682,66	609,28	555,66	444,51	439,76	436,76	435,01	432,72	389,90	236,08	210,46	66,08	17,39	0,00
AZ_6	114814,455	909,29	909,55	910,13	719,35	451,39	427,26	379,01	350,30	332,17	321,59	307,74	272,69	184,04	168,23	110,47	29,07	0,00
KL_1	149327,64	871,64	871,83	872,25	657,40	586,00	412,33	339,36	308,83	306,88	305,74	304,25	271,39	188,29	185,60	181,51	47,77	0,00
HK_61	177365,92	917,99	919,03	921,31	480,79	351,68	333,65	297,60	290,00	282,37	263,87	243,53	227,19	217,17	215,39	198,69	189,87	0,00
AS_2	199141,853	699,97	700,41	701,38	564,42	472,65	463,37	412,39	384,83	359,67	348,75	334,46	255,76	194,28	183,32	146,78	102,94	0,00
KN_10	202262,596	1299,36	1299,57	1300,03	891,30	736,14	720,44	596,28	398,79	385,51	393,59	391,08	350,91	188,12	181,86	129,46	34,07	0,00

Distance (m)

Subsidence history

Table 1:Subsidenec history data set along the transect of Fig.3. The figures in each column indicate the amount of subsidence for each time-line (first row)and within each well (first column). KN-10 and KM-1 are located at the norteastern end and southwestern end of the transect (Fig.3) respectively.

Fig.VII.18: Subsidence curves showing the variations of the Central Zagros basin geometry along the cross section shown in Fig.3. (a) strong variations in subsidence history in form of a few lows and highs have been appeared since 37 Ma., (b) part of the cross section (a) was selected to test the lithispheric deflection modelling for the case of the Asmari Formation (~ 23 Ma.) solely.

We predict extensional bending stresses of 150-200 MPa over the whole bulge. Such stresses are sufficient to yield extensional faulting in the upper crust. Thus all the area covering distances from KN-10 well to KL-1 well, i.e., 100 km, is probably under far-field extensional state of stress induced by plate flexure. We further predict that the plate boundary at which the load is applied was located 80 km to the North of the present position of the KN-10 well.

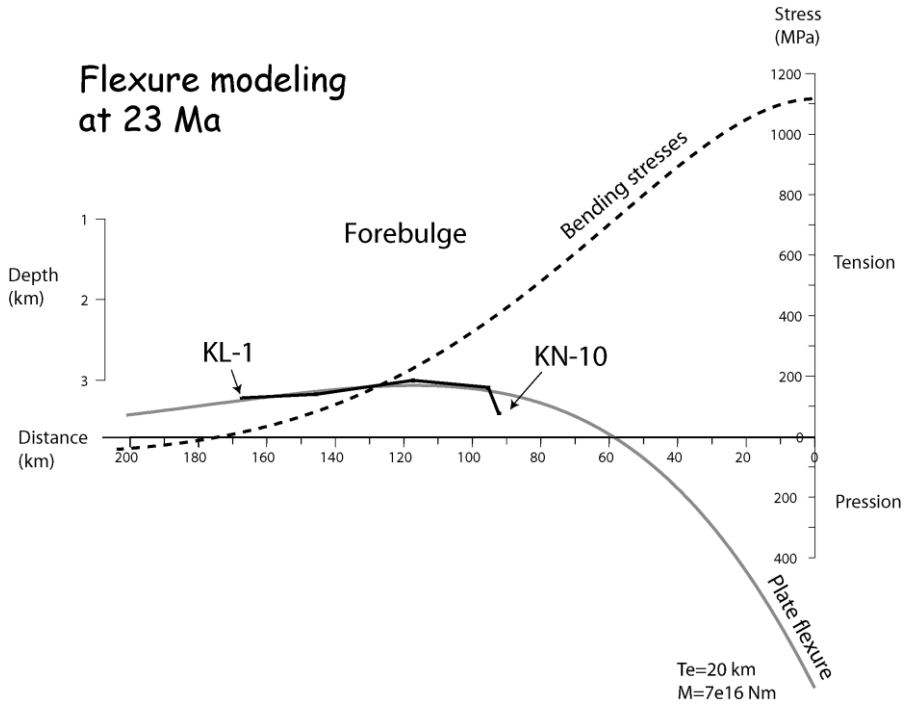

Fig.VII.19: The best fitting plate deflection model for an elastic plate thickness (Te) of 20km modeled for the subsidence history curve of the Asmari Formation (~23 Ma). Extensional bending stresses of 150-200 MPa are predicted over the whole bulge. Such stresses are presumably sufficient to yield extensional faulting and related fracturing in the upper crust during the sedimentation of the Asmari Formation.

Interestingly, for folds located to the south of the KL-1, the model predicts very low tensional stresses and even compression state of stress. This supposes that fracturing within the Asmari reservoirs towards southern part of the Dezful Embayment may not be due to the lithospheric flexure. Such possibility should be tested by comparing the model and the fracture pattern in such structures. In general, data limitation and our weak knowledge about the Zagros basement structure, make it quite difficult to propose a conventional deflected plate model in the Central Zagros.

VII.3.2 Early fracturing in the Asmari carbonates and compressional reactivation of basement faults due to early orogenic stress build-up

Early stage forced folding above compressionally reactivated (inverted ?) basement faults is considered here as one of the main mechanisms in fracture (e.g. set III) initiation within the Asmari carbonates in the Central Zagros. The related extensional stress field in this early fracturing was considered to be localized in the uppermost part of the cover, above inverted underlying basement faults. This requires that stress build-up in the foreland overcome the frictional strength of preexisting basement faults. Among these faults, N-S trending basement faults are presumably steep but a vertical component motion is supposed to be present during their reactivation. This dip-slip component is more important for the group of NW-SE trending basement faults.

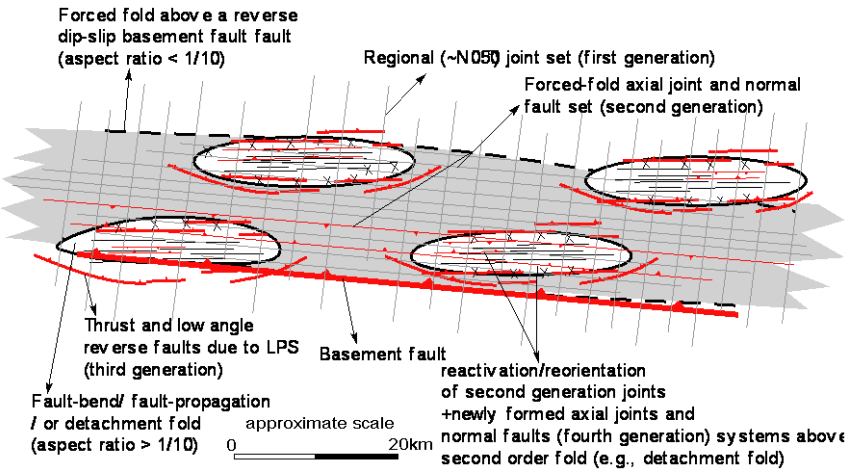

Fig.VII.20: Two superimposed folding event (forced-folding and detachment folding) scenarios and related fracture patterns. Some fracture sets are found in the second order folds (e.g., detachment folds), previously formed above a forced fold and may not be related to the newly formed folds.

Pre-folding fracture sets in the Central Zagros were discussed in detail. Among these fracture sets, a regularly spaced set I fracture (see chapter VI.A) is supposed to have formed regionally and under a compressional stress field. Large-scale forced-folding above the main NW-SE trending basement faults can explain the development of NW-SE trending joints and faults during the first stage deformation in the Zagros. At that time, the sedimentary cover likely underwent layer parallel shortening (LPS) as shown by the earliest N50° earliest joint set (see chapter V for more details). One of the major differences in the geometry of forced folds and buckle folds is their aspect ratio (half wavelength to axial length ratio). As the forcing members that generate the forced folds are generally resulted from long linear steps in the basement, the resulting folds frequently have long aspect ratio and are, although not always, asymmetric (Sattarzadeh et al., 2000). The amount of aspect ratio in buckle folds has been proposed in the range of 1/5 to 1/10 (Sattarzadeh et al., 2000). So, we can expect to find

evidence of early episodes of fracture development above basement faults around the terminations of some present folds in the Zagros (Fig.VII.20). Because the forced folds that result, will have an element of buckling associated with them. However, their geometrical scales are different from buckle folds.

In the following chapter, we will rather adopt the early compressional reactivation of basement faults and the related forced-folding in the overlying cover as the main mechanisms controlling early fracture development in the Zagros.

Conclusion

A major fracture group in the Central Zagros, with no symmetrical relation with the fold geometry based on conventional fold/fracture models, is supposed to have initiated before Mio-Pliocene orogenic episode. Intra-basin architecture and facies changes during Lower Tertiary times suggest that possible forced folding above reactivated basement faults controlled the Asmari sub-basins. Reactivation timing of the main basement faults based on the most important facies marker (i.e., Kalhur Member) was estimated early Aquitanian in age. The presence of a regularly spaced systematically joint set (see chapter VI, set I), striking ~ N40 ± 10°, which predate NW-SE trending forced-fold-related fractures in the Central Zagros suggest that partitioning of N-S convergence into an NE-SW shortening perpendicular to the belt trend and right lateral strike-slip motion along the MRF may have began during the early stage of the Asmari sedimentation (Upper Oligocene-Lower Miocene). The coincidence of the Lower Asmari clastic facies (Ahwaz sand) distribution and even thickness variation and facies changes within Pabdeh/Jahrum basin with the main basement faults even suggest that the onset of deformation and basement forced folding should have started as early as Lower-Middle Eocene times (~50 Ma).

In the episode of plate flexure that followed the deposition of the Asmari limestones at ca. 23 Ma. possibly produced favorable mechanical conditions to trigger extensional faulting in the whole crust. However, this hypothesis should be carefully used by a more complex model of deflected plate for the Central Zagros (e.g. with different elastic thickness and/or the effect of the basement faults).

CHAPTER VIII: Implications for the geodynamic evolution of the Central Zagros

Introduction

Following the discussion in the previous chapter, it is possible now to propose a geodynamic model for deformation in the Central Zagros. The timing in this model is well constrained by early fracture and intra-basin development in the region.

VIII.1.Previous estimates of deformation timing in the Zagros folded-belt

From a geodynamic point of view different models for the evolution of the Zagros mountain system in southern Iran were proposed (e.g. Falcon, 1967; Stocklin, 1968; Wells, 1969; Ricou, 1970; Nowroozi, 1972; Haynes and McQuillan, 1974; Alavi, 1980, 1994; Berberian and King, 1981; Jackson et al., 1981; Ni and Barazangi, 1986; Alavi, 2004). In almost all of them, it was shown that subsequent northward movement of the Arabian plate during Tertiary time resulted in thrust faulting and overfolding in the Imbricated Belt adjoining the trench zone and more gentle folding in the Simply Folded Belt to the southwest. Despite that, the beginning of compression in the Zagros folded-belt is poorly dated. The initial Arabian-Central Iranian continental collision is considered to be Late Cretaceous (Hayenes and McQuillan, 1974; Berberian and King, 1981; Alavi, 1994), Eocene-Oligocene (Hooper, 1994), Oligocene-Miocene (Berberian et al., 1982) or late Miocene in age (Stoneley, 1981; McQuarrie et al., 2003). Berberian and King (1981) proposed that folding in the Zagros folded-belt started around 5Ma and coincides with the second phase of extension in the Red Sea and Gulf of Aden. Based on the unconformity between the Agha-Jari and Bakhtyari formations, Falcon (1961) suggested that the deformation was initiated at the Early Pliocene. On the basis of several unconformities at different stratigraphic levels, Hessami et al. (2001) proposed that deformation occurred by pulses since the end of the Eocene, and reached the front of the folded belt during an end-Pliocene phase. All these estimations are based on ages of unconformities and sediment formations mostly defined by James and Wynd (1965). Documented Holocene anticline growth (Mann and Vita-Finzi, 1988; Vita-Finzi, 2001) and recent seismicity (Jackson and McKenzie, 1984) indicate that deformation in the Zagros belt is still active, especially at deep crustal levels (Homke et al., 2004). Homke et al. (2004) defined the beginning of the deformation in part of Zagros foreland basin (Push-e Kush Arc), 8.1 to 7.2 Ma based on magnetostratigraphy study of Miocene-Pliocene sediments. Allen et al.

(2004) stated that extrapolating present-day deformation rates for 3-7 million years produces displacements that equal or exceed the total deformation on many of fault systems currently active in Arabia-Eurasia collision zone including the Zagros Simple Folded zone and this age range is much shorter than the overall age of the collision, which began in the early Miocene (16-23 Ma) or earlier (Hempton, 1987; Yilmaz, 1993; Robertson, 2000). Accordingly, Agard et al. (2005) documented several major tectonic events that took place at the end of the Cretaceous, during the late Eocene and from the Mid-Miocene onwards (ca. <20-15 Ma) and concluded that collision must have started before ca. 23-25 Ma in northern Zagros.

Based on the variety of estimations given by different authors regarding the absolute timing of collision, providing evidence for the earliest compressional deformation, possibly related to orogenic stresses, is a key point to this respect. The uncertainty on the timing of deformation covers a range from late Cretaceous to Pliocene. To state that this deformation in the Zagros folded belt is diachronous or synchronous depends on the type of deformation and the place where this deformation happened. Most of investigations in this regards were carried out within the sedimentary cover and mostly within the structures which are close to the major tectonic elements in the region (e.g., MZRF, MFF, etc...). Furthermore, our knowledge regarding the role of the Zagros basement in deformation and shortening of the cover is poor.

VIII.2. Possible timing of early fractures and onset of orogenic deformation and stress build-up in the Central Zagros

Fractures directly related to fold geometry are probably either syn- or post-folding, and it is generally difficult to say which (Cosgrove and Ameen, 2000). The relative age of the fractures can sometimes be established using abutting relationships (see chapter III) but the absolute age is more difficult to ascertain. Deformation in the Zagros belt including folding and fracturing is the consequent of Arabia-Eurasia continental collision. The age for initiation of this collision estimated from ~64 Ma (Beberian and King, 1981), using the end of ophiolite obduction, to ~5 Ma (Philip et al., 1989), using the angular unconformity between Bakhtiary conglomerates and the underlying Agha-Jari Formation (Falcon, 1974). Neither of these approaches provides a date for the first time Arabian and Eurasian continental crusts came into contact in response to convergence (Allen et al., 2004). Deformation and syn-tectonic sedimentation took place on the northern side of the Arabian plate in the Early Miocene (~16-23 Ma) (Robertson, 2000), related to the overthrusting of allochthonous nappes originating on the Eurasian side of the Neo-Tethys (Allen et al., 2004). Other studies in the same region put

the initial collision-related deformation in the Oligocene (Yilmaz, 1993), or even in the Middle Eocene (~ 40 Ma) (Hempton, 1987).

Based on evidence of facies changes, forced folding above basement faults in the Central Zagros strongly affected the Asmari basin during Aquitanian time (early Lower Miocene) and possibly continued up to the final stage of deformation during Upper Miocene – Pliocene times. Figs.VIII.1-3 show geodynamic evolution of the Central Zagros basin, based on constructed paleogeographic maps (Figs.VII.10a&b). An almost stable continental platform margin during lower Cretaceous times characterized by thick carbonate series interbeded with shale horizons and followed by a widespread unconformity due to ophiolite obduction at the end of this period (Cenomanian-Turonian). Upper Cretaceous time may be considered as a period in which an unstable basin established in the Central Zagros and facies variety and basin architecture progressively changed at the end of this period and start of the Tertiary times.

VIII.3 Geodynamic implications

North-south convergence across the northwest Zagros is achieved through a combination of northeast-southwest shortening and right-lateral strike-slip faulting on the Main Recent Fault in the NW Zagros (Talebian and Jackson, 2004). Talebian and Jackson (2002) argued an offset of about 50 -70 km along the right-lateral strike-slip Main Recent Fault based on a restoration of the drainage patterns and geological markers. Then they proposed an age of about 3-5 My. for the initiation of the MRF (Main Recent Fault). It means that an average velocity of about 15 mm/yr could be considered for this offset. There are no other major, northwest-southeast, directed seismically active right-lateral strike-slip faults within this part of the Simple Fold Zone that could help partition the overall convergence in this way (Allen et al., 2004). Furthermore, based on recent GPS measurements of convergence between the Central Iranian block and the Arabian plate (Vernant et al, 2004), the Central Zagros accommodates about 7 ± 2mm /yr of north-south shortening. The shortening rate decreases in northern Zagros, implying a right lateral strike-slip rate along the Main Recent Fault (MRF) of 3 ± 2mm /yr, which appear smaller than geological estimates (Talebian and Jackson, 2002) and is compatible with shortening rate estimation (Agard et al., 2005) over the Crush zone after the start of collision at a minimum 3-4 mm/yr. Agard et al. (2005) suggest that strike-slip movement along MRF predated Plio-Quaternary offsets along this fault reported by Talebian and Jackson (2002).

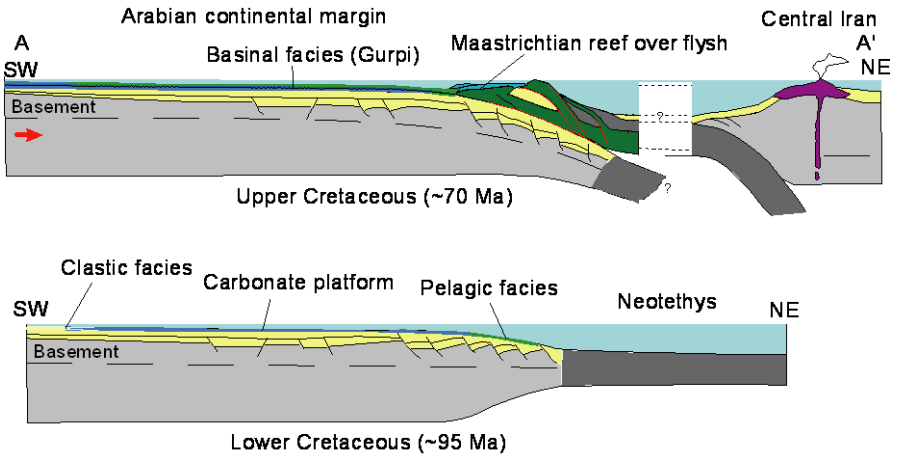

Fig.VIII.1: Geodynamic evolution of the Central Zagros basin during Cretaceous times. While Lower Cretaceous characterized by a stable carbonate platform (lower image) facies variation and platform instability gradually become important following ophiolite obduction along the Main Zagros Reverse Fault (MZRF). The approximate location of the sections were indicated as AA' on the related paleogeographic maps.

The geodynamic evolution of the basin during the lower Tertiary times, at least in the Central Zagros, is not so clear. Most parts of the Paleocene sediments, based on paleolog data in the Dezful Embayment were eroded and this unconformity sometimes reaches Maastrichtian times in this region. Documented emergent zones near N-S direction basement fault (e.g., IZHF, Fig.VII.10b) during the latest Cretaceous and even Paleocene times suggest that N-S trending basement fault may have been reactivated. Progressive basin restrictions, sedimentary flux progradation toward the basin depocenter, and emergent of southern part of the basin (Fig.VII.10d) during Eocene-Oligocene times suggest that basin architecture and the NW-SE trending basement faults presumably affected by a far-field stress which may result from Arabia-Eurasia continental collision. Fig.VII.2 shows a possible scenario of the geodynamic evolution of the Central Zagros during Eocene-Oligocene times.

During early Miocene (Aquitanian) time, as shown in the paleogeographic map (Fig.VII.8e), significant changes in the basin architecture and facies distribution happened. At this time, early reactivation of basement faults (e.g., MFF, DEF) led to possible forced-folding and formation of the Kalhur evaporitic intra-basin which is located between MFF and DEF toward the northeast and southwest respectively. Some important points should be mentioned regarding the present-day coincidence of these linear features (elongated evaporitic basin and basement faults). The amount of calculated shortening based on constructed balanced transects in the Central Zagros, including the High Zagros to the southwest of the Dezful Embayment was reported about 50 km (Sherkati et al., 2005). Furthermore, the differential shortening in the Dezful Embayment (likely less than 15 km) is

quite less than the High Zagros and Izeh zone where the maximum shortening accommodated by a series of imbricate thrust nappes. It means that, the amount of southwest-ward cover displacement on the basement, somewhere between MFF and DEF can be considered negligible for our reconstructions. On the other hand, there is always some discrepancies concerning the (projected) location of basement faults on the present-day cover but in any case, this intra-basin could not be displaced from the Izeh zone, northeast of the MFF, into the Dezful Embayment.

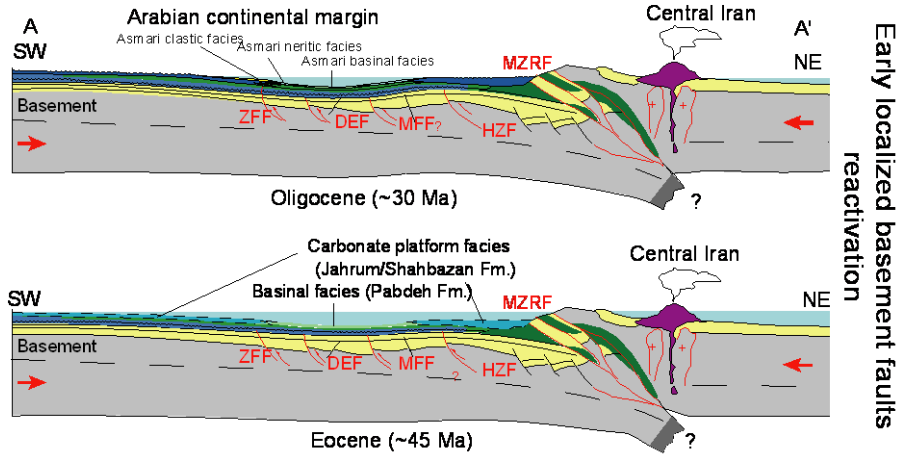

Fig.VIII.2: Geodynamic evolution of the Central Zagros basin during Eocene-Oligocene times based on the paleogeographic and facies distribution in the region. Progressive basin restriction, and sedimentary flux progradation toward the depocenter of the basin suggest the effect of a far-field compressional stress following Arabia-Eurasia continental collision and presumably the start of the NW-SE trending basement faults reactivation.

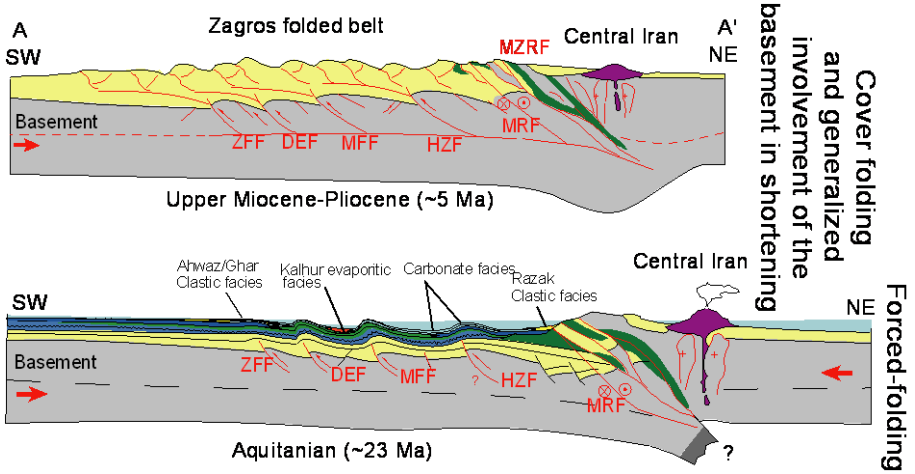

Fig.VIII.3: Geodynamic evolution of the Central Zagros basin during Aquitanian (bottom) and Upper Miocene-Pliocene times. Development of the evaporitic Kalhur intra-basin, and directly on the pelagic facies of the Oligocene Lower Asmari, presumably resulted from the main basement faults (e.g., MFF and DEF) inversion. Finally, whole the sedimentary series and the basement underwent the final phase of deformation during Upper-Miocene-Pliocene times.

Finally, during upper Miocene-Pliocene time, the whole sedimentary series and the basement underwent the final orogenic phase of the Zagros and led to the present day folds

and thrust belt in the region. Fig.VIII.3 shows the geodynamic evolution of the Central Zagros during early Miocene (Aquitanian) and Upper Miocene-Pliocene times.

The group of NW-SE trending fractures is supposed to have formed during the early stage of forced-folding above the main Zagros basement faults, and within the Asmari Formation (and even more ancient formations) during its deposition. Taking into account the earlier group of N050° regional joint set (see chapter V for details) and also the second group which formed above forced folds, it is suggested that partitioning of the N-S convergence into right-lateral shearing along NW-SE trend, and NE-SW shortening should have started, at least, as early as Aquitanian (~23 Ma) time and maybe earlier. In this case, the proposed velocity along the MRF by other workers (i.e., Talebian and Jackson, 2002), supposing the amount of offset is correct, should be quite less and something about 2-3 mm/yr and this is in agreement with the velocity proposed by Vernant et al. (2004) and Agard et al. (2005).

Thickness variations in the Pabdeh Formation, shown in Fig.VII.14b, suggest that the first stage of basement fault reactivation may have started even before the Asmari, possibly during Eocene times (~ 50 Ma) which may more or less mark the onset of compression related to the Arabia-Central Iran continental collision and is also marked by early N050° joint set. The appearance of a sabkha basin between HZF and MFF (or ZFF) with evaporitic facies (Sachun Formation), east of Kazerun fault in the Fars area, could be related to an episode of basement fault reactivation during Eocene times. Then, amplification of basement fault movements during Upper Oligocene to Early Lower Miocene (Chattian- Early Aquitanian, ~ 27- 23 Ma) led to different isolated intra-basins in the studied area and initiated a series of fractures, parallel to general trends of these intra-basins and basement faults. In agreement with Allen et al. (2004), and Agard et al. (2005), deformation partitioning happened probably long before of what has been estimated and 22-30 Ma (Chattian-Aquitanian) is likely to be the minimum range of age for initial plate collision. Because the earliest evidence of compressional trend in the studied area is N50°, similar to that derived from focal mechanisms of thrust earthquakes in the NW Zagros (Talebian and Jackson, 2004), an age of 22-30 Ma could also be acceptable for the onset of partitioning of convergence in the NW Zagros.

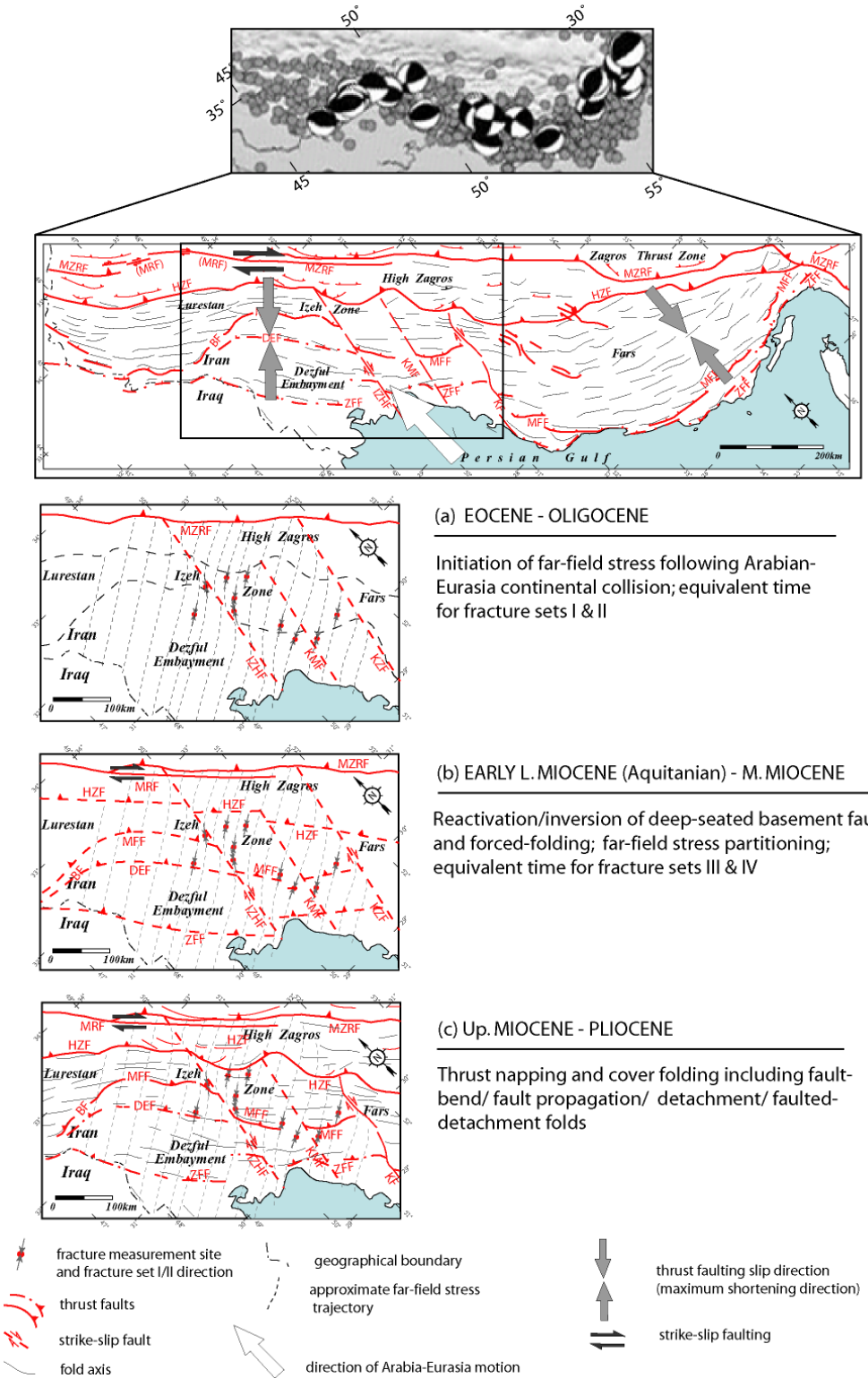

Fig.VIII.4: Deformation episodes in the Central Zagros; see text for more details., at the top: best-double-couple CMT solutions from the Harvard catalogue (http://www.seismology.harvard.edu/CMTsearch.html) for earthquakes with depth ≤30 km, Mw ≥ 5.5 and double-couple component ≥70%, in the interval 1977–2001, epicenters are from the catalogue of Engdahl et al. (1998) (modified from Allen, 2004, big arrows are from Talebian and Jackson, 2004).

VIII.4. Petroleum exploration importance

The marginal zones along the main Zagros basement faults (e.g. MFF) have been poorly explored. Furthermore, deep targeting geophysical and exploration activities still have not been implemented in these zones due to their structural complexities. Regardless of technical problems which may be important from operational point of view, geophysical planing for deep seated traps which may be located above basement faults may lead to explore giant hydrocarbon reservoirs (at least gas reservoirs) which superimposed by Mio-Pliocene conventional detachment, fault-bend, or fault propagation structural traps. There are many giant basement-fault-related structures with oil and gas reservoirs within Paleozoic to Mesozoic horizons beyond the Zagros deformation front in the eastern part of the Arabian plate (e.g., Ghavar in Saudi Arabia, Bourgan in Kuwate, etc...). The presence of such structures should be masked after the Zagros orogeney but they are likely present as potential traps above both NW-SE and N-S trending basement faults in the Zagros folded belt.

Deformation episodes for Tertiary times within the Central Zagros, based on fracture patterns and the geodynamic evolution of the basin, have been summarized in Fig.VIII.4. The trends of regional joint sets (set I & II, see chapter VI) in the studied outcrops were used as indicators for the far-field compressional stress trajectory in the region during Eocene-Oligocene times. As shown in Fig.VIII.4a, joint trend and related stress-filed deflection are supposed to be due to the presence of pre-existing basement linear anomalies (faults). Early Miocene (Aquitanian) to Middle Miocene times were introduced as the period in which basement faults reactivated (Fig.VIII.4b) and followed by thrust napping and cover folding including fault-bend, fault-propagation, detachment, and faulted detachment folds during Upper Miocene to Pliocene times in the studied area (Fig.VIII.4c).

Conclusion

Basement fault movements during Upper Oligocene to Early Lower Miocene (Chattian- Early Aquitanian, ~ 27- 23 Ma) led to different isolated intra-basins in the studied area and initiated a series of fractures, parallel to general trends of these intra-basins and basement faults. Deformation partitioning happened, presumably, long before of what has been estimated and 22-30 Ma (Chattian-Aquitanian) is likely to be the minimum range of age for initial plate collision.

This study emphasizes that early basement block movements have an impact on fracture development in the cover rocks. In addition, the transmission of stress through a

fractured crystalline basement during plate collision can be expected to be heterogeneous and complex, so a deformation front is likely to propagate in an irregular fashion through the basement and the cover leading to a complex chronology of fracture development. Such a complexity should be taken into account in further studies of folded and fractured reservoirs.

Finally, this early deformation phase in form of forced folding above the main basement faults could be important regarding hydrocarbon exploration in the Zagros region as they presumably form the most ancient structural closure for hydrocarbon accumulation in the region.

PART 4
Inherited fracture reactivation and neo-fracturing during folding of sedimentary strata : a mechanical modelling

(This part is the result of a collaboration with M. Guiton and C. Zammali)

Introduction

Different fracture sets and their chronology in the Central Zagros, recognized from intensive field work and aerial/satellite image interpretation, were discussed on different scales (see chapter V). To figure out, more clearly, the brittle deformation mechanisms in the Zagros folds including interaction between deformation style in a typical fold and fracture reactivation, and also neo-fracturing episodes during folding, fracture development and reactivation were modelled numerically. Through a mechanical approach, those fracture data measured in the field, were studied in several models.

The basis of mechanical modelling is to apply the concepts of continuum mechanics to take into account the physical properties of the materials (e.g. following the simulation of the blocks movements along a fault). A mechanical approach permits to calculate the deformation giving the following initial conditions: a geometry, a behaviour law, and displacement and imposed forces to domain boundaries, with their time evolution. Furthermore, such an approach is largely used at asthenospheric and lithospheric scales to understand the evolution of the earth but it is less used at sedimentary basin scale for several reasons:

- The spectrum of rheology for rocks is quite large from brittle to elasto-visco-plastic. In addition, these rheologies could change during time with pressure and temperature variations, and with internal deformation mechanisms which should be homogenized.
- The constitutive law to simulate geological phenomena at large scale are not accessible via direct experiments unlike civil engineering modelling.
- If the boundary conditions, with a high degree of optimism, could be known for the actual state, they become more and more difficult to define and measure through evolution of the basin.
- Such modelling requires the simulation of large deformation and displacements.

The main objective of this part is to test several chronological scenarios of fracture development with respect to folding. For this purpose the Asmari anticline was selected because more information about the fold geometry and its fractures are available from field survey, structural transects and 2D seismic lines of the Asmari anticline than any other anticline. Furthermore, this anticline is quite representative regarding different observed fracture families within different anticlines in the studied area as almost all different azimuthal fracture sets in the region are observed within the Asmari anticline. In this chapter,

first, the basic concepts of kinematic and mechanical modelling are presented, including some terms frequently used in this domain, and then different models with different sets of inherited fractures are tested and are compared to the field observation in the Asmari anticline.

1. Deformation and 3D modelling in structural geology; methodology

The main steps towards deformation modelling of geological structures may be summarized as follow:

- Defining 3D geometry of the structure
- 3D kinematic modelling and restoration
- Mechanical modelling using Finite Element Method and an adaptive constitutive law

The first step which may be considered a static step is based on the preliminary data obtained from constructed geological transect and/or subsurface (seismic) data. The more precise constructed geometrical shape is, the better reconstruction of its evolution will be. Preserved fold shapes usually reveal little about their kinematic evolution (Verges et al., 1996). The first step in reconstruction of geometric evolution of a basin, or simply a fold through time (known as kinematics) consists of definition of an actual state and then the choice of kinematics that leads to a geologically probable initial state (Fig.1). This inverse approach is called restoration and also permits us to validate an actual geometrical interpretation of a structure. Historically, the restoration is principally based on geometrical hypothesis, for example the conservation of the thickness and the length of the sedimentary layers. For this reason, these methods are generally limited to a two-dimensional analysis (2D) because full 3D implementation on a real case is rather complex.

To reconstruct chronological deformation in a sedimentary basin, first, deformational cycles should be derived and then interpreted. To identify this deformation, it is necessary to analyse the internal deformation markers (bed boundaries, micro-faults, stylolites,…) in the bed(s). These markers could be analysed at different scales. These markers, at the scale of a fold, for example, clarify shearing succession, flexure mechanism, and also the quantification of the amount of shortening or elongation applied to the beds. In the earth's crust, internal deformation mechanisms within sedimentary series consist of creep (flow) by diffusion mass transfer under stress (Gratier, 1993), crystalline plasticity (Nicolas, 1984), and also cataclastic deformation with a friction as strength (Knipe, 1989). Each mechanism is accompanied by

characteristic micro structures which allow us to constrain the dynamical conditions of the tectonic events. From mechanical point of view, for small deformation in which the deformed state is close to the initial, non-deformed state, the applied stresses related to deformation follow a linear law. In the case of sedimentary basin deformation, this hypothesis is not valid any more because the final configuration is quite deformed compared to the initial state. In this case, the large displacement formalism is used (Cailletaux et al., 1995).

1.1. Restoration

Our knowledge about the formation mechanisms of structures within geological time scale is limited. The techniques of restoration are classically based on geometrical principles. Among these principals, we essentially mention “the conservation of a target horizontal surface”, “volume conservation” (surface in the 2D case), which are based on the fact that, the geological structures are restored to a non- or little-deformed state without any variation of geological material volume, somehow that the disposition of strata and also length and thickness of each bed is preserved in coherent form. In general the initial stage is chosen to be in form of a horizontal layer. The procedure could be summarized as follow:

- the first step consist of construction of a transect using geological observation and/or geophysical data. This is a primary step for the later kinematic interpretation because it is at this moment that the "lines" (bedding contacts, faults, etc...) on which deformation will be applied, are defined.
- The second step is deformation of these lines with the help of geometrical properties that generally corresponds to the implicit choice of a particular mechanical behaviour. The rheology of natural material is approached by the modes of deformation, for example, flexural-slip in which the deformation in the blocks that limit the faults perform parallel to inter-beds, and vertical or oblique shearing to accommodate, for example, a slip along a listric normal fault (see Rouby et al., 2003 for more details).

The validity of geometrical model is confirmed by trial and error. The other category of kinematical modelling is the modelling by construction (forward or direct), which start from a basin, initially little or non-deformed towards a more deformed state. So, we impose an initial configuration and we test its evolution by comparison with natural structures. Restoration is an iterative process, represented by several steps. A cross section, constructed using a structural interpretation based on seismic data, involve several phases of restoration

before reaching a valid state. In the case of invalid restoration, a new structural interpretation should be done (Fig.2).

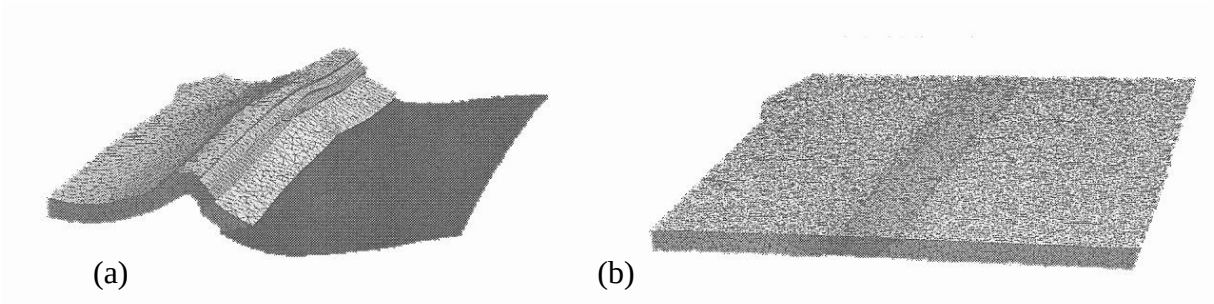

Fig.1: Restoration: (a) initial deformed geometry (actual state) and (b) restored final geometry (non-deformed state), (Moretti et al., 2005).

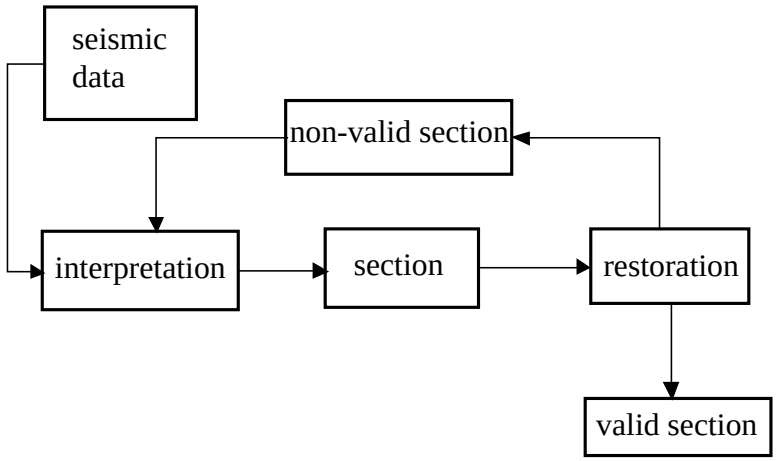

Fig.2: Flowchart of restoration of a cross-section (De Santi et al., 2003)

In this work, we used the methods described in Moretti et al. (2005) in which the volume conservation is imposed using an elastic finite element model with Poisson ratio (ν) close to 0.5. The advantage of this approach is that it allows an effective 3D restoration insuring perfect sliding along faults.

The geological restoration is one of the most practical techniques to obtain a precise and consistent interpretation of seismic data related to a geological cross-section. Its role is to validate the structural and geometrical interpretation of a geological Formation and can lead to define a valid and acceptable model (De Santi et al., 2003). It also represents a preliminary and necessary step of all direct modelling that need an acceptable initial stage to begin with and to precise displacement at their boundaries.

1.2. Direct (mechanical) modeling

Kinematic methods allow reconstruction of the initial configuration from the interpreted present-day structures, and therefore allow validation of an interpretation from a

geometrical point of view. Despite the high interest of such methods, their main drawback lies in the fact that the obtained solution does not necessarily verify mechanical equilibrium and do not have high flexibility in the description of internal deformation. In order to overcome these deficiencies, numerical models which verify the physical equilibrium of the solution have been applied to geological problems. The progress in mechanical formulation of geological deformation, the increase in the super-calculator power, and also improvement in seismic image resolution and quality opens new doors for mechanical modeling of geological structures. It means a representation of evolution of a fold during its geological history with quantification of deformation and stress through time. Such modelling has been allowed with the development of numerical methods such as the finite element method. This method has originally been developed to solve continuum mechanics problems encountered in aeronautics and civil engineering in the framework of infinitesimal strains. Later on, this method was used to study geological problems such as folding (e.g. Parrish, 1973; De Bremaecker and Becker, 1978), fracturing (e.g. Guiton, 2001, Sassi et al., 2003) or other petroleum related structural problems (e.g. Nieuwland and Walters, 1993).

1.2.1. Some basic mechanical notions

The mechanical behaviour of rocks depends on the pressure, temperature and strain-rate. At rapid strain-rates and low temperatures and pressures, most rocks behave in an *elastic* manner. A spring is a simple mechanical analogue for an elastic behaviour (Fig.3a). All strain is recovered when the load is removed. The slope of the stress vs. strain curve is the elastic, or Young's modulus (E) of the rock (Fig.3b).

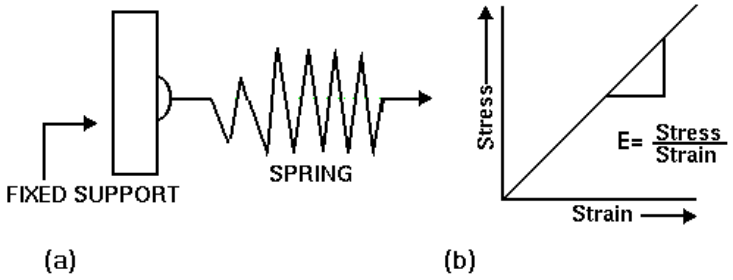

Fig.3: A simple mechanical analogue for an elastic behaviour (a), the slope of the stress vs. strain curve is the elastic, or Young's modulus (E) (b).

At lower strain-rates and elevated temperatures and pressures, rocks behave in a *plastic* manner, showing large deformations at stresses beyond a critical stress level (called

the yield stress, Fig.4b). Strain is not recoverable and deformation is permanent. A block sliding on a plane is a simple mechanical analogue (Fig.4a).

Sometimes the deformation of rocks becomes similar to that of a flowing fluid. The rate of deformation or strain-rate is controlled by the applied stress. Such behavior is called *viscous*. The slope of the stress vs. strain-rate curve is the fluid viscosity (μ, Fig.5b). A dashpot is a simple mechanical analogue for a viscous behavior (Fig.5a). Strain is not recovered. Viscous elements are introduced into models of rock behavior to incorporate time-dependency.

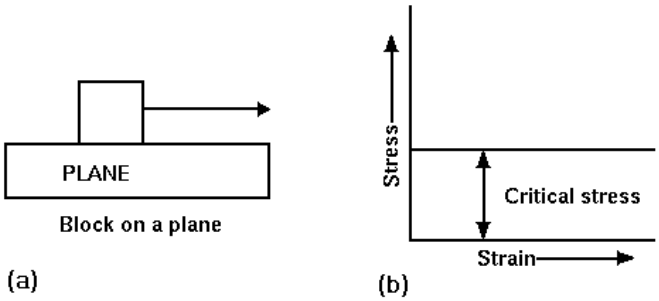

Fig.4: A mechanical analogue for a plastic behaviour (a) shows large deformation at a stress beyond a critical stress level (b).

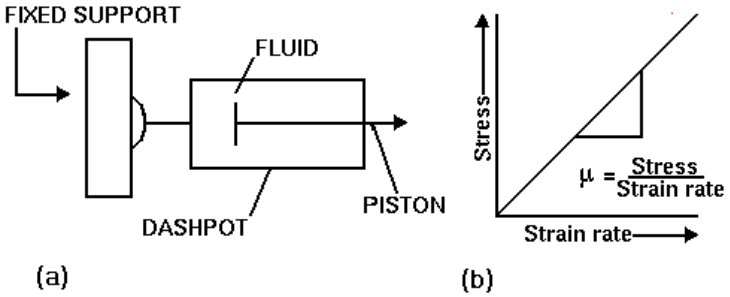

Fig.5: A simple mechanical analogue for a viscous behaviour (a), the slope of the stress vs. strain-rate curve is the fluid viscosity (b).

The *elasto-plastic* model of material behaviour is often used to characterize rocks. It combines elastic and plastic aspects of stress-strain behaviour. A block on a plane attached to a spring is the mechanical analogue (Fig.6). Strain is only recovered for the elastic part of the deformation.

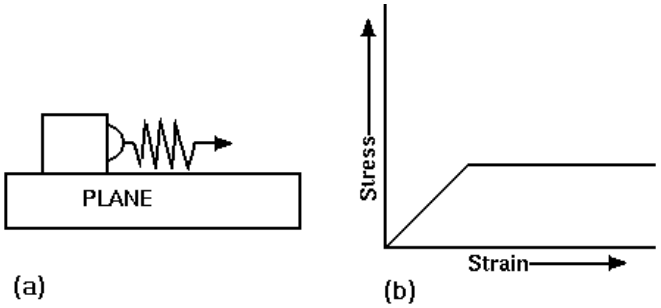

Fig.6: A mechanical analogue for the elasto-plastic model of material behaviour (a) and its stress-strain relationship curve (b).

Rocks fail in different ways depending on the temperature and pressure. At low temperatures and high strain rates rocks are *brittle-elastic*. They deform elastically at stresses up to about 70% of their strength then crack propagation becomes dominant and eventually the rock fails as cracks coalesce to form a large fracture or failure surface. At low strain-rates, elevated temperatures and very high confining pressures the stress strain curve does not have a distinct maximum to indicate failure. Samples show the continuous deformation under load characteristic of *ductile-plastic* materials. Failed cores have a characteristic "barrel" shape (Fig.7). The transition from brittle-elastic behavior to ductile-plastic behavior is favored by: (i) increasing pressure, (ii) increasing temperature. Increasing fluid (pore) pressure should cause a change back to brittle elastic behavior (Engelder, personal communication).

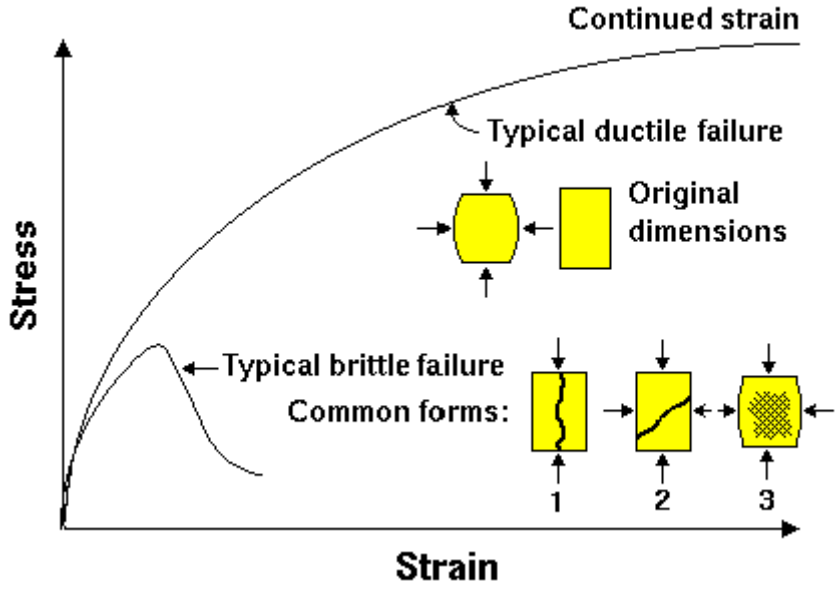

Fig.7: Typical brittle and ductile failure and their common forms; at low confining pressures, shallow depths or near free surfaces, vertical splitting (**1**) is the usual failure mode. At higher confining pressures (deeper) a single shear plane develops (**2**). At even higher confining pressures, a network of inclined shears develops (**3**) (http://homepage.usask.ca/~mjr347/prog/geoe118/geoe118.035.html).

The change in behaviour is called the *brittle-to-ductile transition*. For most rocks it occurs at temperatures and pressures outside the normal range of engineering. However, some shales, fine grained limestones (chalk) and most evaporites (rocksalt, potash, gypsum etc) show ductile behaviour in near-surface, low-temperature environments. In a conventional strength test, the axial stress on a rock core is gradually increased until the rock fails. Rocks will also deform under *constant stress* by a process called *creep*. Creep is time dependent deformation under constant stress.

Structures may be conveniently subdivided into two groups:

- *brittle structures* - recording the brittle-elastic failure of rocks in the past. Faults and joints fall in this broad category.

- *ductile structures* - preserving the permanent viscoplastic deformation of rock throughout geologic time. Some folds and metamorphic foliations are the expression of this type of structure.

The aim of mechanical models is to test different deformation paths to decide which one is compatible with both geological description and mechanical characteristics.

1.2.2. Numerical methods of modeling rock masses, FEM (finite element method)

Rock masses are discontinuous, anisotropic and inhomogeneous. Difficulties arise in numerical modeling due to such complex and non-homogeneous geological conditions of rock mass. The complex combination of its constituents and its long history of formation make rock masses a difficult material for mathematical representation via numerical modeling.

Rock mass can be generally classified into three groups, i.e., (a) continuous, (b) discontinuous and (c) pseudo continuous groups. Type (a) refers to intact rock mass, type (b) represents jointed rock mass and type (c) is for highly fractured or weathered rock mass. The behaviour of type (a) rock mass can be analysed by means of model based on continuum mechanics, while a discontinuous model such as those proposed by Cundall (1971) may be used for analyzing the type (b) rock mass where joint elements in the finite element analysis are also useful. Discontinuous model similar to that of type (b) can be used for type (c) rock mass. However, it is almost impossible to explore all the joint systems and it seems that this type of rock mass behaves just like a continuous body in a global sense. Therefore, a continuum mechanics model can be used with the effect of discontinuities adequately considered in the model. This is achieved by homogenization technique where equivalent continuum properties of the rock mass is derived based on the geometry of the contained fracture systems and physical properties of the intact rock matrix and the fractures.

A number of numerical techniques have been applied to problems in rock mechanics (e.g. finite element, finite difference and boundary integral methods). Finite element is the most widely employed numerical method for the rock mechanics and rock engineering.

- Finite element method (FEM)

The formulation of FEM is based on variational statement of the governing physics. FEM analysis includes three main steps: domain discretisation, local approximation and assemblage and solution of global matrix equation. This method involves the representation of a continuum as an assembly of elements which are connected at discrete points called *nodes*. The problem domain is divided into discrete elements of various shapes, e.g. triangles and quadrilaterals in two-dimension cases and tetrahedrons and bricks in three dimensions. Continuum problem is analyzed in terms of sets of nodal forces and displacements for the problem domain. The displacement components within the finite elements are expressed in terms of nodal displacements. Derivation of these displacements describes strain in the element. The constitutive law that represent the behaviour of the simulated medium is used together with this strain to determine stress in the element. Disadvantage of this method is that considerable time is required in preparing input data for a typical problem. This is particularly crucial in 3D problems and has led to the development of sophisticated mesh generation programs which eliminate much of the tedium involved in data preparation (Sheppard, 1988). FEM is computationally expensive and a large number of simultaneous equations must be solved to obtain a solution. If the problem is non-linear, the computation time increases enormously because the sets of simultaneous equations must be solved a number of times. In practice, a finite element analysis usually consists of three principal steps:

1. *Preprocessing:* The user constructs a *model* of the domain to be analyzed in which the geometry is divided into a number of discrete subregions, or "elements," connected at discrete points (nodes). Certain of these nodes will have fixed displacements, and others will have prescribed loads. Some of preprocessors can overlay a mesh on a preexisting CAD file, so that finite element analysis can be done conveniently as part of the computerized drafting-and-design process.
2. *Analysis*: The dataset prepared by the preprocessor is used as input to the finite element code itself, which constructs and solves a system of linear or nonlinear algebraic equations

$$\mathbf{K}_{ij}\mathbf{u}_j = \mathbf{f}_i$$

where **u** and **f** are the displacements and externally applied forces at the nodal points. The formation of the **K** matrix is dependent on the type of problem to be solved. Commercial codes may have very large element libraries, with elements appropriate to a wide range of problem types. One of FEA's principal advantages is that many problem types can be addressed with the same code, merely by specifying the appropriate element types from the library.

3. *Postprocessing:* In the earlier days of finite element analysis, it was not so easy for the user to manipulate the numbers generated by the code, listing displacements and stresses at discrete positions within the model. It is easy to miss important trends and hot spots this way, and modern codes use graphical displays to assist in visualizing the results. A typical postprocessor display overlays colored contours representing stress levels on the model.

1.2.3. Some applications in fracture study

- Preferential activation of pre-existing planes of weakness

Formation or activation of the fractures is generally controlled by the state of applied stress. The relation between stress and strain, first, introduced by laboratory compressional test and then by theoretical model of Mohr-Coulomb. Based on these theoretical and experimental models, the critical orientation of the faults in an isotropic and homogeneous medium under compression may be predicted. Even activation of pre-existing weak planes of discontinuities could be examined (Sassi et al, 1993). These relations could be used in the nature to construct the stress or strain tensors based on Anderson's theory (1951) or proposed models of inversion (e.g., Carey et Brunier, 1974; Angelier, 1990).

The hypothesis of an isotropic and homogenous material may largely fail if the planes of discontinuities pre-exist in the studied material. It is almost the case of sedimentary rocks in which different fracture sets recorded numerous successive deformation phases and related stress field in their geological history. Unlike newly-formed fractures, these inherited fracture planes have orientations which are not governed by the stress state. Therefore, it is necessary to take into account their geometrical parameters to define their activation threshold in a stress field. This idea is the base on the works of Wallace (1951) and Bott (1959) and can simply be stated by definition of a criteria like Mohr-Coulomb for the resolved normal and shear stresses on the inherited fracture planes. These inherited fracture planes have generally a

mechanical resistance lower than the rocks in which they exist, so they may be activated before the formation of any new fracture, even though they have not optimal orientation relative to the principal stress directions. However, the preferential direction of pre-existing fractures could be sufficient to accommodate applied state of deformation. It means that their presence may inhibit the formation of new fractures. Folding and relative chronology and hierarchical reactivations of inherited fractures, with the application of the plasticity model, presented in Leroy and Sassi (2000), are the main objectives of this chapter. This model provide a simple description of the contribution of planar defects, such as frictional cracks, to the macro-scale irreversible deformation (Guiton, 2002). The details of the numerical algorithms for the elasto-plasticity constitutive relations are found in Guiton et al. (2003). The application of this elasto-plastic model for rock fracturing does not permit us to take into account some complex micro-mechanisms like fracture branching (Kachanov, 1982b; Horii and Nemat-Nasser, 1986; Gambarotta and Lagomarsino, 1993). However, the great advantage of this model is to explain simply and using a number of reduced parameters, the principal mechanisms of fracturing at sedimentary bed scale.

- A mechanical model for pervasively fractured rock and folding

Defining the chronological events of different fracturing episodes is one of the most important and difficult task in a typical fracture study. It is strongly related to evolution in time of the stress field which controls the activation of the discontinuities. In a simple scenario and using the Mohr diagram construction, one may start with some prevailing stress state and evaluate the critical stress state for slip along a given orientation (Wallace, 1951; Bott, 1959; Mandl, 1988). On the other hand, fault-slip data are often used to reconstruct the complete or reduced stress tensor (Carey and Brunier, 1974; Angelier, 1990; Etchecopar and Mattauer, 1988). From the kinematic point of view, a complete data set on fractures (orientation, length, spacing and offsets) is needed to reconstruct the large scale deformation, assuming slip, once the critical stress conditions are met (Reches, 1983; Gauthier and Angelier, 1985). However, because of non-linear response of the rock mass and geometrical effects due to finite rotation during folding (Guiton, 2001), the evolution of the stress tensor beyond first slip is often complex. The proposed mechanical model in the case of the Asmari anticline accounts, in a simple manner, for the presence of inherited fracture sets and the genesis of syn-folding fractures.

1.3. Description of the model and mechanical parameters

Detailed theoretical background of this direct modelling can be found in Guiton et al. (2003) and will not be recalled here. The elastoplasticity model is motivated by comparing the incremental stress-strain response with the macro stress-strain relation based on linear elastic fracture mechanics, for a representative volume element (RVE). RVE described a rock mass which is pervasively transgressed by inherited planar defects (Fig.8a). In this model, RVE correspond to a zone represented by each individual integration point (nod). Each plane contains frictional, penny-shaped cracks (Fig.8b). These inherited discontinuities could be for example, vertical joints or horizontal surfaces marking the separation of two rock sequences. During deformation of the rock mass, every discontinuity, defined by its normal **n** whose orientation is defined by two Euler angles (θ_1: the angle between the normal **n** and the vertical axis, and θ_2: the angle between the projection of **n** in the horizontal plane and the *x* direction) (Fig.8c), responds to the mechanical loading independently in form of either a perfect stick (no activation) or a discontinuity (jump) in displacement (sliding or opening modes). The parameters of the Mohr-Coulomb criterion used to detect the sliding and opening along a given planar surface are: the friction coefficient (μ), the cohesion (c_{s0}), and the tensile strength (c_{o0}) (Fig.8d). The mechanical response of every crack is independent of neighbouring patches, requiring their density to be small or their distribution to be random (Kachanov, 1992, Guiton, 2003). In this case, the exact solution of a penny-shaped crack in an infinite medium can be considered to relate jumps in displacement at the patch-scale to the remote macro-stress (Fig.8e). The number of potential syn-folding set of orientation of fractures is 307 sets (10° step in dip and dip azimuth). If any inherited set is considered , its orientation is chosen in the place of one of these 307 sets.

The permanent macro-deformation is constructed from the contribution of independent orientations of fracture planes [Leroy and Sassi, 2000]. The elastic properties of the RVE are the same as the ones of the matrix and the deformation resulting from the cracks activation is reproduced by the irreversible or permanent deformation. Two yield criteria are proposed to check the activation of a given orientation:

$$\begin{aligned} \phi_s(\boldsymbol{\sigma}, \mathbf{n}, \gamma) &\equiv \tau + \mu\sigma_n - (c_{s0} + c_{s1}\gamma) \leq 0 \\ \phi_o(\boldsymbol{\sigma}, \mathbf{n}, d) &\equiv \sigma_n - (c_{o0} + c_{o1}d) \leq 0, \end{aligned} \qquad (5)$$

corresponding to the sliding and the opening mode, respectively. In equation (5), the scalars c_{S0}, c_{O0}, c_{S1}, c_{O1}, γ, and d are the cohesion, the tensile strength, the hardening moduli in sliding and opening, and two internal variables which mark the accumulated macro-deformation in sliding and opening, respectively. The cohesion and the tensile strength are defined in Fig.8d

and could be estimated in laboratory tests. The other four parameters could be given by physical interpretation in terms of the crack density of the elastic solid defined above (Guiton et al., 2003). Low hardening moduli (c_{s1} and c_{o1}) are considered for weak inherited directions (large fracture densities) and large moduli for new directions (low density of pre-existing flaws).

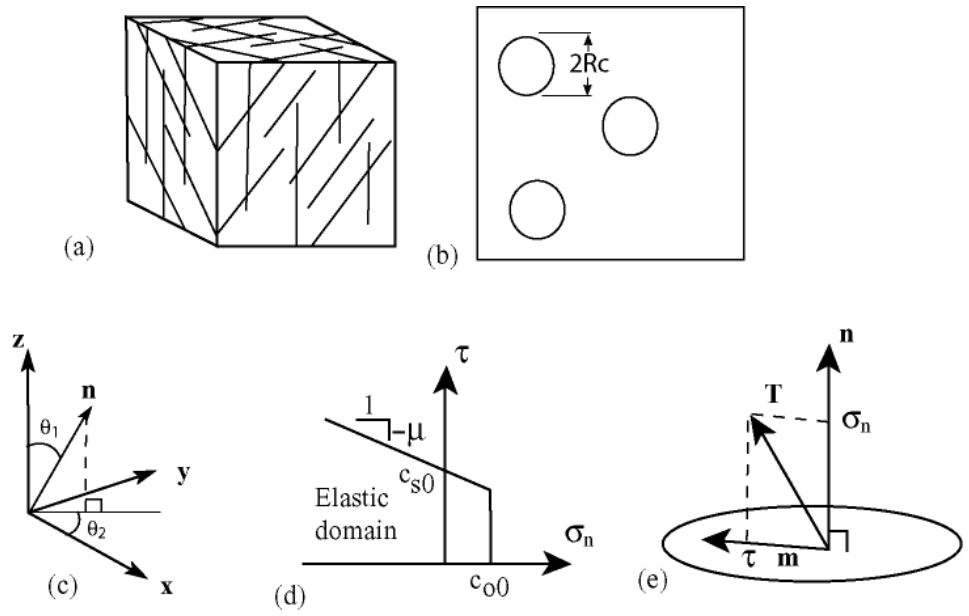

Fig.8: The micro mechanism motivating the constitutive model (Guiton et al., 2003). (a) The representative volume element (RVE) is pervasively transgressed by inherited planar discontinuities. (b) Penny-shaped patches on a given plane with same radius Rc are considered as cracks accommodating sliding and opening. (c) A set of parallel fractures with normal **n** is defined by the two Euler angles θ1 and θ2. (d) The truncated Mohr-Coulomb criterion used to detect the sliding and opening along a given planar surface; μ, c_{S0} and c_{O0} are the friction coefficient, the cohesion, and the tensile strength, respectively. (e) The components of the stress vector T applied on a patch of normal **n**.

2. Modelling of the Asmari anticline

2.1. 3D geometrical model

The 2D geometry of the Asmari anticline was retrieved from constructed regional transect (e.g. Sherkati et al., 2004, LOCACE transect) and a few seismic lines next to this anticline. The main retrieved structural elements from surface (geological map, Fig.9a) and subsurface data (transect, Fig.9b) to construct a 3D geometry include structural surface, and an associated forelimb thrust (Fig.9c & 10).

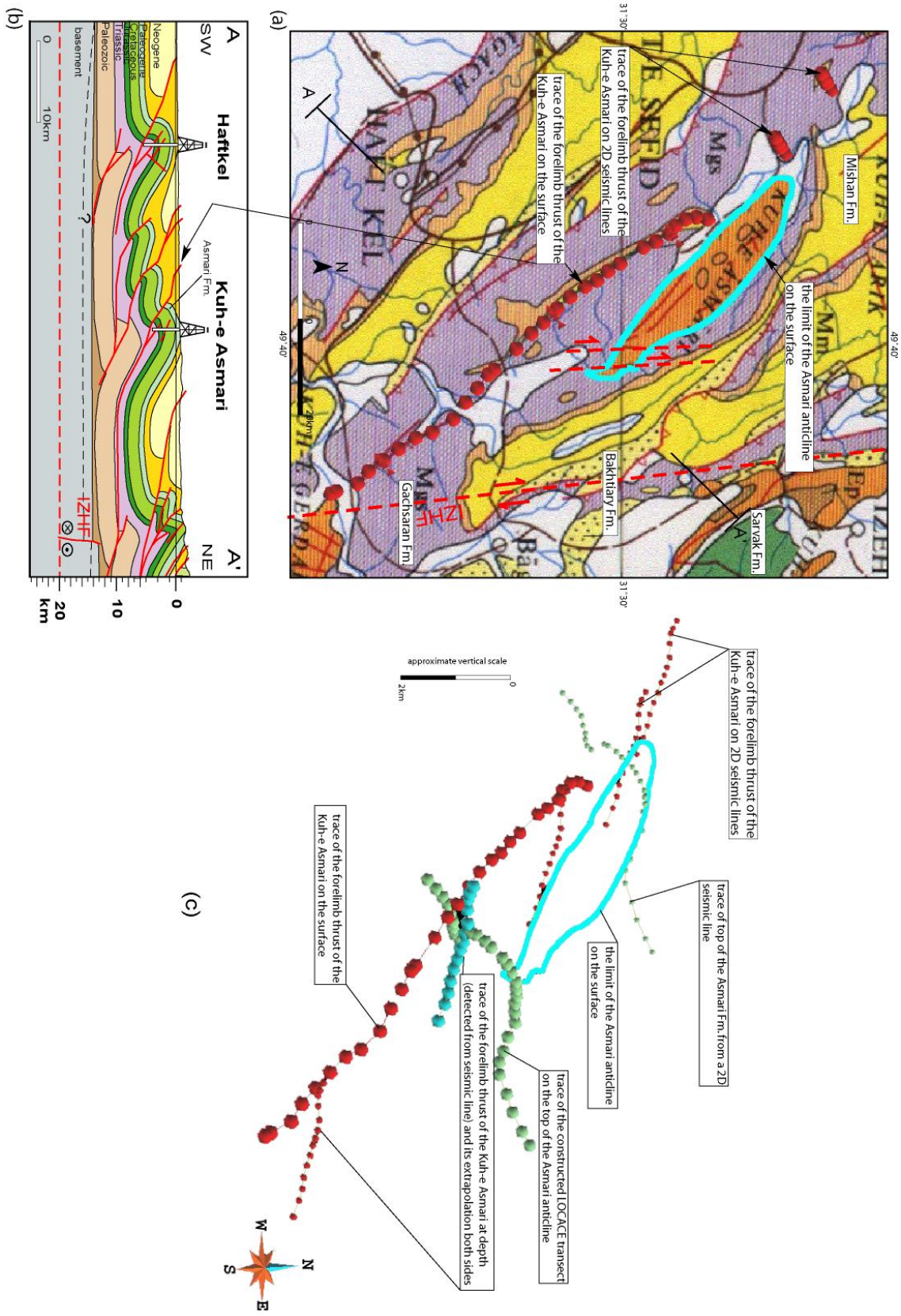

Fig.9: The main geometrical elements used to construct the initial 3D geometrical model of the Asmari anticline, (a) the trace of a forelimb thrust and the limit of the anticline on the surface is seen on the geological map (an x-y plane), (b) the positions of these elements in depths (an y-z plane) could be retrieved from the transect, (c) the 3D positions of retrieved data from geological map and transect.

From a folding mechanism point of view, regional deformation occurred by decoupling of whole sedimentary series from the basal detachment level (Hormuz salt or Lower Palaeozoic shales?) and triggering of main forelimb thrust at this stage (Mio-Pliocene?). Then, progressively, following the propagation of thrust ramp and flat within overlaying strata, the initial, high wave-length, detachment fold evolved into a fault propagation fold or faulted detachment fold. In a certain stage of this evolution, intermediate detachment levels (e.g. Triassic evaporite series, and/or Kazhdumi, Gurpi-Pabdeh argillaceous series) were activated and involved in deformation and secondary short wave length folds developed (Sherkati et al., 2005). The multiple thrusts seen in the cross-section of the Asmari anticline (Fig.9b) are the result of this folding evolution achieved by internal transformation of the main detachment fold into a sequential series of faulted detachment folds from the base towards the top of sedimentary series. In addition to cover shortening, accommodated by early stage layer-parallel shortening and then by fold and thrust propagation, N-S trending dextral strike-slip faults (parallel to IZHF basement fault) accommodated part of shortening in the south-eastern part of this anticline. This can explain the narrow shape geometry, high curvature value (Fig.11) and N-S trending fault pattern (see Fig.V.4 chapter V) in the densely fractured south-eastern termination of the Asmari anticline (Fig.9a).

A great part of the Asmari anticline is located under ground level and the part which crops out at the surface is actually the crest of the fold (Fig.9b). As shown in Fig.10, the geometry of this fold is rather complex. Engagement of intermediate detachment levels (e.g. Triassic Dashtak evaporite and possibly Pabdeh and Gurpi marly formations) affected fold geometry by triggering thrust development and propagation within different sedimentary series, below, inside and in the upper part of the Asmari Formation through younger sedimentary series (Gachsaran and Agha-Jari formations). Development of this forelimb thrust suggests that limb rotation was mostly active during the final stage of folding. The continuation of this forelimb thrust towards the NW termination of the fold, cross-cut a local back-thrust which likely controls the geometry of a small anticline near the NW termination of the Asmari anticline (Fig.10). Fracture data were collected on the structural positions which lay on the upper part of the fold where the fold geometry is rather simple. To reduce geometrical uncertainties and complex fold shape caused by thrust propagation in the forelimb, we focused on the part of the fold displaying the simplest geometry, located at the top of structure and around fracture measurement sites. The portion of the fold whose evolution is modelled is therefore the part in which fracture constraints are available.

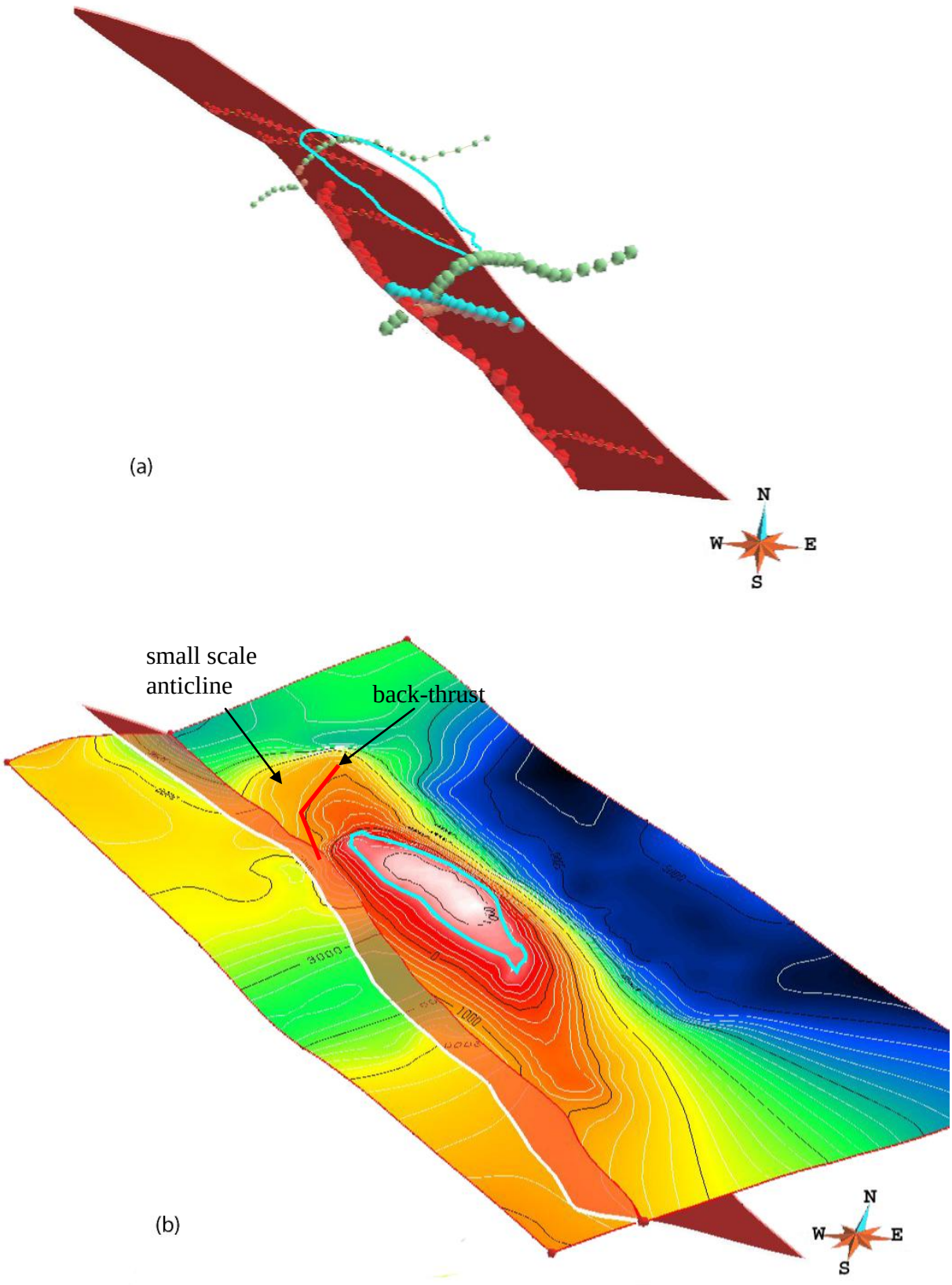

Fig.10: Construction of the main geometrical surfaces, forelimb thrust (a) and structural surface (b) of the Asmari anticline by the extrapolation of traced lines (Fig.8) (picked from the map and transect) in a geomodeler (e.g. Gocad); topographic contour interval is 200m.

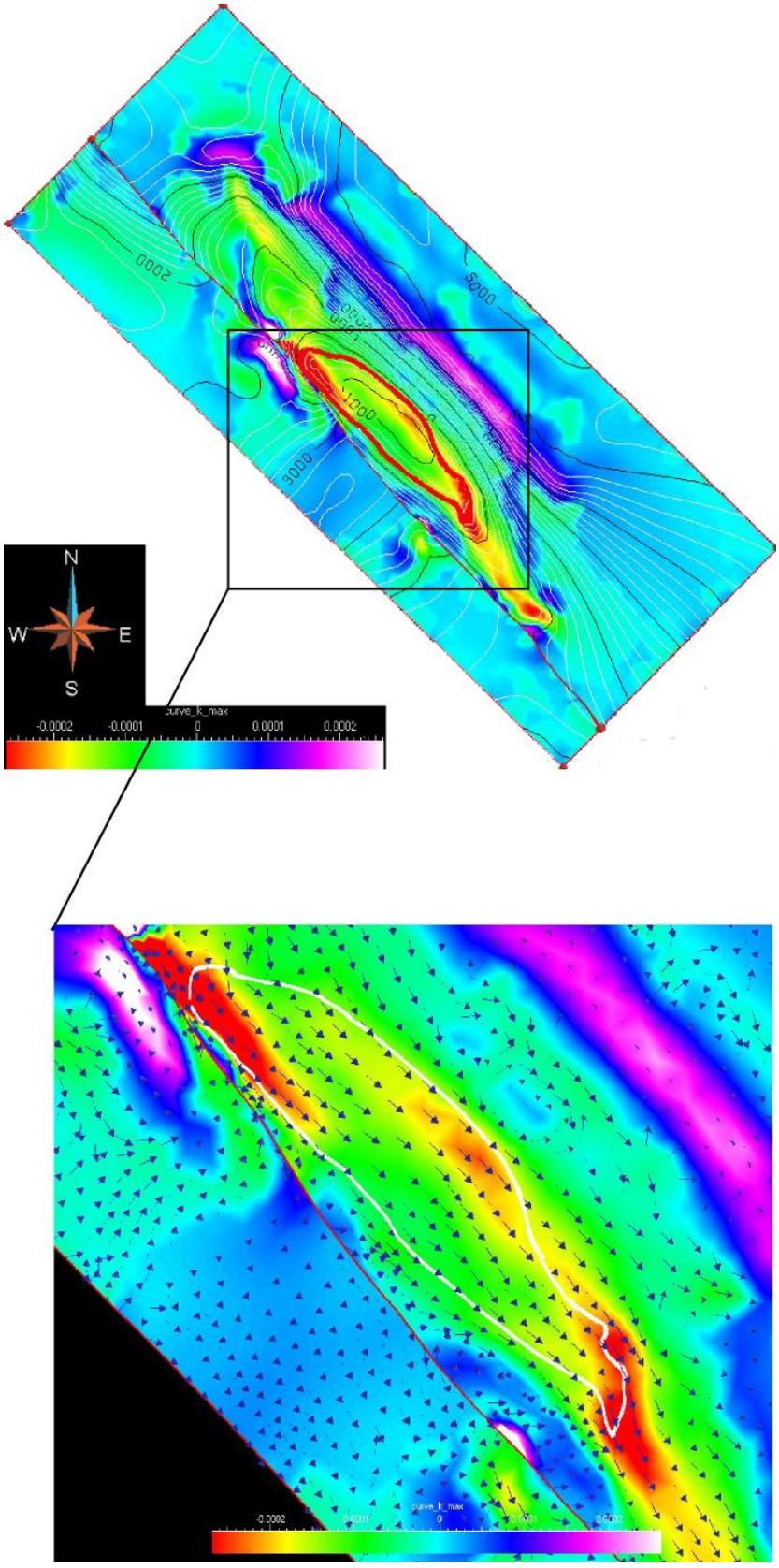

Fig.11: Curvature analysis on the 3D geometrical surface of the Asmari anticline. Only one group of fractures (extrados) may be predicted by this analysis. Structural terminations show the high range of curvature values as both structural dip and trend are changed in these positions. The arrows show the direction of predicted fractures.

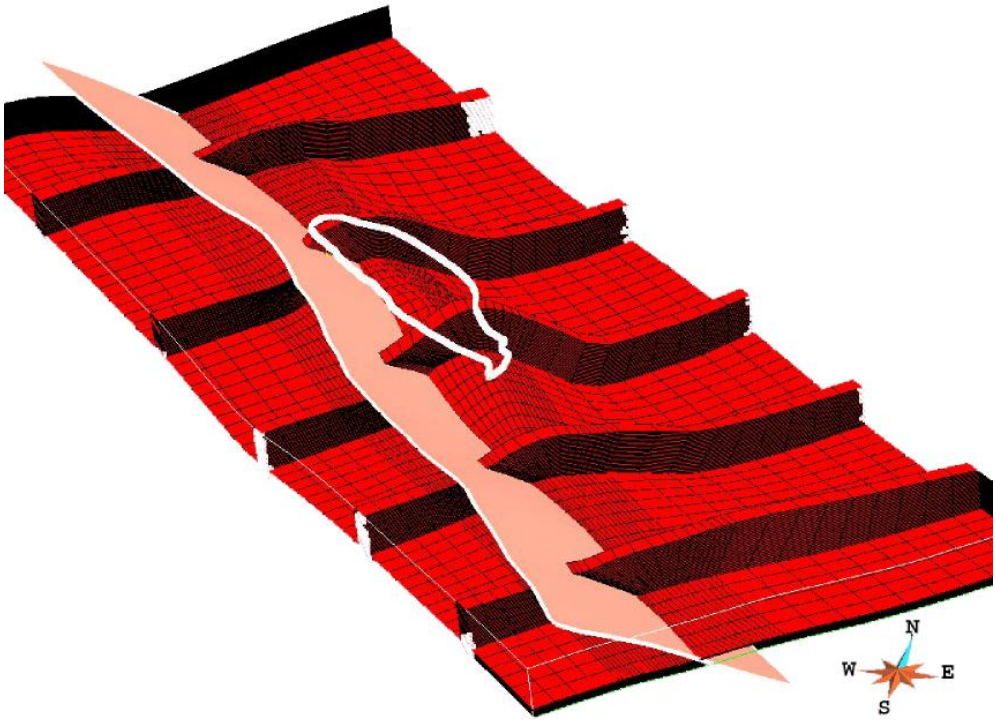

Fig.12: Constructed grid on the 3D geometrical surface of the Asmari anticline in Gocad.

To reduce such a complexity in the Asmari fold geometry, the following simplification and assumptions were applied to the numerical model of the Asmari anticline: (1) An interval between top of the Asmari Formation down to the top of Triassic series has been considered as a single mechanical unit (with about 3km thickness) because the Triassic evaporite in the Dezful Embayment is considered as one of the main intermediate detachment levels, (2) only one single thrust at the level of Triassic evaporite has been taken into account.

The construction of the surfaces from the extrapolation of traced lines (picked either from the map or transect) were done in a geomodeler (Gocad) (Fig.10). The structural and geometrical interpretation of the surface and/or subsurface initial data sets (geological map, transect, seismic lines) are important as any unsuitable interpretation may severely affect the result of the geometrical restoration.

In quantitative structural geology, a curvature analysis is often used to infer the density and location of fractures in the structure in which we assumed that areas of high value of calculated curvature underwent more intensive deformation. This analysis was introduced by many authors as a tool to predict the potential fractures zone in a fold (see Aguilera, 2000 for more details). However, in this analysis, only those fractures which are parallel to the axial trends (outer rim extension) may be predicted and neither heritage nor shear fracturing could be deduced from this analysis. Furthermore, in the case of a pre-fractured

structure the results of curvature analysis may not be applicable and some tests of curvature analysis applied to some of the Asmari reservoirs confirm this point (Motiei, 1995). Fig.11 shows an example of curvature analysis performed on the constructed surface of the Asmari anticline. As shown in this figure, the structural terminations of the fold present high values of curvature as both structural dip and trend are usually changed in these structural positions. The analysis of aerial photos and field data shows that the SE termination of the Asmari anticline has been highly fractured and affected by the faults. The result of curvature analysis predicts only axial fractures whereas mechanical modelling may predict which fracture family was more reactivated at this structural position. Based on the field observation different fracture sets are observed in this structural position and among them N-S fracture set is remarkably developed, see chapter V- Asmari anticline for more details.

Finally, an appropriate grid (Fig.12) was constructed on this initial geometry to be ready for the next steps which include the finite element analysis for 3D geometrical restoration and mechanical modelling.

2.2. 3D restoration

The main goal at this step is to compute a geologically plausible initial state with boundary displacements for the FEM simulations. The restoration of the Asmari anticline was performed by removing the main thrust displacement (throw) and unfolding the hangingwall and footwall blocks of the main thrust (Fig.13). We supposed that whole the sedimentary series (Oligo-Miocene Asmari Formation down to Triassic detachment level), were deformed entirely as coupled units. Furthermore, decompaction phenomenon was not taken into account and we suppose that at the start of the folding, the layers have been already compacted.

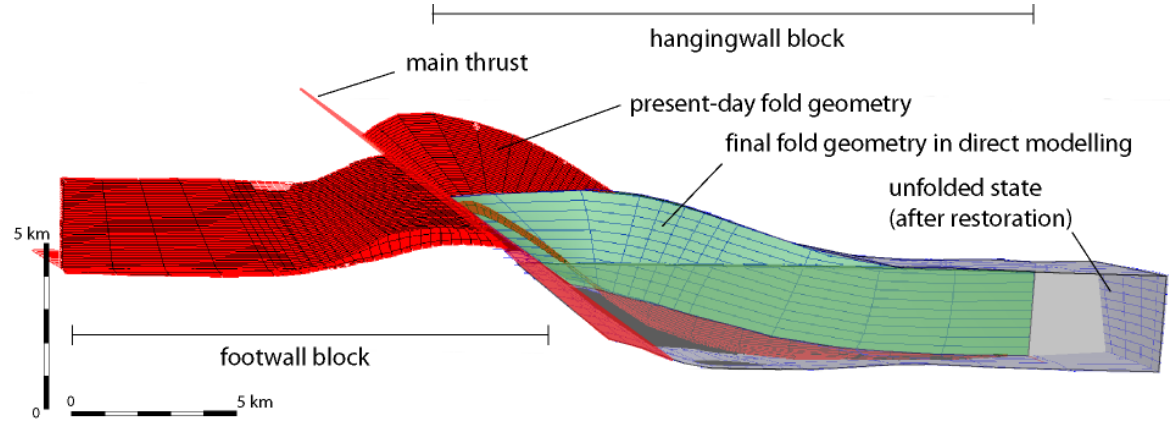

Fig.13: Cross-section shows present-day geometry (red colour), unfolded state (grey colour) after restoration of the hangingwall block, and the final geometry (green colour) obtained by direct mechanical modelling. The reduction of the fold amplitude in direct modelling is presumably due to the loss of convergence in the iterative algorithm for equilibrium search.

2.3. Mechanical modelling of different fracture families in the Asmari anticline

2.3.1. Fracture orientations and chronology in the Asmari anticline (reminder of field observations)

Fracture orientations were measured through 13 sites in the southern flank, crest, north-eastern flank, and south-western plunge of the Asmari anticline (Fig.14). These fractures are normal to sub-normal to bedding planes. The main fracture families in this anticline may be divided into three major and two minor sets: (i) fracture set with N40°±10° trend, (ii) fracture set with N140° ±10° trend, (iii) fracture set with N20°±10°. The minor groups include N-S and E-W trends. Local bedding azimuth in the SW flank, where the maximum measurement sites were located, varied between N120°-N150°. Fig.15 shows the main fracture sets on the southern plunge of this anticline and on the top of the structural surface of the Asmari Formation. Structural dip is quite gentle and near horizontal at this structural position. The first fracture set which is seen in regular pattern like systematic joints (mode I) and without any directional perturbation, shows an azimuth about 50° which is almost perpendicular to the fold axis. The second fracture group is less regular than the first set. This set is almost parallel with the local fold axis and is seen in form of high intensity fracture corridors with persistent continuation. Their cross-cutting relationship with the first set indicate that they likely developed after the first systematic joints. The third and fourth fracture sets consist of N-S and N20°-30° fracture azimuths. The continuation of these sets is less than the two others since they mostly terminated upon (and therefore are restricted by) the two previous fracture families. Some N-S fractures seem to have branched from the second set (≈N130°) in form of dextral shearing (unclear), horsetail fractures. A group of observed N-S trending fracture system on the NE limb of this anticline is thought to be in direct relation with adjacent fault and may be considered as fault related fractures.

N50° systematic joint set is considered as the earliest, pre-folding fracture family. The second one, as was discussed and argued via the Asmari basin facies changes (chapter VII) is thought to have formed initially in the cover above forced-folds and reactivated basement faults. Then, they reactivated during Miocene-Pliocene folding phase of the cover. As the trend of this set is more or less parallel with the general trend of the Asmari anticline, it was easily reopened and intensified especially on the crest of the fold.

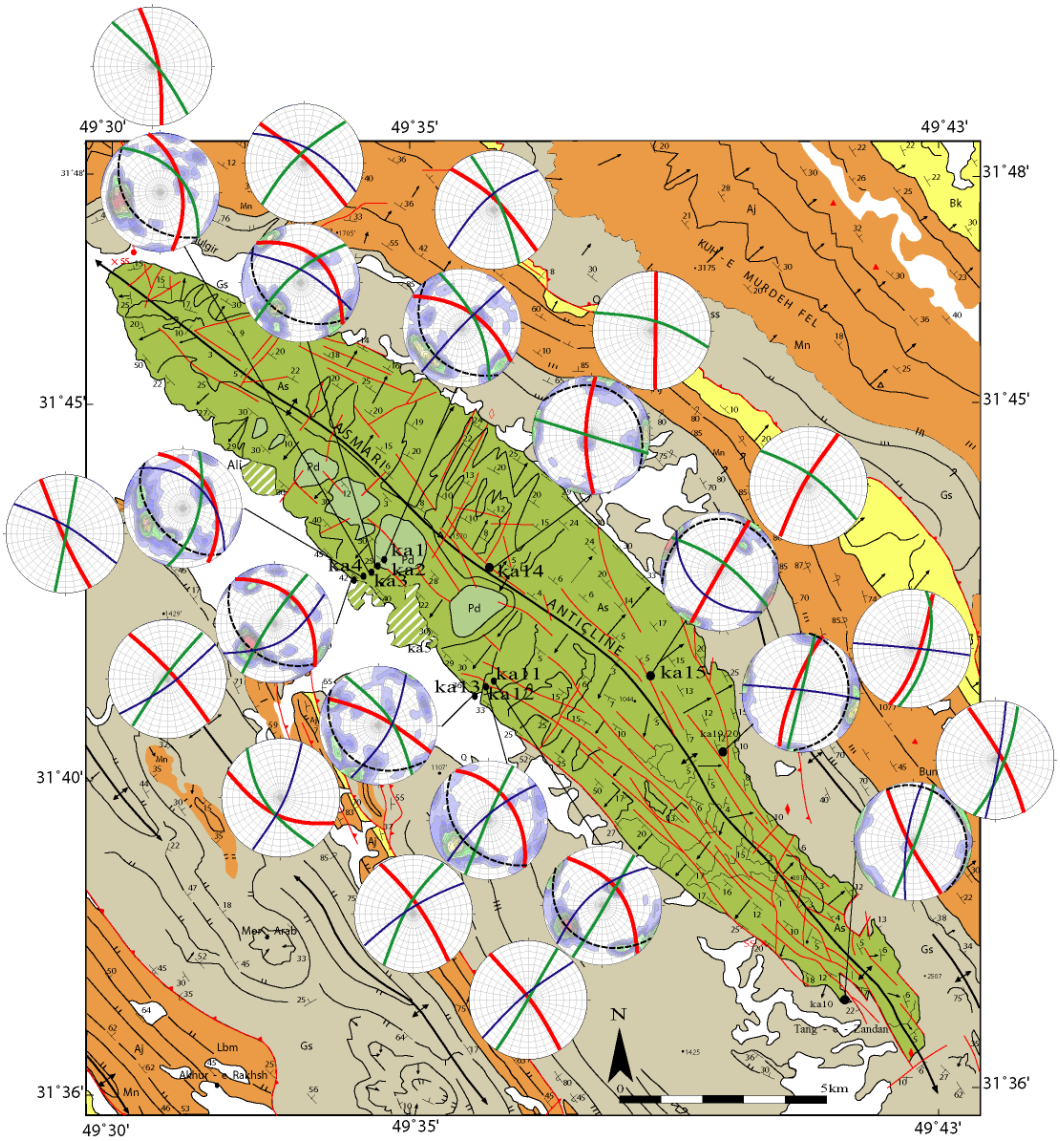

Fig.14: Geological map of the Kuh-e Asmari anticline, fracture measurement sites and fracture diagrams. for more details see chapter V, Asmari anticline section. Green, grey, orange, and yellow colours are the Asmari (Oligo-Miocene), Gachsaran (L.Miocene), Mishan-Agha-Jari (M.-U. Miocene), and Bakhtiary (Pliocene) formations respectively. Schmidt projection of fracture data on lower hemisphere, first, second and third prominent fracture sets are shown by red, green and blue colour semi-circles, respectively, on measured (with density diagram at the background) and unfolded state; dashed semi-circles are bedding planes.

2.3.2. The parameters of the model

The initial plate geometry consists of restorated (unfolded) geometry of the Asmari anticline having almost a square top surface (34 × 86 km) and a thickness *h* of 3 km (Fig.12). It should be mentioned that the elements which were used in this model are hexahedral (with 27 nodes, quadratic) because linear elements take the connection of the deformation gradient in the presence of finite rotation (Guiton et al., 2003). Each cell (element) in our model comprises of 27 nodes which means that RVE = cell size /27 ≈20 m^3 in this model. The plate top surface is at a depth of 2 km and we assume a volumetric mass of 2200 kg/m^3 everywhere.

The vertical principal stress, σv, is calculated from the lithospheric gradient and associated to lithostatic pressure along the inward normal of the top surface. Instead of horizontal forces, the amounts of displacement calculated in restoration (forward modelling) were introduced into the model. To differentiate between new and inherited fractures, the former are assumed to have larger cohesion, tensile strength and hardening moduli. The other parameters used in the simulations are found in Table 1.

Mechanical parameters	new set	inherited set
friction coefficient	0.6	0.2
sliding initial cohesion	20 MPa	10 MPa
sliding work-hardening parameter	10 MPa	1 MPa
opening initial cohesion	5 MPa	0 MPa
opening work-hardening parameter	10 MPa	1 MPa
Elasticity modulus, *E*	1 GPa	1 GPa
Poisson's ratio, ν	0.2	0.2

Table 1: Mechanical parameters used in the simulations without and with the inherited fracture set(s).

For all sets, plastic deformation rate was computed according to a linear overstress viscous model with a viscosity (η) constant and equal to 10^{17} Pa.s, taking into account an estimation of deformation rate (v) about 10^{-8} mm/sec (see Masson et al., 2005) for the Asmari anticline.

2.3.3. Interpretation of the results

Several simulations were performed in this approach. Among them, four simulation are documented here in more detail. One of the simulation was performed for the case in which no inherited fractures was introduced into the model and the others are differentiated by the orientation of the inherited fractures. The results of these simulations are summarized below:

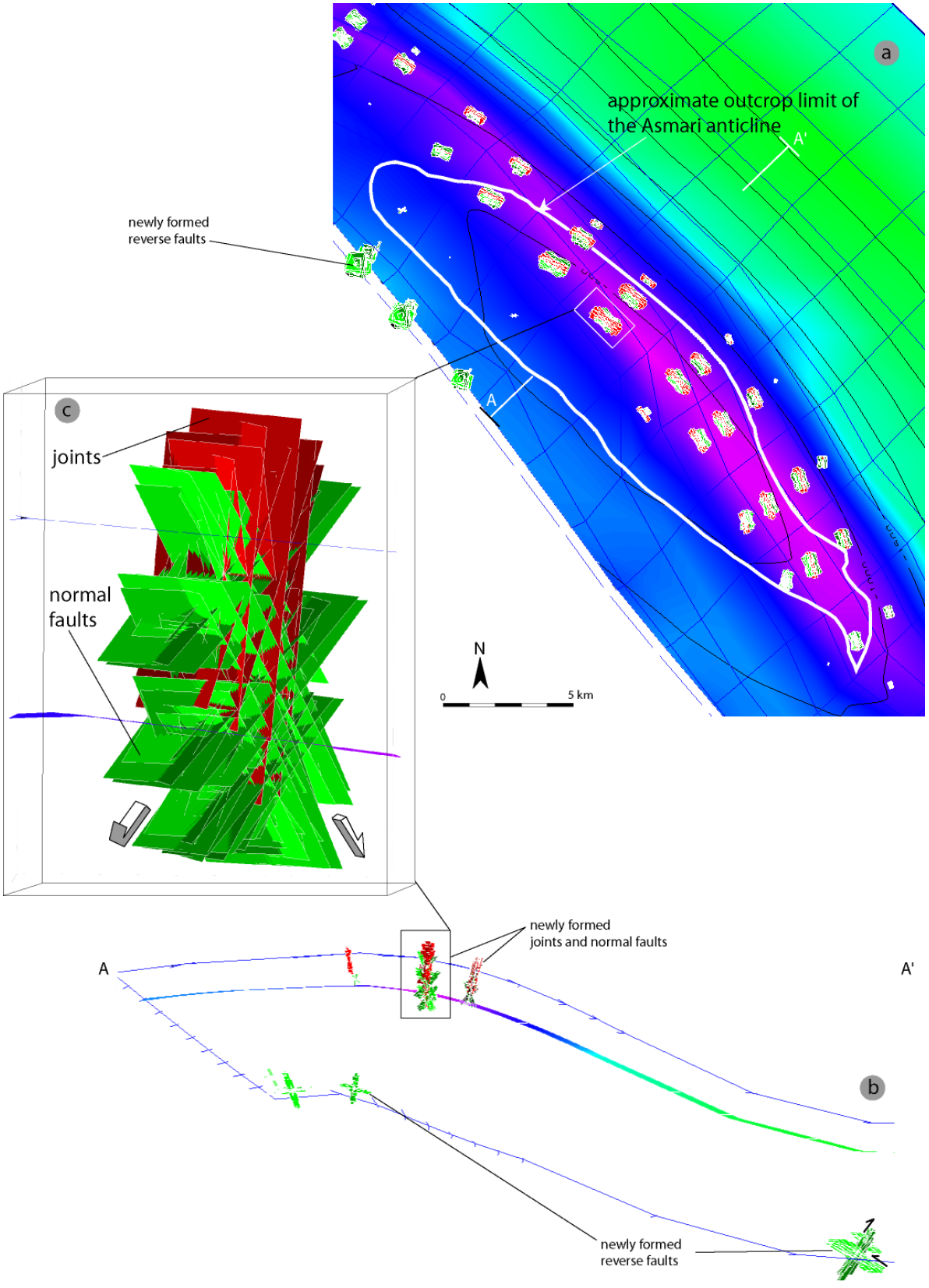

Fig.15: The result of the simulation without any inherited fracture set. (a) a map view on top of the structure with newly formed joints (red colour) and faults (green colour), (b) a cross-section view of the structure shows reverse faults at the base and normal faults and joints developed at the crest of the structure, (c) a zoom on the fractures at the crest.

- newly formed fracturing episode (no inherited fracture introduced)

In this simulation two main groups of fractures are formed during the evolution of the fold. The first group include reverse faults which develop in the flanks of the fold (Fig.15) following the layer-parallel shortening (LPS) or lately in the intrados (inner rim) of the fold. The second group include opening mode fractures (joints) and normal faults which appear on the crest of the fold and are well-known as extrados (outer rim) type fracture family (Fig.15).

- Simulation with N140° and N50° fracture sets

In this simulation two pre-existing fracture sets were introduced into the model including N140° and N50° fracture sets, i.e., the main fracture sets considered as pre-folding fracture families based on field studies. The final result of this simulation shows (Fig.16) that at the crest of the structure, N140° fracture set was reactivated in opening mode while perturbing the direction of newly formed extrados type joint set at this structural position. In the flanks of the fold this fracture set is reactivated in shearing mode. This reactivation is quite remarkable compared to N50° fracture set. One of the main reason is that N50° fracture set is almost parallel with the main compressional direction. Furthermore and interestingly, despite of this favourable stress direction for opening and propagation of N50° fractures, they never reactivate in opening mode and even their shearing mode reactivation is quite rare and local within the SW flank. A field example of this shearing (sinistral) along N50° fracture set was given before in Bangestan anticline (Fig.V.12). Therefore, like the case of the first simulation without any inherited fractures, other mechanical condition should be introduced into the model to be able to create opening mode systematic joint set parallel to the maximum horizontal compressional stress. This may be achieve by changing boundary conditions (in the case of the Asmari Formation and based on the proposed conceptual model, N50° fracture set was initiated quite early and during the sedimentation of the Asmari Formation) and/or introduced different mechanical rock properties.

Another difference between the result of this simulation and the one without inherited fracture sets, is the absence of reverse faults. It means that, pre-existing fracture sets presumably inhibited the development of newly fractures in form of reverse faults and thrusts in the structural position where dominant local stress is compressive (intrados). A probable reason for this phenomenon will be discussed via the results of the last simulation.

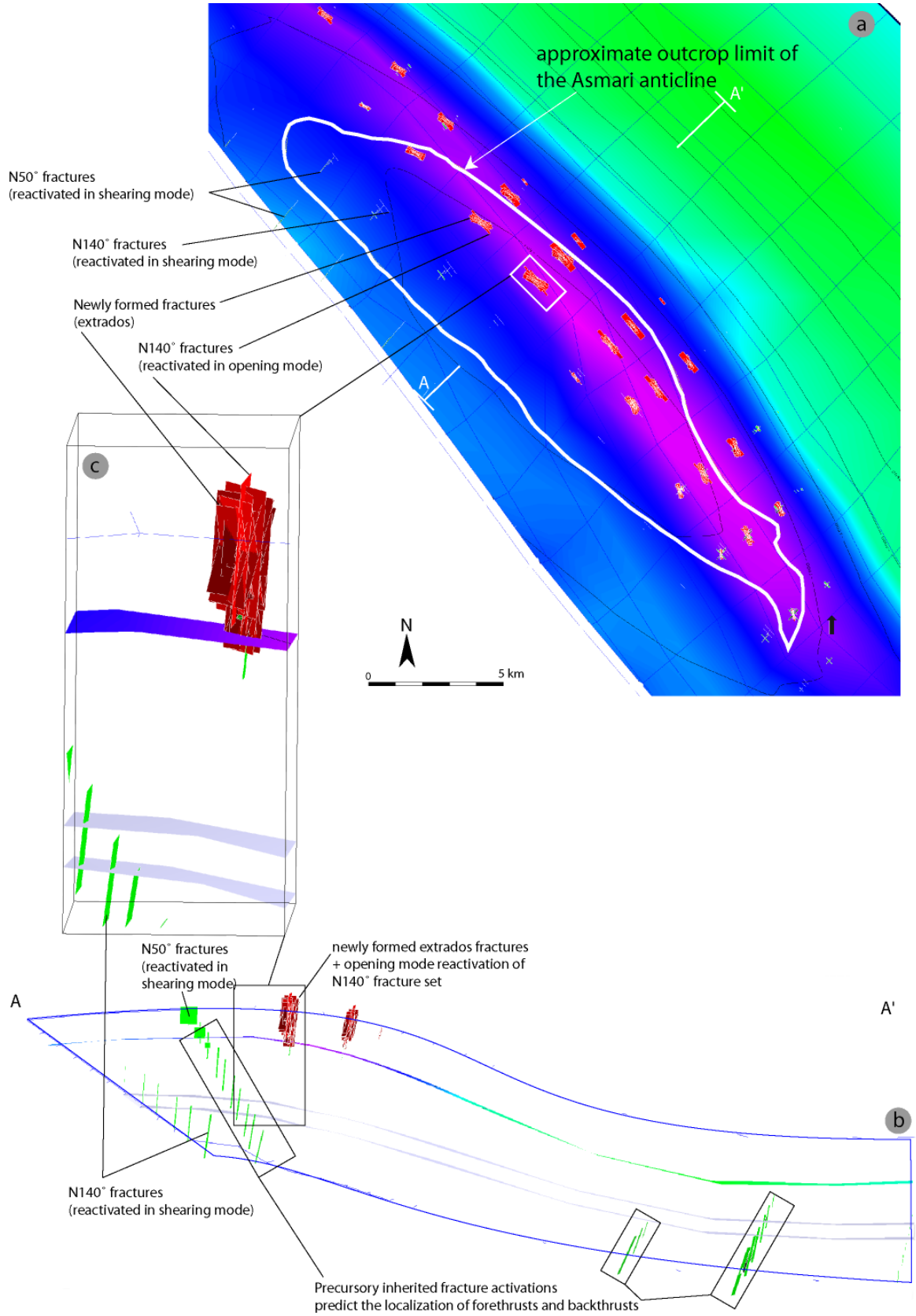

Fig.16: The result of the simulation with two inherited fracture sets (N140° & N50°). (a) a map view on top of the structure with opening mode of newly formed and reactivated (N140°) joint sets (red colour) and reactivation of N140° and N50° fracture sets in shearing mode (green colour), (b) a cross-section view of the structure shows reactivated and newly formed fractures, note that the formation of reverse faults was inhibited by the reactivation of pre-existing joint sets (c) a zoom on the fractures at the crest towards intrados of the structure.

- Simulation with N-S, N140° and N50° fracture sets

In this simulation in addition to the inherited fractures introduced in the previous simulation, a group of N-S striking inherited fractures was added. The reactivation of N140° fracture set is similar to the previous case but N50° fracture set is quite more reactivated especially at the base of the structure. The interesting point in this simulation is the reactivation of N-S striking fracture set which is completely compatible with the direct observation in the outcrop (i.e. the Asmari anticline). The reactivation of this fracture set in both shearing and opening modes around the SE termination of the anticline is noticeable (Fig.17) and is comparable with the dextral shearing fault zone and also prominent joints which were observed and measured in this structural position of the Asmari anticline (Fig.14).

This result confirms that the shortening which was accommodated by N-S (right-lateral) striking fault zone near the SE termination of the Asmari anticline has effectively controlled fracture reactivation in this structural position. Like the previous simulation, newly fracturing episode in form of reverse faults and thrusts in the flanks of the folds was inhibited by the reactivation of these inherited fractures.

- Simulation with N-S, N50° and layer-parallel fracture sets: the effect of flexural-slip mechanism in fracture reactivation

In the simulations discussed above, deformation and fracturing were supposed to have occurred in a thick layer without any heterogeneity and intermediate detachment layer (even internally as a result of the presence of the interbeds of shales within carbonates of the Asmari Formation as is the real case in the field). This is one of the main drawbacks of the model. As discussed in chapter V, an episode of shear fracturing in form of reverse faults and thrusts occurred as new-fracturing in the early stage of the fold development as widely seen especially in the synclines within the Asmari Formation. A beautiful example in this regard is Safid anticline in which duplex structures developed above a few meters of a shale layer within a thick carbonate bed (Fig.V.15). It means that, such an internal small-scale shortening may not happen in the model without introducing inherited planes of weakness parallel to bedding surface. Many examples of parallel-bedding slips, observed within the Asmari anticline, prove that flexural-slip mechanism of folding plays an important role in the internal

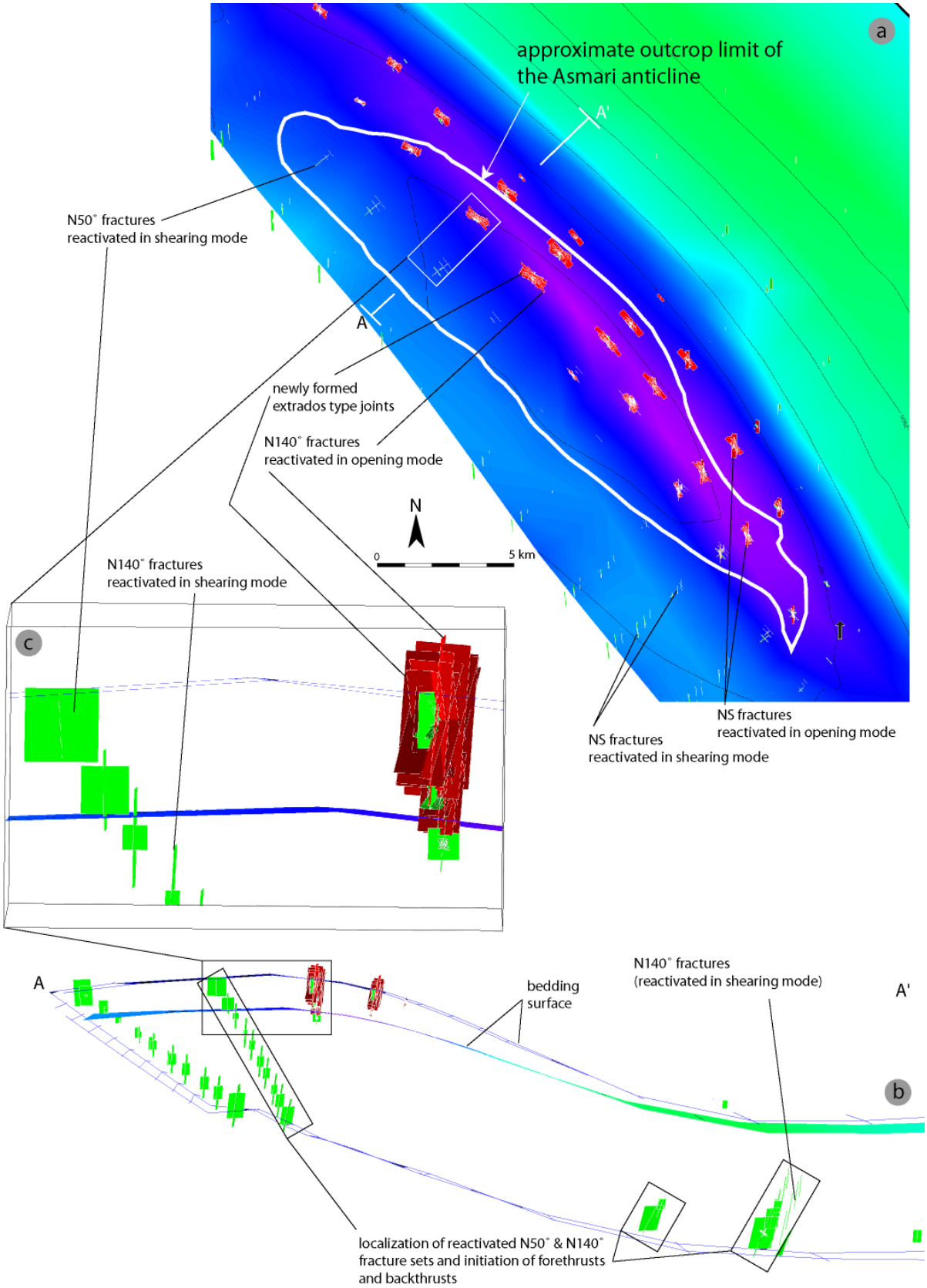

Fig.17: The result of the simulation with three inherited fracture sets (NS, N140°, and N50°). (a) a map view on top of the structure with opening mode of newly formed and reactivated (NS and N140°) fracture sets (red colour) and reactivation of NS, N140° and N50° fracture sets in shearing mode (green colour), (b) a cross-section view of the structure shows reactivated and newly formed fractures, (c) a zoom on the fractures in the upper part of the structure.

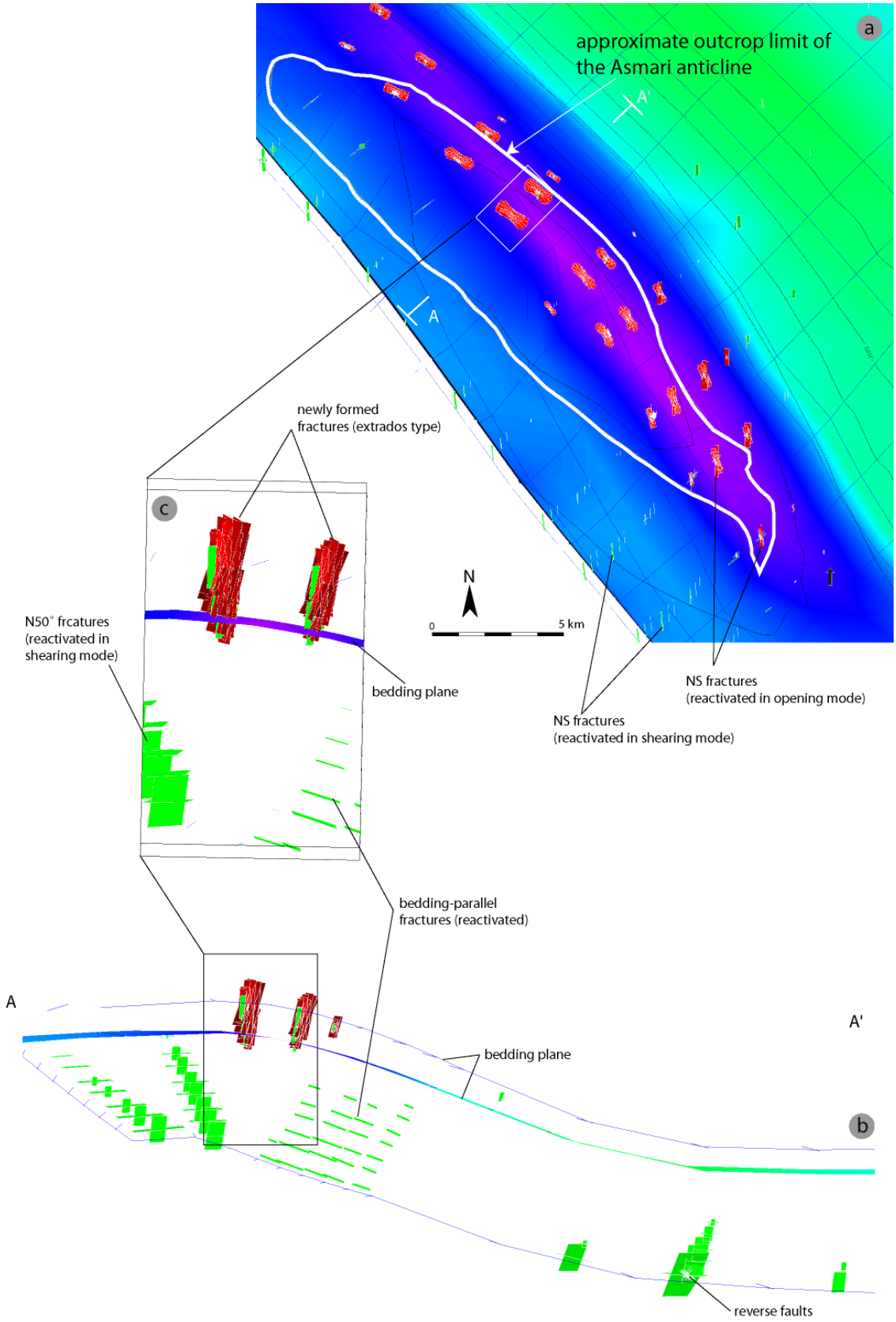

Fig.18: The result of the simulation with three inherited fracture sets (N-S, N50°, and bedding-parallel). (a) a map view on top of the structure with opening mode of newly formed and reactivated (NS) fracture sets (red colour) and reactivation of NS, N50°, and bedding parallel fracture sets in shearing mode (green colour), (b) a cross-section view of the structure shows reactivated and newly formed fractures, note the appearance of reverce faults at the base of the structure following the reactivation of bedding parallel discontinuities, (c) a zoom on the fractures in the from the bottom to the top of the structure.

deformation and shortening within the Zagros folds. Based on field observation in the Central Zagros, structures like thrusts and duplexes within the beds of few centimetres to a few meters are accompanied by underlying and overlying minor shaly layers. These minor detachment levels play an effective role in brittle deformation, leading to parallel-bedding slips and small scale thrust formation.

To take into account somehow this mechanism, the last simulation was done by introducing a bedding-parallel inherited fracture set in addition to two other pre-existing joint sets (e.g. N-S and N50° fracture sets). Again, N-S fracture set was reactivated at the crest and the flanks of the fold especially around the SE termination of the anticline (Fig.18), both in shearing and opening modes like the previous simulation. The N50° joint set, again, was limitedly reactivated in shearing mode in the SW flank and the crest of the structure. The interesting point is the activation of introduced parallel-bedding fracture set in both flanks (and not in the crest) of the fold which confirm the flexural-slip mechanism as internal brittle deformation following the evolution of the fold. As shown in Fig.18b, at the base of the NE flank, new reverse faults and thrusts again limitedly appeared like in the simulation without pre-existing fractures. This result shows that, unlike the other simulation with inherited fracture sets, newly fracturing (i.e. reverse faults) episode is again triggered by the presence of the parallel-bedding weakness in the model, otherwise other inherited fractures inhibit this fracturing episode.

Conclusion

Direct mechanical modelling can be used as an effective tool not only to verify interpretation of fracture data acquired in the field but also to predict the fracturing pattern and genesis for an entire fold structure. However, precise and detailed field works are essential to constrain field data and synthesis in the model and to reduce the uncertainties regarding fracture orientation and chronologies. The results of this step is one of the most important backup for the modelling approach. These results may not be achieved in the case of the Central Zagros folds without a regional scale fracture study. Even if a precise field work and fracture data acquisition would be performed in a single anticline, the result likely could not suggest a reasonable inherited fracturing episodes and to make a link between the regional structural evolution and fracturing style within the Asmari Formation of the Central Zagros folds.

The modelling approach showed that the varieties of different observed fracture groups within the Asmari anticline can not have formed following a deformation and folding of a rock mass without any pre-existing discontinuities. Extrados type fracture set was the only fracture group which formed at the crest of the structure in all the performed simulations. However their directions were perturbed following the introduction of other pre-existing fracture sets in the model. On the other hand, the reactivation of N-S fracture set around the SE termination of the anticline is proved by field observations and measurement in addition to lineament interpretation on aerial images (Fig.V.5). This fracture set reactivated in opening and shearing mode and both reactivation have been predicted by the model. Newly fracturing episode in the model achieved by introducing parallel-bedding fractures in the model as bedding discontinuities, otherwise newly fracturing in form of reverse faults and thrusts may be inhibited by the reactivation of other pre-existing fracture sets which is not the real case in the observed anticlines of the region.

As mentioned before, curvature analysis was previously introduced as a numerical method to predict more intensive fractured zone(s) in a structure. This method usually applied on a surface (a 2D approach). Furthermore, only the intensity of axial fracture set, as a newly fracturing episode, may be predicted by this method and no information about activation of other sets and local stress field may be derived because curvature analysis is just a kind of geometrical attribute analysis. These deficiencies of curvature analysis are effectively improved in mechanical modelling in which entire structure (a 3D approach) could be examined and different fracturing episodes (both newly formed and inherited) and also their modes of activation (opening, shearing) could be predicted by direct mechanical modelling.

The geometry of the folds and the history of their deformation may severely change the activation of pre-existing fracture set(s). This requires to build a precise geometry and evolution history through time of the fold (or reservoir) implementing an acceptable 3D restoration. In the case of subsurface reservoirs, this essential step may achieved more effectively having a high resolution and quality 3D seismic data which can effectively reduce the uncertainties at the first step of mechanical modelling (restoration). Then, the results of simulations can be compared with reservoir dynamic data (e.g. well tests, production data,…) and image logs (e.g. FMS, FMI, UBI, …) instead with direct observation on an outcrop. This is one of the main objectives of the fractured reservoir modelling and this procedure may routinely be used for development of these kind of reservoirs especially in the petroleum province of the Zagros folded belt.

General conclusion and prospective

General conclusion

Fracture patterns in the Asmari carbonates, one of the main reservoirs in SW Iran, their relationships with fold geometry, and their relative and probable absolute chronologies were the main objectives of this thesis.

The first part was devoted to elementary aspects of the fold and fracture mechanisms through an intensive bibliography on the basic and principal mechanical elements of fractures. Joints, faults, and stylolites were introduced as the main features of the brittle deformation. The interpretation of these features, from genesis and chronological points of view and also in paleostress definition, was taken into account. This chapter served the main theoretical background concerning fracture study in this work. Previous fracture studies and their results were briefly mentioned as well as ambiguities and some important aspects which were not fully covered in these studies. This part introduced the main geological features and principal tectonic elements as a preliminary data base to support the latter parts of this thesis.

The second part, started by chapter III in which paleogegaphy, geological setting, and structural style of the Zagros folded belt presented and followed by introducing the Asmari Formation, in chapter IV, as the main lithostartigraphical unit in which fracture study was performed regionally in the Izeh and the northern part of the Dezful Embayment.

The third part started by an introduction on previous fracture studies in the Arabian cover including the Asmari Formation (Chapter V) and followed by chapter VI in which the results of fracture study in the Asmari Formation through several intensive field works in the Central Zagros were presented. The main important message in this part, based on observations on the studied outcrops, was that the most fracture sets in the Asmari Formation have quite weak symmetrical relationship with the fold geometry or are not compatible with conventional fold-related fracture models. Then using chronology of different fracture sets, fault-slip data interpretation, and aerial/satellite image interpretation it was concluded that most of these fracture sets predate the present-day folds in the studied area. Finally, a conceptual model was proposed based on which the formation of different fracture sets through different stages were presented. In this model, fracture set I, striking ~ N050° was considered as the first joint set which initiated regionally in the studied area. However, some observed azimuthal deflection and reorientation of this joint set (indicated as set II) was suggested to be due to a far-field stress perturbation near large-scale N-S trending basement faults. Then initiation of ~N140° and N-S trending fracture sets were argued to be in direct relation with the main deep seated basement faults reactivation in the studied area. Finally, the

last episode of fracturing in form of reverse faults and thrusts and a group of conjugate fractures with an bisect of acute angle perpendicular to fold axis was suggested to be the products of layer-parallel-shortening (LPS) phase followed by Miocene-Pliocene folding event in the Central Zagros. In addition, reactivation of pre-existing fracture sets in form of reopening, shearing and reorientation was happened in this stage. Part three is finished by some complementary remarks on the aspects (some complicate features of N-S and E-W fractures, diagenesis, and paleostress definition in the Central Zagros using calcite twins). Then in chapter VII development of those fractures which proposed to be related to deep-seated basement faults was discussed. Through sedimentological evidence and constructed stratigraphical transects and paleogeographical maps, it was shown that facies variations within the Asmari basin was strongly controlled by reactivation of basement faults. Then it was concluded that forced-folding in the Central Zagros predated the final Mio-Pliocene orogenic event and it was suggested that deformation in the cover started quiet early, possibly Aquitanian time or even as early as Eocene-Oligocene times. One of the main conclusions obtained from this part and also proposed conceptual model of previous part is that, convergence partitioning, resulted by an oblique convergence between the Arabian and Eurasia Plates was initiated quite earlier compare to what proposed by the others (e.g., Talebian and Jackson, 2002). A geodynamic model was proposed at the end of this part (Chapter VIII).

Finally, in part four, reactivation of different fracture sets which were explained and argued based on field works and data interpretation, was tested by a direct (mechanical) modelling on a typical anticline (Asmari anticline). The results of different performed simulations are compatible with the field observations. The obtained results in the modelling approach prove that a link between fold kinematics and mechanical modelling may give a powerful tool to predict fracture activation and development in a fold (or reservoir). Outcrop observations and measurements (or subsurface data set) provide an essential part to reduce the uncertainties in the modelling approach whose result provide the valuable information for any fracture reservoir development.

Prospective

The significance of fracture study in the Asmari carbonate reservoirs has arisen since the role of fractures in hydrocarbon production appeared to be important. The main results obtained in this thesis are indebted to a regional fracture study approach in which fracture

initiation and development during different deformation stages in the Central Zagros were argued. At quite early stage of this study, it was predicted that the role of basement in cover deformation within the Zagros region is noticeable and any effort toward the better understanding of deep seated basement structures will effectively reduce the uncertainties and ambiguities which are encountered during the interpretation of cover structures. It was shown that localization of the early stage fractures has direct relation with the underneath basement faults. Reactivation chronology of these pre-existing fractures during the growth of a fold and their possible effect on fold geometry through analogical and/or numerical modelling approaches are essential targets which should be taken into account for the next studies.

Recently, deeper carbonated reservoir horizons in the Dezful embayment are under development. Upper Cretaceous Sarvak Formation is one of these targets in which fracture study have never been performed seriously. Furthermore, based on outcrop observation and production data within a few limitedly developed oil fields, joints poorly developed in the Sarvak Formation. Regional and local (reservoir-scale) study of fractures distribution in this Formation could be one of the main research prospectives in the development plan of the Sarvak reservoirs.

Based on my experience during the Asmari fracture study, paleostress analysis appeared to be an essential part in this work and should be considered to perform in any joint study project. Different approaches may be implemented in this regard. Fault-plane striations and stylolite peaks are generally used as the most practical data sets which can be measured easily on the outcrops. Furthermore, calcite twins were introduced by some authors as another applicable mean in paleostress analysis (see e.g., Lacombe, 1992 for details). However, this type of data set should be cautiously treated both during the sampling on the outcrop and also laboratory preparation steps and microscopic interpretations. Paleostress analysis in the Zagros folded belt have been poorly covered and if it is performed properly within a few sectors of this region, some ambiguities regarding the timing of deformation episodes and fracture pattern complexities (e.g., E-W fractures), will be better understood. Making a comparison between pre- and post-Gachsaran fracture patterns could be a complementary part towards defining different deformation episodes using paleostress analysis.

Fracture swarms have not been even touched in the Zagros region seriously. Their patterns and their relations with structures are not clear. This fracture group had presumably an important role in the secondary oil migration from source rock (e.g., the Kazhdumi Formation) into the Asmari carbonates. Their chronology compare to other fracture sets, and

their relative development intensity within different reservoir horizons could be the main topics in their study.

Finally, Diagenesis of the carbonate reservoirs and more precisely the role of fractures in this phenomenon and visa versa, still are new domains of study in the Zagros region. This part could be studied both in a basin and reservoir scale. Different diagenetical zones are presumably controlled and bordered by large-scale faults and fractures in this area. For example, dolomitization can be widely seen within the Asmari carbonates of different fields in the Dezful Embayment but such a diagenetical process weakly developed in the outcrops of this Formation in the Izeh zone.

References

Adams, T., D., 1969, The Asmari Formation of Lurestan and Khuzestan Provinces, IOOC report, No. 1154, 34p.

Adams, T. D., and Bourgeois, F., 1967, Asmari biostratigraphy, Geological and Exploration Div. IOOC report No.1074, 34p.

Agar, R. A., 1985, The Najd fault system revisited; a two-way strike-slip orogen, *Journal of Structural Geology* 9, 41-48.

Agard, P., Omrani, J., Jolivet, L., and Mouthereau F., 2005, Convergence history across Zagros (Iran): constrains from collisional and earlier deformation, Int. J. Earth Sc., 94, 401-419, doi 10.1007/S00531-005-0481-4

Ahmadhadi, F., Daniel, J.M., and Lacombe, O., 2005, Fracture development within Asmari carbonates in the Central Zagros folded belt, SW Iran: An insight into the role of basement faults on Lower Tertiary facies changes and possible forced folding (abs.), Thrust Belt and Foreland Basins, International Meeting, France.

Allen, M., 2004, Late Cenozoic reorganization of the Arabian-Eurasian collision and comparison of short-term and long-term deformation rates, *TECTONICS*, vol.. 23, TC2008, doi:10.1029/2003TC001530,

Allen, P.A. and Allen, J.R., 2005, *Basin Analysis*, Principles and Applications. Blackwell publishing, 549 pp.

Alavi, M., 1980, Tectonostratigraphical evolution of the Zagrosides of Iran, Geology, vol.8, p.144-149.

Alavi, M., 1994, Tectonics of the Zagros Orogenic belt of Iran: new data and interpretations. Tectonophysics, 229, 211-238.

Alavi, M., 2004, Regional stratigraphy of the Zagros fold-thrust belt of Iran and its proforeland evolution, American Journal of Science, vol.304, p.1-20.

Al-Kadhi, A., and Hancock, P. L., 1980, Structure of the Durma-Nisah segment of the central Arabian graben system, *Saudi Arabian Directorate General of Mineral Resources*, Bulletin 16, 40p.

Al-Khatieb, S. O., and Norman, J. W., 1982, Photogeological evidence of the continuation of Al Amar Idsas basement fault under the Phanerozoic rocks, central Saudi Arabia, *Trans. Inst. Min. & Metall*., 91 B169-B174.

Al-Laboun, A., A., 1986, Stratigraphy and hydrocarbon potential of the Palaeozoic succession in both the Tabuk and Widyan basins, Arabia, In: M. T. Halbouty (Ed.), *Future Petroleum Provinces of the World*, AAPG Mem., 40, 399-425.

Allen M. , Jackson J., and Walker R., 2004, Late Cenozoic reorganization of the Arabia-Eurasia collision and the comparison of short-term and long-term deformation rates, *Tectonics*, 23, TC2008, doi:10.1029/2003TC001530

Al-Sawari, A. M., 1980, tertiary faulting beneath Wadi Al-Batin (Kuwait), *Bull. geol. Soc. Am*. 91, 610-618.

Al-Sayari, S. S., and Zotl, J. G., 1978, Quarternary Period in Saudi Arabia (eds.), Springer, New York.

Al Shanti, A.M.S. and Gass, G.M., 1983, The upper Proterozoic ophiolite melange zones of the easternmost Arabian shield, *Jour. Geol, London*, v. 14016, p. 867-876.

Alvarez, W., Engelder, T., and Geiser, P. A., 1978, Classification of solution cleavage in pelagic limestones, *Geology*, 6, 263-266.

Ambraseys, N.N., 1978, Middle East- A reappraisal of seismicity, *Q.J. Eng. Geol*., v. 11, pp. 19-32.

Ameen, M. S., 1988, Folding of layered cover due to dip-slip basement faulting, Ph.D. thesis, University of London.

Ameen, M. S., 1990, Macrofaulting in the Purbeck-Isle of Wight monicline, *Proceeding of the geologists' Association*, 101, 31-46.

Ameen, M. S., 1991, Alpine geowarpings in the Zagros-Taurus range: Influence on hydrocarbon migration and accumulation, *J. Pet. Geol*. V. 14, no. 4, p. 417-428.

Amrouch, K., 2005, Quantification des orientations des paléocontrainrtes tertiaires dans les deux anticlinaux de Dezful (Kuh-e Dil et Kuh-e Khaviz) par l'analyse des macles de la calcite, *l'apport intern de l'IFP*.

Anderson, E. M., 1951, The dynamics of faulting and dyke formation with application to Britain, 2nd edition, Oliver and Boyd, 206pp.

Angelier, J., 1984, Tectonic analysis of fault slip data sets, J. Geophy. Res., 89, B7, pp.5835-5848.

Angelier, J., 1990, Inversion of field data in fault tectonics to obtain the regional stress-III. A new rapid direct inversion method by analytical means, Geophys., J., Int., 103, 363-376.

Angelier, J., and Goguel, J., 1979, Sur une méthod sipmle de détermination des axes principaux des contraintes pour une population de faille, C.R.Acad.Sci. Paris, 288, Sér. D, 307-310.

Angelier, J., Tarantola, A., Vallete, B., and Manoussis, S., 1982, Inversion of field data in fault tectonics to obtain the regional stress: I Single phase fault populations; a new method of computing stress tensor, Geophys. J. R. Astr. Soc., 69, pp. 607-621.

Angevine, C.L., Heller, P.L. and Paola, C., 1990, Quantitative Sedimentary Basin Modeling, *American Association of Petroleum Geologists Short course* (Note Series 32): 247.

Armijo, R., Carey, E., and Cisternas, A., 1982, The inverse problem in microtectonics and the separation of tectonic phases, Tectonophysics, 82, pp.145-160.

Arthaud, F., 1969, Méthode de déterminatioft graphique dês directions de raccourcissement, d'allongement et intermédiaire d'une population de failles. *Bull. Soe. Géol. France*, **11**:729-737

Arthaud, F., and Mattauer, M., 1969, Exemples de stylolites d'origine tectonique dans le Languedoc, leurs relation avec la tectonique cassante, Bull. Soc. Géol. Fr., 7, Ser. XI, 738-744.

Athy, L.F., 1930, Density, porosity and compaction of sedimentary rocks, *American Association of Petroleum Geologists Bulletin*, 14: 1-24.

Aguilera, R., 1995, Naturally fractures reservoirs, 2nd ed., PennWell Books, Tulsa, Oklahoma, 521pp.

Babcock, E. A., 1973, Regional joints in southern Alberta, *Canadian Journal of earth Sciences*, vol. 10, no. 12, p. 1769-1781.

Babcock, E. A., 1974a, Photolineaments and regional joints: Lineation density and terrain parameters, south-central Alberta, *Bulletin of Canadian Petroleum Geology*, vol. 22, no. 2, p. 89-105.

Babcock, E. A., 1974b, Jointing in central Alberta, *Canadian Journal of Earth Science*, vol. 11, no. 8, p. 1181-1186.

Badgley, P.C., 1965, Structural and Tectonic Principles, Harper and Row, New York.

Bahat, D., 1991, Tectonofractography, Springer verlag, 354p.

Bahroudi, A., and C. J. Talbot, 2003, The configuration of the basement beneath the Zagros basin, Journal of Petroleum Geology, vol.26 (3), p. 257-283.

Baker, C., Jackson, J., and Priestly K., 1993, Earthquakes on the Kazerun line in the Zagros mountains of Iran: strike-slip faulting within a fold-and-thrust belt, *Geophys. J. Int*., 115, p.41-61.

Barber, D. J., and Wenk, H. R., 1976, Detects in deformed calcite and carbonate rocks, In: *Electron Microscopy in Mineralogy* (edited by Wenk, H.R.), Springer Verlag, Berlin, 428-442.

Barnes, B. B., 1987, Recent developments in geophysical exploration for hydrocarbons, In: *Short course on hydrocarbon exploration*, KFUPM Press, Dhahran, 12p.

Bazalgette, L., 2004, Relation plissement/fracturation multi échelle dans les multicouches sédimentaires du domaine élastique/fragile: Accomodation discontinue de la courbure par la fracturation de petite échelle et par la articulations; implication dynamique dans les écoulements des réservoir, Thèse de Doctorat, Université Montpellier, 275p.

Barzegar, F., 1994, Basement fault mapping of E Zagros folded belt (S.W. Iran) based on space-born remotely sensed data, *Proceedings of the 10th thematic conference on geologic remote sensing: exploration, environment, and engineering*. 10, 455-466, San Antonio, Texas, USA.

Beach, A., 1975, The geometry of en-echelon vein array, *Tectonophys*, 28, 245-264.

Beach, A., 1977, Vein array, hydraulic fractures and pressure-solution structures in a deformed flysch sequence, S.W. England, *Tectonophys*, 40, 201-225.

Bellahsen, N., Fiore, P. E., and Pollard, D. D., 2005, The role of fractures in the structural interpretation of Sheep Mountain anticline, Wyoming, *Tectonics* (submitted).

Bellen, R. C., Van, 1956, Stratigraphy of the main limestone of Karkuk Bai Hassan, and Qarah Chauq Dagh structures in North Iraq, *Jour. Inst. Petrol*., vol. 42, no. 393, p. 233-263.

Berberian, M., 1976, An explanatory note on the first seismotectonic map of Iran; a seismotectonic review of the country, In: contribution to the seismotectonics of Iran (Part II), Berberian, M., (ed.), *Geological Survey of Iran*, no.39, pp.7-141.

Berberian, M., 1979, Evaluation of the instrumental and relocated epicenters of Iranian earthquakes, *Geophys. J. R. Astron. Soc*., 58, 625-630.

Berberian, M., 1981, Active faulting and tectonics of Iran, In: H. K. Gupta and F. M. Delaney (Editors), Zagros-Hindu Kush-Himalaya Geodynamic evolution, Am. Geophys. Union, Geodyn. Ser., vol.3, p.33-69.

Berberian, M. 1983, The southern Caspian: A compressional depression floored by a trapped, modified oceanic crust, *Can. J. Earth Sci.*, 20(2): 163-183.

Berberian, M. 1986, Seismotectonics and earthquake-fault hazard study of the Karkheh river project

Berberian, M., 1995, Master blind thrust faults hidden under the Zagros folds: active basement tectonics and surface morphotectonics, Tectonophysics, 241, pp. 193-224.

Berberian, M. and King, G.C.P., 1981, Paleogeography and tectonic evolution of Iran, *2nd. Jour. Of Earth Science*, v. 18, p.210-265.

Berberian, M., and Tchalenko, J., 1976a, Earthquakes of the southern Zagros (Iran): Bushehr region, Geol. Surv. Iran, vol.39, p.343-370.

Berberian, M. and King, G. C. P., 1981, Towards a paleogeography and tectonic evolution of Iran, *Can. J. Earth Sci*., 18(2): 210-285.

Berberian, F.; Muir, I. D., Pankhurst, R. J. and Berberian, M., 1982, Late Cretaceous and early Miocene Andean-type plutonic activity in northern Makran and Central Iran, *J. Geol. Soc. London*, 139(5): 605-614.

Bergbauer, S., Pollard, D., 2004, New conceptual fold-fracture model includes prefolding joints, based on field data from Emigrant Gap anticline, Wyoming, GSA Bulletin, v.116, no.3/4, p.294-307.

Beydoun, Z. R., 1988, The Middle East: Regional geology and petroleum resources (eds.), Beaconsfield, Hants Scientific Press.

Beydoun, Z. R., 1989, Hydrocarbon potential of the deep (pre-Mesozoic) formations in Middle East Arab countries, In: technical Papers, Presented at the Seminar on Deep formations in the Arab Countries: Hydrocarbon potential and Exploration Techniques, Abu Dhabi National Oil Co;, Abu Dhabi, UAE, 1989.

Beydoun, Z. R., 1991, Arabian plate hydrocarbon, Geology and Potential – A Plate tectonic approach, AAPG, Studies in Geology 33, 77 p.

Biot, M. A.,1961, Theory of folding of stratified visco-elastic media and its application on tectonics and orogenise, Geol. Soc. Am. Bull., 72, 1595-1620.

Blanc, E. J.-P., Allen, M. B., Inger, S., and Hassani, H., 2003, Structural style in the Zagros simple folded zone, Iran, *Journal of the Geological Society, London*, vol. 108, p. 401-412.

Bland, S., Griffiths, P., Hodge, D., 2004, Restoring the seismic image with a geological rule base, Petroleum Geosciences, pp. 51-55.

Bohannon, R. G., 1986, Tectonic configuration of the western Arabian continental margin, southern red Sea; *Tectonics*, v. 5, no. 4, p. 477-499.

Bond, G.C. and Kominz, M.A., 1984, Construction of tectonic subsdience curves for the early Paleozoic miogeocline, southern Canadian Rocky Mountains: implications for subsidence mechanisms, age of breakup, and crustal thinning, *Geological Society of America Bulletin*, 95: 155-173.

Bonini, M., Detachment folding, fold amplification, and diaprism in thrust wedge experiments, *Tectonics*, 224/1-4/26,1065 doi: 10.1029/2002TC001458

Bott, M. H. P., 1959, The mechanism of oblique slip faulting, Geol. Mag., 12, 3, pp. 109-117.

Bouroz, C., 1990, Les joints et leur signification tectonique en domaine tabulaire: exemples dans le plateau du Colorado (Utah, Arizona, Nouveau Mexique). Thèse Doctorat, Paris VI, 257 p.

Brace, W.F. 1964, Brittle fracture of rocks. IN: *State of Stress in the Earth's Crust* (edited by Judd, R.). Elsevier New York, 111-180.

Brace, WF, BW Paulding, Jr., and CH Scholz, 1966, Dilatancy in the fracture. of crystalline rocks, *J. Geophys. Res.* 73, 3295-3302.

Brown, G. F, 1972, Tectonic map of the Arabian Peninsula, *Geol. Map AP-2*, 1:4,000,000, Saudi Arabia Dir. Gen. Miner. Resour., Jiddah.

Brown, G. F. and R. O. Jackson, 1960, The Arabian shield; 21st Int. Geol. Cong. Proc., Section 9, p. 69-77.

Byerlee, J. D., 1968, Brittle-ductile transition in rocks, J. Geophys. Res., 73, 4741-4750.

Cailletaux, G., J. Y. Cognard, C. Cornuault and G. Dhatt, 1995, Mécanique non-linéaire des solides et des structures, Volume 1, *Institut pour la Promotion des Sciences de l'ingénieur*.

Calvez, J. Y., C. Alsac, J. Delfour, J. Kemp, and C. Pellaton, 1983, Geological evolution of western, central and eastern parts of the northern Precambrian shield, Kingdom of Saudi Arabia: *Directorate General of Mineral Resources, Saudi Arabia*, BRGM-OF-03-17, 57 p.

Carey, E., 1976, Analyse numérique d'un modèle mécanique élémentaire appliqué à l'étude d'une population de failles: calcul d'un tenseur moyen des contraintes à partir des stries de glissement, Thèse de Doctorat, Paris XI, 138p.

Carey, E., and Brunier, B., 1974, Analyse théorique et numérique d'un modèle mécanique élémentaire appliqué à l'étude d'un population de failles, C.R.A.S., 279, 891-894.

Cornu, T., 2002, Modélisation cinématique discrète de la déformation 3D des bassins sédimentaire, *Thèse de Doctorat*, Université de Joseph Fourier, Fracnce.

Cundall, P. A., 1971, A Computer Model for Simulating Progressive Large Scale Movements in Blocy Rock Systems. *Proc. Sympo. Int. Soc. Rock Mech.*

Chu, D., and Gordon, R., G., 1998, Current plate motion across the Red Sea, Geophys. J. Int., 135, 313-328.

Colletta, B., Letouzey, J., Pinedo, R., Ballard, J. F. & Bale, P., 1991. Computerized X-ray tomography analysis of sandbox models; examples of thin-skinned thrust systems, *Geology*, 19, 1063-1067.

Colman-SADD, S. P., 1978, Fold Development in Zagros Simply Folded Belt, Southwest Iran, The American Association of Petroleum Geologists Bulletin, V. 62, No.6, pp. 984-1003.

Cook, A. C., and K. R. Johnson, 1970, Early joint formation in sediments, *Geol. Mag.*, v. 107, no. 4, p. 361-368.

Cooper, M., 1992, The analysis of fracture systems in subsurface thrust structures from the foothills of the Canadian Rockies, in McClay, K. R., ed., Thrust tectonics, London, Chapman and Hall, p.391-405.

Cosgrove, J. W., & Ameen, M. S. (eds.), 2000, Forced Folds and Fractures. Geological Society, London, Special Publications, 169, © The Geological Society of London.
Coulomb, J. J., J. Felenc and J. Testard, 1981, Volcanisme et mineralisation a ZN-Cu de la ceinture d'Al Amar (Royuaume d'Arabie Saoudite): *Bureau de recherches Géologiques et Minières Bulletin*, series 2, p. 41-71.
Couzens-Schultz, B.A., Vendeville, B.C., and Wiltschko, D.V., 2003, Duplex style and triangle zone formation: insights from physical modeling, *Journal of Structural Geology*, 25, 1623-1644.
Coward, M. P., Dewey, J. F. & Hancock, P. L. (eds), 1987, Continental Extension Tectonic, Geological Society Special Publication No. 28, pp. 127-137.
Cruickshank, K. M., Zhao, G., and Johnson, A. M., 1991, Analysis of minor fractures associated with joints and faulted joints, J. Struct. Geol., 13, pp. 865-886.
Currie, J.B., Patnode, H.W., and Trump, R.P., 1962, Development of folds in sedimentary strata, *The Geological Society of America Bulletin*, 73, 655-674.
Dahlstrom, C.D.A., 1990, Geometric constraints derived from the law of conservation of volume and applied to evolutionary models for detachment folding, *AAPG Bulletin*, 74(3), 336-344.
Davis, D., and Engelder, T., 1985, The role of salt in fold-and-thrust belts: *Tectonophysics*, v. 119, p. 67–88.
De Bremaecker, J.-Cl., and Becker, E. B., 1978, Finite element models of folding, *Tectonophysics*, v. 50, p. 349-367.
Dehghani, G.A. and Makris, J., 1983, The gravity field and crustal structure of Iran, *Rep. No. 51*, p. 51-70.
De Jong, K. A., 1982, Tectonics of the Persian Gulf, Gulf of Oman and Southern Pakistan region, In: The oceanic basins and margins, vol. 6, The Indian Ocean, edited by A. E. M. Narin and F. G. Stehli, pp. 315-351, Plenum, New York.
De Mets, C. , Gordon, D. F. and Stein, S., 1990, Current plate motions, *Geophys.* J. Int., 101: 425-478.
De Mets, C., Gordon, R. G., Argus, D. F., and Stein, S., Effects of recent revision to the geomagnetic revers time scale on estimates of current plate motions, Geophysical research Letters, p. 2191-2194.
Donath, F. A., 1962, Role of Layering in geologic deformation; N. Y. *Acad. Sci. Trans*., v. 24 p. 236-249.
De Paor, D., 1988a, Balanced section in thrust belts, part 1: construction, AAPG Bulletin, vol.72, no.1, pp.73-90.
De Paor, D., 1988b, Balanced section in thrust belts, part 2: compterized line and area balancing, Geobyte, pp.33-37.
De Paor, D. G., C. Simpson, C. M. Bailey, K. J. W. McCaffrey, E. Beam, R. J. W. Gower, and G. Aziz, 1991, The role of solution in the formation of boudinage and transverse veins in carbonate rocks at Rheems, Pennsylvania, *Geological Society of America Bulletin*, 103, 1552 – 1563.
De Santi, M. R., Marth, L. F., Campos, J. L. E., 2003, 3D restoration using a finite element approach, Tecgraph/PUC-Rio, Brazil, pp.1-6.
De Sitter, L. U., 1956: Structural geology, New York, McGraw-Hill, 552p.
Dunne W. M. and Hancock, P. L., 1994, Paleostress Analysis of Small-Scale Brittle Structures, In: *Continental. Deformation* (ed Hancock PL), pp. 101-118.
Dzulinski, S., and Kotlarczyk, J., 1965, Tectoglyphs on slickensided surfaces, Bull. Acad. Polonaise Sci. Sér. Géol. Géogr. XIII, 149-154.
Edgell, H. S., 1987, Structural analysis of hydrocarbon accumulation in Saudi Arabia, In: Short course on hydrocarbon exploration, KFUPM, Press, Dhahran, 26p.
Edgell, H. S., 1992, Basement tectonic of Saudi Arabia as related to oil field structures, In: Rickard et al. (eds.), Basement tectonic 9, Kluwer Academic Publishers, Dordrecht, p. 169-193.
Elliott, D., 1976, The energy balance and deformation mechanisms of thrust sheets, *Phil. Trans. R. Soc.*, 283A, 289-312.
Elliot, D., 1983, The construction of balanced cross-sections, J. Struct. Geol, vol.5, no.2, p.101.
Endignoux, L., and Wolf, S., 1990, Thermal and kinematic evolution of thrust basins: A 2D numerical model, *in* Letouzey, J., ed., Petroleum and tectonics in mobile belts: Paris, Editions Technip, p. 181–192.
Engdahl, E. R., R. van der Hilst, and R. Buland, 1998, Global teleseismic earthquake relocation with improved travel times and procedures for depth determination, *Seismol. Soc. Am. Bull*., 88, 722 – 743.
Engelder, T. 1982, Reply to comments by A.E. Scheidegger on "Is there a genetic relationship between selected regional joints and contemporary stress within the lithospher of North America?", *Tectonics*, 1, 465-470.
Engelder, T. 1985, Loading paths to joint propagation during a tectonic cycle: an example from the Appalachian Plateau, U.S.A. *J. Struct. Geol.* 7. 459-476.
Engelder, T., 1987, Joints and shear fractures in rock, in Fracture Mechanics of Rock, Copyright © by Academic Press Inc. (London) Ltd.
Engelder, T., and Geiser, P., 1980, On the use of original joint sets as trajectories of paleostress fields during the development of the appalachian plateau; U.S.A., J. Geophys. Res. 85, 6319-6341.

Engelder, T., and Marshak, S., 1985, Disjunctive cleavage formed at shallow depths in sedimentary rocks, *Journal of Structural Geology*, v. 7, p. 327-343.
Engelder, T., Fischer, M.P., and Gross, M.R., 1993, Geological aspects of fracture mechanics: Short Course Manual, *Annual Meeting of the Geological Society of America*, Boston, Massachusetts.
Etchecopar, A., and Mattauer, M., 1988, Méthodes dynamique d'analyse de population de faille, *Bulletin de la Société Géologique de France*.
Etchecopar, A., Vasseur, G., and Daignieres, M., 1981, An inverse problem in microtectonics for the determination of stress tensor from fault striation analysis, J. Struct. Geol., 3, pp.51-65.
Evan, A. G., 1974, Slow crack growth in brittle materials under dynamic loading conditions, Int. J. of Fract. 10, p. 251-259.
Fahmi, K. J., M. A. Al-Salmi, and B. S. Ayar, 1986, Recent earthquake activity in the Lesser Zab region, northeastern Iraq, Building Research Center, *Iraq Scientific Research Council Report* RP104/86.
Falcon, N.L., 1961, Major earth-flexing in the Zagros Mountains of southwest Iran., *Q. J. Geol. Soc. London*, 117(4): 468: 367-376.
Falcon, N., 1967, The geology of the north-east margin of the Arabian basement shield, Adv. Sci., v.24, p.31-42.
Falcon, N.L., 1969, Problems of relationship between surface structures and deep displacements illustrated by the Zagros range, In: Time and place in orogeny: *Geol. Soc. London, Spec. Pub*. 3, 9-22.
Falcon, N. L., 1974, Southern Iran: Zagros mountains, In: A. M. spencer (Editor), Mesozoic-Cenozoic Organic belts, data for orogenic studies, *Geol. Soc. London, Spec. Pub*., 4: 199-211.
Favre, G., 1975, Structures in the Zagros orogenic belt, OSCO, Report no. 1233, (Unpub.).
Fischer, M., and M. Coward, 1952, Strains and folds within thrust sheets: an analysis of the heilam sheet, northwest scotland, *Tectonophysics*, vol.88, pp.291-312.
Fischer, M. P., and Wilkerson, M. S., 2000, Predicting orientations of joints from fold shape, results of pseudo-three-dimensional modeling and curvature analysis, Geology, v.28, p.15-18.
Fletcher, R. C., and Pollard, D. D., 1981, Anticrack model for pressure solution surfaces, *Geology*, 9, 415-424.
Forsyth, D.W., 1985, Subsurface loading and estimates of the flexural rigidity of continental lithosphere, *J. Geophys. Res*., 100, pp. 9761-9788.
Freund, R., Garfunkle, Z., Zak, I., Goldberg, M., Weisbrod, T., and Derin, B., 1970, The shear along the Dead Sea Rift, *Philosophical Transactions Royal Society London*, 167, 107-130.
Friedman, M., 1964, Petrofabric tectonics for the determination of principal stress directions in rocks, In: *State of Stress in the Earth's crust* (edited by Judd, W. R.), Am. Publ.Comp., New York.
Frisch, W., and A. M. Al Shanti, 1977, Ophiolite belts and the collision of island arcs in the Arabian shield: *Tectonophysics*, v. 43, p. 293-306.
Fürst, M., 1970, Stratigraphic und Werdegang der Ostlichen Zagrosketten (Iran), Erlanger, *Geol. Abh.*, Heft 80, p. 1-51.
Gambarotta, L., and Lagomarsino, S., 1993, A microcrack damage model for brittle materials, International Journal of Solides and Structures, 30, 177-198.
Gauthier, B. D. M., and Angelier, J., 1985, Fault tectonics and deformation: a method of quantification using field data, *Earth and planetary Science letters*, 74, pp.137-148.
Geiser, P. A, and Sansone, S., 1981, Joints, microfractures, and the formation of solution cleavage in limestone, *Geology*, v. 9, p. 280-285
Gholipour, A. M., 1998, Patterns and Structural Positions of Productive Fractures in the Asmari Reservoirs, Southwest Iran, The Journal of Canadian Petroleum Technology, Vol. 37, No. 1.
Ghosh, S. K., 1993, Structural geology: Fundamental and modern development (ed.), Pergamon Press, Oxford, 598p.
Gibbs, A., 1983, Balanced cross-section construction from seismic sections in extentional tectonics, J. Struct. Geol., vol.5, PP.153-160.
Giese, P. et al., 1983, Seismic crustal studies in southern Iran between central Iran and Zagros belt, geodynamic Project in Iran, *GST report No. 51-1983*, p. 71-102.
Goetze, C., and Kohlstedt, D. L., 1977, The dislocation structure of erxperimentally deformed marble, Contr. Miner. Petrol., 59, 293-306.
Goguel, J, 1948, Introduction à l'étude mécanique des déformation de l'écorce terrestre, *Mem. Expl. Carte Geol. Fr*., 530p.
Goff, Jeremy C., Jones, Robert W., Horbury, Andrew D., 1994, Cenozoic basin evolution of the northern part of the Arabian plate and its control on hydrocarbon habitat, GeoArabia, pp.402-412.
Gramberg, J., 1965, Axial cleavage fracturing, a significant process in mining and geology, Engineering Geology, 1, 31-72.
Granier, TH., 1986, Initiation, évolution et amortissement des failles en domaine fragile, Thèse de Doctorat, Université de Montpellier II, 224p.

Gratier, J.-P., 1993, Le fluage des roches par dissolution – cristallisation sous contrainte, dans la croûte supérieur, *Bull. Soc. Geol. Fr*., vol. 164, no.2, pp. 267-287.
Griffith, A. A., 1920, The phenomena of rupture and flow in solids, Phil. Trans. Roy. Soc. Lond., Ser A 221, 163-198.
Griffith, A. A., 1924, Theory of rupture, First Int. Conf. Applied Mechanics, 55-63.
Groshong, R. H., Jr., 1972, Strain calculated from twinning in calcite, *Bull. geol. Soc. Am.* 83, 2025-2048.
Groshong, R. H., Jr., 1974, Experimental test ol the least squares strain gage calculation using twinned calcite, *Bull. geol. Soc.* 4nz, 85, 1855-1864
Groshong, R. H., Jr., 1974, 'Slip' cleavage caused by pressure solution in buckle fold, *Geology*, 3, 411-413.
Guiraud, M., Laborde, O., and Philip, H., 1989, Characterization of various types of deformation and their corresponding deviatoric stress tensors using microfault analysis, Tectonophysica, 170, 289-316.
Guiton, M., 2001, Contribution de la fracturation diffuse à la déformation f'ensemble durant le plissement de roches sédimentaires, Thèse de Doctorat, Ecole Polytechnique de Paris, 256p.
Guiton, M.L.E., Leroy, Y.M., Sassi, W., 2003, Activation of diffues discontinuities and folding of sedimentary layers, J. Geophys. Res., vol.108, no.C4, 2183, doi: 10.1029/2002JB001770.
Halbouty, M. T., 1980, Geologic significance of Landsat data for 15 Giant Oil and Gas fields, *AAPG Bull*., 64, 8-36.
Hancock, P. L., 1985, Brittle microtectonics: principles and practice, *Journal of Structurel Geology*, Vol. 7, pp. 437 to 457.
Hancock, P. L., 1994, Continental Deformation (eds.), Pergamon Press, 421p.
Hancock, P. L., and T. Engelder, 1991, Neotectonic joints: Reply, Geol. Soc. Am. Bull., 103, 432-433.
Hancock, P. L., S. O. Al Khatieb, and A. Al Kadhi, 1981, Structural and Photogeological evidence for the boundaries to an East Arabian block, *Geol. Mag*., 118, 533-538.
Hancock, P. L., Al Kadhi, A., Sha'at, N. A., 1984, Regional joint sets in the Arabian platform as indicators of interplate processes, Tectonics, V.3, No.1, pp. 27-43.
Hancock, P. L., and Al-Kadhi, A., 1985, Structure of Qirdan segment of the Central Arabian Graben System, Kingdom of Saudi Arabia, Deputy Ministry for Mineral Resources, *Professional paper No. PP-2*, 63-74.
Hancock, P. L., and Bevan, T. G., 1987, Brittle modes of foreland extension, In: Coward, M. P., Dewey, J. F., and Hancock, P. L., (eds.), Continental extension tectonic, *Geol. Soc. London, Spec. Pub*. No.28, 127-137.
Handin, J., 1969, On the Coulomb-Mohr failure criterion, J. Geophys. Res., 74, 5343-5348.
Handin, J., and R. V. Hager, 1957, Experimental deformation of sedimentary rocks under confining pressure; Tests at room temperature on dry samples, AAPG Bull., vol. 41, p. 1-50.
Hanks, C.L., and Krumhardt, A.P., 1995, Distribution and character of fractures in deformed carbonates of the Lisburne group, northeastern Brooks range, Alaska, public data file 95-26, state of Alaska, department of natural resourses.
Haq, B.U., Hardenbol, J. and Vail, P.R., 1987, Chronology of Fluctuating Sea-Levels since the Triassic, *Science*, 235: 1,156-1,167.
Harison, J. C., and Bally, A. W., 1988, Cross sections of the Devonian to Mississippian fold belt on Melville Island, Canadian Arctis Islands, Canadian Society of Petroleum Geologists, 36, p.311-332.
Harris, J. F., Taylor, G. L., and Walper, J.L., 1960, Relation of deformational fractures in sedimentary rocks to regional and local structures, American Association of Petroleum Geologist Bulletin, v.44, p.1853-1873.
Hayens, S. J., and McQuillan, H., 1974, Evolution of the Zagros suture zone, southern Iran, *Geol. Soc. Amer. Bull.*, vol. 85, 739-744.
Hempton, M. R., 1987, Constraints on Arabian plate motion and extensional history of the Red Sea, *Tectonics*, 6, 687 – 705.
Hennings, P. H., Olson, J. E., and Thompson, L. B., 2000, Combining outcrop data and three dimensional structural models to characterize fractured reservoirs: an example from Wyoming, American Association of Petroleum Geologist Bulletin, v.84, p.830-849.
Henson, F. R. S., 1951, Observation on the geology and petroleum occurrences of the Middle East., 3rd World Petroleum Congress, The Hague, Proceedings, section 1, 118-140.
Hessami, K., 2002, Tectonic history and present-day deformation in the Zagros fold-thrust-belt, Uppsala University, Ph.D. thesis, 13pp.
Hessami, K., Koyi, H.A. and Talbot, C.J., 2001, The significance of strike-slip faulting in the basement of the Zagros fold and thrust belt, *Journal of Petroleum Geology*, 24, 5-28.
Hessami, K., Koyi, H.A., Talbot, C.J., Tabasi, H., and Shabanian, E., 2001, Progressive unconformities within an evolving foreland fold-thrust belt, Zagros Mountains: Journal of the Geological Society of London, v. 158, p. 969-981.

Hessami, K., Jamali, F., Tabassi, H., 2003, Major active faults of Iran, Edition 2003, International Institute of Earthquake Engineering and Seismology, 1 Sheet.
Hills, E. S., 1963, Elements of structural geology; New York, John Wiley and Sons, 483p.
Hobbs, B.E., Means, W.D. & Williams, P.F., 1976, *An Outline of Structural Geology*, Wiley, New York.
Hodge, D., Roques, D., Bland, S., 2003, Techniques and benefits of combining seismic manipulation with cross section restoration, Z-99, pp. 1-3.
Hodgson, R. A., 1961a, Regional study of jointing in Comb Ridge-Navajo Mountain area, Arizona and Utah, *AAPG Bull*., vol. 45, no. 1, p. 95-97.
Holst, T. B., 1982, Regional jointing in the northern Michigan Basin, Geology, 10, 273-277.
Hooper, R. J., Baron, I. R., Agah, S., Hatcher, R. D., Jr., 1994, The Cenomanian to recent development of the Southern Tethyan Margin in Iran, in: M.I. Al-Husseini (Ed.), Middle East Petroleum Geosciences GEO, vol. II, pp. 505– 516.
Hoppin, R. A,, 1961, Precambrian rocks and their relationship to Laramide structure along the east flank of the Bighorn Mountains near Buffalo, Wyoming, *Geological Society of America Bulletin*, v. 72, p. 351-368.
Horii, H. and Nemat-Nasser, S., 1986, Brittle failure in compression: splitting, faulting and brittle-ductile transition, *Phil, Trans. Royal Society of London*, A-319: 337-374.
Homke, S., J. Verges, M. Garces, H. Emami and R. Karpuz, 2004, Magnetostratigraphy of Miocene-Pliocene Zagros foreland deposits in the front of the Push-e Kush Arc (Lurestan Province, Iran), *Earth and Planetary Science Letters*, 225(3-4), p. 397-410.
Houseknecht, D. W., 1987, Intergranular pressure solution in four quartzose sandstones, J. Sedim. Pet., 58, 228-246.
Hubbert, M.,1937, Theory of scale models as applied to the study of geologic structures, *Geol. Soc. Am. Bull.*, 48, 1459-1520.
Huber, H., 1977, Geological map of Iran, 1:1,000,000 with explanatory note. *Natl. Iran Oil Co., Explor. Prod. Affaris*, Tehran.
Hull, Cedric E. and Warman, Harry R., 1970, Asmari Oil Fields of Iran, Memoir-AAPG, pp. 428-437.
Husseini, M. I., 1988, The Arabian Infracambrian extensional system, Tectonophysics, 148, pp.93-103.
Husseini, M. I., 1989, Tectonic and deposition model of Late Precambrian-Cambrian Arabian and Adjoining plates, The American Association of Petroleum Geologists Bulletin, V. 73, No. 9, pp. 1117-1131.
Husseini, MI 2000, Origin of the Arabian plate structures: Amar collision and. Najd rift, *GeoArabia*, 5, 527–542
Ibrahim Shah, 1980, Stratigraphy and economic geology of central salt range, *Geol. Surv. Of Pakistan records*, v. 52.
Jackson, J. A., 1980, Reactivation of basement faults and crustal shortening in orogenic belts, Nature, v. 283, p. 343-346.
Jackson, J. A., and Fitch, T., 1981, Basement faulting and the focal depths of the larger earthquakes in the Zagros mountains (Iran), Geophys. J. R. Astron. Soc., 64, 561-586.
Jackson, J. A. and McKenzie, D. P., 1984, active tectonic of the Alpian-Himalayan belt between western Turkey and Pakistan, *Geophys, J. R. Astron. Soc*., 77, 185-264.
Jackson, J. A., Fitch, Ti., and McKenzie, D. P., 1981, Active thrusting and evolution of the Zagros fold belt. In: K. McClay and N. Price Editors, Geol. Soc. London, Spec. Publ., 9: 371-379.
Jaeger, J.C. & Cook, N.G.W., 1976, *Fundamentals of Rock Mechanics*. (2nd ed.), Chapman & Hall, London.
James, N. P. and Coquette, P. W., 1988, eds., *Paleokarst*: Springer-Verlag. New York, 421 p.
James, N. P.,1984, Limestones- the meteoric diagenetic environment, *Geoscience Canada* v.11 No.4.
Jackson, J. A. and Mckenzie, D. P., 1984, active tectonic of the Alpian-Himalayan belt between western Turkey and Pakistan, *Geophys*, J. R. Astron. Soc., 77: 185-264.
James, G. S., and Wynd, J. G., 1965, Stratigraphic nomenclature of Iranian Oil Consortium Agreement area, *Am. Assoc. Pet. Geol.*, 49(12): 2182-2245.
Jamison, W. R., 1987, Geometric analysis of fold development in overthrust terranes, *Journal of Structural Geology*, v.9, p.207-219.
Jamison, W. R., 1997, Quantitative evaluation of fractures on Monkshood anticline, a detachment fold in the foothills of western Canada, American Association of Petroleum Geologists Bulletin, v.81, p.1110-1132.
Jamison, W. R. & Spang, J. H., 1976, Use of calcite twin lamellae to infer differential stress, *Bull. geol. Soc. Am.*, 87, 868-872
Jestin, F., Huchon, P., and Gaulier, J. M., 1994, The Somalia plate and the East African Rift system, present-day kinematics, Geophys. J. Int., 116, 637-654.
Johnson, P.R., 1998, Tectonic Map of Saudi Arabia and Adjacent areas., Ministry of Petroleum and Mineral Resource, Saudi Arabia.

Kachanov, M. L., 1982b, A microcracked model of rock inelasticity part II : propagation of microcracks, *Mechanics of Materials*, 1, 29-41

Knipe, R., 1989, Deformation mechanisms recognition from natural tectonites, J. Strct. Geol., vol.11, no.1-2, pp.127-146.

Kelly, V. C., and N. J. Clinton, 1960, Fracture systems and tectonic elements of the Colorado plateau, *University of New Mexico Publication in Geology*, no. 6, 104 p.

Kent, P.E., Slinger and Thomas, 1951, Stratigraphical exploration surveys in Southwest Persia, Third world Petroleum Cong. The Hauge Sec. 1, p. 141-161.

Kent, P.E., 1958, Recent studies of south Persian salt plugs: *AAPG Bull.*, v. 42, p. 2951-2972.

Kent, P.E., 1970, The salt plugs of the Persian Gulf region; Leicester Literary and Philos. Soc. Trans., v. 64, p. 56-88.

Kent, P.E., 1979, The emergent Hormuz salt plugs of southern Iran, Journal of Petroleum Geology, , 2(2), pp.117-144.

Kerrich, R., Beckinsale, R. D., and Durham, J. J., 1977, The transltion between deformation regimes dominated by intercrystalline diffusion and intracrystailine creep evaluated by oxygen isotope thermometry, Tectonophysics 38, 241-257.

Koop, W. J., and Stoneley, R., 1982, Subsidence history of the Middle East Zagros basin, Permian to Recent. In: Kent, P. E., Bott, M. H. P., McKenzie, D. P., and Williams, C. A., (eds.), The evolution of sedimentary basins, *Philosophical Transactions of the Royal Society*, Part A, v. 305, p. 149-168.

Koyi, H., and Sans, M., 2003, Modeling the formation front of fold-thrust belts containing multiple weak horizons, *AAPG international conference* (abstract).

Kranz, R. L., 1979, *Int. J. Rock Mech. Min. Sci.* **16**, 37-47.

Kugler, A., 1970, An interpretation of the aeromagnetic pilot-survey of southwest Iran IOOC *report No. 1176b (unpub.).*

Kuh-é Asmari Geological Compilation Map, 1966, geological and exploration division, Iranian oil operating companies.

Kulander, B.R., and Dean, S.L., 1985, Hackle plume geometry and joint propagation dynamics, In: *Proc; Int. Symposium Fundamentals of Rocks Joints*, Björkliden, 85-94.

Lacombe, O., 1992, Maclage, fracturation et paleocontraintes intraplaques: application à la plate-forme carbonatee Ouest-Europeenne, Thèse de Doctorat, Université P. et M. Curie, 316p.

Lacombe, O., and Laurent, P., 1992, Determination of principal stress magnitudes using calcite twins and rock mechanics data, Tectonophysics, 202, pp. 83-93.

Lacombe, O., Mouthereau, F., Kargar, S., Meyer, B., 2006, Late Cenozoic and modern stress fields in the western Fars (Iran): implications for the tectonics and kinematic evolution of Central Zagros, *Tectonics*, vol. 25, TC1003, doi:10.1029/2005TC001831.

Lajtai, E.Z., 1971, A theoretical and experimental evaluation of the Griffith theory of brittle fracture, Tectonophysics, 11, 129-156.

Laurent, P., 1987, Shear-sense determination on striated faults from *e* twin lamellae in calcite, *Journal of Structural Geology*, vol.9, no.5/6, pp.591-595.

Laurent, P., Bernard, P., Vasseur, and G., Etchecopar, A., 1981, Stress tensor determination from the study of twins in calcite: a linear programing method, Tectonophysics, 78, pp. 651-660.

Laurent, P., Tourneret, C., and Laborde, O., 1990, Determining deviatoric stress tensors from calcite twins; application to monophased synthetic and natural polycrystals, Tectonics, 9, 3, pp. 379-389.

Lawn, B.R., and Wilshaw, T.R., 1975, Fracture of brittle solids, Cahn R.W et al. (eds). *Cambridge Univ. Press*, 204 p.

Le Bel, L. and M. Laval, 1986, Felsic plutonism in the Al Amar-Idsas area, Kingdom of Saudi Arabia, *Journal of African Earth Science*, v. 4, p. 87-98.

Lees, G.M., 1948, Some structural and stratigraphical aspects of the oil fields in the Middle East; Internat. Geol. Congress, London, pt. VI.

Lees, G.M., 1952, Foreland folding: *Geol. Soc. London*, Quart. Jour., v. 108, p. 1-34.

Lees, G.M., 1950, Some structural and stratigraphical aspects of the oil fields of the Middle East: *18th Int. Geol. Cong., Great Britain, Proc.*, pt. 6, p. 26-33.

Lees, G. M., 1955, Recent earth movements in the Middle East, *Geol. Rundsch*. 43, 221 pp.

Lees, G. M. and Falcon, N. L., 1952, The geographical history of the Mesopotamian plains, *Geogr. J.*, 118: 24-39.

Leroy, Y. M., and Sassi, W., 2000, A plasiticity model for discontinua, In: *Aspects of tectonic faulting*, Lehner, F., and Urai, J.(ed.), Springer – Verlag

Letouzey, J., and Trémolière, P., 1980, Paleostress field around the Mediterranean sincethe Mesozoic derived from microtectonics : comparison with plate tectonic data, In: Géologie des chaines alpines issues de la Téthys, 26eme C.G.I., Paris, Mém. BRGM, 115, pp. 261-273.

Letouzey, J., B. Colletta, R. Vially, and J. C. Chermette, 1995, Evolution of salt related structures in compressional setting, In: Jackson, M. P. A., D. G. Roberts, and S. Snelson (Eds.), Salt tectonics: a global perfective, AAPG Memoir, 65, p.41-60.

Letouzey, J., Colletta, B., Vially, R., Bale, P. & Chermette, J. C., 1992, Analysis of physical models using X-ray tomography, with application to seismic interpretation of basin inversion. In: Eynon, G. (Ed), American Association of Petroleum Geologists, 1992 annual convention; abstracts. *Annual Meeting Abstracts - American Association of Petroleum Geologists and Society of Economic Paleontologists and Mineralogists*. American Association of Petroleum Geologists and Society of Economic Paleontologists and Mineralogists, 75.

Letouzey, J., Sherkati, S., Mengus, J.M., Motiei, H., Ehsani, H., Ahmadnia, M., and Rudkiewicz, J.L., 2002, A regional structural interpretation of the Zagros mountain belt in Northern Fars and High Zagros (SW Iran), *AAPG Annual Meeting* (abstract).

Lisle, R.J., 1994, Detection of zones of abnormal strains in structures using Gaussian curvature analysis, AAPG Bulletin 78[12], 1811.

Lisle, R.J., 2000, Predicting patterns of strain from three-dimensional fold geometries; neutral surface folds and forced folds, Geological Society Special Publications 169, 213, United Kingdom, Geological Society of London: London, United Kingdom.

Lorenz, J. C., Teufel, L. W., and Warpinski, N. R., 1991, Regional fractures I: A mechanism for the formation of regional fractures at depth in flat-lying reservoirs, AAPG Bull., 75, 11, 1714-1737.

McClay, K. R., and Price, N. J., (eds.), 1981, Thrust and Nappe tectonics, *Geol. Soc. London Spec. Pub*. No. 7, 371-379.

Maggi, A., Jackson, J. A., Priestley, K., and Baker, C., 2000, A re-assessment of focal depth distributions in southern Iran, Tien Shan and northern India: do earthquakes really occur in the continental mantle? Geophys. J. Int., vol.143, p.629-661.

Malavieille, J., 1984, Modélisation expérimentale des chevauchements imbriqués: application aux chaînes de montagnes, Bulletin de la Société géologique de France XXVI(1), p. 129-138.

Mann, C. D., Vita-Finzi, C., 1988, Holocene serial folding in the Zagros, in: M. Audley-Charles, A. Hallam (Eds.), Gondwana and Tethys, Special Publication Geological Society, vol. 37, pp. 51–59.

Mandl, G., *Mechanics of tectonic faulting*, 1988, Elsevier, New-York.

Martinod, J., Davy, P., Cobbold, P.R., 1991, The control of lithospheric instabilities (buckling) on thrusting in experiments and Central Asia., *Eur. Un. Geosc. VIth Annual Meeting*, Strasbourg.

McClusky S. M., Reillinger, R., Mahmoud, S., Ben Sari, D., and Tealeb, A., 2003, GPS constraints on Africa (Nubia) and Arabia plate motions, Geophys., J., Int., 155, 126-133.

McCall, G. J. H., 1996, The inner Mesozoic to Eocene ocean of south and central Iran and associated microcontinents, Geotectonics, 29, 490-499.

McClintok, F. A., and Walsh, L. B., 1962, Friction on Grifith cracks under pressure, Proc. Fourth U.S. Nat. Congress of Appl. Mech., pp. 1015-1021.

McCoard, D. R., 1974, Regional geology of the Asmari in Ahwaz and Marun areas, NIOC internal report, (Unpub.).

McEven, T. J., 1981, Brittle deformation in pitted pebble conglomerates, *J. Struct. Geol*., 3, 25-37.

McQuarrie, N., 2004, Crustal scale geometry of the Zagros fold-thrust belt, Iran, Journal of Structural Geology, 26, 519-535.

McQuillan, H., 1973, Small-Scale Fracture Density in Asmari Formation of Southwest Iran and its Relation to Bed Thickness and Structural Setting, The American association of Petroleum Geologists, V. 57, No. 12, pp. 2367-2385.

McQuillan, H., 1974, Fracture Patterns on Kuh-e Asmari Anticline, Southwest Iran, The American Association of Petroleum Geologists, V. 58, No. 2, pp. 236-246.

McQuillan, H., 1985, Carbonate Petroleum Reservoirs ,(Roehl & Choquette), Springer-Verlag New York , Inc.

McKenzie, D. P., 1972, Active tectonics of the Mediterranean region, *Geophysical Journal of the Royal Astronomical Society* 30, 109-185.

McKenzie, D. P., 1978b, Some remarks on the development of sedimentary basins, Earth Planet. Sci., Lett., 40, p.25-32.

Mercier, E., 1995, Les plis de propagation de rampe: cinématique, modélisation numèrique, et importance dans la tectogénès, *Habilitation à diriger des recherches*, Université de Cergy-Pontoise, France.

Mercier, J., and Vergely, P., 1992, Tectonique, © Dunod, Paris, p. 214.

Mina, P., Razaghnia, M. T., and Paran, Y., 1967, Geological and geophysical studies and exploratory drilling of the Iranian continental shelf, Persian Gulf, 7th World Petroleum Congress, Mexico, Proceedings P. D. 9, 179-222.

Mitra, S., 2002, Fold accommodation faults, AAPG Bull., 86 (4), 671-693.

Mitra, S., 2002, Structural models of faulted detachment folds, AAPG Bull., 86 (9), 1673-1694.

Mogi, K., 1974, On the pressure dependence of strength of rocks and the coulomb fracture criterion, *Tectonophysics*, 21, 273-285.
Molinaro, M., P. Leturmy, J. C. Guezou, and D. Frizon de Lamotte, 2005, The structures and kinematics of the southeastern Zagros fold-thrust belt, Iran: from thin-skinned to thick-skinned tectonics, Tectonics, 24, TC3007, p.1-19.
Moore, J. M., and Al-Shanti, A. M., 1979, Structure and mineralization in the Najd fault system, Saudi Arabia, In : S . Talhoun (Editor), *Evolution and mineralization of the Arabian-Nubian shield, 2. Pergamon, New York*, N. Y., 17-28.
Moretti, I., Lepage, F., Guiton, M., 2005, KINE3D: a new 3D restoration method based on a mixed approach linking geometry and geomechanics, Oil and Gas Technology, accepted.
Morris, P., 1977, Basement structure as suggested by aeromagnetic surveys in southwest Iran. Proc. Of Second Geological Symposium of Iran, March 1977, Iranian Petroleum Institute, Tehran.
Motiei, H., 1993, Geology of Iran, Zagros stratigraphy, (eds.), *Geological Society of Iran Publications, (in Persian).*
Motiei, H., 1995, Petroleum Geology of Zagros, vol. 1 & 2, *Geological Society of Iran Publications*, (in Persian).
Mullenax, A. C., and Gray, D. R., 1984, Interaction of bed-parallel stylolites and extension veins in boudinage, *J. Struct. Geol*., 6, 63-72.
Muriss, R. J., 1981, Middle east: Stratigraphic evolution and oil habitat, *Geol. Mijnbouw*., 60, 467-486.
National Iranian Oil Company, 1969, Geological map of Zagros, 1:1000,000, *NIOC Exploration Publications*, Iran.
Nawab, Z. A., 1979, Geology of the AL Amar-Idsas region of the Arabian shield, in A. M. AL Shanti ed., *Evolution and mineralization of the Arabian-Nubian shield*: New York, Pergamon Press, v. 2, p. 29-40.
Nelson, R. A., 1979, Natural fracture systems, description and classification, *AAPG Bull*., vol. 63, no. 12, p; 2214-2221.
Nelson, R. A., 1985, Geologic analysis of naturally fractured reservoirs, (eds.), *Gulf Publishing*, Houston, Texas, Contr. In Petrol. Geol. And Eng., no. 1, 320 p.
Nelson, R.A., 2001, Geological analysis of naturally fractured Reservoirs, Second Edition, *Gulf Professional Publishing*.
Nelson, R; A., and Serra, S., 1995, Vertical and lateral variations in fracture spacing in folded carbonate sections and its relation to locating horizontal wells, Journal of Canadian Petroleum Technology, v.34, no. 6, p.51-56.
Nelson, R. A., and D. W. Stearns, 1977, Intraformational Control of Regional Fracture Orientation, In: Rocky Mtn. Assoc. Geol., 1977 Field Trip Guidebook, Exploration Frontiers, Central and Southern Rockies, p. 95-101.
North, F. K., 1985, Petroleum Geology (ed.), *Allen and Unwin*, Boston, 607 p.
Nelson, R. A. 1981. Significance of fracture sets associated with stylolite zones. *Bull. Am. Ass. Petrol. Geol.* 65, 2417-2425.
Nelson, R.A., 2001, Geological analysis of naturally fractured Reservoirs, Second Edition Gulf Professional Publishing, pp. 1-18.
Ni, J., and M. Barazangi, 1986, Seismotectonics of the Zagros continental collision zone and a comparison with the Himalayas, *Journal of Geophysical Research*, vol. 91, part B8, 8205-8218.
Nicolas, A., 1984, Principes tectonique, Masson, 196p.
Nieuwland, D. A., and J. V. Walters, 1993, Geomechanics of the South Furious field. An integrated approach towards solving complex structural problems, including analogue and finite-element modelling, *Tectonophysics*, 229, pp. 143-166.
Nino, F., Philips, H., and Chery, J., 1998, The role of bedding parallel slip in the formation of blind thrust faults, *J. Struct. Geol*., 13, 503-516.
Nitecki, M. H., 1962, Observations on slickolites, J. Sedim. Pet., 32, 435-439.
Nowroozi, A. A., 1972, Focal mechanism of earthquakes in Iran, Turkey, West Pakistan and Afghanistan and plate tectonics of the Middle East, Bull. Seismol. Soc. Am., vol.62, no.3, p.823-850.
Oberlander, T., 1965, The Zagros streams, *Syracuse Geogr. Ser*. 1.
O'Brien, C.A.E., 1950, Tectonic problems of the oil field belt of southwest Iran, *18th Int. Geol. Cong.*, Great Britain, Proc., pt. 6, p. 45-58.
O'Brien, C.A.E., 1953, Discussion of fractured reservoir subjects, *AAPG Bull*., v. 37, no. 2, p. 325.
Odé, H., 1960, Faulting as velocity discontinuity, In: D. T. Griggs and J. Handin (eds.), Rock deformation, Mem. Geol. Soc. Am., 79, 293-321.
Odonne, F., and Vialon, P., 1983, Analogue model s of folds above a wrench fault ; *Tectonophysics*, 99, 31-46.
Oliver, D., 1987, The development of structural patterns above reactivated basement faults; Ph.D. thesis, university of London.

Onyedim, G. C. and Norman, J. W., 1986, Some appearances and causes of lineaments seen on landsat images, Journal of Petroleum Geology, 9, 2, pp. 179-194.
Owen, R.M.S. and S.N. Nasr, 1958, Stratigraphy of the Kuwait-Basra Area. In: 'Habitat of Oil', *American Association Petroleum Geologist Memoir* 1, p. 1252-1278
Park, W. C., and Schot, E. H., 1968, Stylolites; their nature and origin: *Jour. Sed. Petrology*, v.38, p. 175-191.
Parker, J. M., 1942, Regional systematic jointing in slightly deformed sedimentary rocks, Geol. Soc. Am. Bull., 53, 381-408.
Parrish, D. K., 1973, A nonlinear finite-element fold model, *Am. J. Sci.* , 273, 318-334.
Paterson, M. S., 1978, *Experimental Rock Deformation-The Brittle Field*, Springer, Heidelberg.
Payne, A., 1990, A structural interpretation of the Zagros Fold Belt, SW Iran-NE Iraq, British Petroleum Co. Ltd, internal report.
Petit, J. P., 1987, Criteria for the sense of movement on fault surfaces in brittle rocks, J. Struct. Geol., 9, 5/6, 597-608.
Petit, J. P., and Barquins, M., 1988, Can natural faults propagate under mode II conditions ?, Tectonics, 7, 6 , 1243-1256.
Pfiffner, O. A., and Burkhard, M., 1987, Determination of paleostress axes orientations from, twin and earthquake data, *Annales Tectonicae*, 1, pp. 48-57.
Philip, H., A. Cisternas, A. Gvishiani, and A. Gorshkov, 1989, The Caucasus: An actual example of the initial stages of a continental collision, *Tectonophysics*, 161, 1 – 21.
Piper, J. D. A., 1983, Dynamic of the continental crust in Proterozoic times : GSA Memoir 161, p. 11-34.
Player, R.A., 1969, The Hormuz salt plugs of southern Iran: *Ph.D.; thesis*, Reading Univ., 300p.
Pohn, H.A. 1981, Joint spacing as a method of locating faults. Geology 9, 258-261.
Pollard, D.D., and Aydin A., 1988, Progress in understanding jointing over the past century, *G.S.A. Bulletin*, 100, 1181-1204.
Powers, R. W., L. F. Ramirez, C. D. Redmond, and E. L. Elberg, 1966, Geology of the Arabian Peninsula-sedimentary geology of Saudi Arabia, *Prof. Pap. U. S. Geol. Surv.*, 560D, D1-D147.
Price, N. J., 1959, Mechanics of jointing in Rocks, *Geological magazine*, vol. 46, no. 2, p. 149-167.
Price, N. J., 1966, *Fault and joint development in brittle and semi-brittle rock*, Pergamon Press, London, 176 p.
Price, N. J., 1974, The development of stress systems and fracture patterns in undeformed sediments, Proc. 3rd Cong. Intern. Rock Mech., TA 487-496.
Price, R. A., 1967, The tectonic significance of mesoscopic sub-fabrics in the Southern Rocky Mountains of Alberta and British Columbia, Canadian Journal of Earth Sciences, v.4, p.39-70.
Price, N. J., and J. W. Cosgrov, 1990, Analysis of geological fractures, *Cambridge University Press*, Cambridge.
Ramberg, H., 1970, Folding of laterally compressed multilayers in the field of gravity,1. *Phys. Earth Planet. Interiors*, 2, 203--232
Ramberg, H. R., and Stephanson, O., 1964, Compression of floating elastic and viscous plates affected by gravity, a basis for discussing crustal buckling, Tectonophysics, 1, 101-120.
Ramsay, J. G., 1967, folding and fracturing of rocks: International series in the earth and planetary sciences, McGraw-Hill Book Co., pp. 392-402.
Ramsay, J. G., 1977, Pressure solution – the field data, *J. Geol. Soc. Lond*., 134, 72.
Ramsay, J. G., 1980, The crack-seal mechanism of rock deformation, Nature, 284, 135-139.
Ranalli, G. & Yin, Z.M., 1990, Critical stress difference and orientation of faults in rock with strength anisotropies: the two-dimensional case. *Journal of Structural Geology* **12,** 1067-1071.
Raynaud, S., 1987, Les premiers stades de la deformation dans une zone de relais entre decrochements: exemples naturels et experi- mentaux. *Bull. Soc. geol. Ft.* 8,583-590.
Reches, Z., 1983, Faulting of rocks in three-dimensional strain fields II: theoretical analysis, *Tectonophysics*, 95, 133-156.
Reches, Z., 1987, Determination of tectonic stress tensor from slip along faults that obey the Coulomb yield criterion, Tectonics, 6, 6, pp. 849-861.
Regard, V., O. Bellier, J.-C. Thomas, D. Bourlès, S. Bonnet, M. R. Abbassi, R. Braucher, J. Mercier, E. Shabanian, Sh. Soleymani, and Kh. Feghhi, 2005, Cumulative right-lateral fault slip rate across the Zagros-Makran transfer zone: role of the Minab-Zendan fault system in accommodating Arabia-Eurasia convergence in southeast Iran, Geophys. J. Int., 162, 177-203.
Richard, P., 1990, Champs de failles au dessus d'un décrochement de socle: modélisation expérimentale, *Thèse de Doctorat*, Université de Rennes, France.
Richard, P., 1991, Experiments on faulting in a two-layer cover sequence overlying a reactivated basement fault with oblique-slip, *J. Struct. Geol.*, vol.13, no.4, 459-469.
Richard, P., and Krantz, R. W., 1991, Experiments on fault reactivation in strike-slip mode, *Tectonophysics*, 188, 117-131.

Richard, P., Mocquet, B., and Cobbold, P. R., 1991, Experiments on simultaneous faulting and folding above abasement wrench fault, *Tectonophysics*, 188, 133-141.
Richardson, R. K., 1924, Lower Fars stratigraphy summary of outcrop evidences, AIOC report, No. 611 (unpub.).
Ricou, L. E., 1970, Comments on radiolarites and ophiolite nappes in the Iranian Zagros mountains, *Geological Magazine*, v.107, p.479-480.
Ricou, L. E., 1974, L'évolution géologique de la région de Neyriz (Zagros iranien) et l'évolution structurale des Zagrides, *Thése d'état*, Université d'Orsay, France.
Rispoli, R., 1981, Stress fields about strike-slip faults inferred from stylolites and tension gashes, *Tectonophysics*, 75, T29-T36.
Rives, T., 1992, Mécanismes de formation des diaclases dans les roches sédimentaires: Approche expérimentale et comparaison avec quelques exemples naturels, *Thèse de Doctorat*, Université Montpellier II, 250p.
Rives, T., Rawnsley, K. & Petit, J.P., 1994. Analogue simulation of orthogonal joint set formation in brittle varnish. Journal of Structural Geology, 7, N° 3, p. 419-429,
Roberts, J. C., 1961, Feather-fracture, and the mechanics of rock jointing, Am. J. Sci., 259, 481-492.
Roberts, A.M., Kusznir, J.N., Yielding, G., and Style, P., 1998, 2D flexural backstripping of extensional basins: the need for a sideways glance, *Petroleum Geoscience*, vol.4, pp.327-338.
Robertson, A. H. F., 2000, Mesozoic-Tertiary tectonicsedimentary evolution of a south Tethyan oceanic basin and its margins in southern Turkey, in Tectonics and Magmatism in Turkey and the Surrounding Area, edited by E. Bozkurt, J. A. Winchester, and J. D. A. Piper, *Geol. Soc. Spec. Publ.*, 173, 97–138.
Rouby, D., Xiao, H., Suppe, J., 2000, 3-D restoration of complexly folded and faulted surfaces using multiple unfolding mechanisms, AAPG Bulletin, 84(6) pp.805-829.
Roure, F., and Sassi, W., 1995, kinematic of deformation and petroleum system appraisal in Neogene Foreland Fold and Thrust belt, Petroleum Geosciences, 1, pp.253-269.
Rowe, K. J., and Rutter, E. H., 1990, Paleostress estimation using calcite twinning: experimental calibration and application to nature, J. Struct, Geol., 12, 1, pp. 1-17.
Rumsey, I. A. P., 1971, Relationship of fractures in unconsolidated superficial deposits to those in underlying bedrock, *Modern Geology* 3, (1) 25-41.
Rutter, E. H., 1976, The kinetic of rock deformation by pressure solution, *Phil. Trans. Roy. Soc. Lond*, A. 283, 43-54.
Salam, A. M. and H. Arab, 2001, Tectonic development of the Arabian Gulf, AAPG annual meeting, Denver, Colorado.
Salençon, J., 1995, *Mécanique des milieux continues*, Tomes I and II, Ecole Polytechnique.
Sangree, J.B., Masson, P.H., McQuillan, H., and Twernbold, E.F., 1961, Asmari fracture study, IOOC, report no. G-963 (Unpub.).
Sassi, W., and J. L. Faure, 1997, Role of faults and layer interfaces on the spatial variation of stress regime in basins: Inference from numerical modeling, *Tectonophysics*, 266, 101– 119.
Sassi, W., Colletta P., Balé T., & Paquereau T., 1993, Modelling of structural complexity in sedimentary basins: the role of pre-existing faults in thrust tectonics. *Tectonophysics* **226,** 97-112.
Sattarzadeh, Y., J. W. Cosgrove, and C. Vita-Finzi, 2000, The interplay of faulting and folding during the evolution of the Zagros deformation belt, In: Cosgrov, J. W., & Ameen, M. S., (eds.), Forced folds and fractures, Geol. Soc. Lon. Spec. Pub., 169, 187-196.
Savalli, L., Engelder, T., 2005, Mechanisms controlling rupture shape during subcritical growth of joints in layered rocks, *GSA Bulletin*, v. 117; no. 3-4; p. 436-449; DOI: 10.1130/B25368.1
Schader, F., 1988, Symmetry of pebble-deformation involving solution pits and slip-lineations in the northern Alpine Molasse Basin, J. Struct. Geol., 10, 41-52.
Schmidt, D. L., D. G. Hadley, and D. B. Stoesser, 1979, Late Proterozoic crustal history of the Arabian shield, southern Najd Province, Kingdom of Saudi Arabia, in *S. A. Talhoun, ed., Evolution and mineralization of the Arabian-Nubian shield: New York, Pergamon Press*, v. 2, p. 41-58.
Secor, D. T., 1965, Role of fluid pressure in jointing, Am. J. SCI., 263, 633-646.
Segall, P. and D. D. Pollard, 1980, Mechanics of discontinuous. faults, *Journal of Geophysical Research*, 85, p. 4337-. 4350
Sella, G.F., Dixon, T.H., and A. Mao, 2002, A model for recent plate velocities from space geodesy, Journal of Geophysical Research, 107, 11-30.
Sepehr, M., 2001, The tectonic significance of the Kazerun Fault Zone, Zagros fold–thrust belt, Iran, *Ph.D. Thesis*, Imperial College, University of London.
Sepehr, M., and Cosgrove, J.W., 2004, Structural framework of the Zagros fold-thrust belt, Iran, *Marine and Petroleum Geology*, 21, 829-843.
Sepehr, M., and Cosgrove, J.W., 2005, Role of the Kazerun fault zone in the formation and deformation of the Zagros fold-thrust belt, Iran, Tectonics, vol. 24, TC5005, doi:10.1029/2004TC001725.

Setudehnia, A., 1972, Iran du sud-ouest, Lexique Stratigraphique International III, Fascicule 9b, Iran, Centre National de la Recherche Scientifique, Paris, pp.285-376.
Setudehnia, A., 1975, The Paleozoic sequence at Zardkuh and Kuh-e-Dinar, Bulletin of the Iranian Petroleum Institute, 60, pp.16-33.
Shanti, A. M. al-, and I. G. Gass, 1983, The upper Proterozoic ophiolite melange zones of the easternmost Arabian shield, *J. Geol. Soc. London*, v. 140, p. 867-876.
Shanti, A. M. al-, and A. H. G. Mitchell, 1976, Late Precambrian subduction and collision in the Al Amar-Idsas region, Arabian shield, Kingdom of Saudi Arabia, *Tectonophysics*, v. 30, p. 41-47.
Shephered, M. F., Twerenbold, E. F., Sajjadi, F., 1961, The geology of Iraq border structures, IOOC internal report, no.911 (Unpub.).
Sheppard, M. S., 1988, Approaches to the Automatic Generation and Control of Finite Element Meshes, *Appl. Mech. Rev.*, 41, pp. 169-185.
Sherkati, S., 2004, Tectonic style and kinematics of folding in the Iranian Zagros (Izeh zone): with special emphasis on petroleum systems, Ph.D. Thesis, Cergy-Pontoise University, France.
Sherkati, S., and Letouzey, J., 2004, Variation of structural style and basin evolution in the central Zagros (Izeh zone and Dezful Embayment), Iran, *Marin and Petroleum Geology*, 21, 535-554.
Sherkati, S., Letouzey, J., and Frizon de Lamotte, D., 2005, The central Zagros fold-thrust belt (Iran): New insights from seismic data, field observation and sandbox modelling, *Journal of Structural Geology*, in press.
Sharland, P. R., R. Archer, D. M. Casey, R. B., Davies, S. H. Hall, A. P. Heward, A. D. Horbury, and M. D. Simmons, 2001, Arabian Plate Sequence Stratigraphy, *GeoArabia Special Publication* 2.
Sibson, R. H., 1974, Frictional constraints on thrust, wrench and normal faults, *Nature*, 249:542-44.
Sibson, R. H., 1985, A note on fault reactivation. Journal of structural geology, 7(6):751-54.
Sibson, R. H., 1989, Earthquake faulting as a structural process, J. Struct. Geol, vol. 11, p. 1-14.
Silliphant, L.J., Engelder, T., Gross, M.R., 2002, The state of the stress in the limb of the Split Mountain anticline, Utah: constraints placed by transects joints, *Journal of Structural Geology*, 24, p.155-172.
Smith, A. G., A. M. Hurley, and J. C. Briden, 1981, Phanerozoic paleocontinental world map: Cambridge, *Cambridge University press*, 102 p.
Spang, J. H., 1972, Numerical method for dynamic analysis of calcite twin lamellae. *Bull. geol. Soc. Am.* 83,467-472.
Sperner, B., Ott, R., and Ratschbacher, L., 1993, Fault-striae analysis: a turbo pascal program package for graphical presentation and reduced stress-tensor calculation. - Computers & Geosciences, 19(9):1361-1388; Manchester.
Stacey, J. S., D. B. Stoesser, W. R. Greenwood, and L. B. Fisher, 1984, U-Pb zircon geochronology and geological evolution of the Halaban-Al Amar region of the eastern Arabian shield, Kingdom of Saudi Arabia, J; Geol. Soc. London, v. 142, p. 1189-1203.
Stearns, D. W.,1968a, Fracture as a mechanism of flow in naturally deformed layered rock, In: *Kink Bands and Brittle deformation*, A. J. Baer and D. K. Norsis, Eds., Geol., Surv. Can., 68-52, p. 79-95.
Stearns, D. W.,1968b, Certain aspects of fractures in naturally deformed rocks, In: NSF Advanced Science Seminar in Rock Mechanics, R. E. Rieker, ED., Special report, Air Force Cambridge Research Laboratories, Bedford, Massachusetts, AD 6693751, p. 97-118.
Stearns, D. W.,1972, Structural interpretation of the fractures associated with the Bonita fault, Guidebook 23rd Field Conf., New Mexico, Geol. Soc., East Central New Mexico, p. 161-164.
Stearns, D. W.,1978, Faulting and forced folding in the rocky mountains foreland, *Geol. Soc. Am. Bull.*, 151, 1-37.
Stearns, D. W., and M. Friedman, 1972, Reservoirs in fractured rock, *AAPG Memoir* 16, p. 82-100.
Stern, R. J., 1985, The Najd fault system, Saudi Arabia and Egypt: a late Precambrian rift-related transform system?, *Tectonics*, 4, 497-511.
Stewarts, S. A., and Wynn, T. J., 2000, Mapping spatial variation in rock properties in relationship to scale-dependent structure using spectral curvature, Geology, v.28, p.691-694.
Stöcklin, J., 1968a, Structural history and tectonics of Iran: a review: *AAPG Bulletin*, v. 52, p. 1229-1258.
Stöcklin, J., 1968b, Salt deposits of the Middle East, In: Saline deposits, *Geol. Soc. America, Spec. Paper* 88, p. 158-181.
Stöcklin, J., 1977, Structural correlation of the Alpine ranges between Iran and Central Asia, Mémoire Hors-Série No.8 de la Société Géologique de France.
Stoesser, D. B. and V. E. Camp, 1985, Pan-African microplateaccretion of Arabian shield: *GSA Bulletin*, v. 96, p. 818-826.
Stoesser, D. B., J. S. Stacey, W. R. Greenwood, and L. B. Fischer, 1984, U-Pb zircon geochronology in the southern part of the Nabitah mobile belt and Pan-African continental collision in the Saudi Arabian shield: USGS Open-File Report TR-04-05, 88p.

Stoneley, R., 1976, On the origin of ophiolite complexes in the southern Tethys region, Tectonophysics, 25, pp.303-322.
Stoneley, R., 1981, The geology of the Kuh-e Dalneshin area of southern Iran, and its bearing on the evolution of southern Tehys, Journal of Geological Society, London, v. 138, p. 509-526.
Storti, F., F. Salvini, and K. McClay, 1997, Fault related folding in sandbox analogue models of thrust wedges, J. Struc. Geol., vol. 19, nos. 3-4, p. 583-602.
Suppe, J., 1985, Principles of structural geology, Prentice Hall, Inc, Englewood cliffs, New Jersey.
Szabo, F., and Kheradpir, A., 1978, Permian and Triassic stratigraphy, Zagros basin, south-west Iran, Journal of Petroleum Geology, 1(2), pp.57-82.
Talbot, C. J., and Alavi, M., 1996, The past of a future syntaxis across the Zagros, *in* Alsop, G. I., Blundell, D. J., and Davidson, I., editors, Salt tectonics: London, Geological Society Special Publication 100, p. 89–109.
Talbot, C. J., and Jarvis, R. J., 1984, Age, budget and dynamics of an active salt extension in Iran, *J. Struc. Geol.* 6, 521-533.
Talebian, T., and J. Jackson, 2002, Offset on the Main Recent Fault of NW iran and implications for the late Cenozoic tectonics of the Arabia-Eurasia collision zone, Geophys. J. Int. v. 150, p. 422-439.
Talebian, M., and Jackson, J. A., 2004, A reappraisal of earthquake focal mechanism and active shortening in the Zagros mountains of Iran, Geophysical Journal International, vol.156, p.506-526.
Tatar, M., 2001, Etude sismotectonique de deux zones de collision continentale: le Zagros Central et l'Alborz (Iran), Thése de l'Université de Gronoble.
Tatar, M., D. Hatzfeld, J. Martinod, A. Walpersdorf, M. Ghafori-Ashtiany, and J. Chéry, 2002, The present-day deformation of the central Zagros from GPS measurements, Geophys. Res. Lett., 29 (19), 1927, doi: 10.1029/2002GL015427.
Tatar, M., D. Hatzfeld, and M. Ghafori-Ashtiany, 2004, Tectonics of the Central Zagros (Iran) deduced from microearthquakes seismicity, Geophys. J. Int., p.255-266.
Tensi, T., F. Mouthereau, and O. Lacombe, 2006, Lithospheric bulge in the western Taiwan Basin, *Basin Research* (submitted)
Thomas, A.N., 1948, The Asmari limestone of Southwest Iran, AIOC Report, no.705, (Unpub.).
Thomas, A.N., 1949, Tentative isopach map of Upper Asmari limestone, the Oligocene and Lower Miocene in Southwest Iran, AIOC internal report, No.731 (Unpub).
Timoshenko, S., and Woinowsky-Krieger, S, 1959, Theory of plates and shells: New York, McGraw-Hill, 580p.
Tjia, H. D., 1971, Fault movement, reoriented stress field and subsidary structures, Pacific Geol., 5, 49-70.
Trapp, B., and Cook, J., 1988, Pressure solution zone propagation in naturally deformed carbonate rocks, Geology, ?, 182-185.
Tullis, T. E., 1980, The use of mechanical twinning in minerals as a measure of shear stress magnitudes, J. Geophys. Res., 85, pp. 6262-6268.
Turcotte, D.L. and Schubert, G., 1982, Geodynamics: Applications of Continuum Mechanics to Geological Problems, Wiley, New York.
Turner, F. J., 1962, "Compression" and "tension" axes determined from $\{0112\}$ twinning in calcite (abs.): J. Geophys. Res., v. 67, p. 1660.
Van Hinte, J.E., 1978, Geohistory Analysis - Application of Micropaleontology in Exploration Geology. *American Association of Petroleum Geologists Bulletin*, 62: 201-222.
Verges, J., D. W. Burbank, and A. Meigs, 1996, Unfolding: an inverse approach to fold kinematics, *Geology*, v. 24; no. 2; p. 175-178.
Vernant, P., F. Nilforoushan, D. Hatzfeld, M. R. Abbassi, C. Vigny, F. Masson, H. Nankali, J. Martinod, A. Ashtiani, R. Bayer, F. Tavakoli, and J. Chéry, 2004, Present day crustal deformation and plate kinematics in the Middle East constrained by GPS measurements in Iran and northern Oman, Geophys. J. Int., v. 157, p. 381-398.
Vita-Finzi, C., 1979, Rates of Holocene folding in the coastal Zagros near Bandar Abbas, Iran, *Nature*, 278(5705): 632-634.
Vita-Finzi, C., 2001, Neotectonics at the Arabian plate margins, Journal of Structural Geology 23, 521– 530.
Voight, B., and St. Pierre, H. P., 1974, Stress history and rock stress, Proc. 3rd Rock Mech. Congr., ISRM 2, 580-582.
Walker, D.J., 1969, Distribution of sandstone in the Marun Asmari Reservoir, IOEPC, internal Memo. (Unpub).
Wallace, R. E., 1951, Geometry of shearing stress and relation to faulting, J. Geol., 59, PP. 118-130.
Wang, Y., and J-C. Mareschal, 1999, Elastic thickness of the lithosphere in the Central Canadian Shield, *Geophysical Research Letters*, vol.26, no.19, pp.3033-3035.
Watson, S.E., 1962, Lower Fars key bed correlation in Aghajari, *IOOC report* No. 1014 (Unpub.).
Watts, A.B., 2001, Isostasy and Flexure of the Lithosphere, Cambridge University Press, Cambridge.

Watts, A.B. and Ryan, W.B.F., 1976, Flexure of the lithosphere and continental margin basins, *Tectonophysics*, 36: 25-44.
Watts, N. L., 1983, Microfractures in chalks of Albuskjell Field, Norwegian Sector, North Sea; possible origin and distribution AAPG Bulletin, 67: 201-234
Wells, A. J., 1969, The crush zone of the Iranian Zagros mountains, and its implications, Geological magazine, v.106, p.358-394.
Weijermars, R., 1998, Plio-Quaternary movement of the East Arabian block, GeoArabia, 3, 509-540.
Wissmann, H. von, Rathjens, C., & Kossmat, F., 1942, Beiträge zur tektonik Arabiens, *Geologisches Rundschau* 33, 221-353.
Yilmaz, Y., 1993, New evidence and model on the evolution of the southeast Anatolian orogen, *Geol. Soc. Am. Bull*., 105, 251 – 271.
Yin, Z.M. & Ranalli, G., 1992, Critical stress difference, fault orientation and slip direction in anisotropic rocks under non-Andersonian stress systems. *Journal of Structural Geology* 14**,** 237-244.
Ziony, J. I., 1966, Analysis of systematic jointing in part of the monument upwarp, Southern Utah, Ph.D. Dissertation, University of California, Los Angeles, California, 152 pp.

Annex 1
Some remarks on SPOT 5 imagery

An SPOT 5 satellite image which cover part of our studied area was used to define the most important lineaments (large scale fractures/faults) on the studied outcrops. The image-scale lineament directions were compared to the field measurement results to see, first if they are coherent and second, to define if the observed anomalies in the measurement could be the effect of a local tectonic feature, like a fault near measurement site(s).

The definition of high resolution satellite imaging systems is not fixed, it depends upon the application. For meteorological satellites even 1 km may belong to high resolution. For the topographic mapping purposes it starts approximately at a ground sampling distance (GSD) of 10 m. Ground sampling distance is the distance of the centre of neighbored pixels projected to the ground. This appears as pixel size on the ground even if the real ground pixel size is influenced by over- or under sampling. The first digital images available for civilian application came from Landsat in 1972, but its GSD was not usable for topographic maping; this was possible at first with SPOT 1 in 1986.

The SPOT satellites have been designed especially for mapping with the potential of a stereoscopic coverage from neighboured orbits. The SPOT system is designed to achieve optimum image quality in terms of resolution and solar illumination and to respond quickly to user requests. The SPOT satellites orbit the Earth at an altitude of 822 km at the Equator. To maintain a costant resolution, the orbit is circular. The orbit is also near polar, which means the satellite can acquire images of any point on the globe. Because of the Earth's rotation, the subsatellite point follows a regular pattern of ground tracks on the Earth's surface.

The orbit is phased so that a satellite passes over the same point every 26 days. The satellite thus repeats the same ground tracks and the maximum distance between tracks at the Equator is 108 km. The combined field of view of the two instruments in twin-vertical configuration is 117 km, so a satellite covers the Earth in a single 26-day cycle (Fig.VI.1a). The SPOT imaging instruments' oblique viewing capability means they can acquire imagery of any point on the globe within less than five days at the Equator, and in less than three days at temperate latitudes (45°). Oblique viewing also makes it possible to acquire stereopair images of the same area of interest from different viewing angle (Fig.VI.1b).

The areas of interest in satellite images were derived from a single high resolution pseudo-color SPOT 5 satellite image (Fig.VI.2) with a coverage of about 60 x 60 km (24 x 24

KPixel). This image was taken by HRG instrument of SPOT 5 satellite. The image resolution was 2.5m/Pixel. Table VI.1 shows other technical parameters of this image.

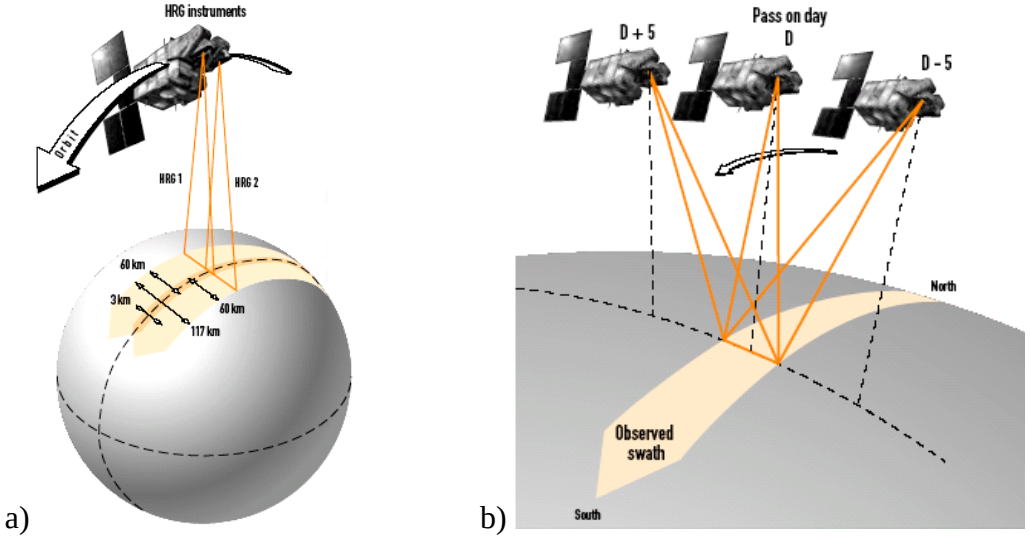

Fig.VI.1: (a) HRG instruments in twin-vertical viewing configuration; each HRG instrument covers a 60 km swath. Together, the two instruments thus image a combined swath of 117 km, with a 3 km overlap. In thsi mode SPOT covers the entire earth in 26 days since the maximum distance between adjacent ground tracks at the Equator is 108 km. (b) Oblique viewing offers two key advantages: fast and flexible acquisition of repeat imagery and imaging from different viewing angles to yield stereopairs (http://www.cnes.tv.com/dossiers/spot5)

Scene ID	5 150-288 04/01/21 07:27:29 1 T+X
K-J identification	150-288
Date	2004-01-21 07:27:29
Instrument	HRG 1
Shift Along Track	0
Preprocessing level	1A
Spectral mode	T+X
Number of spectral bands	3
Spectral band indicator	XS1 XS2 XS3
Gain number	2 2 3
Absolute calibration gains	(W/m2/sr/µm) 0.672115 0.804593 1.098000
Orientation angle	13.038583 degree
Incidence angle	R4.959938 degree
Sun angles (degree)	Azimut:155.851474 Elevation:35.433134
Number of lines	24000
Number of pixel per line	24000
Scene Center Location	
Latitude	N30°56'54"
Longitude	E050°08'03"
Pixels number	12001
Line number	12001
Corners Location	
Corner Latitude Longitude Pixel n° Line n°	
1 N31°16'25" N49°53'49" 1 1	
2 N31°09'03" N50°30'45" 24000 1	
3 N30°37'23" N50°22'03" 24000 24000	
4 N30°44'44" N49°45'20" 1 24000	

Table VI.1: Scene parameters of SPOT 5 satellite image used for lineament interpretation.

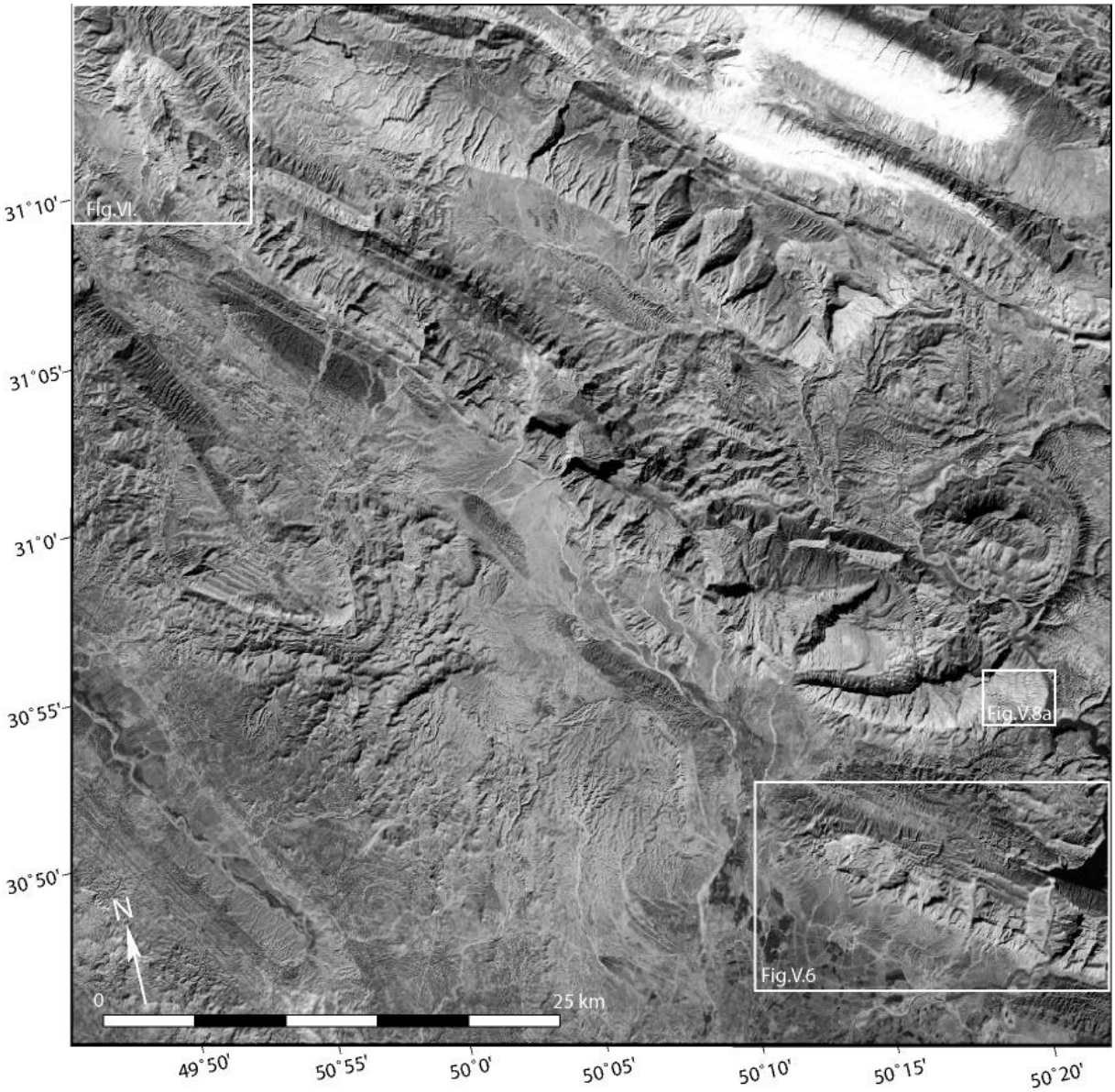

Fig.VI.2: SPOT 5 satellite image used for lineaments interpretation in some studied anticlines (selected parts on the image shown by rectangles). Analysis of the images indicated by the white rectangles are provided in the chapter V.

Annex 2
Field examples of fracture patterns in some anticlines

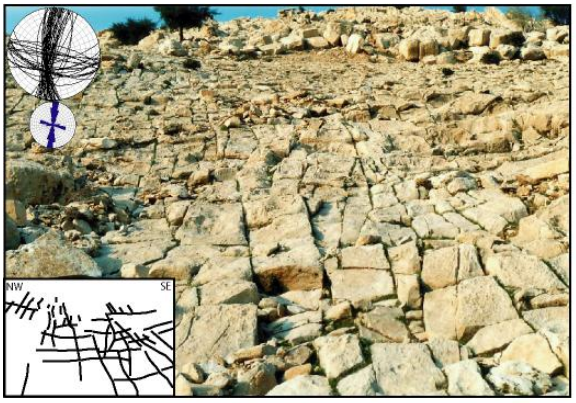

Bangestan anticline

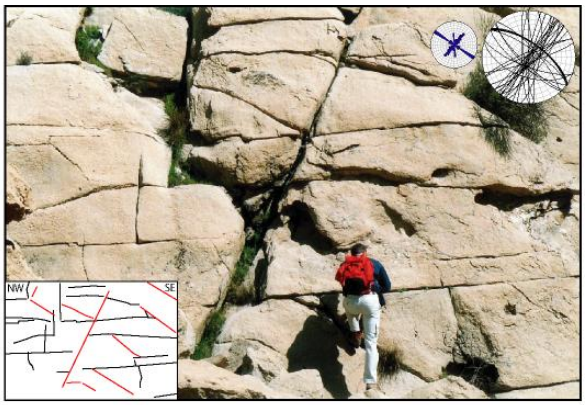

Mish anticline (Tang-e Gorgoda)

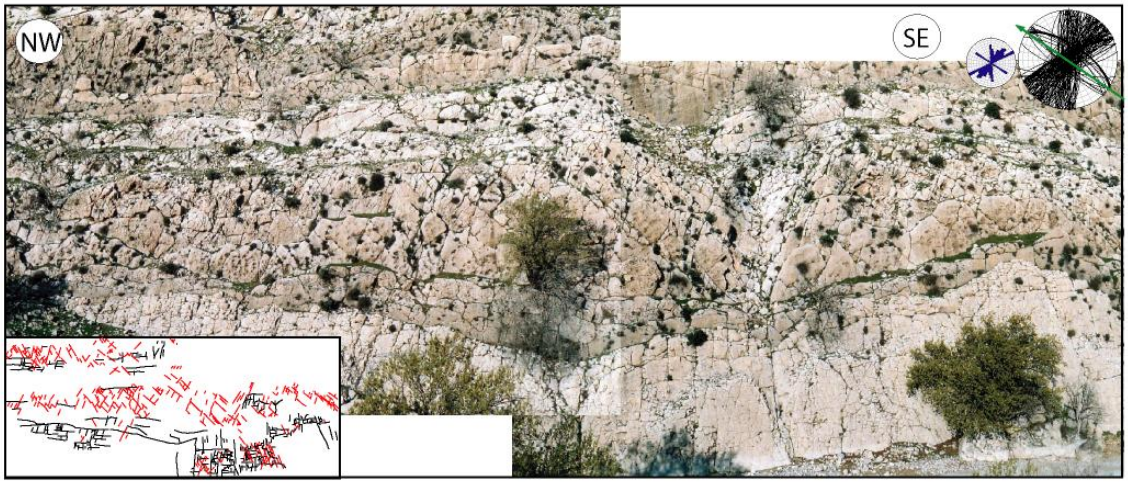

Mish anticline (Top Asmari)

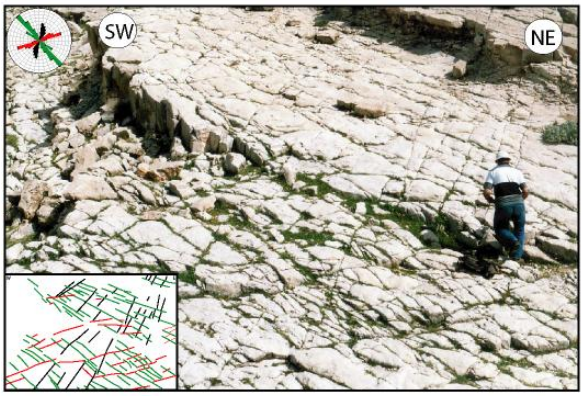

Khaviz anticline (SE nose)

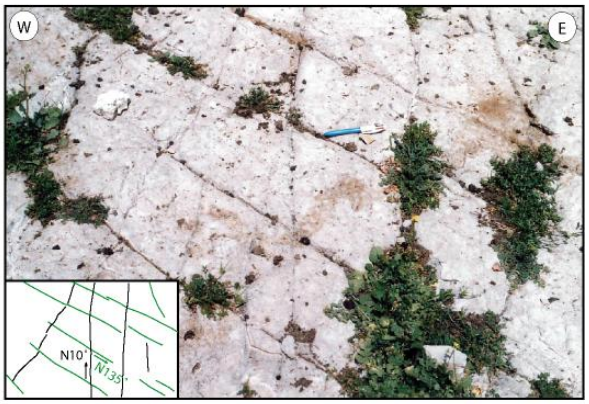

Bangestan anticline (SE nose)

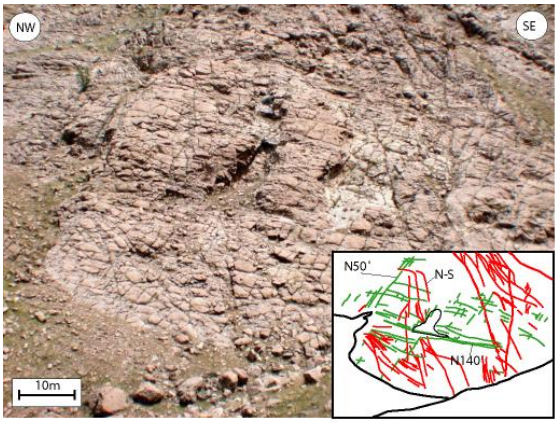

Asmari anticline

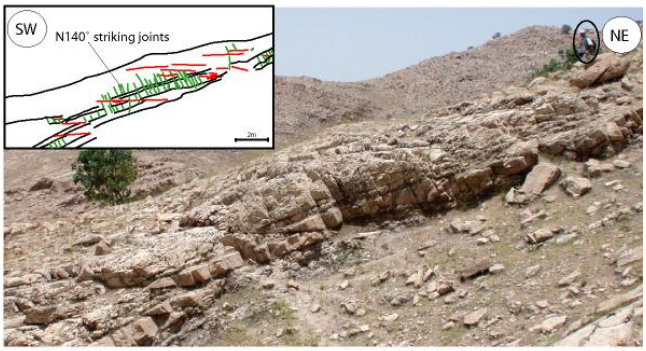

Asmari anticline

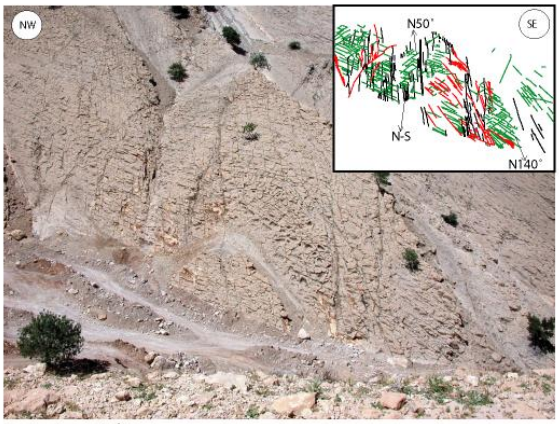

Asmari anticline

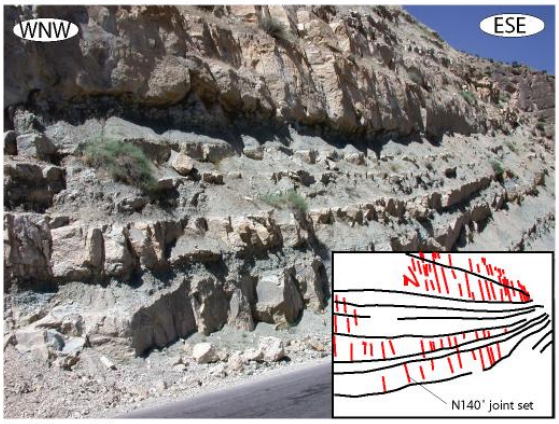

Safid anticline

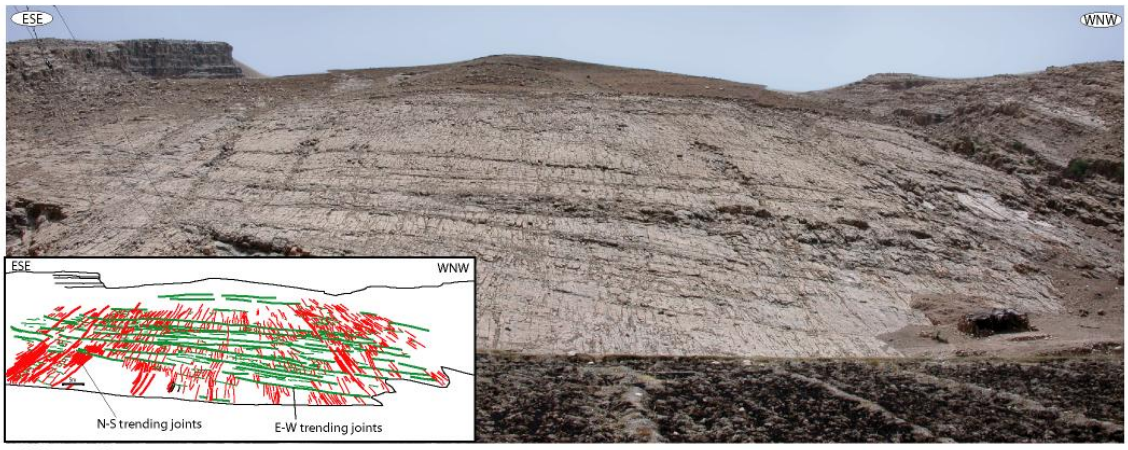

Sulak anticline